BioMed Research International

Oncogenic Processes

Guest Editors: Rita de Cassia Stocco, Franco Peppino Roperto, Lubna Nasir, and Marcelo Palma Sircili

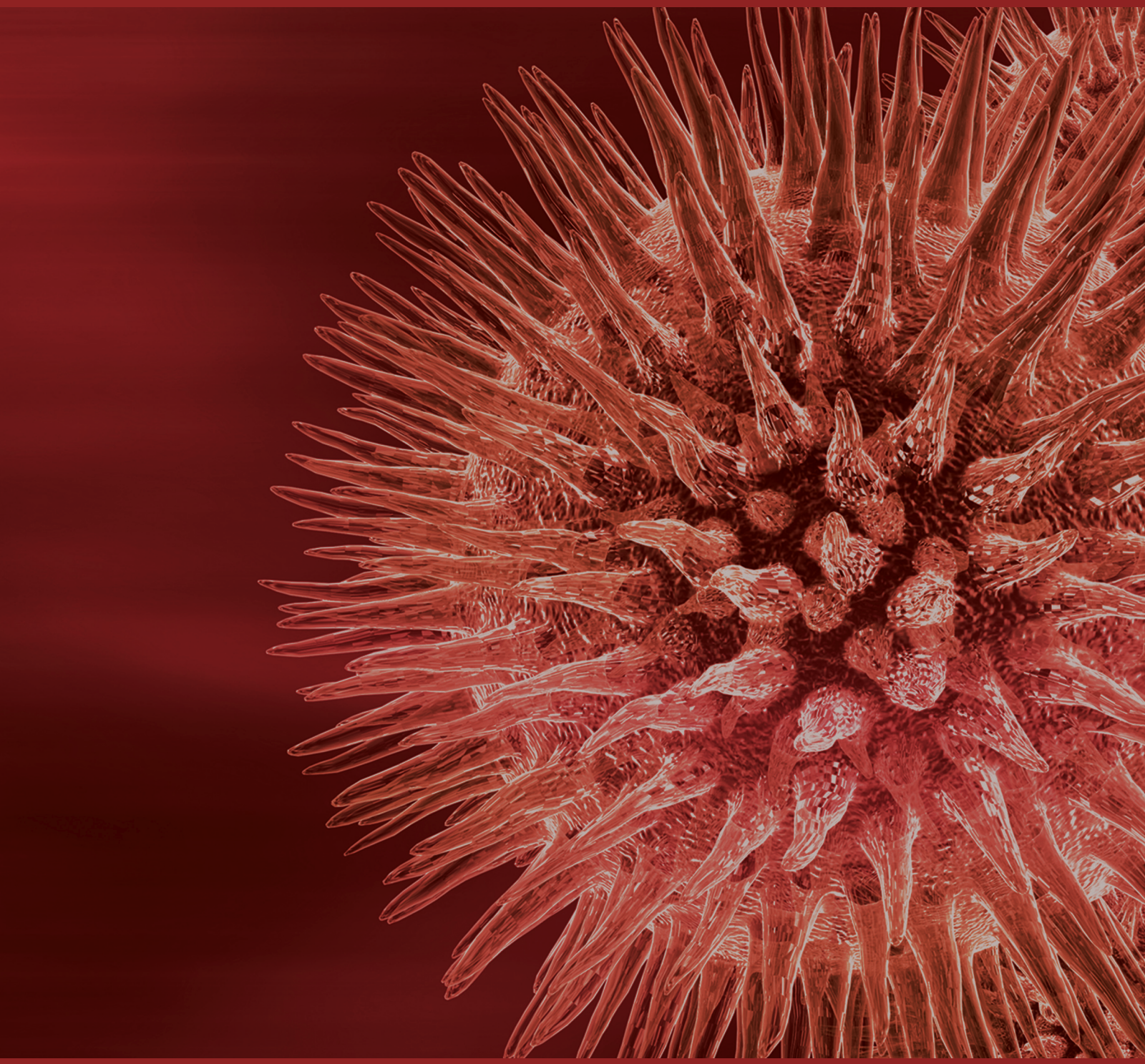

Oncogenic Processes

BioMed Research International

Oncogenic Processes

Guest Editors: Rita de Cassia Stocco,
Franco Peppino Roperto, Lubna Nasir,
and Marcelo Palma Sircili

Contents

Hindawi Publishing Corporation
BioMed Research International
Volume 2014, Article ID 879013, 4 pages
http://dx.doi.org/10.1155/2014/879013

Editorial
Oncogenic Processes

Rita de Cassia Stocco,[1] Franco Peppino Roperto,[2] Lubna Nasir,[3] and Marcelo Palma Sircili[1]

[1] *Laboratório de Genética, Instituto Butantan, Secretaria de Estado da Saúde, Avenida Vital Brasil, 1500 Butantã, 05503-900 São Paulo, SP, Brazil*
[2] *Department of Biology, Naples University Federico II, Via Mezzocannone 16, 80134 Naples, Italy*
[3] *Institute of Infection, Immunity and Inflammation, College of Medical, Veterinary and Life Sciences, MRC-University of Glasgow Centre for Virus Research, Bearsden Road, Glasgow G61 1QH, UK*

Correspondence should be addressed to Rita de Cassia Stocco; ritastocco@butantan.gov.br

Received 13 November 2013; Accepted 13 November 2013; Published 16 January 2014

The relevance of cancer to human health is extremely high and the efforts to understand and control the processes related to the oncogenic modifications that take place in cells have increased, dramatically, in the past few decades [1–3]. The special issue presents a broad view of this subject.

Actually, oncogenic process was discussed by the authors that contributed to the Special Issue and have clearly demonstrated that this process involves the action of different agents on the cell [1, 4–7].

The major contribution achieved was the diversity of the approaches; the studies have brought together important aspects of cell transformation and also concerted efforts directed towards therapeutic procedures. The editors hope that this issue can help partially to the complex problems involved in these processes.

When we consider the etiology of tumor cells, papillomaviruses come immediately to mind: the relevance of HPVs (human papillomavirus) in female cervical cancer has obtained the priority in the virus-cancer relationship discussion [1, 2, 4, 8–10]. Its incidence turns it in a worldwide human health problem. In this volume, we have the opportunity to study persistence or clearance in HPV infection in order to allow the identification of risk groups, cofactors, and strategies for prevention of cervical cancer. At the same time, the issue presents results of research on less common HPV types that might be involved in cervical lesions and that some of these variants can be found in B-cell and T-cell epitopes [11–15].

Animal models have played a contributions to the understanding of oncogenic processes [5, 10, 16–26]. One of them deserves special attention: *Bovine papillomavirus*. This group of viruses is directly related to serious clinical consequences in bovine, namely papillomatosis, esophagus tract carcinoma, and urinary bladder carcinoma leading to animal death and in equids, sarcoid tumours that presents similar results [10, 18, 27]. These diseases lead to dramatic economic hazards. BPV animal model has been studied in several aspects, as illustrated in the different papers included in this issue, since many aspects of bovine papillomavirus infection and pathogenesis remain still to be clarified [28]. The oncogenesis process is mainly associated with different viral oncoprotein expressions, which are involved in cell transformation [7, 12, 19, 29]. The accuracy of diagnostic processes and the distribution of the different viral types [14, 26, 30–32] indicate which types and variants deserve the special attention [8, 9, 25, 33, 34]. The expression and characterization of recombinant viral oncoproteins are required to obtain biotechnological products as antibodies and potential vaccines [9, 15, 35–37]. Further studies show association of oncoproteins and cell compounds, as PDGFβ receptor and their actions in transformation of epithelial cell to mesenchymal cell as well as epithelial carcinogenesis of the urinary bladder [17, 33, 38]. The oncoproteins also act on host cell chromatin, in epithelial and blood cells [18, 23, 27, 39]. The virus DNA sequences have been described in semen, urine, and other non conventional host cells [10, 17, 20, 21, 23, 29, 33]. However, the initial event of the malign process remains not determined.

Chromosome aberrations can be detected in very diverse neoplastic process; bovine leukemia virus (BLV) was investigated and reported presenting chromosome breakage in

lymphocytes [16] and in the central nervous system (CNS) of cattle with neurological syndrome. While in papillomavirus, the chromosome aberrations occur at random, in tumor cells, virus sequences can be integrated in specific sites or the malign process can be related to products as in leukemia, fusion protein RUNX1/ETO that is generated by the chromosomal translocation t(8; 21) [40–43].

The oncogenic process can have another trigger, not specifically chromatin lesions. Gap junctions are communicating junctions which are important for tissue homeostasis, and their disruption is involved in carcinogenic process; connexin 43 deficiency is a clear example [44–46]. Cell surface proteins are related as targets for the beginning of the cancer development and consequently for cancer therapy or diagnosis [47–50]. These aspects have been well discussed in oncogenic processes; the expression of different genes in breast tumors, alternative TrkAIII splice variant expressed by advanced stage human neuroblastomas (NBs).

In a final evaluation, the papers pointed very clearly the complexity of the events leading to cancer. This complexity, obviously, reaches the diagnosis and therapy possibilities. In the ongoing studies, molecules are being analyzed to create ways to interfere with the tumor cell. In the special issue, viral oncoproteins were also considered through bioinformatics approach. The volume includes a detailed review of a purified peptide from South American rattle snake, a venom chemical crotamine [51–53] that is being discussed as a vector to reach the malign cell.

Our major aim in organizing this volume was to emphasize that the first step in oncogenic process is until now under discussion and therefore is the key for prophylaxis, diagnosis, and therapy. An attractive possibility is that the key remains in any alteration in the natural history of a cell; any cell, as any organism, has beginning, development, ageing, and death. When this route is modified, due to a large range of events, this cell can follow a different way and compete with its similar tissue cells, and, when this occurs in advantage, tumor cells win and the cancer happens.

The special issue (*oncogenic processes*) is celebrating the 80th birthday of Prof Dr. Willy Beçak, former Director of Instituto Butantan and remarkable researcher in cancer etiology studies and in the developing of vaccines.

We hope that this special issue (*oncogenic processes*) can contribute to this scientific area, bringing to readers accurate data and important discussions about this subject; but, mainly, we hope that this special issue will initiate new discussions relating to the elucidation of mechanisms and oncogenic process.

Rita de Cassia Stocco
Franco Peppino Roperto
Lubna Nasir
Marcelo Palma Sircili

References

[1] H. Zur Hausen, "Papillomaviruses and cancer: from basic studies to clinical application," *Nature Reviews Cancer*, vol. 2, no. 5, pp. 342–350, 2002.

[2] M. S. Campo, "Papillomavirus and disease in humans and animals," *Veterinary and Comparative Oncology*, vol. 1, pp. 3–14, 2003.

[3] J. N. Eble, G. Sauter, J. I. Epstein, and I. A. Sesterhenn, *Pathology and Genetics of Tumours of the Urinary System and Male Genital Organs*, IARC WHO Classification of Tumours, IARC Press, Lyon, France, 2004.

[4] X. Castellsagué and N. Muñoz, "Chapter 3: cofactors in human papillomavirus carcinogenesis—role of parity, oral contraceptives, and tobacco smoking," *Journal of the National Cancer Institute. Monographs*, no. 31, pp. 20–28, 2003.

[5] M. S. Campo, B. W. O'Neil, R. J. Barron, and W. F. H. Jarrett, "Experimental reproduction of the papilloma-carcinoma complex of the alimentary canal in cattle," *Carcinogenesis*, vol. 15, no. 8, pp. 1597–1601, 1994.

[6] M. S. Campo, W. F. H. Jarrett, R. Barron, B. W. O'Neil, and K. T. Smith, "Association of bovine papillomavirus type 2 and bracken fern with bladder cancer in cattle," *Cancer Research*, vol. 52, no. 24, pp. 6898–6904, 1992.

[7] G. Borzacchiello, G. Lovane, M. L. Marcante et al., "Presence of bovine papillomavirus type 2 DNA and expression of the viral oncoprotein E5 in naturally occurring urinary bladder tumours in cows," *The Journal of General Virology*, vol. 84, no. 11, pp. 2921–2926, 2003.

[8] P. M. Miranda, B. C. Pitol, M. S. Moran et al., "Human papillomavirus infection in Brazilian women with normal cervical cytology," *Genetics and Molecular Research*, vol. 11, no. 2, pp. 1752–1761, 2012.

[9] H.-U. Bernard, S.-Y. Chan, M. M. Manos et al., "Identification and assessment of known and novel human papillomaviruses by polymerase chain reaction amplification, restriction fragment length polymorphisms, nucleotide sequence, and phylogenetic algorithms," *Journal of Infectious Diseases*, vol. 170, no. 5, pp. 1077–1085, 1994.

[10] L. Nasir and M. S. Campo, "Bovine papillomaviruses: their role in the aetiology of cutaneous tumours of bovids and equids," *Veterinary Dermatology*, vol. 19, no. 5, pp. 243–254, 2008.

[11] D. G. DeNardo, M. Johansson, and L. M. Coussens, "Immune cells as mediators of solid tumor metastasis," *Cancer and Metastasis Reviews*, vol. 27, no. 1, pp. 11–18, 2008.

[12] B. Marchetti, G. H. Ashrafi, E. Tsirimonaki, P. M. O'Brien, and M. S. Campo, "The bovine papillomavirus oncoprotein E5 retains MHC class I molecules in the Golgi apparatus and prevents their transport to the cell surface," *Oncogene*, vol. 21, no. 51, pp. 7808–7816, 2002.

[13] H. Zur Hausen, "Papillomavirus infections—a major cause of human cancers," *Biochimica et Biophysica Acta*, vol. 1288, no. 2, pp. F55–F78, 1996.

[14] G. Cornut, S. Gagnon, C. Hankins et al., "Polymorphism of the capsid L1 gene of human papillomavirus types 31, 33, and 35," *Journal of Medical Virology*, vol. 82, no. 7, pp. 1168–1178, 2010.

[15] T. A. Hall, "BioEdit: a user-friendly biological sequence alignment editor and analysis program for Windows 95/98/NT," *Nucleic Acids Symposium Series*, vol. 1, pp. 95–98, 1999.

[16] N. H. Castro, J. Walter, R. C. dos Santos et al., "Cytogenetic study of cattle affected by persistent lymphocytosis," *Zentralblatt für Veterinarmedizin A*, vol. 35, no. 5, pp. 380–384, 1988.

[17] S. Roperto, G. Borzacchiello, R. Brun et al., "A review of bovine urothelial tumours and tumour-like lesions of the urinary bladder," *Journal of Comparative Pathology*, vol. 142, no. 2-3, pp. 95–108, 2010.

[18] R. C. Stocco dos Santos, C. J. Lindsey, O. P. Ferraz et al., "Bovine papillomavirus transmission and chromosomal aberrations: an experimental model," *The Journal of General Virology*, vol. 79, no. 9, pp. 2127–2135, 1998.

[19] G. Borzacchiello, V. Russo, C. Spoleto et al., "Bovine papillomavirus type-2 DNA and expression of E5 and E7 oncoproteins in vascular tumours of the urinary bladder in cattle," *Cancer Letters*, vol. 250, no. 1, pp. 82–91, 2007.

[20] C. de Carvalho, A. C. de Freitas, O. Brunner et al., "Bovine papillomavirus type 2 in reproductive tract and gametes of slaughtered bovine females," *Brazilian Journal of Microbiology*, vol. 34, no. 1, pp. 82–84, 2003.

[21] C. J. Lindsey, M. E. Almeida, C. F. Vicari et al., "Bovine papillomavirus DNA in milk, blood, urine, semen, and spermatozoa of bovine papillomavirus-infected animals," *Genetics and Molecular Research*, vol. 8, no. 1, pp. 310–318, 2009.

[22] S. R. C. Campos, C. Trindade, O. P. Ferraz et al., "Can established cultured papilloma cells harbor bovine papillomavirus?" *Genetics and Molecular Research*, vol. 7, no. 4, pp. 1119–1126, 2008.

[23] A. Yaguiu, M. L. Z. Dagli, E. H. Birgel Jr. et al., "Simultaneous presence of bovine papillomavirus and bovine leukemia virus in different bovine tissues: in situ hybridization and cytogenetic analysis," *Genetics and Molecular Research*, vol. 7, no. 2, pp. 487–497, 2008.

[24] V. Turusov and U. Mohr, *Pathology of Tumours in Laboratory Animals: Tumors of the Mouse*, IARC Scientific Publication (WHO), Lyon, France, 2nd edition, 1994.

[25] S. Roperto, R. Brun, F. Paolini et al., "Detection of bovine papillomavirus type 2 in the peripheral blood of cattle with urinary bladder tumours: possible biological role," *The Journal of General Virology*, vol. 89, no. 12, pp. 3027–3033, 2008.

[26] N. Diniz, T. C. Melo, J. F. Santos et al., "Simultaneous presence of bovine papillomavirus in blood and in short-term lymphocyte cultures from dairy cattle in Pernambuco, Brazil," *Genetics and Molecular Research*, vol. 8, no. 4, pp. 1474–1480, 2009.

[27] J. You, "Papillomavirus interaction with cellular chromatin," *Biochimica et Biophysica Acta*, vol. 1799, no. 3-4, pp. 192–199, 2010.

[28] T. Haga, J. Dong, W. Zhu, and R. D. Burk, "The many unknown aspects of bovine papillomavirus diversity, infection and pathogenesis," *Veterinary Journal*, vol. 197, pp. 122–123, 2013.

[29] S. Roperto, S. Comazzi, E. Ciusani et al., "PBMCS are additional sites of productive infection of bovine papillomavirus type 2," *The Journal of General Virology*, vol. 92, no. 8, pp. 1787–1794, 2011.

[30] D. Geraets, L. Alemany, N. Guimera et al., "Detection of rare and possibly carcinogenic human papillomavirus genotypes as single infections in invasive cervical cancer," *The Journal of Pathology*, 2012.

[31] T. Ogawa, Y. Tomita, M. Okada, and H. Shirasawa, "Complete genome and phylogenetic position of bovine papillomavirus type 7," *The Journal of General Virology*, vol. 88, no. 7, pp. 1934–1938, 2007.

[32] T. Vincze, J. Posfai, and R. J. Roberts, "NEBcutter: a program to cleave DNA with restriction enzymes," *Nucleic Acids Research*, vol. 31, no. 13, pp. 3688–3691, 2003.

[33] S. Roperto, V. Russo, A. Ozkul et al., "Bovine papillomavirus type 2 infects the urinary bladder of water buffalo (Bubalus bubalis) and plays a crucial role in bubaline urothelial carcinogenesis," *The Journal of General Virology*, vol. 94, pp. 403–408, 2013.

[34] H.-U. Bernard, R. D. Burk, Z. Chen, K. van Doorslaer, H. Z. Hausen, and E.-M. de Villiers, "Classification of papillomaviruses (PVs) based on 189 PV types and proposal of taxonomic amendments," *Virology*, vol. 401, no. 1, pp. 70–79, 2010.

[35] Y. Modis, B. L. Trus, and S. C. Harrison, "Atomic model of the papillomavirus capsid," *The EMBO Journal*, vol. 21, no. 18, pp. 4754–4762, 2002.

[36] Y. Liu and J. D. Baleja, "Structure and function of the papillomavirus E6 protein and its interacting proteins," *Frontiers in Bioscience*, vol. 13, no. 1, pp. 121–134, 2008.

[37] Y. Modis, B. L. Trus, and S. C. Harrison, "Atomic model of the papillomavirus capsid," *The EMBO Journal*, vol. 21, no. 18, pp. 4754–4762, 2002.

[38] F. Tavora, O. N. Kryvenko, and J. I. Epstein, "Mesenchymal tumours of the bladder and prostate: an update," *Pathology*, vol. 45, pp. 104–115, 2013.

[39] T. C. Melo, N. Diniz, S. R. C. Campos et al., "Cytogenetic studies in peripheral blood of bovines afflicted by papillomatosis," *Veterinary and Comparative Oncology*, vol. 9, no. 4, pp. 269–274, 2011.

[40] K. Döhner and H. Döhner, "Molecular characterization of acute myeloid leukemia," *Haematologica*, vol. 93, no. 7, pp. 976–982, 2008.

[41] F. Rosenbauer and D. G. Tenen, "Transcription factors in myeloid development: balancing differentiation with transformation," *Nature Reviews Immunology*, vol. 7, no. 2, pp. 105–117, 2007.

[42] A. T. Look, "Oncogenic transcription factors in the human acute leukemias," *Science*, vol. 278, no. 5340, pp. 1059–1064, 1997.

[43] J. R. McWhirter, D. L. Galasso, and J. Y. J. Wang, "A coiled-coil oligomerization domain of Bcr is essential for the transforming function of Bcr-Abl oncoproteins," *Molecular and Cellular Biology*, vol. 13, no. 12, pp. 7587–7595, 1993.

[44] M. Mesnil, "Connexins and cancer," *Biology of the Cell*, vol. 94, no. 7-8, pp. 493–500, 2002.

[45] M. L. Z. Dagli and F. J. Hernandez-Blazquez, "Roles of gap junctions and connexins in non-neoplastic pathological processes in which cell proliferation is involved," *The Journal of Membrane Biology*, vol. 218, no. 1–3, pp. 79–91, 2007.

[46] B. Cogliati, T. C. da silva, T. P. A. Aloia et al., "Morphological and molecular pathology of CCL4-induced hepatic fibrosis in connexin43-deficient mice," *Microscopy Research and Technique*, vol. 74, no. 5, pp. 421–429, 2011.

[47] C. M. Perou, T. Sørile, M. B. Eisen et al., "Molecular portraits of human breast tumours," *Nature*, vol. 406, no. 6797, pp. 747–752, 2000.

[48] L. Harris, H. Fritsche, R. Mennel et al., "American Society of Clinical Oncology 2007 update of recommendations for the use of tumor markers in breast cancer," *Journal of Clinical Oncology*, vol. 25, no. 33, pp. 5287–5312, 2007.

[49] L. J. van't Veer, H. Dai, M. J. van de Vijver et al., "Gene expression profiling predicts clinical outcome of breast cancer," *Nature*, vol. 415, no. 6871, pp. 530–536, 2002.

[50] J. P. C. da Cunha, P. A. F. Galante, J. E. de Souza et al., "Bioinformatics construction of the human cell surfaceome," *Proceedings of the National Academy of Sciences of the United States of America*, vol. 106, no. 39, pp. 16752–16757, 2009.

[51] G. Nicastro, L. Franzoni, C. de Chiara, A. C. Mancin, J. R. Giglio, and A. Spisni, "Solution structure of crotamine, a Na^+ channel affecting toxin from Crotalus durissus terrificus venom," *European Journal of Biochemistry*, vol. 270, no. 9, pp. 1969–1979, 2003.

[52] C. Plank, B. Oberhauser, K. Mechtler, C. Koch, and E. Wagner, "The influence of endosome-disruptive peptides on gene transfer using synthetic virus-like gene transfer systems," *Journal of Biological Chemistry*, vol. 269, no. 17, pp. 12918–12924, 1994.

[53] M. Zorko and Ü. Langel, "Cell-penetrating peptides: mechanism and kinetics of cargo delivery," *Advanced Drug Delivery Reviews*, vol. 57, no. 4, pp. 529–545, 2005.

Hindawi Publishing Corporation
BioMed Research International
Volume 2014, Article ID 675985, 9 pages
http://dx.doi.org/10.1155/2014/675985

Review Article

State of the Art in the Studies on Crotamine, a Cell Penetrating Peptide from South American Rattlesnake

Irina Kerkis,[1] Mirian A. F. Hayashi,[2] Alvaro R. B. Prieto da Silva,[1] Alexandre Pereira,[1] Paulo Luiz De Sá Júnior,[1] Andre J. Zaharenko,[1] Gandhi Rádis-Baptista,[3] Alexandre Kerkis,[1] and Tetsuo Yamane[4]

[1] *Laboratório de Genética, Instituto Butantan, Av. Vital Brasil, 1500 05503-900 São Paulo, SP, Brazil*
[2] *Departamento de Farmacologia, Universidade Federal de São Paulo (UNIFESP), São Paulo, SP, Brazil*
[3] *Labomar-Instituto de Ciências do Mar, Universidade Federal do Ceará, Fortaleza, CE, Brazil*
[4] *Universidade Estadual da Amazônia (UEA) e Laboratório de Bioquímica e Biologia Molecular, Centro de Biotecnologia da Amazônia (CBA), Manaus, AM, Brazil*

Correspondence should be addressed to Irina Kerkis; ikerkis@butantan.gov.br
and Alvaro R. B. Prieto da Silva; alvaroprieto@butantan.gov.br

Received 15 March 2013; Revised 5 August 2013; Accepted 8 August 2013; Published 15 January 2014

Academic Editor: Marcelo Palma Sircili

Animal venoms comprise a naturally selected cocktail of bioactive peptides/proteins and other molecules, each of which playing a defined role thanks to the highly specific interactions with diverse molecular targets found in the prey. Research focused on isolation, structural, and functional characterizations of novel natural biologics (bioactive peptides/proteins from natural sources) has a long way to go through from the basic science to clinical applications. Herein, we overview the structural and functional characteristics of the myoneurotoxin crotamine, firstly isolated from the South American rattlesnake venom. Crotamine is the first venom peptide classified as a natural cell penetrating and antimicrobial peptide (CPP and AMP) with a more pronounced antifungal activity. In contrast to other known natural CPPs and AMPs, crotamine demonstrates a wide spectrum of biological activities with potential biotechnological and therapeutic values. More recent studies have demonstrated the selective *in vitro* anticancer activity of crotamine. *In vivo*, using a murine melanoma model, it was shown that crotamine delays tumor implantation, inhibits tumor cells proliferation, and also increases the survival of mice engrafted with subcutaneous melanoma. The structural and functional properties and also the possible biotechnological applications of minimized molecules derived from crotamine are also discussed.

1. Introduction

Snake venoms contain a complex cocktail of toxins (proteins and enzymes), which are designed to assault the cardiovascular system (hemotoxic), to target specific tissues or muscle types (cytotoxic), and to go directly into the brain and nervous system (neurotoxic) of the prey. Crotamine, which is one of the major components of the venom of the South American rattlesnake *Crotalus durissus terrificus*, combines the cytotoxic and neurotoxic properties. Crotamine is a low molecular weight, nonenzymatic, and noncytolytic small protein, composed of about 42 amino acid residues. Among them, 11 are basic amino acid residues (nine lysines and two arginines), and six are cysteine residues that form three disulfide bridges [1]. These basic amino acids provide a highly positive charge for this peptide. Crotamine has two isoforms found in different subspecies, and they differ by the presence of an isoleucine residue in position 19 instead of leucine. The 3D solution structure of crotamine was determined by proton NMR spectroscopy [1], showing that crotamine structure encompasses a short N-terminal α-helix (involving the residues 1–7), two stranded anti-parallel β-sheets (residues 9–13 and 34–38), and two β-turns (residues 14–16 and 27–34). Consequently, it was suggested that the toxin is arranged in $\beta_1\alpha\beta_2\beta_3$ topology, where both the first and second strands run antiparallel to the third one, while the β-sheet twisted in a right-handed fashion. this β-sheet is stabilized by four hydrogen

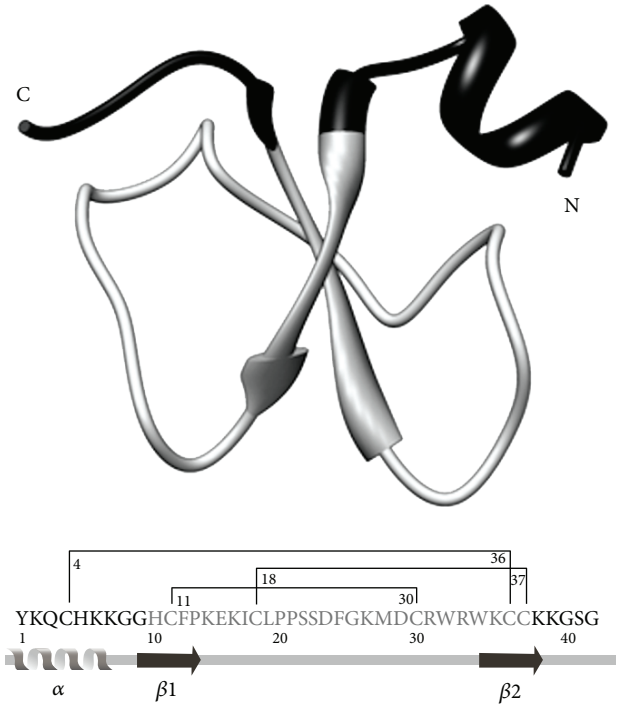

Figure 1: The crotamine derived peptide NrTP1 structure. NrTP1 synthetic peptide combines the N- and C-terminus of crotamine and embraces the first nine residues that are linked to the last residues 38–42, which are depicted in black in structure of the crotamine molecule above. NrTP1 and analogues are capable of membrane translocating and they localize in the nucleolus of tumor cells. Crotamine structure contains 42 residues arranged in a topology $\alpha\beta_1\beta_2$: one α-helix with residues 1–7 and two-stranded antiparallel β-sheets with residues 9–13 and 34–38. The structure is stabilized by three disulfide bridges C_4–C_{36}; C_{11}–C_{30}; C_{18}–C_{37} [1, 2]. This figure was adapted from [5].

bonds between the strands β_1 and β_3, (extending from the residues 10–37 and 12–35) and by other two hydrogen bonds between the strands β_2 and β_3 (residues 25–36). However, soon later, other authors described the presence of only two β-sheets [2], which is in accordance with others [3, 4]. Interchain disulfide bonds promote protein cross-linking (Cys^4–Cys^{36}, and Cys^{18}–Cys^{37}) between the strand β_3 with the α-helix and the first loop (Pro^{13}–Ser^{23}), respectively, while the Cys^{11}–Cys^{30} bond promotes the connection of β_1-sheet with the second loop (Gly^{26}–Trp^{34}) [1, 4] (Figure 1, Table 1).

1.1. Genomic Structure and Chromosomal Localization of the Gene for Crotamine. In the Crotalus genus, which belongs to the Viperidae family, the karyotype is composed of 36 chromosomes: eight macrochromosome and ten microchromosome pairs. The sex determining system in this genus is heteromorphic in females (ZZ/ZW), and the fourth pair of macrochromosomes is the sex pair [7]. Fluorescent in situ hybridization (FISH) revealed that crotamine gene is localized at the end of the long arm of chromosome 2. However, the consistent difference in the intensity of the FISH signals between homologous chromosomes was evidenced, suggesting a variable number of copies of the gene on each chromosome [8]. This in turn would be a possible explanation for the variable amounts of crotamine found in the venom of crotamine-positive *C. d. terrificus* [9–11].

1.2. Crotamine Cytotoxicity. Toxins, by definition, are effective and specific poisonous bullets produced by the living organisms. The biological activities of crotamine were tested by intraperitoneal (IP) injection into mice in sublethal doses corresponding to 2.5 mg of toxin/kg body mass, which provokes the hind limb paralysis and the necrosis of the muscle cells of mice [9]. *In vitro,* at final concentration 10 μg/mL, crotamine was demonstrated to be toxic for muscles cells, promoting muscle tissue necrosis [10, 11]. In contrast, crotamine, at final concentration ranging from 1 to 10 μg/mL, was not cytotoxic to other normal cells of different types (e.g., human and mouse fibroblasts, muscle cells, human endothelial cells (HUVEC), lymphoblast (immortalized lymphocytes), mouse 3T3 cells line, mouse embryonic stem (mES) cells and others), even after 72 h of exposure [12].

1.3. Cell Penetrating Activity of Crotamine. Cell penetrating peptides (CPPs) are a class of bioactive molecules, also known as protein transduction domains (PTDs), membrane translocating sequences (MTSs), and Trojan peptides [13]. They are short peptides (usually ≤40 amino acid residues), with the ability to gain the access into the inner side of almost any cell [13]. Crotamine similar to other CPPs showed a rapid translocation (within 5 min) into all cell types investigated up to now [12]. Distinctly from other CPPs, crotamine demonstrates a preferential and expressive accumulation in actively proliferating cells [12]. Some CPPs show nuclear localization, as well as crotamine. Interestingly, in the nucleus, it binds to chromosomes and centrioles during the cell division. In metaphase chromosomes, fluorescently labeled crotamine binding to the chromosome produces a specific banding pattern, which is different from that presented by known DNA intercalation dyes, such as those that allow observing the G-banding or Giemsa banding and others such as the fluorescent stain 4′,6-diamidino-2-phenylindole (DAPI), which are commonly used in cytogenetic to produce a visible karyotype by staining condensed chromosomes [12]. The double helix of DNA is highly and negatively charged due to all the negatively charged phosphates in the backbone. Our recent study reported that positively charged crotamine binds noncooperatively to negatively charged DNA, covering about 5 nucleotide residues when it connects to a single or double stranded molecules [14]. Our data suggest that specific banding pattern observed on chromosomes results from electrostatic interaction between DNA phosphates and crotamine. This intrinsic biophysical property also distinguishes crotamine from other CPPs [15]. *In vivo*, crotamine penetrates into mice tissues, such as liver, skeletal muscle, bone marrow, and kidney [16]. Crotamine also crosses the blood-brain barrier (BBB), as the fluorescently labeled crotamine [16] as well as the radiolabeled form [17] was found in the brain. Three steps for the transcytosis of crotamine through the BBB can be suggested: (1) binding and internalization through

Table 1: Crotamine main characteristics, properties, and potential biotechnological applications*.

Name	Crotamine
Organism	*Crotalus durissus terrificus* South American rattlesnake Common name: Cascavel
Taxon authority	[6]
Geographic range	Brazil, Peru, Bolivia, Paraguay, Uruguay, Argentina*
Classification	Myoneurotoxin, cell-penetrating peptide, antimicrobial peptide, and defensin-like peptide
Molecular weight	4726,63 daltons
Isoelectric point	pI 9.54, highly positive
Length	Polypeptide of 42 amino acids
Primary sequence	KQCHKKGGHCFPKEKICLPPSSDFGKMDCRWRWKCCKKGSG
Isoform	Crotamine-Ile 19 (isoleucine substitution at position 19)*
Chemical formula	$C_{346}H_{530}N_{90}O_{82}S_8$ (isoform 1)*
Solubility	Highly soluble in water and physiological solutions
Stability	Highly stable in solution, relative large pH range, and temperature
Folding	Crotamine is arranged in a $\alpha\beta_1\beta_2$ topology stabilized by 3 disulfide bridges: an α-helix with residues 1–7 and a two-stranded antiparallel β-sheets with residues 9–13 and 34–38.
Disulfide bonds	C_4–C_{36}; C_{11}–C_{30}; C_{18}–C_{37}
Physiological and neurological activity	Hind limb paralysis in mice in final concentration 2.5 mg of toxin/kg body mass Necrosis of muscle cells
Electrophysiology activity	Mammalian $K_v1.1$, $K_v1.2$, and $K_v1.3$ blocker with $IC_{(50)}$ of 286.53 ± 91.72 nM
In vitro toxicity (normal cells)	Nontoxic (concentration ranged from 0.1 to 10 μM)
Embryotoxicity	Nontoxic (concentration ranged from 0.1 to 10 μM)
Cell penetrating activity (*in vitro*)	Selective: dividing (actively proliferating cells) Concentration, cell type, and cell-cycle dependent
Intracellular localization	Cytosol, vesicles, nucleus, centrioles, and chromosomes
Mechanism of DNA-crotamine interaction	Only electrostatic: crotamine (+charged)—DNA (−charged) aggregate
Uptake	Within 5 minutes, and permanence in the cells for approximately 24 hours
Mechanism of penetration	Membrane heparan sulfate proteoglycans binding and clathrin-dependent endocytosis
Cell penetrating activity (*in vivo*)	Selective: dividing (actively proliferating cells), for example stem cells in bone marrow, spleen, liver, lung, and so force.
Localization in brain	Able to cross blood-brain barrier, and localization in brain cells
Molecular carrier	Intracellular delivery of DNA (both circular and linear molecules) *in vivo* and *in vitro.* Final complex size dependent delivery.
Antimicrobial activity	Modest against Gram-positive and Gram-negative bacteria, with some exceptions, for example *Micrococcus luteus*, and with no detectable activity against the filamentous fungus *Aspergillus fumigatus* and *Trichophyton rubrum* at concentrations up to 125 μg/mL.
Antimycotic (-fungal) activity	Significant activity against yeast *Candida* spp.
Cancer cells toxicity	Toxic (concentration ranged from 0.1 to 10 μM) Inoffensive for normal cells
Anticancer activity (*in vitro)*	Strong against melanoma cells *in vitro*
Anticancer activity (*in vivo*)	Inhibition and delay of melanoma growth *in vivo* in mouse model
Mechanism of tumor inhibition	Mitochondrial depolarization Intracellular calcium release
Immunogenicity	Low
Biotechnological and biomedical applications	Marker of centrioles and cell cycle; marker of actively proliferating normal cells; biomolecules carrier; tool for cancer cells investigation; marker of cancer cells *in vitro* and *in vivo*, and as antifungal and anticancer agent. Prototype for new drug design.

*Several old data about crotamine need to be revised using modern approaches.

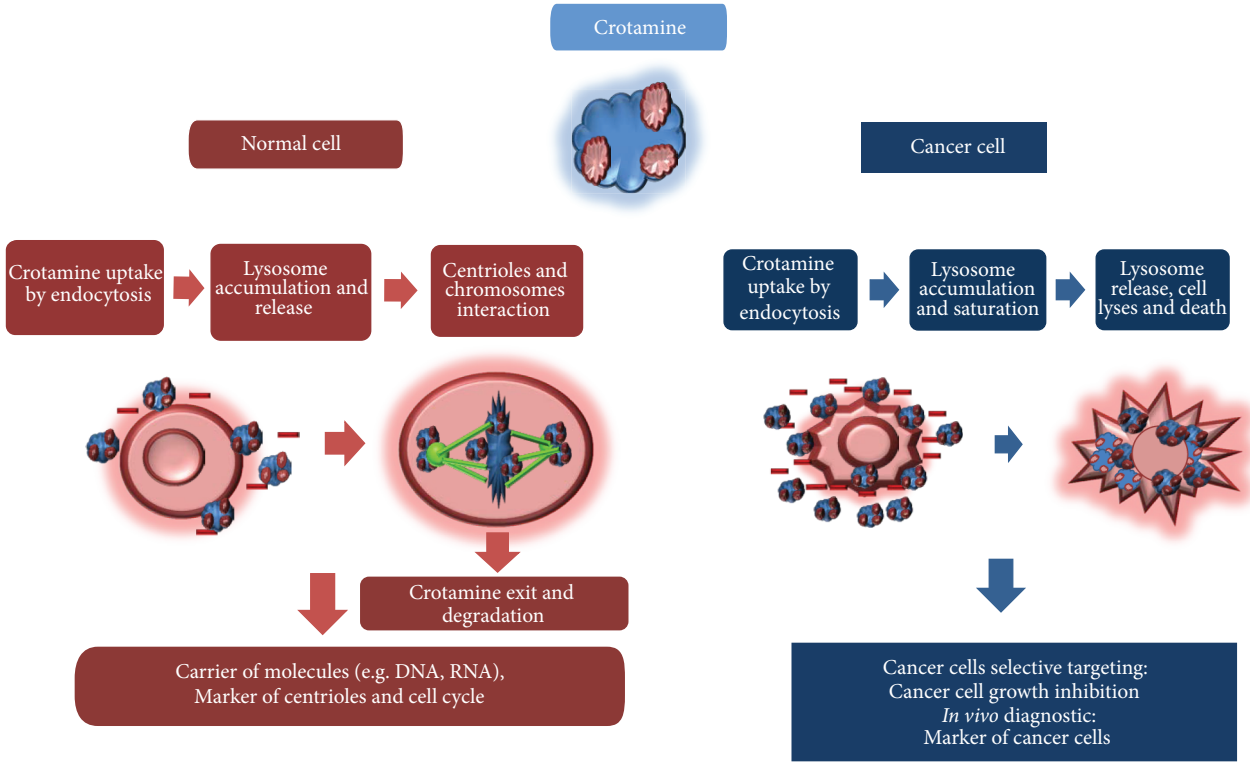

Figure 2: Crotamine action in normal (red) and cancer (blue) cells. Crotamine is a positively charged (blue) protein. In normal cells, crotamine uptake occurs through clatrin-dependent endocytosis followed by lysosome accumulation, followed by its release in the cytosol due to the disruption of the vesicles containing crotamine. In normal cells, crotamine interacts electrostatically with centrioles and chromosomes and can be used as a biotechnological tool, as carrier of bioactive molecules, and as a marker of cell cycle. Cancer cells, which have more negatively charged molecules on their surface compared to normal cells, potentially attract crotamine strongly. In cancer cells, crotamine intracellular concentration appears to be higher than that observed in normal cells, thus probably leading to cell lyses and cell death. In cancer cells, crotamine inhibits tumor growth and kills tumor cells, besides representing a potential tool for *in vivo* cancer cells identification.

endocytosis at the luminal side of endothelial cell membrane, which is negatively charged due to the presence of chondroitin and heparan sulfate molecules, (2) CPPs diffusion via the cytoplasm, and (3) externalization from endothelial cells [18, 19]. All these pathways are in accordance to the previously described mechanism of crotamine intracellular penetration [20].

1.4. Crotamine-Targeted Delivery of Plasmid DNA. The common feature among the CPPs is their capacity to deliver biologically active molecules into the cells both *in vitro* and *in vivo*. The majority of CPPs do not present any cell specificity for the translocation into the cells [21]. In contrast, crotamine displays specificity for actively proliferating cells, even when employed as gene delivery agent [16, 20]. This feature of crotamine could be advantageous to allow for an efficient and selective transfection of rapidly dividing cells, for example, normal stem cells, without strongly affecting the cell viability, and cancer stem cells in contrast to the currently widely used procedure, such as electroporation that causes the death of about 90% of the cells [22]. In addition, crotamine provides a successful *in vivo* transfection of bone marrow (BM) cells of mice after IP injection of crotamine-pEGFP-N1 plasmid DNA complex [16]. The proportion of BM cells displaying GFP fluorescence (about 10–20% of total) is in good agreement with the described ratio of proliferating cells present in the BM tissue. The GFP fluorescent signal was also detected in the liver and lung cells of mice [16]. In other words, the observed crotamine-mediated transfection *in vivo* [16] is similar to the previously described *in vitro* selectivity [12].

1.5. Mechanism of Crotamine Penetration and Cargo Delivery into Cells. Using pharmacological inhibitors and low-temperature conditions, we also demonstrated that crotamine internalization is dependent of endocytosis. Its penetration was decreased by 92.3% in the presence of chloroquine [23], which disrupts endosomal pathway by interfering with the acidification of the endosome, due to the inhibition of ion-transporting ATPase. Additionally, crotamine partially relied on the clathrin-dependent pathway for the cell uptake, since chlorpromazine (an inhibitor of clathrin mediated endocytosis) inhibited crotamine penetration by 65%. The inhibition of lipid rafts (dynamic microdomains of cholesterol, sphingolipids, and proteins clusters of the membrane) endocytosis, and also macropinocytosis did not interfere with crotamine internalization. On the other hand, low temperature (4°C) affected negatively the cell uptake of crotamine, since the efficiency of internalization could be drastically

reduced showing the retention of the crotamine on the cell surface [17].

2. Crotamine Derived Peptides

2.1. CyLoP-1. The nuclear translocation process resides on lysine- and arginine-rich nuclear localization signals (NLSs). Kerkis and coworkers [12] suggested that crotamine has two putative NLS motifs, $Crot_{2-18}$ (KQCHKKGGHCFPKEKIC) and $Crot_{27-39}$ (KMDCRWRWKCCKK), which could be responsible for crotamine nuclear localization. The synthesis of one of such NLS motifs as thetridecapeptide $Crot_{27-39}$ (KMDCRWRWKCCKK), which included 3 cysteine residues, and one tryptophan, aspartic acid, and methionine, along with 6 basic amino acid residues (arginine and lysine) has also been reported by Jörn Engelmann group from Germany that named this synthetic peptide as CyLoP-1 (Cytosol Localizing Peptide-1) [24]. The cell uptake of this peptide coupled to FITC presents in NIH-3T3 cell line mainly cytosol localization, instead of a nuclear distribution pattern. In order to determine the optimal length for the cell penetrating properties, single deletions of the residues from the N-terminus of CyLoP-1 have been done. Newly produced CyLoP-1 derived peptide 4 (CRWRWKCCKK) demonstrated about 20% higher cellular uptake efficiency compared to the CyLoP-1, and the best homogeneous distribution in the cell cytosol was found for this CyLoP-1 derived peptide 4. Interestingly, peptide 4 was found to be uniformly distributed in the cytoplasm along with an endosomal and vesicular fluorescence localization. The substitution of one to three cysteines by serine residue(s) led to the loss in the uptake efficiency of CyLoP-1 derived peptide 4. Based on the intracellular distribution pattern observed for this peptide, such as the perinuclear localization of the peptide, vesicles-filled fluorescent, or the cytosolic spread in different cell types, the authors concluded that, at least, CyLoP-1 derived peptide 4 uptake and its cytosolic distribution is dependent on the cell type. The carrier ability of CyLoP-1 was compared to other well-characterized CPPs, namely, Tat, penetratin, and octaarginines. D-Tat_{49-57} (RKKRRQRRR) and D-octaarginine (RRRRRRRR) and penetratin (RQIKIWFQNRRMKWKK) are also highly cationic. In addition, penetratin and CyLoP-1 derived peptide 4 (CRWRWKCCKK) are rich in hydrophobic residues. Long-term incubation of these CPPs [2.5 μM] showed a lower cellular internalization in comparison to the CyLoP-1 derived peptide 4 [24]. Albeit, the same CPPs composed of D-amino acid residues showed an increased cell uptake. Indeed, the CyLoP-1 derived peptide 4, composed of L-amino acid residues was found to be the most efficient CPP for a long-term labeling [24]. Moreover, similarly to crotamine, the uptake of CyLoP-1 derived peptide 4 is strongly dependent on the cell type. Successful delivery of cargoes by CyLoP-1 also depends on their sizes. The differences in sizes and charge hydrophobicity or function of cargos in the delivery of resulting conjugates formed with CyLoP-1 derived peptide 4 were evaluated in NIH-3T3 cell line, after 18 h incubation, using the concentration of 2.5 μM. As expected, the increase in molecular size resulted in an overall decrease in the intracellular uptake [24].

2.2. Nucleolar-Targeting Peptides (NrTPs). It has been reported that the native crotamine also targets nucleolus, which is a nuclear structure composed by RNA, DNA, and proteins, that has different functions, such as ribosomal subunit assembly, mRNA biogenesis, and nucleolus organizer region, in immortalized and cancer cell lines, such as CHO (Chinese hamster ovary) and murine melanoma B16-F10 [16]. Rádis-Baptista and coworkers [5] designed and synthesized the nucleolar-targeting peptides (NrTPs) based on two structural simplified sequences of crotamine: Peptide 1 (YKQCHKKGGKKGSG) and Peptide 2 (YKQCHKKGGXKKGSG), both containing only one single cysteine residue (Figure 1). In HeLa cells, they were found at the nucleus and in nucleolus. Similarly to the native crotamine, these peptides bind to DNA and chromosomes at different stages of the cell cycle [15].

3. Crotamine Antimicrobial and Antifungal Activity

The antimicrobial peptides (AMPs) are small cationic peptides, responsible for the adaptive immunity in the external surface of skin and mucus of several organisms across the evolutionary spectrum [25]. The AMPs are a unique class composed of varying molecules grouped into subgroups based on their amino acid composition and structure. AMPs are classified into three major groups: (i) peptides with an α-helical conformation (insect cecropins, magainins, etc.), (ii) cyclic and open-ended cyclic peptides with pairs of cysteine residues (defensins, protegrin, etc.), and (iii) peptides with an overrepresentation of some amino acids (proline-rich, histidine-rich, etc.) [26]. AMPs present a rapid killing and broad-spectrum antimicrobial activities [27]. AMPs are usually composed of 12 to 50 amino acid residues, and they show at least two or more positively charged residues, generally represented by arginine, lysine, or histidine, in acid environments, and with a high content of hydrophobic residues (usually >50%) [28]. Moreover, most AMPs display hydrophobic and cationic properties, have a molecular mass below 25–30 kDa, and adopt an amphipathic structure (alpha-helix, beta-hairpin-like beta-sheet, beta-sheet, or alpha-helix/beta-sheet mixed structures) [29]. The ability to associate with the cell membrane is a key feature of the AMPs, although the membrane permeabilization is not an essential requirement for their activity [30]. Different peptides act in different ways and the exact mechanisms are only beginning to be elucidated. Some intracellular targets have also been described [31]. In fact, speculations that transmembrane pore formation is not the only mechanism of microbial killing suggest that translocated peptides can alter cytoplasmic membrane septum formation, inhibit cell-wall synthesis, inhibit nucleic acid synthesis, inhibit protein synthesis, or inhibit enzymatic activity [30]. It seems that crotamine is also a potential candidate to be included in this class of compounds with antimicrobial activities [32]. More interestingly, it is likely that crotamine and the well-known AMP defensin could have been derived from a common ancestor gene [33]. This was suggested by Nicastro and coworkers [1], who first described the similarities of

the disulfide bonds pattern of these molecules. However, significant differences in the primary structure/amino acid composition are observed for these molecules [34]. Despite the well-known broad antimicrobial spectrum of defensins [35], crotamine shows a modest activity towards both Gram-negative and Gram-positive bacteria [36].

Yount and collaborators [33] also suggested the potential antibacterial and antifungal activity of crotamine. A more careful determination of minimal inhibitory concentration (MIC) of crotamine towards a broad range of microorganisms was only recently determined by Mirian Hayashi's group [36]. Crotamine's important activity against several fungi of *Candida* spp., in particular *C. albicans*, including against clinical resistant strains, was observed [36]. It is of note that this Candida species are among the most common bloodstream pathogens in the United States and rank seventh among etiologic agents in Europe [37], and the pronounced effective antifungal activity observed by our group for crotamine opens new perspectives for the use of this venom component in biomedicine, more specifically for infectious disease treatments [36]. Moreover, some AMPs are also found to possess translocating activity across the cell membrane, which can interfere with critical cellular functions leading to cell death [38]. Similar apoptotic activity in combination with cell penetration was described for crotamine by our group for several cell types [39]. Moreover, the AMPs are thought to have other polyanions, such as DNA or RNA, as their ultimate target [40].

4. Crotamine Anticancer Cells Activity

Actually, it is well accepted that the majority of antimicrobial compounds might also have antitumor activity [41]. It could be simply due to the 3D structural similarities or even due to an evolutionary relationship, which still remains to be determined [42]. The cationic feature might also be determinant of both activities [43]. The electrostatic interactions between the negatively charged components of the membrane of cancer cells and the positively charged peptide are believed to play a major role in the strong binding of the peptide and its ability to selectively disrupt the membrane of cancer cells [44].

Investigation of crotamine anticancer cells toxicity and their *in vitro* and *in vivo* efficacy in mouse model of melanoma was examined by Kerkis's group [45, 46]. This toxin at concentrations of 1–5 μg/mL was used to test the viability of B16-F10 (murine melanoma), SK-Mel-28 (human melanoma cells), and Mia PaCa-2 (human pancreatic carcinoma cell line). The nonmalignant neoplastic murine fibroblasts 3T3 cell line was used as control. Interestingly, that crotamine at final concentration of 5 μg/mL was lethal to B16-F10, Mia PaCa-2, and SK-Mel-28 cells, while it was inoffensive to normal cells [45]. Additionally, we showed that differently from several anticancer drugs, crotamine targets primary lysosomes and mitochondria, leading to increases of intracellular free calcium concentrations in cancer cells [16]. Once the balance of cellular uptake and efflux determines drug accumulation, we also measured the crotamine permanence in cancer cells. Using Cy3-crotamine, which was added to B16-F10 cells, it was possible to observe that at least 70% of the cells hold the fluorescence signal during approximately 20 h, suggesting a long-term retention of crotamine in these cells [45]. *In vivo*, in mouse model for melanoma, crotamine demonstrates selective penetration into tumor melanoma cells, predominantly observed within the cells in tumor masses, in the cells around the tumor necrotic areas, and in rapidly dividing metastatic cells, but not in normal cells surrounding the tumors [39, 45].

Fluorescent crotamine traces metastatic invasion of B16-F10 cells, suggesting its possible applications as an imaging agent and metastasis marker in living organisms [39].

Delay of melanoma tumors implantation was also observed after 21 days of chronic treatment with crotamine (1 μg per animal, per day), in a mice model that received B16-F10 cells (10^5 cells) by subcutaneous injection. This treatment, started at the first day after melanoma cells injection, allowed to observe that crotamine significantly inhibits the tumor growth, as evaluated by measuring the tumor mass weight, and also prolongs the lifespan of these mice bearing B16-F10 tumor [45]. Histological examination also confirmed that crotamine is nontoxic to normal cells and normal tissues, such as kidney and liver, at the used concentrations, as well as that crotamine does not demonstrate any immunotoxic effect after *in vivo* long-term treatment of mice bearing melanoma tumors [39, 45]. The low immunogenicity of some snake venom toxins is a well-known feature, which in the case of crotamine could be attributed to its small size [46].

More recently, using noninvasive optical imaging procedure that permits *in vivo* real-time monitoring of fluorescent molecules uptake, crotamine localization into remote subcutaneous tumors engrafted in nude mice was confirmed [39]. Additionally, this study also demonstrated that the inhibition of tumor growth involves mitochondrial depolarization and intracellular calcium release. These data indicated that the cytotoxic peptide crotamine could potentially be used for a dual purpose: to target and detect growing tumor tissues and also to selectively trigger tumor cell death [39].

Interestingly, infections caused by *Candida* spp. are frequent and serious in oncology patients [47]. Definitely, a more precise evaluation of the structure-function relationship for both antimicrobial and antitumor activity of crotamine might allow for the discovery and proposal of potential novel mechanisms or of new structural models for the treatment of cancer and/or for the development of a more selective antimicrobial compounds that might not act on mammals host cells. Comparative studies to further understand the determinants of antimicrobial and antitumor activities of crotamine are considered by our group to be highly significant.

4.1. Crotamine-Like Peptides. Crotamine shares similar structure features with the defensins, which are a family of small cysteine-rich cationic proteins found in both vertebrates and invertebrates. Similarly to crotamine, defensins (from vertebrates) present a compact structure and consist of 18–45 amino acid residues, including the presence of six to eight conserved cysteine residues [48]. Biologically active

crotamine-like peptides (CLPs) were also described in the venom of some sauropsid reptiles (lizards and snakes), scorpions (*Scorpio maurus palmatus*), and in small mammals such as Platypus (*Ornithorhynchus anatinus*), a semiaquatic mammal from Eastern Australia [49]. The mechanism of action of CLPs is very wide, including targets as the voltage-gated Na^+ (Na_vs) [50], K^+ (K_vs) [51], and acid-sensing ion channels (ASICs) [52]. Crotamine was also supposed to present similar effect. In fact, Peigneur et al. [53] reported that crotamine potently and selectively blocks mammalian voltage-gated $K_v1.3$, although it was also demonstrated that crotamine does not act on $Na_{(\upsilon)}$ channels [54]. This was the first study, which shows a neurotoxin from the snakes of Crotalus genus targeting an ion channel.

5. Conclusions

Indeed, learning more about the way cancer cells is different from normal cells will allow us to identify and target specific proteins in cancer cells. Any new treatment proposal aims to be more efficient and with fewer side effects. Since cancer cells hardly differ physiologically from healthy cells, anticancer drugs do not specifically affect only cancer cells, but mistakenly also affect all other normal dividing cells. Compared to other known anticancer targeted drugs, only crotamine was shown to have the ability to selectively target actively proliferating living cells, both *in vitro* and *in vivo*, without visible effect on normal dividing cells.

Similarly to AMPs, crotamine is highly soluble in water and is capable of interacting strongly with biological membranes. This might be due to its N-terminal polyarginine domain, which may allow its interaction with negatively charged phosphate moieties in the cell membranes, which is suggestive of a cell-penetrating domain [55]. Crotamine is also selectively attracted to negatively charged microbial membranes [36]. Additionally, it presents significant antifungal and antitumor activity [36]. Inside the several cell types, crotamine interacts with secondary targets, thus being able to interrupt vital metabolic processes [16]. Moreover, the recent findings by Peigneur et al. [53] demonstrated that crotamine selectively blocks mammalian $K_v1.3$, heterologously expressed in *Xenopus laevis* oocytes. It also sheds more light on the possible role of voltage-gated potassium channels blockage in its anticancer effect, but more studies are still required to clarify it.

In Table 1, we summarized the possible biotechnological applications of crotamine and their derivatives. We demonstrate that crotamine acts differently in normal actively proliferating (dividing) and cancer cells (Figure 2). This study provides new insights, which may contribute to unveil the differences among the normal and cancerous cells using as a tool the crotamine, which is a versatile and multifunctional peptide, as described here. On the other hand, crotamine and their derivates represent already a potential biotechnological tool. Further studies need to become crotamine derivates marketable. Although, they are potentially ready to be used both *in vitro* and *in vivo* as molecular carrier, marker of cell cycle and of centrioles, and as biomarker of cancer cells.

Conflict of Interests

The authors declare that there is no conflict of interests regarding the publication of this paper.

Acknowledgments

The authors thank the snake for providing the native crotamine for our studies, which is so exciting, interesting, and valuable. Our studies were supported by the following Brazilian foundations: the National Council for Scientific and Technological Development (CNPq), San Paulo Research Foundation (FAPESP), and the Coordination for the Improvement of Higher Level or Education-Personnel (CAPES). This work is dedicated to Dr. Willy Beçak Emeritus Professor of genetics and the founder of the Laboratory of Genetics, at Butantan Institute, São Paulo, Brazil. Professor W. Beçak is an open mind and outstanding scientist who inspired several generation in Brazil with his own exemplar to follow studies in biology always with high ethical and human pattern.

References

[1] G. Nicastro, L. Franzoni, C. De Chiara, A. C. Mancin, J. R. Giglio, and A. Spisni, "Solution structure of crotamine, a Na+ channel affecting toxin from *Crotalus durissus terrificus* venom," *European Journal of Biochemistry*, vol. 270, no. 9, pp. 1969–1979, 2003.

[2] V. Fadel, P. Bettendorff, T. Herrmann et al., "Automated NMR structure determination and disulfide bond identification of the myotoxin crotamine from *Crotalus durissus terrificus*," *Toxicon*, vol. 46, no. 7, pp. 759–767, 2005.

[3] A. M. Siqueira, N. F. Martins, M. E. De Lima et al., "A proposed 3D structure for crotamine based on homology building, molecular simulations and circular dichroism," *Journal of Molecular Graphics and Modelling*, vol. 20, no. 5, pp. 389–398, 2002.

[4] M. A. Coronado, A. Gabdulkhakov, D. Georgieva et al., "Structure of the polypeptide crotamine from the Brazilian rattlesnake Crotalus durissus terrificus," *Acta Crystallographica D*, vol. 69, pp. 1958–1964, 2013.

[5] G. Rádis-Baptista, B. G. de la Torre, and D. Andreu, "Insights into the uptake mechanism of NrTP, a cell-penetrating peptide preferentially targeting the nucleolus of tumour cells," *Chemical Biology and Drug Design*, vol. 79, no. 6, pp. 907–915, 2012.

[6] Crotalus durissus terrificus (Laurenti, 1768) Taxonomy ID: 8732.

[7] W. Beçak, M. L. Beçak, H. R. S. Nazareth, and S. Ohno, "Close karyological kinship between the reptilian suborder serpentes and the class aves," *Chromosoma*, vol. 15, no. 5, pp. 606–617, 1964.

[8] G. Rádis-Baptista, T. Kubo, N. Oguiura et al., "Structure and chromosomal localization of the gene for crotamine, a toxin from the South American rattlesnake, *Crotalus durissus terrificus*," *Toxicon*, vol. 42, no. 7, pp. 747–752, 2003.

[9] J. M. Gonçalves and E. G. Arantes, "Estudos sobre venenos de serpentes Brasileiras. III-determinação quantitativa de crotamina no veneno de cascavel Brasileira," *Anais da Academia Brasileira de Ciências*, vol. 28, pp. 369–371, 1956.

[10] N. Oguiura, M. E. Camargo, A. R. P. Da Silva, and D. S. P. Q. Horton, "Quantification of crotamine, a small basic myotoxin,

in South American rattlesnake (*Crotalus durissus terrificus*) venom by enzyme-linked immunosorbent assay with parallel-lines analysis," *Toxicon*, vol. 38, no. 3, pp. 443–448, 2000.

[11] D. L. Cameron and A. T. Tu, "Chemical and functional homology of myotoxin a from prairie rattlesnake venom and crotamine from South American rattlesnake venom," *Biochimica et Biophysica Acta*, vol. 532, no. 1, pp. 147–154, 1978.

[12] A. Kerkis, I. Kerkis, G. Rádis-Baptista et al., "Crotamine is a novel cell-penetrating protein from the venom of rattlesnake *Crotalus durissus terrificus*," *FASEB Journal*, vol. 18, no. 12, pp. 1407–1409, 2004.

[13] I. Kerkis, M. A. F. Hayashi, N. F. Lizier et al., "Pluripotent stem cells as an *in vitro* model of neuronal differentiation," in *Embryonic Stem Cells-Differentiation and Pluripotent Alternatives*, Kallos, Ed., pp. 81–98, InTech, Rijeka, Croatia, 2011.

[14] P. C. Chen, M. A. Hayashi, E. B. Oliveira et al., "DNA-interactive properties of crotamine, a cell-penetrating polypeptide and a potential drug carrier," *PLoS ONE*, vol. 7, no. 11, Article ID e48913, pp. 1–11, 2012.

[15] G. Rádis-Baptista and I. Kerkis, "Crotamine, a small basic polypeptide myotoxin from rattlesnake venom with cell-penetrating properties," *Current Pharmaceutical Design*, vol. 17, no. 38, pp. 4351–4361, 2011.

[16] M. A. Hayashi, F. D. Nascimento, A. Kerkis et al., "Cytotoxic effects of crotamine are mediated through lysosomal membrane permeabilization," *Toxicon*, vol. 52, no. 3, pp. 508–517, 2008.

[17] M. Boni-Mitake, H. Costa, V. S. Vassilieff, and J. R. Rogero, "Distribution of 125I-labeled crotamine in mice tissues," *Toxicon*, vol. 48, no. 5, pp. 550–555, 2006.

[18] J. P. Blumling III and G. A. Silva, "Targeting the brain: advances in drug delivery," *Current Pharmaceutical Biotechnology*, vol. 13, no. 12, pp. 2417–2426, 2012.

[19] E. C. de Lange, "The physiological characteristics and transcytosis mechanisms of the blood-brain barrier (BBB)," *Current Pharmaceutical Biotechnology*, vol. 13, no. 12, pp. 2319–2327, 2012.

[20] F. D. Nascimento, M. A. F. Hayashi, A. Kerkis et al., "Crotamine mediates gene delivery into cells through the binding to heparan sulfate proteoglycans," *Journal of Biological Chemistry*, vol. 282, no. 29, pp. 21349–21360, 2007.

[21] D. Sarko, B. Beijer, R. G. Boy et al., "The pharmacokinetics of cell-penetrating peptides," *Molecular Pharmaceutics*, vol. 7, no. 6, pp. 2224–2231, 2010.

[22] J. Gehl, "Electroporation: theory and methods, perspectives for drug delivery, gene therapy and research," *Acta Physiologica Scandinavica*, vol. 177, no. 4, pp. 437–447, 2003.

[23] G. M. Poon and J. Gariépy, "Cell-surface proteoglycans as molecular portals for cationic peptide and polymer entry into cells," *Biochemical Society Transactions*, vol. 35, no. 4, pp. 788–793, 2007.

[24] D. Jha, R. Mishra, S. Gottschalk et al., "CyLoP-1: a novel cysteine-rich cell-penetrating peptide for cytosolic delivery of cargoes," *Bioconjugate Chemistry*, vol. 22, no. 3, pp. 319–328, 2011.

[25] F. Schweizer, "Cationic amphiphilic peptides with cancer-selective toxicity," *European Journal of Pharmacology*, vol. 625, no. 1–3, pp. 190–194, 2009.

[26] N. Boulanger, C. Lowenberger, P. Volf et al., "Characterization of a defensin from the sand fly Phlebotomus duboscqi induced by challenge with bacteria or the protozoan parasite Leishmania major," *Infection and Immunity*, vol. 72, no. 12, pp. 7140–7146, 2004.

[27] G. Maróti Gergely, A. Kereszt, É. Kondorosi, and P. Mergaert, "Natural roles of antimicrobial peptides in microbes, plants and animals," *Research in Microbiology*, vol. 162, no. 4, pp. 363–374, 2011.

[28] Y. Park, S. N. Park, S. Park et al., "Synergism of Leu-Lys rich antimicrobial peptides and chloramphenicol against bacterial cells," *Biochimica et Biophysica Acta*, vol. 1764, no. 1, pp. 24–32, 2006.

[29] P. Bulet, R. Stöcklin, and L. Menin, "Anti-microbial peptides: from invertebrates to vertebrates," *Immunological Reviews*, vol. 198, pp. 169–184, 2004.

[30] K. A. Brogden, "Antimicrobial peptides: pore formers or metabolic inhibitors in bacteria?" *Nature Reviews Microbiology*, vol. 3, no. 3, pp. 238–250, 2005.

[31] M. L. Crouch, L. A. Becker, I. S. Bang, H. Tanabe, A. J. Ouellette, and F. C. Fang, "The alternative sigma factor σE is required for resistance of Salmonella enterica serovar Typhimurium to antimicrobial peptides," *Molecular Microbiology*, vol. 56, no. 3, pp. 789–799, 2005.

[32] A. M. S. Mayer, A. D. Rodríguez, R. G. S. Berlinck, and N. Fusetani, "Marine pharmacology in 2007-8: marine compounds with antibacterial, anticoagulant, antifungal, anti-inflammatory, antimalarial, antiprotozoal, antituberculosis, and antiviral activities; Affecting the immune and nervous system, and other miscellaneous mechanisms of action," *Comparative Biochemistry and Physiology C*, vol. 153, no. 2, pp. 191–222, 2011.

[33] N. Y. Yount, D. Kupferwasser, A. Spisni et al., "Selective reciprocity in antimicrobial activity versus cytotoxicity of hBD-2 and crotamine," *Proceedings of the National Academy of Sciences of the United States of America*, vol. 106, no. 35, pp. 14972–14977, 2009.

[34] G. Rádis-Baptista, N. Oguiura, M. A. F. Hayashi et al., "Nucleotide sequence of crotamine isoform precursors from a single South American rattlesnake (*Crotalus durissus terrificus*)," *Toxicon*, vol. 37, no. 7, pp. 973–984, 1999.

[35] G. Maróti Gergely, A. Kereszt, É. Kondorosi, and P. Mergaert, "Natural roles of antimicrobial peptides in microbes, plants and animals," *Research in Microbiology*, vol. 162, no. 4, pp. 363–374, 2011.

[36] E. S. Yamane, F. C. Bizerra, E. B. Oliveira et al., "Unraveling the antifungal activity of a South American rattlesnake toxin crotamine," *Biochimie*, vol. 95, no. 2, pp. 231–240, 2013.

[37] T. Calandra and O. Marchetti, "Clinical trials of antifungal prophylaxis among patients undergoing surgery," *Clinical Infectious Diseases*, vol. 39, supplement 4, pp. S185–S192, 2004.

[38] G. Kragol, L. Otvos Jr., J. Feng, W. Gerhard, and J. D. Wade, "Synthesis of a disulfide-linked octameric peptide construct carrying three different antigenic determinants," *Bioorganic and Medicinal Chemistry Letters*, vol. 11, no. 11, pp. 1417–1420, 2001.

[39] F. D. Nascimento, L. Sancey, A. Pereira et al., "The natural cell-penetrating peptide crotamine targets tumor tissue *in vivo* and triggers a lethal calcium-dependent pathway in cultured cells," *Molecular Pharmaceutics*, vol. 9, no. 2, pp. 211–221, 2012.

[40] Y. Lan, Y. Ye, J. Kozlowska, J. K. W. Lam, A. F. Drake, and A. J. Mason, "Structural contributions to the intracellular targeting strategies of antimicrobial peptides," *Biochimica et Biophysica Acta*, vol. 1798, no. 10, pp. 1934–1943, 2010.

[41] D. W. Hoskin and A. Ramamoorthy, "Studies on anticancer activities of antimicrobial peptides," *Biochimica et Biophysica Acta*, vol. 1778, no. 2, pp. 357–375, 2008.

[42] A. R. Lizzi, V. Carnicelli, M. M. Clarkson, A. Di Giulio, and A. Oratore, "Lactoferrin derived peptides: mechanisms of action

and their perspectives as antimicrobial and antitumoral agents," *Mini-Reviews in Medicinal Chemistry*, vol. 9, no. 6, pp. 687–695, 2009.

[43] B. Findlay, G. G. Zhanel, and F. Schweizer, "Cationic amphiphiles, a new generation of antimicrobials inspired by the natural antimicrobial peptide scaffold," *Antimicrobial Agents and Chemotherapy*, vol. 54, no. 10, pp. 4049–4058, 2010.

[44] N. Papo and Y. Shai, "Host defense peptides as new weapons in cancer treatment," *Cellular and Molecular Life Sciences*, vol. 62, no. 7-8, pp. 784–790, 2005.

[45] A. Pereira, A. Kerkis, M. A. Hayashi et al., "Crotamine toxicity and efficacy in mouse models of melanoma," *Expert Opinion on Investigational Drugs*, vol. 20, no. 9, pp. 1189–1200, 2011.

[46] G. León, L. Sánchez, A. Hernández et al., "Immune response towards snake venoms," *Inflammation and Allergy-Drug Targetsno*, vol. 10, no. 5, pp. 381–398, 2011.

[47] K. A. Marr, "The changing spectrum of candidemia in oncology patients: therapeutic implications," *Current Opinion in Infectious Diseases*, vol. 13, no. 6, pp. 615–620, 2000.

[48] C. Zhao, T. Nguyen, L. Liu, R. E. Sacco, K. A. Brogden, and R. I. Lehrer, "Gallinacin-3, an inducible epithelial β-defensin in the chicken," *Infection and Immunity*, vol. 69, no. 4, pp. 2684–2691, 2001.

[49] B. G. Fry, "From genome to "venome": molecular origin and evolution of the snake venom proteome inferred from phylogenetic analysis of toxin sequences and related body proteins," *Genome Research*, vol. 15, no. 3, pp. 403–420, 2005.

[50] E. Wanke, A. J. Zaharenko, E. Redaelli, and E. Schiavon, "Actions of sea anemone type 1 neurotoxins on voltage-gated sodium channel isoforms," *Toxicon*, vol. 54, no. 8, pp. 1102–1111, 2009.

[51] S. Diochot, A. Baron, L. D. Rash et al., "A new sea anemone peptide, APETx2, inhibits ASIC3, a major acid-sensitive channel in sensory neurons," *EMBO Journal*, vol. 23, no. 7, pp. 1516–1525, 2004.

[52] S. Diochot and M. Lazdunski, "Sea anemone toxins affecting potassium channels," *Progress in molecular and subcellular biology*, vol. 46, pp. 99–122, 2009.

[53] S. Peigneur, D. J. Orts, A. R. Prieto da Silva et al., "Crotamine pharmacology revisited: novel insights based on the inhibition of KV channels," *Molecular Pharmacologyno*, vol. 82, no. 1, pp. 90–96, 2012.

[54] C. T. Rizzi, J. L. Carvalho-de-Souza, E. Schiavon, A. C. Cassola, E. Wanke, and L. R. P. Troncone, "Crotamine inhibits preferentially fast-twitching muscles but is inactive on sodium channels," *Toxicon*, vol. 50, no. 4, pp. 553–562, 2007.

[55] M. Rodrigues, A. Santos, B. G. de la Torre et al., "Molecular characterization of the interaction of crotamine-derived nucleolar targeting peptides with lipid membranes," *Biochimica et Biophysica Actano*, vol. 818, no. 11, pp. 2707–2717, 2012.

Hindawi Publishing Corporation
BioMed Research International
Volume 2013, Article ID 578276, 6 pages
http://dx.doi.org/10.1155/2013/578276

Research Article

Persistence or Clearance of Human Papillomavirus Infections in Women in Ouro Preto, Brazil

P. M. Miranda,[1] N. N. T. Silva,[2] B. C. V. Pitol,[2] I. D. C. G. Silva,[3] J. L. Lima-Filho,[4] R. F. Carvalho,[1,5] R. C. Stocco,[1,5] W. Beçak,[1,6] and A. A. Lima[2]

[1] *Laboratório de Genética, Instituto Butantan, Avenida Vital Brasil 1500, 05503-900 São Paulo, SP, Brazil*
[2] *Departamento de Análises Clínicas Escola de Farmácia, Universidade de Ouro Preto (UFOP), Rua Costa Sena 171, 35400-000 Ouro Preto, MG, Brazil*
[3] *Laboratório de Tocoginecologia, Departamento de Ginecologia, Universidade Federal de São Paulo, 04039-032 São Paulo, SP, Brazil*
[4] *Laboratório de Imunopatologia Keizo Asami (LIKA), Universidade Federal de Pernambuco (UFPE), 50670-901 Recife, PE, Brazil*
[5] *Programa de Pós-Graduação Interunidades em Biotecnologia, Universidade de São Paulo, 05508-900 São Paulo, SP, Brazil*
[6] *Departamento de Biologia, Universidade Federal da Integração Latino-Americana (UNILA), 85867-970 Foz do Iguaçú, PR, Brazil*

Correspondence should be addressed to R. C. Stocco; ritastocco@butantan.gov.br

Received 2 April 2013; Accepted 6 September 2013

Academic Editor: Marcelo Palma Sircili

Persistent high-risk (HR) human papillomavirus (HPV) infection is necessary for development of precursor lesions and cervical cancer. We investigate persistence and clearance of HPV infections and cofactors in unvaccinated women. Cervical samples of 569 women (18–75 years), received for routine evaluation in the Health Department of Ouro Preto, Brazil, were collected and subjected to PCR (MY09/11 or GP5+/6+ primers), followed by RFLP or sequencing. All women were interviewed to collect sociodemographic and behavioral information. Viral infection persistence or clearance was reevaluated after 24 months and was observed in 59.6% and 40.4% of women, respectively. HPVs 16, 33, 59, 66, 69, and 83 (HR) were the most persistent types whereas HPVs 31, 45, and 58 were less persistent. Clearance or persistence did not differ between groups infected by HPVs 18, 53, and 67. In low-risk (LR) types, HPV 6 infected samples were associated with clearance, while HPV 11, 61, 72, or 81 infected samples were persistent in the follow-up. No statistically significant association was detected between persistent HPV infections and sociodemographic and behavioral characteristics analyzed. To study persistence or clearance in HPV infection allows the identification of risk groups, cofactors, and strategies for prevention of cervical cancer.

1. Introduction

Human papillomavirus (HPV) infections are the most commonly diagnosed sexually transmitted disease. More than 100 HPV types have been identified. They infect the skin squamous epithelia and mucosa and usually cause benign papillomas or warts. Persistent infection with oncogenic high-risk HPV causes all cervical cancers, most anal cancers, and a subset of vulvar, vaginal, penile, and oropharyngeal cancers [1–3].

The major steps in cervical carcinogenesis include HPV infection, HPV persistence for a certain period of time, progression to precancer, and invasion [4, 5].

HPV infection alone may not be sufficient to cause cervical cancer, and other factors influence the risk of progression to cervical cancer. High parity, smoking, long-term use of oral contraceptives, sexual behavior, genetic factors, and coinfection with other sexually transmitted infectious agents such as herpes simplex virus 2 (HSV-2) and *Chlamydia trachomatis* have been established as cofactors for cervical cancer among women with persistent infections [6–9].

Although these environmental and genetic factors are considered to act as HPV cofactors contributing to progression from viral infection to cervical cancer, few prospective studies have addressed the roles that these risk factors play in the natural history of precursor lesions. The knowledge of

epidemiology and natural history of HPV infection (acquisition, clearance, and persistence) is relevant and can direct interventions to prevent preneoplastic lesions and cervical cancer [4].

There is evidence that most HPV infections are transient and clear spontaneously within 12–24 months after first detection. Persistent HPV infection with elevated risk of cervical cancer occurs in only a small percentage of virus infected women [5, 10]. The reasons of this fact are still unknown.

The importance of HPV clearance/persistence has been recognized recently, and the number of studies addressing these issues has increased substantially during the past few years. However, data are still incomplete and in part inconsistent as to the cofactors that regulate these events [11, 12].

In Ouro Preto, MG, Brazil, a recent study showed prevalence of HPV infections in women with normal cervical cytology. Different subtypes of high-risk HPV (mainly HPV 16) were predominant. Furthermore, age, literacy, residence, marital status, smoking status, and number of sexual partners were independently associated with HPV infection [13].

HPV-positive women in this prevalence study have been accompanied to assess the natural history of viral infection. Therefore, the aim of this study was to investigate persistence and clearance of HPV infections in unvaccinated women and cofactors correlated with such events.

2. Material and Methods

Ethical Statements. The protocols used in this study were approved by the Ethical Committee in Research of the Universidade Federal de São Paulo (number 0832.08) assigned by the president of this committee.

The sample was composed of 569 women (aged 18 to 75 years) living in Ouro Preto, MG, Brazil. Women were randomly selected when they visited health units for routine gynecological evaluation and they were not enrolled in the study if they were pregnant, diagnosed with mental incompetence, or diagnosed with carcinoma, except the cervical cancer. This project was reviewed and approved by the Institutional Ethic Committee, and informed consent was obtained from private interviews at the time of gynecological evaluation.

Sociodemographic characteristics, smoking status, alcohol consumption, bracken fern diet, and sexual and reproductive behavior were obtained from private interviews with the women at the time of the gynecological evaluation. Subjects were considered as nonsmokers or nonalcohol consumers if they have never smoked or drunk. Speculum examination was performed by gynecologists; cervical samples were obtained using an extended tip "Ayre" spatula. The conventional cervical smear was spread onto a glass slide and the tip of the spatula was broken off and placed in a container containing preservation solution for HPV testing.

2.1. HPV-DNA Typing. For the extraction of DNA from cervical samples, we used a GenomicPrep Blood kit (GE Healthcare), with proteinase K digestion. HPV was detected by the amplification of DNA by using a standard polymerase chain reaction (PCR) protocol with L1 consensus primer pair MY09 and MY11, which promotes amplification of an approximately 450 bp product and can detect more than 40 distinct low- and high-risk genital HPV types. Positive and negative controls were used in all tests. The amplification was performed according to the following protocol: 94°C for 30 s, 51.5°C for 30 s, and 72°C for 30 s for 35 cycles, followed by a final step at 72°C for 7 min [14, 15]. The β-actin gene primers were used as internal controls.

We used RT-PCR with primers GP5+/6+ for HPV detection in samples with no conclusive diagnosis using primers MY09/11. The reactions were performed using SYBR Green PCR Master Mix (Applied Biosystems) and conducted in ABI 7000 Applied Biosystems.

HPV-DNA-positive specimens were typed by restriction fragment length polymorphism (RFLP), according to Bernard et al. 1994 [16]. Samples with positive HPV viral types not identified by RFLP were identified by sequencing of the PCR product using BigDye Terminator kit (Applied Biosystems). Sequences were generated on ABI model 377 automated sequencer (Applied Biosystems) and aligned to HPV sequences at Genbank using BioEdit Sequence Alignment Editor 7.0.9.0.

2.2. Follow-Up Study. HPV infection was detected in 133 women, who were invited to participate in a follow-up study, consisting of a second cervical scrape specimen collection 24 months from first recruitment, using the same procedure as the initial examination. 89 women (66.9%) completed the survey and were tested for HPV in 24 months. 44 women (33.1%) were lost in the follow-up.

After 24 months (second cervical scrape specimen for cytology and HPV testing), all women were interviewed again, with the same questionnaire used in first collection, and the information was updated.

Persistent type-specific HPV infection was defined as the detection of the same HR-HPV type at both examinations (first study and follow-up study). Clearance was defined as the proportion of women who were initially HR-HPV positive (first collection), but the same HR-HPV type was not found at the follow-up [12].

2.3. Statistical Analysis. Descriptive statistics were used for the analysis of persistence and clearance of type-specific HPV infection. Particularly, Pearson's x^2 test was used to verify the association between all independent variables and the response variable. $P < 0.05$ was considered statistically significant. Statistical analyses were performed using SPSS software for Windows (version 18.0).

3. Results and Discussion

3.1. Results

3.1.1. Profile of the Initial Sample. Analyses of this study were performed with samples of 89 women, mean age of 37.7 (±12.6) years.

Table 1: Evolution of HPV infection related to virus oncogenic risk and type of infection.

	Total *N*	Clearance *n* (%)	Persistence *n* (%)	*P*
Infection				
Single	80	34 (42.5)	46 (57.5)	0.210
Multiple	9	2 (22.2)	7 (77.8)	
Oncogenic risk				
LR-HPV	17	5 (29.4)	12 (70.6)	
IR-HPV	17	10 (58.8)	7 (41.2)	0.082
HR-HPV	55	21 (38.2)	34 (61.8)	

These samples were composed predominantly of women with the following characteristics: age ≥30 years (68.5%); resident in urban areas (76.4%); only one sexual partner in lifetime (51.7%); no use of oral contraceptives (52.8%); alcohol consumption (61.8%); 1–5 pregnancies (66.3%); bracken fern consumption in usual diet (68.5%); smoking (40.4%). Only 20.2% of women in the group had early onset of sexual activity (≤15 years).

Simple infections, by a single viral type, were predominant (80 women, 89.9%) and multiple HPV infections were detected in 10.1%.

High-risk (HR) HPV types (mainly HPV16) were more prevalent in the study samples. HR-HPV was detected in 55 (61.8%) women, indeterminate risk (IR) HPV in 17 (19.1%) and low risk (LR) in 17 (19.1%) women.

3.1.2. Evaluation after 24-Month Follow-Up. Among the 89 women HPV positive at baseline, 53 (59.6%) had persistent infection and 36 (40.4%) had clearance of the infection after 24 months.

Table 1 shows clearance or persistence of viral infection in relation to number and risk of HPV types.

Most women with multiple infections (77.8%) showed persistence after 24 months of follow-up. However, presence of multiple infections was not statistically associated with persistent HPV infection (Table 1).

Similarly, in relation to risk oncogenic HPV types, no statistical difference was observed between persistence of viral infection and HR-HPV types. The infection persisted after follow-up in 61.8% of samples infected by HR-HPV and in 70.6% by LR-HPV (Table 1).

Among specific HR-HPV types, HPV 16, 33, 59, 66, 69, and 83 were the most persistent types whereas HPVs 31, 45, and 58 were the less persistent. Clearance or persistence did not differ between groups infected by HPVs 18, 53, and 67 (Table 2).

Regarding specific LR-HPV types, HPV 6 infected samples were associated with clearance. In contrast, HPV 11, 61, 72, or 81 infected samples were associated with persistent infections in the 24-month follow-up (Table 3).

Table 4 shows that no statistically significant association was detected between persistent HPV infections and sociodemographic and behavioral characteristics evaluated.

Table 2: Persistence or clearance of specific high-risk (HR) HPV infection after follow-up.

HPV types	Clearance *n* (%)	Persistence *n* (%)	Total *N*
16	12 (35.3)	22 (64.7)	34
18	3 (50)	3 (50)	6
31	2 (100)	0 (0)	2
33	0 (0)	2 (100)	2
45	1 (100)	0 (0)	1
53	1 (50)	1 (50)	2
58	1 (100)	0 (0)	1
59	0 (0)	1 (100)	1
66	0 (0)	1 (100)	1
67	1 (50)	1 (50)	2
69	0 (0)	1 (100)	1
83	0 (0)	2 (100)	2
HR-HPV	21 (38.2)	34 (61.8)	55

Table 3: Persistence or clearance of specific low-risk (LR) HPV infection after follow-up.

HPV types	Clearance *n* (%)	Persistence *n* (%)	Total *N*
6	4 (66.7)	2 (33.3)	6
11	0 (0)	2 (100)	2
61	1 (14.3)	6 (85.7)	7
72	0 (0)	1 (100)	1
81	0 (0)	1 (100)	1
LR-HPV	5 (29.4)	12 (70.6)	17

4. Discussion

We have analyzed the prevalence of HPV infection in women presenting normal cervical cytology [13] and in women living in rural and urban areas of Ouro Preto, MG, Brazil [17]. HPV-positive women were followed for 24 months. In general, persistence of HPV infection was 59.6% and clearance was 40.4%. It is believed that HPV infections "clear" within 2 years in more than 90% of individuals [5, 18–20]. Therefore, the percentage of HPV clearance was low in our study but similar results were also obtained by Banura et al., 2010 [21], and Guo et al., 2010 [22].

Considering only HR-HPV infections, the persistence was 61.8% and clearance was 38.2%. This result was similar to that reported in studies in Brazil [23] and other countries [12, 24, 25].

However, unlike what is expected we observed high persistence (70.6%) and low clearance (29.4%) of LR-HPV infections, proportions similar to those obtained for HR-HPV types. This may be due to the small number of women with each viral type or time of follow-up. Banura et al., 2010 [21], showed clearance LR-HPV ranged between 50% and 100%. Other studies also observed that clearance proportion was similar in HR-HPV and LR-HPV [21, 26]. We found

Table 4: Evolution of HPV infection related to sociodemographic and behavioral characteristics.

	Total *N*	Clearance *n* (%)	Persistence *n* (%)	*P*
Age groups (years)				
>30	28	11 (39.3)	17 (60.7)	0.657
30 to 39	20	7 (35.0)	13 (65.0)	
40 to 49	25	11 (44.0)	14 (56.0)	
>50	16	7 (40.4)	9 (56.3)	
Residence				
Rural	21	10 (47.6)	11 (52.4)	0.303
Urban	68	26 (38.2)	42 (61.8)	
Age at first intercourse (years)				
≤15	18	8 (44.4)	10 (56.6)	0.449
>15	71	28 (39.4)	43 (60.6)	
Number of lifetime sexual partners				
1	46	18 (39.1)	28 (60.9)	0.051
2 to 4	28	8 (28.6)	20 (71.4)	
5 or more	15	10 (66.7)	5 (33.3)	
Oral contraceptive use				
No	47	19 (40.4)	28 (59.6)	0.583
Yes	42	17 (40.5)	25 (59.5)	
Parity				
0	19	8 (42.1)	11 (57.9)	0.509
1 to 5	59	25 (42.4)	34 (57.6)	
6 or more	11	3 (27.3)	8 (72.7)	
Bracken fern consumption				
No	28	12 (42.9)	16 (57.1)	0.466
Yes	61	24 (39.3)	37 (60.7)	
Smoking				
No	53	19 (35.8)	34 (64.2)	0.197
Yes	36	17 (47.2)	19 (52.8)	
Alcohol consumption				
No	34	13 (38.2)	21 (61.8)	0.457
Yes	55	23 (41.8)	32 (58.2)	

that HPV 16, 33, 59, 66, 69, and 83 infections were the most persistent. Studies have reported that HPV 16 was significantly more likely to persist than were all other viral types [21, 25, 27]. Moreover, Sammarco et al., 2013 [12], observed that HPV types with the highest likelihood of persistence were 31, 39, and 73, whilst HPV 16 was the least persistent. Persistent infections have a higher risk of progression to precursor lesions and cervical cancer.

In this study, most of women with multiple infections showed persistence after 24 months of follow-up. Similar results were obtained by Trottier et al., 2008 [28], Nielsen et al., 2010 [27], Castle et al., 2011 [29], and Schmeink et al., 2013 [26], who reported that infection with multiple HPV types is associated with longer persistence of HPV infection. This association was not observed by Sammarco et al., 2013 [12].

In the literature, associations of HPV persistence or clearance with cofactors vary widely due to the sample size, population characteristics, and study design. In this study, there was no significant association between HPV persistence or clearance and the analyzed cofactors. Schmeink et al., 2013 [26], suggest that HPV clearance is mainly related to the host immune response or other intrinsic host factors and not to present behavior factors.

There are reports that women with persistent HR-HPV infections were younger than those who cleared their infections [12, 30, 31]. Others showed that persistence increased with age [29]. However, no association between HPV persistence and age was found in this study as in Trottier et al., 2008 [28], and Muoz et al., 2009 [32].

Likewise in this work, some studies found no association between persistent HPV infection and smoking, number of sexual partners, oral contraceptive use, and high parity [12, 26, 27, 30, 33].

Persistent high-risk HPV infection also was associated with high viral load [22, 34].

The main limitations of this study were sample size and follow-up period. This prevented extensive discussion of some results and direct comparison with other studies. Furthermore, it is important to emphasize that our data were based solely on the detection of DNA in cervical samples.

HR-HPV persistence plays a key role in the progression of preneoplastic lesions and in the development of cervical cancer. Thus, epidemiological and biological understanding of the natural history of HPV infection is critical to guide the implementation of strategies for prevention and control of cervical cancer.

Conflict of Interests

All authors declare that there is no conflict of interests regarding the research, authorship, and/or publication of this paper. The authors inform that all materials and trademarks mentioned were used just as part of experimental protocol and there are no financial gains or favoritism of business.

Acknowledgments

The authors would like to thank the *Ministério de Ciência, Tecnologia e Inovação/Conselho Nacional de Desenvolvimento Científico e Tecnológico* (CNPq Proc. 554816/2006-7), *PRONEX/FACEPE* (APQ-0781-4.01/06), FAPESP (Proc. 2006/02439-6), FAPEMIG, Fundação Butantan, and Coordenação de Aperfeiçoamento Pessoal de Nível Superior (CAPES) for the financial support and thank Carolina da Paz Sabino for her editorial support.

References

[1] H. Z. Hausen, "Papillomaviruses and cancer: from basic studies to clinical application," *Nature Reviews Cancer*, vol. 2, no. 5, pp. 342–350, 2002.

[2] M. Steben and E. Duarte-Franco, "Human papillomavirus infection: epidemiology and pathophysiology," *Gynecologic Oncology*, vol. 107, no. 2, pp. S2–S5, 2007.

[3] H. Z. Hausen, "Human papillomavirus and cervical cancer," *Indian Journal of Medical Research*, vol. 130, no. 3, p. 209, 2009.

[4] M. Schiffman, N. Wentzensen, S. Wacholder, W. Kinney, J. C. Gage, and P. E. Castle, "Human papillomavirus testing in the prevention of cervical cancer," *Journal of the National Cancer Institute*, vol. 103, no. 5, pp. 368–383, 2011.

[5] P. E. Gravitt, "The known unknowns of HPV natural history," *Journal of Clinical Investigation*, vol. 121, no. 12, pp. 4593–4599, 2011.

[6] X. Castellsagué and N. Muñoz, "Chapter 3: cofactors in human papillomavirus carcinogenesis—role of parity, oral contraceptives, and tobacco smoking," *Journal of the National Cancer Institute Monographs*, no. 31, pp. 20–28, 2003.

[7] L. A. Dahlström, K. Andersson, T. Luostarinen et al., "Prospective seroepidemiologic study of human papillomavirus and other risk factors in cervical cancer," *Cancer Epidemiology Biomarkers and Prevention*, vol. 20, no. 12, pp. 2541–2550, 2011.

[8] H. Yetimalar, B. Kasap, K. Cukurova, A. Yildiz, A. Keklik, and F. Soylu, "Cofactors in human papillomavirus infection and cervical carcinogenesis," *Archives of Gynecology and Obstetrics*, vol. 285, no. 3, pp. 805–810, 2012.

[9] K. E. Jensen, S. Schmiedel, B. Norrild, K. Frederiksen, T. Iftner, and S. K. Kjaer, "Parity as a cofactor for high-grade cervical disease among women with persistent human papillomavirus infection: a 13-year follow-up," *The British Journal of Cancer*, vol. 108, no. 1, pp. 234–239, 2013.

[10] K. Syrjänen, "Mechanisms and predictors of high-risk human papillomavirus (HPV) clearance in the uterine cervix," *European Journal of Gynaecological Oncology*, vol. 28, no. 5, pp. 337–351, 2007.

[11] M. Confortini, F. Carozzi, M. Zappa et al., "Human papillomavirus infection and risk factors in a cohort of Tuscan women aged 18–24: results at recruitment," *BMC Infectious Diseases*, vol. 10, article 157, 2010.

[12] M. L. Sammarco, I. Del Riccio, M. Tamburro, G. M. Grasso, and G. Ripabelli, "Type-specific persistence and associated risk factors of human papillomavirus infections in women living in central Italy," *European Journal of Obstetrics and Gynecology and Reproductive Biology*, vol. 168, no. 2, pp. 222–226, 2013.

[13] P. M. Miranda, B. C. Pitol, M. S. Moran et al., "Human papillomavirus infection in Brazilian women with normal cervical cytology," *Genetics and molecular research*, vol. 11, no. 2, pp. 1752–1761, 2012.

[14] M. H. Schiffman, H. M. Bauer, A. T. Lorincz et al., "Comparison of Southern blot hybridization and polymerase chain reaction methods for the detection of human papillomavirus DNA," *Journal of Clinical Microbiology*, vol. 29, no. 3, pp. 573–577, 1991.

[15] W. G. Qu, G. Jiang, Y. Cruz et al., "PCR detection of human papillomavirus: comparison between MY09/MY11 and GP5+/GP6+ primer systems," *Journal of Clinical Microbiology*, vol. 35, no. 6, pp. 1304–1310, 1997.

[16] H. U. Bernard, S. Y. Chan, M. M. Manos et al., "Identification and assessment of known and novel human papillomaviruses by polymerase chain reaction amplification, restriction fragment length polymorphisms, nucleotide sequence, and phylogenetic algorithms," *Journal of Infectious Diseases*, vol. 170, no. 5, pp. 1077–1085, 1994.

[17] B. C. V. Pitol, P. M. Miranda, M. S. Moran et al., "Prevalence of HPV infection and risk factors in rural and urban women," Unpublished results.

[18] E. L. Franco, L. L. Villa, J. P. Sobrinho et al., "Epidemiology of acquisition and clearance of cervical human papillomavirus infection in women from a high-risk area for cervical cancer," *Journal of Infectious Diseases*, vol. 180, no. 5, pp. 1415–1423, 1999.

[19] C. B. J. Woodman, S. Collins, H. Winter et al., "Natural history of cervical human papillomavirus infection in young women: a longitudinal cohort study," *The Lancet*, vol. 357, no. 9271, pp. 1831–1836, 2001.

[20] N. Muñoz, F. Méndez, H. Posso et al., "Incidence, duration, and determinants of cervical human papillomavirus infection in a cohort of Colombian women with normal cytological results," *Journal of Infectious Diseases*, vol. 190, no. 12, pp. 2077–2087, 2004.

[21] C. Banura, S. Sandin, L. van Doorn et al., "Type-specific incidence, clearance and predictors of cervical human papillomavirus infections (HPV) among young women: a prospective study in Uganda," *Infectious Agents and Cancer*, vol. 5, no. 1, article 7, 2010.

[22] Y. Guo, K. You, J. Qiao, Y. Zhao, C. Liu, and L. Geng, "Natural history of infections with high-risk HPV in Chinese women with abnormal cervical cytology findings at baseline," *International Journal of Gynecology and Obstetrics*, vol. 110, no. 2, pp. 137–140, 2010.

[23] M. I. Rosa, J. M. G. Fachel, D. D. Rosa, L. R. Medeiros, C. N. Igansi, and M. C. Bozzetti, "Persistence and clearance of human papillomavirus infection: a prospective cohort study," *The American Journal of Obstetrics and Gynecology*, vol. 199, no. 6, pp. 617.e1–617.e7, 2008.

[24] E. R. Howe, Z. Li, R. C. McGlennen, W. L. Hellerstedt, and L. S. Downs Jr., "Type-specific prevalence and persistence of human papillomavirus in women in the United States who are referred for typing as a component of cervical cancer screening," *The American Journal of Obstetrics and Gynecology*, vol. 200, no. 3, pp. 245.e1–245.e7, 2009.

[25] X. Carcopino, N. Bolger, M. Henry et al., "Evaluation of type-specific HPV persistence and high-risk HPV viral load quantitation in HPV positive women under 30 with normal cervical cytology," *Journal of Medical Virology*, vol. 83, no. 4, pp. 637–643, 2011.

[26] C. E. Schmeink, L. F. Massuger, C. H. Lenselink et al., "Prospective follow-up of 2, 065 young unscreened women to study human papillomavirus incidence and clearance," *International Journal of Cancer*, vol. 133, no. 1, pp. 172–181, 2013.

[27] A. Nielsen, S. K. Kjaer, C. Munk, M. Osler, and T. Iftner, "Persistence of high-risk human papillomavirus infection in a population-based cohort of Danish women," *Journal of Medical Virology*, vol. 82, no. 4, pp. 616–623, 2010.

[28] H. Trottier, S. Mahmud, J. C. M. Prado et al., "Type-specific duration of human papillomavirus infection: implications for human papillomavirus screening and vaccination," *Journal of Infectious Diseases*, vol. 197, no. 10, pp. 1436–1447, 2008.

[29] P. E. Castle, A. C. Rodríguez, R. D. Burk et al., "Long-term persistence of prevalently detected human papillomavirus infections in the absence of detectable cervical precancer and cancer," *Journal of Infectious Diseases*, vol. 203, no. 6, pp. 814–822, 2011.

[30] S. Syrjänen, I. Shabalova, N. Petrovichev et al., "Factors predicting persistence of high-risk human papillomavirus (HPV) infections in women prospectively followed-up in three new

independent states (NIS) of the former Soviet Union," *European Journal of Gynaecological Oncology*, vol. 26, no. 5, pp. 491–498, 2005.

[31] E. Fukuchi, G. F. Sawaya, M. Chirenje et al., "Cervical human papillomavirus incidence and persistence in a cohort of HIV-negative women in zimbabwe," *Sexually Transmitted Diseases*, vol. 36, no. 5, pp. 305–311, 2009.

[32] N. Muoz, G. Hernandez-Suarez, F. Méndez et al., "Persistence of HPV infection and risk of high-grade cervical intraepithelial neoplasia in a cohort of Colombian women," *The British Journal of Cancer*, vol. 100, no. 7, pp. 1184–1190, 2009.

[33] N. Muñoz and R. Herrero, "Prevention of cervical cancer in women's hands: Mexico leads the way," *The Lancet*, vol. 378, no. 9806, pp. 1829–1831, 2011.

[34] J. Bae, S. Seo, Y. Park et al., "Natural history of persistent high-risk human papillomavirus infections in Korean women," *Gynecologic Oncology*, vol. 115, no. 1, pp. 75–80, 2009.

Hindawi Publishing Corporation
BioMed Research International
Volume 2013, Article ID 618475, 6 pages
http://dx.doi.org/10.1155/2013/618475

Research Article

Higher Incidence of Lung Adenocarcinomas Induced by DMBA in Connexin 43 Heterozygous Knockout Mice

Krishna Duro de Oliveira, Marcello Vannucci Tedardi, Bruno Cogliati, and Maria Lúcia Zaidan Dagli

Department of Pathology, School of Veterinary Medicine and Animal Science, University of São Paulo, Avenue Professor Dr. Orlando Marques de Paiva 87, 05508-900 Sao Paulo, SP, Brazil

Correspondence should be addressed to Maria Lúcia Zaidan Dagli; mlzdagli@yahoo.com.br

Received 22 March 2013; Accepted 8 August 2013

Academic Editor: Sircili MP

Gap junctions are communicating junctions which are important for tissue homeostasis, and their disruption is involved in carcinogenic processes. This study aimed to verify the influence of deletion of one allele of the Connexin 43 gene on cancer incidence in different organs. The 7, 12-dimethylbenzanthracene (DMBA) carcinogenic model, using hebdomadary doses by gavage of 9 mg per animal, was used to induce tumors in Connexin 43 heterozygous or wild-type mice. The experiment began in the eighth week of the mice life, and all of them were euthanized when reaching inadequate physical condition, or at the end of 53 weeks. No statistical differences occurred for weight gain and cancer survival time ($P = 0.9853$) between heterozygous and wild-type mice. $Cx43^{+/-}$ mice presented significantly higher susceptibility to lung cancer ($P = 0.0200$) which was not evidenced for benign neoplasms ($P = 0.3449$). In addition, incidence of ovarian neoplasms was 2.5-fold higher in $Cx43^{+/-}$ mice, although not statistically significant. Other organs showed a very similar cancer occurrence between Cx43 groups. The experiment strengthens the evidence of the relationship between Connexin 43 deficiency and carcinogenesis.

1. Introduction

Gap junction, first described in the beginning of the 1960's [1], is a cell membrane junction responsible for cell-to-cell communication, being one of the mechanisms involved in tissue homeostasis, proliferation, and differentiation [2–5]. Connexins are the basic units of these junctions, being expressed by 21 genes in human and 20 in mice [6]. The union of 6 of these proteins is responsible to form a connexon, a hemichannel structure normally allocated in cell membrane [5, 7, 8]. When connexons from neighbor cells connect, they allow the interchange of substances with 1,000 Da or less, like water, ions, sugars, small peptides, amino acids, fatty acids, and drugs [5, 9].

Cell growth, proliferation, and apoptosis are regulatory mechanisms shared between cells, and any disruption of this process may allow the development of many disorders. Cell-to-cell communication pathway has been studied to better understand inflammatory, regenerative, and oncogenic processes [3, 7, 10]. A considerable number of studies after the classic Loewenstein and Kanno [11] publication have shown the correlation between the lower communication capacity and the development of cancer.

This study has been performed in order to verify if the heterologous deletion of one allele of Cx43 could contribute to enhance the incidence of different cancers in mice, when compared to wild-type mice. DMBA carcinogenesis was the model of choice, based on previously conducted experiment, where breast, lung, skin, lymphoid, digestive tract, and ovary cancers were evidenced [12].

2. Materials and Methods

2.1. Animals. The heterozygous knockout mice for Connexin 43 ($Cx43^{+/-}$) were generated by replacing exon-2 of the Cx43 gene by neomycin resistance gene [13]. This animal model was used because Connexin 43 knockout mice ($Cx43^{-/-}$)

die after birth due to cardiac congenital abnormalities [13]. Animals were kindly provided by International Agency for Research on Cancer (IARC, Lyon, France) and originally were produced in the C57BL/6 strain. Their background was subsequently changed to CD1 by serial breeding at the IARC. The Cx43 expression was characterized by real-time polymerase chain reaction (PCR) and Western blot in these $Cx43^{+/-}$ mice, showing reduced mRNA amount and lower Cx43 levels than wild types according to previouse studies from our group [14]. 155 female mice wild-type ($Cx43^{+/+}$) and heterozygote ($Cx43^{+/-}$) mice were randomly provided by the Animal Facility of the Department of Pathology, School of Veterinary Medicine and Animal Science of the University of São Paulo. The experiment was blind; the authors were not informed if animals were wild types or heterozygotes during the mice life time, necropsy, and histopathology procedures. Only female mice were used to favor breast cancer development.

The animals were kept in a room with ventilation (16–18 air changes/hour), relative humidity (45–65%), controlled temperature (20–24°C), and light/dark cycle 12:12 and were given water and balanced diet *ad libitum*. The study has been approved by the Committee on Bioethics of the School of Veterinary Medicine and Animal Science of the University of São Paulo, Proc. no. 1876/2010.

2.2. Carcinogenesis. Carcinogenesis was induced by f 7, 12-dimethylbenzanthracene (Sigma), diluted in corn oil and administered by gavage [12]. Each animal received 1 mg per week until completing the total dose of 9 mg. Control group was composed of 20 mice, receiving only corn oil, also by gavage. Animals were weighted and received careful clinical examination weekly. The experiment began in the eighth week of life of animals, and all animals were euthanized when reaching inadequate physical condition, or at the end of 53 weeks.

2.3. Necropsy and Histopathology Study of Tumors. Necropsy was performed in all animals of the experiment, and tumors, mammary glands, gastrointestinal tract, liver, spleen, heart, lung and kidneys were collected and fixed in 10% formaldehyde solution. All mouse tumors were classified according to IARC Scientific Publication no. 111 [15].

2.4. Genotyping. DNA from each mouse was obtained from tail biopsies. Mice were genotyped for Connexin 43 gene by polymerase chain reaction (PCR) as described by Yamakage and collaborators (1998) [16]. The primers were used in respect to the following sequence: CCC-ACTCTCACCTATGTCTCC-3′ and antisense 5′-ACTTTT-GCCGCCTAGCTATCCC-3′ observed at 520 bp; neo-sense 5′-GGCCACA GTCGATGAATCCAG-3′ and antisense 5′-TATCCATCATGGCTGATGCAA-3′ observed at 294 bp.

2.5. Statistical Analysis. Statistical analysis was performed using the GraphPad Prism (version 5.0, GraphPad Software Inc., USA). Chi-square test and Fisher's exact test were used to compare incidence between both $Cx43^{+/-}$ and $Cx43^{+/+}$ groups. Odds ratio and relative risk and descriptive studies of the mean of tumors per animal in each group were also assessed. Logrank test was performed in order to evaluate the survival difference between $Cx43^{+/+}$ and Cx $43^{+/-}$ mice. The significance level was set at $P < 0.05$.

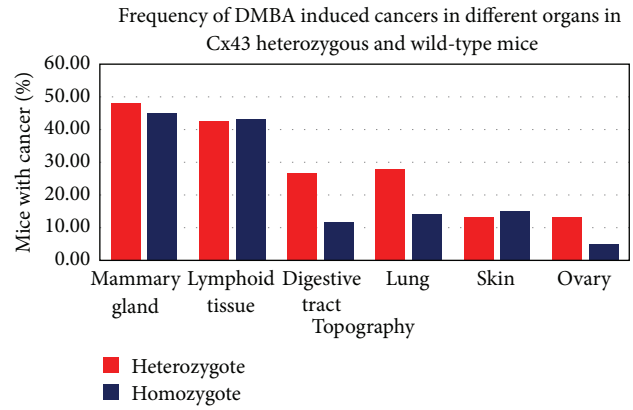

FIGURE 1: Bar graphic showing the proportional incidence among different topographies compared with the $Cx43^{+/-}$ and $Cx43^{+/+}$ groups.

3. Results

Control group after genotype was composed of 10 homozygote animals (wild types) and 10 heterozygous animals for Cx43, and none of them developed any type of neoplasia. 135 mice that received DMBA after genotype were divided in two groups, composed of 60 wild-type mice and 75 Cx43 heterozygous mice.

Neoplasms began to appear in the 8th week after DMBA injection and affected 100% of DMBA treated mice.

No significant statistical differences were observed in weight gain and survival time ($P = 0.9853$) between $Cx43^{+/-}$ and $Cx43^{+/+}$ DMBA induced groups (data not shown). Incidence rate of neoplasms in different organs and the histopathological classification of the neoplasms are presented in Table 1 and Figure 1.

Chi-square test and Fisher's Exact test were performed to the observe difference in incidence of cancers in different locations between $Cx43^{+/-}$ and $Cx43^{+/+}$ DMBA induced groups.

It has been detected a statistically significant difference in the incidence of lung adenocarcinomas, where $Cx43^{+/-}$ mice presented a 1.4-fold higher risk than wild-type animals (Table 2). Histopathology images of lung cancer are presented in Figure 2.

Benign lung neoplasia was diagnosed in 8 and 3 animals from $Cx43^{+/-}$ and $Cx43^{+/+}$ DMBA treated animals, respectively. The relative risk for developing papillary lung adenoma in heterozygous group, when compared with wild-type animals, was 2.133 (IC 95% 0.5913–7.696), and odds ratio were 2.269 (IC 95% 0.5745–8.959). The P value was 0.3449 for Fisher's Exact Test, and therefore, there was no difference

Table 1: DMBA induced cancer incidence in $Cx43^{+/-}$ and $Cx43^{+/+}$ mice divided by topography and tumor histopathological classification.

Cancer	$Cx43^{+/-}$ ($n = 75$)		$Cx43^{+/+}$ ($n = 60$)	
	Number of tumors	%	Number of tumors	%
Mammary gland	$n = 36$	48.00	$n = 27$	45.00
Adenoacanthoma	20	47.62	10	34.48
Adenocarcinoma type A	5	11.90	4	13.79
Adenocarcinoma type C	1	2.38	0	0.00
Carcinosarcoma	0	0.00	0	0.00
Cystic adenocarcinoma	12	28.57	12	41.38
Fibrosarcoma	1	2.38	0	0.00
undifferentiated type	1	2.38	0	0.00
Organoid	2	4.76	0	0.00
Total	**42**	**100.00**	**29**	**100.00**
Digestive tract	$n = 20$	26.67	$n = 16$	26.67
Squamous cell carcinoma	20	95.24	16	5.52
Gastric adenocarcinoma	1	47.61	0	0.00
Total	**21**	**100.00**	**16**	**100.00**
Lymphoid tissue	$n = 32$	42.67	$n = 26$	43.33
Lymphoma	32	100.00	26	100.00
Total	**32**	**100.00**	**26**	**100.00**
Skin	$n = 10$	13.33	$n = 9$	15.00
Squamous cell carcinoma	10	100.00	9	100.00
Total	**10**	**100.00**	**9**	**100.00**
Lung	$n = 21$	28.00	$n = 7$	11.66
Papillary adenocarcinoma	21	95.45	7	100.00
Bronchial carcinoma	1	4.45	0	0.00
Total	**22**	**100.00**	**7**	**100.00**
Ovary	$n = 10$	13.33	$n = 3$	5.00
Granulosa cell carcinoma	10	100.00	3	100.00
Total	**10**	**100.00**	**3**	**100.00**
Total	**137**		**90**	
Number of cancer histological types per animal	1.83		1.50	

Note: there are more tumors than mice in the experiment because some animals developed more than one type of cancer in the same or different organs.

in the incidence of lung papillary adenomas in $Cx43^{+/-}$ and $Cx43^{+/+}$ mice.

4. Discussion

The aim of this study was to verify if the deficiency in Connexin 43 could increase the susceptibility to different types of neoplasms in mice. For this purpose, the DMBA carcinogenesis model was used, since it has previously been shown, in BALB/c mice, that this carcinogen induces not only mammary tumors but also lung, digestory, lymphoid, and other neoplasms [12].

The 100% of cancer occurrence in DMBA induced mice in this study is in accordance with the incidence rate of cancers in the study presented by Tedardi et al. [12]. The purpose was to investigate possible correlations of the deletion of one Cx43 allele on cancer development in different organs. The statistical analysis demonstrated a higher incidence of lung cancer in $Cx43^{+/-}$ mice when compared to wild-type animals.

Gap junctions are known to be involved in lung carcinogenesis. This information can be clearly demonstrated by Cesen-Cummings et al. study [17]. They cultivated human and mouse cell lines of normal and neoplastic lung tissues and compared the cell-to-cell transfer of Lucifer Yellow coupling dye, observing a higher dye transfer in nonaffected tissue than in cancerous ones (represented by lung small cell carcinoma, squamous cell carcinoma, adenocarcinoma and large cell carcinoma in human cell lines and carcinoma in mouse cell line) [17]. Coculturing the normal and cancer cells, they still noted the lower capacity of neoplastic cells to communicate with each other and with normal cells [17].

Several studies evidenced the correlation of Cx43 expression in lung carcinogenesis. Human and mouse lung cancer

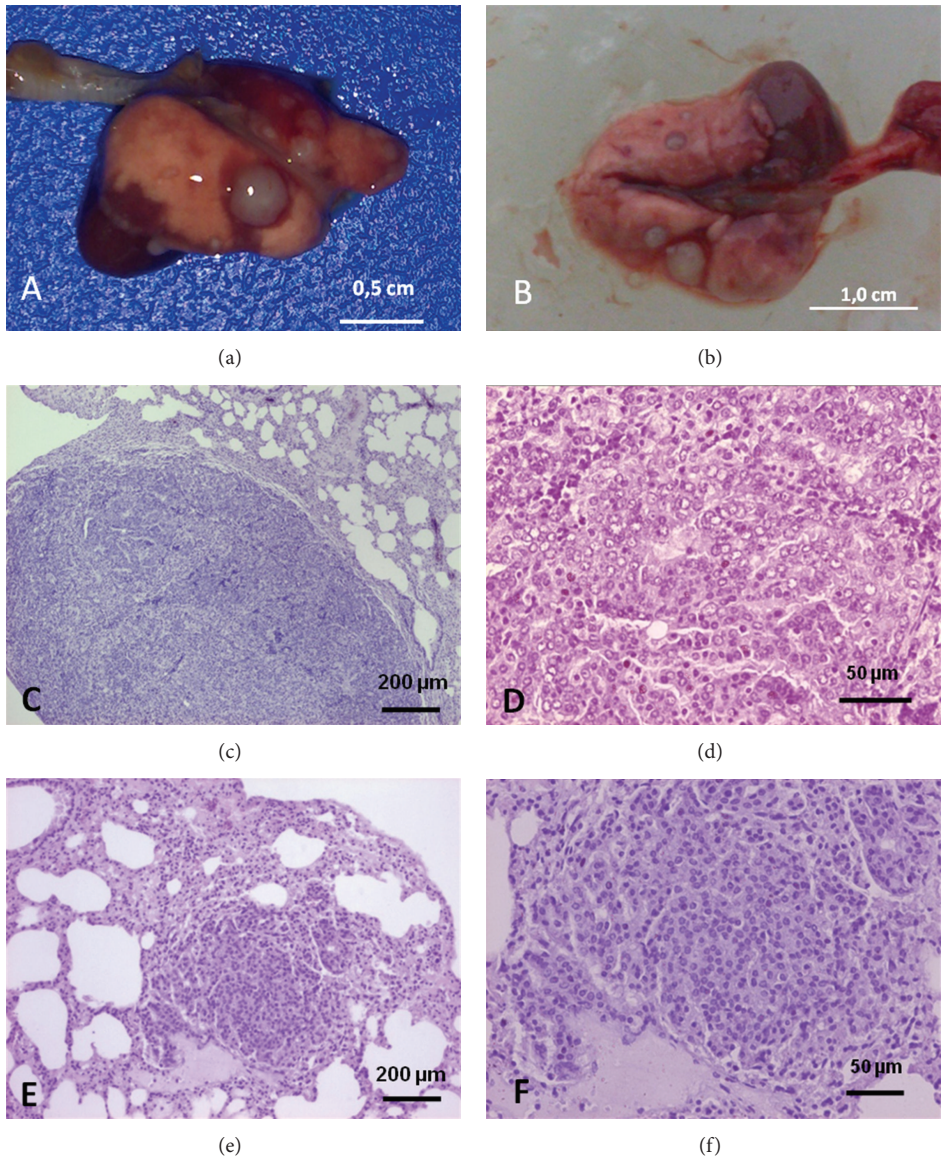

FIGURE 2: (a) Gross picture of $Cx43^{+/-}$ mouse lung, showing gray nodules of 0.1–0.3 cm of diameter. (b) Gross picture of $Cx43^{+/+}$ mouse lung, showing red and grey nodules of 0.3 cm or less of diameter. Bar = 0,5 cm, and bar = 1,0 cm. (c) and (d). Lung bronchial carcinoma, H&E, bar = 200 μm, and bar = 50 μm. (e) and (f). Lung with solid papillary adenomas, H&E, 200 μm, and 50 μm.

cell lines had a lower expression of connexin 43 by Western blot and Southern blot analysis [17] and immunohistochemistry. In a study with 107 samples of human lung cancers, it has been shown a decrease in numbers of Cx43 spots and loose of membrane stain with replacement by cytoplasm subcellular localization of connexins [18]. The relation of decreased expression of both Connexin 43 and E-cadherin was associated with a poor differentiation, advanced TNM stage, and lymph node metastasis [18]. The expression decay occurred progressively from normal distant tissue to adjacent tissue and cancer nodules and is related to nodal lung micrometastasis [19]. Connexin 43 expression also correlated with the cancer degree of differentiation. It has been shown that poorly differentiated lung adenocarcinoma and squamous cell carcinoma expressed lower levels than well-differentiated and moderate-differentiated cancers [20]. This aberrant expression could be explained by promoter methylation, probably for AP1 binding, [19].

Higher incidence of lung tumors was initially described by our research group. Heterozygous knockout mice $Cx43^{+/-}$ presented statistically more lung papillary adenomas and with a higher number of cells stained for PCNA than wild-type animals. Furthermore, the lesions had larger areas, and these animals presented lower expression or Cx43 mRNA [14]. This experiment used urethane induction, and mice lived only 6 months; maybe the short experiment duration and the different carcinogen used could explain why we found correlation with malignant tumors and not with benign ones.

Another study from our group using NNK for lung carcinogenesis induction corroborates the $Cx43^{+/-}$ susceptibility

Table 2: Cancer incidence in DMBA wild-type and heterozygote mice induced groups.

Cancer topography	Heterozygote ($Cx43^{+/-}$)	Wild-type ($Cx43^{+/+}$)	Odds ratio (95% IC)[1]	Relative risk (95% IC)[1]	*P* value
Mammary gland	36	27	1.128 (0.5708–2.230)	1.067 (0.7399–1.538)	0.7285
Lymphoid tissue	32	26	0.9732 (0.4902–1.932)	0.9846 (0.6662–1.455)	0.9380
Digestive tract	20	16	1.000 (0.4640–2.155)	1.000 (0.5694–1.756)	1.0000
Lung	21	7	2.944 (1.155–7.506)	2.400 (1.094–5.264)	0.0200*
Skin	10	9	0.8718 (0.3296–2.306)	0.8889 (0.3859–2.047)	0.7820
Ovary	10	3	2.923 (0.7664–11.150)	2.667 (0.7678–9.262)	0.1436
Total	**75**	**60**	—	—	—

[1]Values calculated using wild-type mice ($Cx43^{+/-}$) cancer incidence for reference to compare with cancer incidence with heterozygote group ($Cx43^{+/+}$).
*Results of *P* value less than 5%.

to spontaneous and induced lung cancer and demonstrates that in the heterozygous mice, nodules were larger and surprising expressing higher levels of Cx43 mRNA [21]. Lung neoplasms, spontaneous, or chemical induced are known to be generated by alveolar type II epithelial cells (APTIIs) [22, 23]. $Cx43^{+/-}$ animals had a lower cell-to-cell communication capacity and elevated proliferation of APTIIs [22], and the transfection of *Gja1* (Cx43 gene) gene in E9 APTII neoplasia cells, in other study, reestablished and rendered these cells to a nonneoplastic state [23]. The role of Cx43 must be extensively studied for molecular carcinogenesis processes comprehension in the lung.

Another point to highlight is the ovarian cancer occurrence in this experiment. It is known that the connexin 43 is expressed in ovarian tissue, being governed by gonadotropins in transcription, translation, and posttranslational modification. Within their physiological functions, Cx43 plays a role in the control of follicular genesis and oogenesis and seems to act here as a tumor suppressor gene [24]. According to Fernstrom et al. (2002) [25], gap junction proteins are often reduced in neoplastic cells, including cells of ovarian carcinoma. The same group of researchers conducted an interesting study *in vitro* to gene therapy, using the Cx43 directed to ovarian cancer. Transfecting ovarian carcinoma cells with Cx43 gene decreased cell proliferation and increased sensitivity to adriamycin, suggesting that communication by gap junction and/or Connexin 43 is able to suppress the neoplastic phenotype of ovarian carcinoma cells and its low expression is involved in neoplastic transformation of these cells. Although our observations in this paper have not found statistically significant differences in values between the groups, in absolute numbers, in the group with heterologous deletion of Cx43, there was a higher incidence of ovarian neoplasms, above twice than manifested in wild group. It is possible that if a larger number of animals were studied, the correlation would demonstrate what strongly corroborate with this role assigned to Cx43, whose depletion could favor the ovarian carcinogenesis.

5. Conclusion

The Cx43 deficient mice predisposition to lung neoplasms had been demonstrated as well as the gap junction role in the carcinogenic process in this organ. Our study strengthens the evidence by DMBA carcinogenic protocol, which is not a lung-specific carcinogen. In addition, the predisposition of ovary granulosa cell carcinoma for Connexin 43 deficiency had a consistent literature basement, and the authors suggest further studies to correlate both *in vivo* in a more specific carcinogenic model for this kind of tumor.

Acknowledgments

This work is part of the Ph.D. thesis of Krishna Duro de Oliveira, in the Postgraduation Program in Experimental and Comparative Pathology, School of Veterinary Medicine and Animal Science, University of São Paulo. Marcello Vannucci Tedardi participated in this project as a Scientific Initiation Fellow of Fundação de Amparo a Pesquisa do Estado de São Paulo, FAPESP, proc. 2010/00874-2. The project has also received a financial support from FAPESP, proc. 2010/08480-3.

References

[1] M. Mesnil, "Connexins and cancer," *Biology of the Cell*, vol. 94, no. 7-8, pp. 493–500, 2002.

[2] M. Vinken, T. Vanhaecke, P. Papeleu, S. Snykers, T. Henkens, and V. Rogiers, "Connexins and their channels in cell growth and cell death," *Cellular Signalling*, vol. 18, no. 5, pp. 592–600, 2006.

[3] M. L. Zaidan Dagli and F. J. Hernandez-Blazquez, "Roles of gap junctions and connexins in non-neoplastic pathological processes in which cell proliferation is involved," *Journal of Membrane Biology*, vol. 218, no. 1–3, pp. 79–91, 2007.

[4] K.-K. Luiza, S. Stanislaw, K. Mariusz, W. Andrzej, R. Tadeusz, and M. Mariola, "The role of connexins in carcinogenesis:

review of current knowledge," *Current Signal Transduction Therapy*, vol. 2, no. 1, pp. 49–56, 2007.

[5] D. S. Sanches, C. G. Pires, H. Fukumasu et al., "Expression of connexins in normal and neoplastic canine bone tissue," *Veterinary Pathology*, vol. 46, no. 5, pp. 846–859, 2009.

[6] R. Kar, N. Batra, M. A. Riquelme, and J. X. Jiang, "Biological role of connexin intercellular channels and hemichannels," *Archives of Biochemistry and Biophysics*, vol. 524, no. 1, pp. 2–15, 2012.

[7] L. N. Torres, J. M. Matera, C. H. Vasconcellos, J. L. Avanzo, F. J. Hernandez-Blazquez, and M. L. Z. Dagli, "Expression of connexins 26 and 43 in canine hyperplastic and neoplastic mammary glands," *Veterinary Pathology*, vol. 42, no. 5, pp. 633–641, 2005.

[8] J. C. Sáez, V. M. Berthoud, M. C. Brañes, A. D. Martínez, and E. C. Beyer, "Plasma membrane channels formed by connexins: their regulation and functions," *Physiological Reviews*, vol. 83, no. 4, pp. 1359–1400, 2003.

[9] J. K. Chipman, A. Mally, and G. O. Edwards, "Disruption of gap junctions in toxicity and carcinogenicity," *Toxicological Sciences*, vol. 71, no. 2, pp. 146–153, 2003.

[10] B. Cogliati, T. C. Da silva, T. P. A. Aloia et al., "Morphological and molecular pathology of CCL4-induced hepatic fibrosis in connexin43-deficient mice," *Microscopy Research and Technique*, vol. 74, no. 5, pp. 421–429, 2011.

[11] W. R. Loewenstein and Y. Kanno, "Intercellular communication and the control of tissue growth: lack of communication between cancer cells," *Nature*, vol. 209, no. 5029, pp. 1248–1249, 1966.

[12] M. V. Tedardi, K. D. Oliveira, G. U. Avanzo et al., "Chemical carcinogenesis by 7, 12- dimethylbenzanthracene in BALB/c mice," Annals of the 4th Symposium of the Latin American Society of Toxicologic Pathology, LASTP, http://www.alaptox.net .

[13] A. G. Reaume, P. A. De Sousa, S. Kulkarni et al., "Cardiac malformation in neonatal mice lacking connexin43," *Science*, vol. 267, no. 5205, pp. 1831–1834, 1995.

[14] J. L. Avanzo, M. Mesnil, F. J. Hernandez-Blazquez et al., "Increased susceptibility to urethane-induced lung tumors in mice with decreased expression of connexin43," *Carcinogenesis*, vol. 25, no. 10, pp. 1973–1982, 2004.

[15] V. Turusov and U. Mohr, *Pathology of Tumours in Laboratory Animals: Tumors of the Mouse*, IARC Scientific Publication (WHO), Lyon, France, 2nd edition, 1994.

[16] K. Yamakage, Y. Omori, C. Piccoli, and H. Yamasaki, "Growth control of 3T3 fibroblast cell lines established from connexin 43-deficient mice," *Molecular Carcinogenesis*, vol. 23, pp. 121–128, 1998.

[17] K. Cesen-Cummings, M. J. Fernstrom, A. M. Malkinson, and R. J. Ruch, "Frequent reduction of gap junctional intercellular communication and connexin43 expression in human and mouse lung carcinoma cells," *Carcinogenesis*, vol. 19, no. 1, pp. 61–67, 1998.

[18] H.-T. Xu, Q.-C. Li, Y.-X. Zhang et al., "Connexin 43 recruits E-cadherin expression and inhibits the malignant behaviour of lung cancer cells," *Folia Histochemica et Cytobiologica*, vol. 46, no. 3, pp. 315–321, 2008.

[19] J.-T. Chen, Y.-W. Cheng, M.-C. Chou et al., "The correlation between aberrant connexin 43 mRNA expression induced by promoter methylation and nodal micrometastasis in non-small cell lung cancer," *Clinical Cancer Research*, vol. 9, no. 11, pp. 4200–4204, 2003.

[20] Y. Jinn, M. Ichioka, and F. Marumo, "Expression of connexin32 and connexin43 gap junction proteins and E-cadherin in human lung cancer," *Cancer Letters*, vol. 127, no. 1-2, pp. 161–169, 1998.

[21] H. Fukumasu, J. L. Avanzo, D. S. Sanches, G. Mennecier, C. M. C. Mori, and M. L. Z. Dagli, "Higher susceptibility of spontaneous and NNK-induced lung neoplasms in connexin 43 deficient CD1×AJ F1 mice: paradoxical expression of connexin 43 during lung carcinogenesis," *Molecular Carcinogenesis*, vol. 52, no. 7, pp. 497–506, 2013.

[22] J. L. Avanzo, G. Mennecier, M. Mesnil et al., "Deletion of a single allele of Cx43 is associated with a reduction in the gap junctional intercellular communication and increased cell proliferation of mouse lung pneumocytes type II," *Cell Proliferation*, vol. 40, no. 3, pp. 411–421, 2007.

[23] K. A. Peebles, M. W. Duncan, R. J. Ruch, and A. M. Malkinson, "Proteomic analysis of a neoplastic mouse lung epithelial cell line whose tumorigenicity has been abrogated by transfection with the gap junction structural gene for connexin 43, Gja1," *Carcinogenesis*, vol. 24, no. 4, pp. 651–657, 2003.

[24] E. Gershon, V. Plaks, and N. Dekel, "Gap junctions in the ovary: expression, localization and function," *Molecular and Cellular Endocrinology*, vol. 282, no. 1-2, pp. 18–25, 2008.

[25] M. J. Fernstrom, L. D. Koffler, G. Abou-Rjaily, P. D. Boucher, D. S. Shewach, and R. J. Ruch, "Neoplastic reversal of human ovarian carcinoma cells transfected with Connexin43," *Experimental and Molecular Pathology*, vol. 73, no. 1, pp. 54–60, 2002.

Hindawi Publishing Corporation
BioMed Research International
Volume 2013, Article ID 976816, 11 pages
http://dx.doi.org/10.1155/2013/976816

Research Article

The Human Cell Surfaceome of Breast Tumors

Júlia Pinheiro Chagas da Cunha,[1,2] Pedro Alexandre Favoretto Galante,[1,3] Jorge Estefano Santana de Souza,[1,4] Martin Pieprzyk,[5] Dirce Maria Carraro,[6] Lloyd J. Old,[7] Anamaria Aranha Camargo,[1,3] and Sandro José de Souza[1,8]

[1] *Ludwig Institute for Cancer Research, São Paulo 01308-050, SP, Brazil*
[2] *Center for Applied Toxinology, Butantan Institute, São Paulo 05503-900, SP, Brazil*
[3] *Centro de Oncologia Molecular Hospital Sírio-Libanês, São Paulo 01308-050, SP, Brazil*
[4] *Instituto de Bioinformática e Biotecnologia, Natal 59064-560, RN, Brazil*
[5] *Fluidigm Inc., South San Francisco 94080, CA, USA*
[6] *Hospital AC Camargo, São Paulo 01509, SP, Brazil*
[7] *Ludwig Institute for Cancer Research, New York 10017, NY, USA*
[8] *Brain Institute, Federal University of Rio Grande do Norte, Natal 59064-560, RN, Brazil*

Correspondence should be addressed to Júlia Pinheiro Chagas da Cunha; julia.cunha@butantan.gov.br

Received 21 March 2013; Accepted 22 July 2013

Academic Editor: Lubna Nasir

Introduction. Cell surface proteins are ideal targets for cancer therapy and diagnosis. We have identified a set of more than 3700 genes that code for transmembrane proteins believed to be at human cell surface. *Methods*. We used a high-throuput qPCR system for the analysis of 573 cell surface protein-coding genes in 12 primary breast tumors, 8 breast cell lines, and 21 normal human tissues including breast. To better understand the role of these genes in breast tumors, we used a series of bioinformatics strategies to integrates different type, of the datasets, such as KEGG, protein-protein interaction databases, ONCOMINE, and data from, literature. *Results*. We found that at least 77 genes are overexpressed in breast primary tumors while at least 2 of them have also a restricted expression pattern in normal tissues. We found common signaling pathways that may be regulated in breast tumors through the overexpression of these cell surface protein-coding genes. Furthermore, a comparison was made between the genes found in this report and other genes associated with features clinically relevant for breast tumorigenesis. *Conclusions*. The expression profiling generated in this study, together with an integrative bioinformatics analysis, allowed us to identify putative targets for breast tumors.

This paper is in the memory of Lloyd J. Old

1. Introduction

Breast tumors are among the most common fatal cancers, accounting for half of the total cancer deaths in women [1]. It has been shown that breast cancer is a very heterogeneous disease with four different molecular profiles based on the expression pattern of ERBB2, estrogen and progesterone receptors, and histological grade. These classes are also associated with distinct clinical outcomes and responses to therapy [2].

According to the American Society of Clinical Oncology [3], breast cancers express some additional markers that have been shown to be useful in clinic: CA15-3, CA27.29, carcinoembryonic antigen (CEA), urokinase plasminogen activator, and plasminogen activator inhibitor 1, among others. Several of these markers are cell surface transmembrane proteins, including ERBB2 and CEA. In addition, gene signatures identified by gene-expression profiling of breast tumors, such as the MammaPrint [4], which calculates a

prognostic score for node-negative patients at stage I or II based on the expression of a pool of 70 genes, contain more than 10% of trans-membrane (TM) proteins believed to be at the cell surface [5].

Some of these cell surface markers are used as targets for therapies against breast cancer. Targeted therapies, such as lapatinib (Tykerb) [6], bevacizumab (Avastin) [7], and trastuzumab (Herceptin), are gaining special attention in cancer treatment as they act directly to cancer cells avoiding the destruction of healthy cells. Two of them are monoclonal antibodies that block directly or indirectly the activation of a trans-membrane receptor. Herceptin binds to the extracellular domain of ERBB2 and is used routinely in the treatment of patients with ERBB2 positive breast tumors. However, ERBB2 is just over expressed in 20–25% of invasive breast tumors [8, 9]. These facts emphasize the importance of exploring cell surface proteins in tumors to identify new tumor targets. Besides being targets for monoclonal antibodies that block their function, trans-membrane proteins can also be used to allow the entrance of drugs or radioactive material directly into cancer cells.

A catalog of 3,702 genes coding for TM proteins located at the surface of human cells (human cell surfaceome) was generated by us through the use of bioinformatics approaches [5]. New targets for colorectal and glioblastoma (GBM) tumors have been identified using this collection of cell surface proteins. Here we explored the human cell surfaceome searching for breast tumors targets using a high-throughput quantitative real-time PCR (qPCR) in tumor samples and tumor cell lines. Furthermore, we compared our data with other expression profiles publically available taking into consideration some clinical features important for breast tumors.

2. Materials and Methods

2.1. Public Data. Breast cancer somatic mutations were obtained from Sjöblom et al. [10] and Wood et al. [11]. Homozygotic deletions and genomic amplifications in breast cancer were retrieved from Leary et al. [12]. The genomic coordinates for these alterations were determined through a local mapping using BLAT and crossed against surfaceome genes coordinates. Gene pathways were downloaded from KEGG (http://www.genome.jp/kegg/). To build the protein protein interaction (PPI) database, data from MINT (December 2007 version), BIOGRID (2.0.37), INTACT (January 2008 version), HPRD (September 2007 version), BIND (May 2006 version), and DIP (January 2008 version) were used. Data obtained exclusively from functional interactions (e.g., genetic interactions present in BIOGRID) and mass spectrometry-based methods were excluded.

2.2. Samples. The twelve breast tumor samples (ERBB2 negative) were obtained from the Tumor Tissue Biobank of the Medical and Research Center, A.C. Camargo Hospital, São Paulo, after local ethics committee approval. Human tumor breast cell lines (HCC1954, MCF7, MDA231, MDA435, MDA436, MDA468, and SK-BR 3) were obtained from American Type Culture Collection (ATCC) and cultured following ATCC instructions. A nontumorigenic and non-transformed breast cell line (HB4A) was obtained from reduction mammoplasty tissue [13]. Total RNA derived from 21 normal human tissues (thymus, prostate, fetal brain, trachea, skeletal muscle, fetal liver, uterus, small intestine, heart, bone marrow, kidney, stomach, liver, spleen, spinal cord, lung, testis, placenta, brain whole, breast, and colon) was purchased from Clontech.

2.3. Primer Design. Primers and the specific UPL probes were designed using the Universal ProbeLibrary Assay Design Center (http://qpcr.probefinder.com/organism.jsp) by automatically selecting an intron spanning assay. Rpl27 (NM_021574.2—ribosomal protein l27) and bcr (NM_021574.2—breakpoint cluster region) were used as the references genes. All primers and probes used are available in [5].

2.4. RNA Extraction, cDNA Synthesis, and Preamplification Reaction. RNA extraction, cDNA synthesis, and pre-amplification reaction were performed as previously described in [5]. Briefly, total RNA was extracted by using Trizol (Invitrogen), and its integrity, checked by Bioanalyser (Agilent). SuperScript III First-Strand Synthesis SuperMix (Invitrogen) was used to synthesize cDNA from 200 ng of DNA-free RNA. For the pre-amplification reaction, one fourth of cDNA (synthesized as described above) was pooled with all primers (50 nM), 10 μL of 2 X PreAmp Master Mix (Applied Biosystems) in a cycling program of 14 cycles of 95°C for 15 sec and 60°C for 4 min.

2.5. qPCR. The qPCR reactions for 573 genes were performed in 96.96 dynamic array chips (Fluidigm) as previously described [5] following the manufacturer's instructions. In summary, the assay inlets of the M96 Dynamic Array were loaded with 2 μM forward primer, 2 μM reverse primer, 1 μM UPL probe, and 0.025% Tween 20 while each sample inlets was loaded with 2.5 μL of PreAmp sample, 3.25 μL of 2 X AB Universal TaqMan Master Mix (Applied Biosystems), and 0.32 μL of 20 X DA Sample Loading Solution (Fluidigm). The cycling program used consisted of 2 min at 50°C, 10 min at 95°C followed by 35 cycles of 95°C for 15 sec, 70°C for 5 sec, and 1 min at 60°C. All reactions were performed in triplicates.

2.6. Data Processing of qPCR and Selection of Overexpressed Genes. The BioMark Gene Expression Data Analysis was used to obtain the CT values and to discriminate between high-quality and low-quality reactions. Low-quality reactions and CTs higher than 30 were excluded from these analyses and named as not available (NA). The $2^{-\Delta\Delta CT}$ [14] method was used to obtain the relative gene expression values; normal whole breast (from Clontech) was used as a reference, and Rpl27 and bcr were used as reference genes. Genes were considered overexpressed in breast tumors if 3 or more primary breast tumors had a fold change higher than three times the standard deviation in all three replicates. Genes expressed in 5 or less normal tissues were considered restrictedly expressed. In order to be considered expressed,

the gene/sample must have a fold change value higher than 0.1 in two qPCR experiments. Expression in fetal brain, fetal liver, brain, placenta, and testis was not considered in this analysis.

2.7. Comparative Analysis Using ONCOMINE. For the analysis of overexpression in other tumor types, the ONCOMINE website (http://www.oncomine.org) was used for searching individually ("Gene search") the presence of each of the 77 overexpressed genes in the studies that compare "Cancer & Normal" with P value < 0.01. For the correlation analysis of over expression and prognosis, tumor grade and stage, we searched ("Profile Search") genes over expressed (P-value < 0.01) on breast studies using the filters "Prognosis," "Grade" and "Stage" existing at the ONCOMINE website (http://www.oncomine.org). Manual inspections of the studies were performed in others to select the most concordant (regarding samples types) in each category.

3. Results and Discussion

3.1. Genes Differentially Expressed in Breast Tumors. Recently, we have generated a catalog of 3,702 genes that codes for trans-membrane proteins located at cell surface [5]. In that report, we further selected 573 cell surface genes as the most promising candidates for cancer diagnostics and therapy based on their expression profiling through the use of Massively Parallel Signature Sequencing (MPSS) and Serial Analysis of Gene Expression (SAGE) libraries. We validated this strategy by finding potential new human targets for GBM and colorectal tumors. Here, we analyzed the expression of these 573 genes in 12 primary breast tumors, 1 normal breast tissue, 7 breast tumor cell lines, and 1 normal breast cell line using a high-throughput qPCR platform. We also analyzed these 573 genes in a panel of 21 normal samples obtained from our previous publication [5].

An ideal candidate for breast cancer diagnostics and therapy would be a gene product that is over expressed in breast tumors and expressed in a restricted pattern in normal tissues. Based on that, our qPCR data was analyzed for genes expressed in less than 6 normal tissues and overexpressed in at least 3 primary breast tumors when compared to normal breast tissue. We found two genes showing this expression pattern: C3orf57 and LRRC26. According to our data, the former is expressed in brain, prostate, and stomach while the latter in colon and prostate. C3orf57 (also known as ADMP), a putative G-protein coupled receptor, is also expressed in prostate epithelium and was shown to be downregulated by androgens in mice cells [15]. LRRC26, a leucine-rich repeat protein, has been previously shown to be increased in breast, prostate, colon, and pancreatic cancers. However, its subcellular localization is still a matter of debate in spite of the presence of a trans-membrane domain [16].

Irrespective of the expression pattern in normal tissues, we found 77 genes that were over expressed (in relation to normal breast) in primary breast tumors (Figure 1). Interestingly, these genes are enriched in specific genomic locations. Eight (CADM4, FXYD5, GPR77, PSENEN, SPINT2, TMEM147, TYROBP, and UPK1A) out of 77 genes are localized at chromosome 19q (P-value 0.006). In addition, an enrichment at the chromosome cytoband 1p35 (IFI6, PTPRU, SERINC2, and SLC2A1) is also observed (P-value 4.5E-4). Interestingly, this cytoband is associated with sporadic colorectal cancer, an Epstein-Barr virus integration site, and with some hormone-dependent syndromes such as serkal syndrome, mullerian aplasia, and hyperandrogenism (OMIM—http://www.ncbi.nlm.nih.gov/Omim/getmap.cgi?ll32850). SLC2A1, also known as GLUT-1, is a glucose transporter, that is mutated in GBM and pancreatic tumor. Furthermore, it is expressed in various tumors, like oral squamous cell carcinoma [17], primary renal tumors [18], ovarian carcinoma [19], colorectal tumors [20], thyroid carcinomas [21], and gallbladder carcinomas [22]. Differential expression of this gene in breast tumors emphasizes the importance of glucose transporters in the glucose requirements in cancer cells. As we used only ERBB2 negative samples in this study, this gene accordingly was not present in our list of over expressed genes.

Next, we looked at protein-protein interaction (PPI) networks, KEGG, and the literature to find common interaction partners among differentially expressed surfaceome genes, as we did in [5] (Figure 2). Four genes (TNFRSF19, TNFRSF12A, TMEM109, and TMBIM6) interact with members of the TRAF family. TRAF proteins are TNF receptor-associated factors that serve as adapter proteins for a wide variety of cell surface receptors. They regulated the activation of many signal transduction pathways, such as JNK, ERK, and NF-κB culminating in regulation of cell survival, apoptosis, and differentiation [23].

Furthermore, we found that GIPC1, a member of PDZ domain containing family that has already been detected as overexpressed in breast tumors [24], interacts with four genes of our list of overexpressed surfaceome genes (SDC3, SDC4, SLC2A1, and FDZ3). GIPC1 leads to an increase of TGF beta receptors and may interfere with TGF beta signaling [25]. SDC3 and SDC4 are syndecans that contain heparan and chondroitin sulfates chains that play a role in cell-cell and cell-matrix interactions [26]. Orend et al. [27] proposes that SDC4 may play an important role in the control of anchorage-dependent cellular proliferation of fibroblasts. The FZD3, a member of frizzled gene family, contributes to the Wnt signaling pathway which leads to an increase of the beta-catenin in the nucleus promoting specific gene expression [28]. MPSS analysis also confirms that this gene is over expressed in breast tumors (data not shown).

3.2. Further Validation of Overexpressed Genes. To gain more information on the surfaceome genes over-expressed in breast tumors, a comparison with expression data from other sources was performed. We first compared our list of genes with our previous study [5] in which the expression of the same set of genes was evaluated in colorectal tumors and GBM. Seven (GPR172A, IFI6, NPFFR2, REEP6, SLC2A1, SQLE, and TNFRSF12A) and 13 (CD300LF, CD72, CMTM3, GPR172A, MMP14, P2RY11, SERINC2, TMEM134, TNFRSF12A, TNFRSF19, TYROBP, VSIG4, and ZDHHC12) genes are also over expressed in colorectal tumors and GBM,

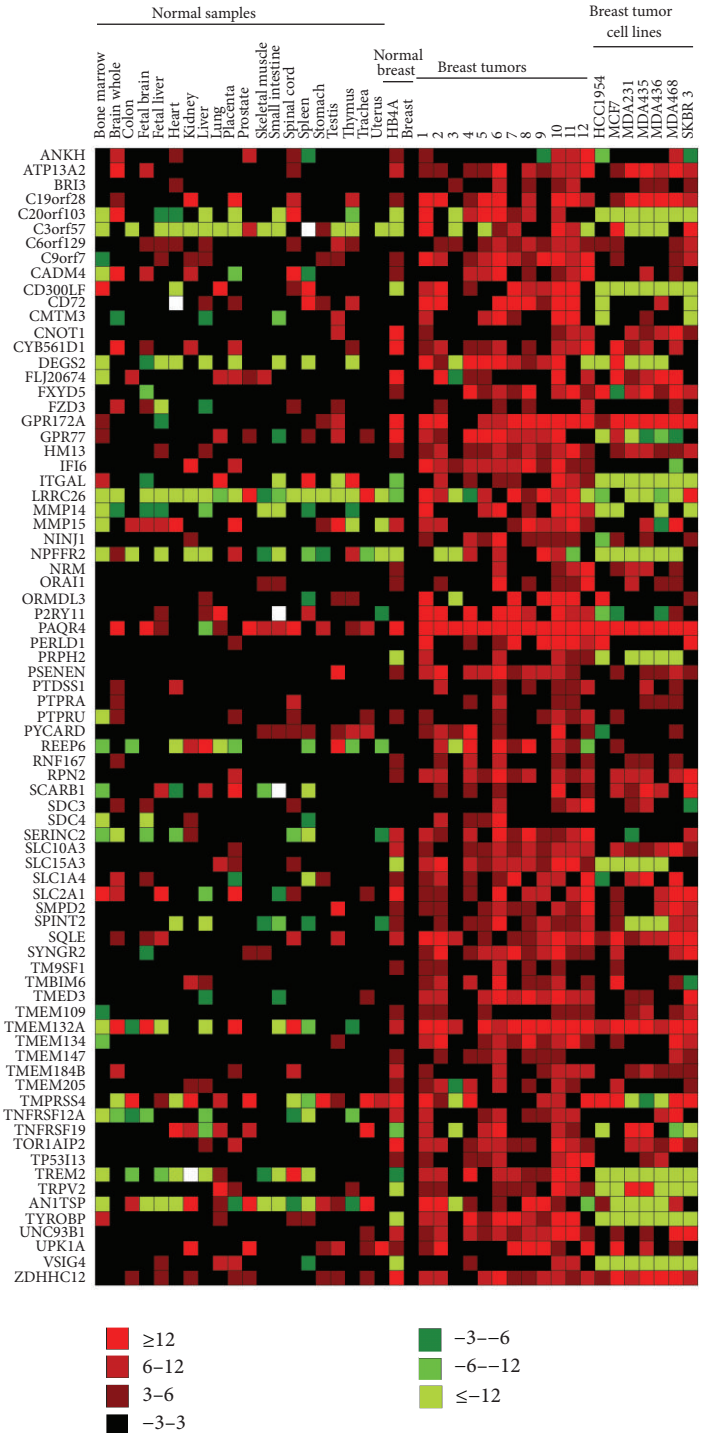

Figure 1: Expression profile of surfaceome genes in normal tissues, breast cancer cell lines, and breast tumor samples. Expression data for normal tissues was obtained from [5]. Colors represent the fold changes values obtained by qPCR (average of three qPCRs experiments) using normal breast as a reference sample and Rpl.27 as a reference gene. Red, green and black squares represent, respectively, genes over-expressed (fold changes ranging from 3 to 5.99, 6 to 11.99, and higher than 12 standard deviation values), genes downregulated (fold changes ranging from −3 to −5.99, −6 to −11.99, and lower than −12 standard deviation values), or genes equally expressed between the respective sample and reference. White squares represent noninformative data points.

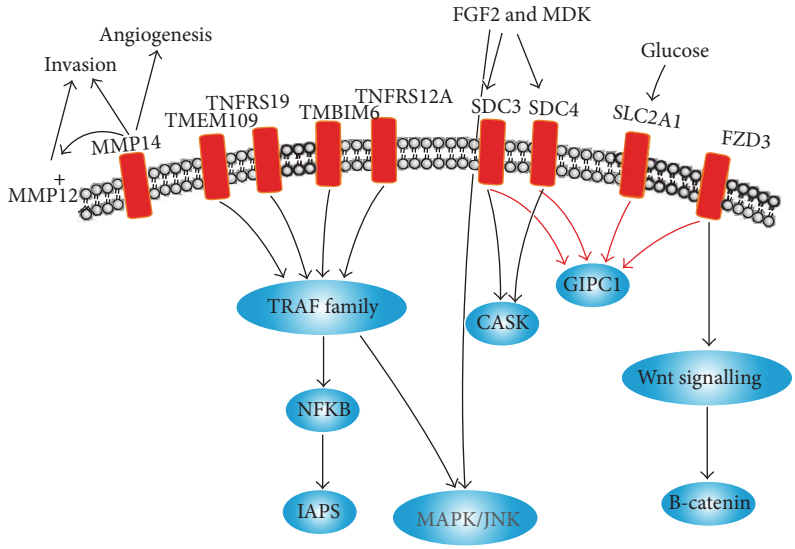

Figure 2: Schematic view of key pathways represented in the set of surfaceome genes overexpressed in breast tumors (see text for more details). Interactions represented by black arrows were derived from protein-protein interaction networks while interactions represented by red arrows were derived from either the literature or KEGG database.

respectively. Among them, MMP14, a membrane-bound matrix metalloprotease (MMP), seems one of the most interesting. It has been associated with tumorigenesis, metastasis, and angiogenesis [29–31] and activates pro-MMP2 [32, 33], a MMP known to be critically involved in tumor spreading. Recently, Devy et al. [34] identified a human antibody that is a potent and highly selective inhibitor of MMP-14. It reduces the incidence of metastases in orthotopic mouse model, displayed anti-invasive activity, and inhibited angiogenesis. The authors propose that this inhibitor could be used for the treatment of solid tumors.

Moreover, we compared the expression of our set of overexpressed surfaceome genes in breast tumors to 16 other tumor types, including breast, using microarray data from studies available at ONCOMINE (http://www.oncomine.org). As shown in Table 1, we confirmed that more than a half (57,1%) of our genes are overexpressed in at least another study using breast tumors. The other part, however, most probably reflects different experimental sensitivities between qPCR and microarray as well as different breast tumor types. In addition, 53 out of 77 are over expressed in more than 4 tumor types.

It is also important to know whether any of our over expressed surfaceome genes is associated with a clinically relevant characteristic. Genes that are overexpressed (P values < 0.01) in studies that compared samples with distinct prognosis, grades, or stages of breast tumors were selected by looking at the ONCOMINE dataset (Table 2). Thirty-seven out of 77 genes were expressed (in at least one study) in breast tumors of higher grades. Concerning the staging of breast cancer using the TNM classification, six genes (FXYD5, MMP15, PTPRU, SQLE, TM9SF1, and TNFRS12A) are overexpressed in samples with increased spread to lymph nodes, while one gene (TYROBP) is over expressed when breast tumors samples without and with metastasis were compared. Twenty-five out of 77 genes are over expressed in samples derived from patients with high mortality rate within 5 years while 24 out of 77 genes are over expressed in samples derived from patients that relapsed within 5 years.

The result of these comparisons strongly suggests that the set of surfaceome genes generated in this report is enriched with genes important for breast tumor.

3.3. Surfaceome Genes and Genetic Alterations in Breast Tumors. We also analyzed whether the human surfaceome is associated with genes commonly altered in breast tumors based on previously published data [35] that investigated the presence of homozygous deletion, chromosome amplification, and somatic mutation in breast tumor samples. Eighteen surfaceome genes (BVES, C9orf11, CDH3, FAT, LINGO2, LRRC19, MTNR1A, OR4C6, OR4S2, PCDH8, POPDC3, PTCHD3, PTPLAD2, ROBO2, SGPP1, SLITRK1, TEK, and TLR3) were found previously to be homozygously deleted in breast tumors. Not surprisingly, none of them are present in our list of over expressed genes. In contrast, 116 surfaceome genes are localized in genomic regions that contain focal amplifications in cancer (Figure 3 and See Table S1 in Supplementary Material available online at http://dx.doi.org/10.1155/2013/976816). GPR172A, ORMDL3, PERLD1, PRPH2, and TREM2 are presented in our list of over expressed genes. Among them, PERLD1 is located in a chromosome 17 locus together with well known oncogenes (MYC, ERBB2, MET, and FGFR2 among others) that are frequently amplified in gastric and breast cancers [36]. However, the subcellular localization of some of these genes is still a matter of debate.

Two hundred and thirty-five surfaceome genes (6,35% of the total surfaceome collection) have been previously identified as having somatic mutations in breast tumor [10, 11]. Four of them (C19orf28, HM13, ITGAL, and MMP15) are

Table 1: Evaluation of breast tumor overexpressed genes in other tumor types according to ONCOMINE.

Gene	Tumors														
	Bladder	Bone marrow	Brain	Breast	Colon	Esophagus	Head and neck	Kidney	Leukemia	Liver	Lung	Ovary	Pancreas	Prostate	Skin
ANKH	—	—	—	—	•	—	•	•	•	—	—	—	•	—	—
ATP13A2	•	—	—	—	—	•	•	—	—	—	—	—	—	•	•
BRI3	—	—	•	•	—	—	•	—	—	—	—	—	—	—	—
C19orf28	•	•	—	•	—	—	—	—	—	—	—	•	•	•	•
C20orf103	—	—	—	•	•	—	•	—	—	—	—	—	•	•	—
C6orf129	—	—	•	•	—	—	•	—	—	—	—	•	—	•	—
C9orf7	•	—	•	•	—	—	—	—	—	—	—	•	—	•	•
C3orf57	—	—	—	—	—	—	—	—	—	—	—	—	—	—	—
CADM4	—	—	•	—	—	—	—	—	—	•	•	—	—	—	•
CD300LF	—	—	—	•	—	—	—	—	—	—	—	—	—	—	—
CD72	•	—	—	•	—	—	•	—	—	—	•	—	—	—	—
CMTM3	—	—	•	•	—	—	—	•	—	—	—	—	—	•	—
CNOT1	•	—	•	•	•	—	—	—	•	—	•	—	—	•	—
CYB561D1	—	•	—	—	—	—	—	—	—	•	—	—	—	•	—
DEGS2	—	—	—	—	—	—	—	—	•	—	—	—	—	—	—
FLJ20674	•	—	•	•	—	—	—	—	—	—	—	—	—	—	—
FXYD5	•	—	•	•	•	—	—	•	—	—	—	•	•	—	—
FZD3	—	—	—	—	—	—	•	—	—	—	•	—	—	—	•
GPR172A	•	—	•	•	•	•	•	—	—	•	•	•	•	•	•
GPR77	—	—	—	—	—	—	•	—	—	—	—	—	—	—	•
HM13	—	—	•	•	•	—	—	—	—	—	—	•	•	—	—
IFI6	•	•	•	•	—	•	•	•	—	•	—	—	•	•	•
ITGAL	—	—	•	—	—	—	—	—	—	—	—	—	—	—	—
LRRC26	—	—	—	—	—	—	—	—	—	—	—	—	—	—	—
MMP14	•	—	•	•	•	•	•	—	—	•	•	•	•	•	•
MMP15	•	—	•	—	—	•	—	—	—	—	•	•	—	•	—
NINJ1	—	—	•	—	•	—	•	•	—	—	—	—	—	—	•
NPFFR2	—	—	—	•	—	—	—	—	—	—	—	—	—	—	—
NRM	—	—	•	•	—	—	—	—	•	•	•	—	—	•	•
ORAI1	—	—	•	—	•	•	—	—	—	—	•	—	—	•	—
ORMDL3	—	•	•	—	•	—	—	•	—	—	—	—	—	—	—
P2RY11	—	—	•	—	—	—	—	—	—	—	—	•	—	•	•
PAQR4	•	—	—	•	—	—	•	—	•	•	•	•	•	—	•
PERLD1	•	—	—	•	—	—	—	•	•	—	—	•	—	—	—
PRPH2	—	—	—	—	—	—	—	—	—	—	—	—	•	—	—
PSENEN	—	—	—	—	—	—	—	—	—	•	—	—	—	—	—
PTDSS1	•	•	•	•	•	•	•	—	•	•	•	•	—	•	•
PTPRA	•	•	•	•	—	•	—	•	•	—	•	—	•	—	•
PTPRU	•	—	—	—	—	•	—	—	•	—	•	•	—	•	•
PYCARD	•	—	•	•	—	—	•	•	—	—	—	—	—	—	—
REEP6	—	•	—	•	—	—	—	•	•	—	—	—	—	—	—
RNF167	—	•	—	—	—	—	—	—	—	—	•	—	—	•	—
RPN2	•	—	•	•	•	•	•	—	•	—	•	•	•	—	•

Table 1: Continued.

Gene	Tumors														
	Bladder	Bone marrow	Brain	Breast	Colon	Esophagus	Head and neck	Kidney	Leukemia	Liver	Lung	Ovary	Pancreas	Prostate	Skin
SCARB1	•	•	—	—	—	•	•	•	—	—	•	—	—	•	•
SDC3	—	—	•	•	—	•	•	•	—	—	•	—	—	•	•
SDC4	•	—	—	—	—	•	•	—	—	—	—	•	—	•	—
SERINC2	—	—	•	•	—	—	—	—	—	•	•	•	•	•	—
SLC10A3	•	•	•	•	—	—	—	—	—	•	—	—	—	—	—
SLC15A3	•	—	•	•	—	•	•	•	—	—	—	—	—	—	—
SLC1A4	—	—	•	•	•	—	•	•	•	•	•	•	—	•	—
SLC2A1	•	•	—	•	•	—	•	•	•	—	•	•	•	—	—
SMPD2	•	—	•	—	—	—	—	•	—	•	•	•	—	—	•
SPINT2	•	—	—	•	—	—	•	•	—	—	•	•	•	•	—
SQLE	•	—	•	•	—	—	•	—	—	•	•	•	—	•	•
SYNGR2	•	—	—	•	•	—	—	•	—	—	•	•	•	•	—
TM9SF1	•	—	•	—	—	—	•	—	•	•	•	•	—	•	—
TMBIM6	•	—	•	—	—	—	—	—	—	—	•	•	•	•	—
TMED3	•	•	•	—	•	—	—	•	•	—	•	—	—	•	•
TMEM109	—	•	—	•	—	—	—	—	•	—	—	—	—	—	•
TMEM132A	•	—	—	•	—	—	•	—	—	—	•	•	•	•	—
TMEM134	•	—	•	—	—	—	—	—	—	—	•	•	—	•	—
TMEM147	—	—	•	—	•	—	—	—	—	•	•	•	—	•	—
TMEM184B	•	—	—	—	—	•	•	•	•	•	•	•	•	•	•
TMEM205	—	—	—	—	—	—	—	—	—	—	—	—	—	—	—
TMPRSS4	—	—	—	—	•	—	—	—	—	—	•	•	—	—	—
TNFRSF12A	—	•	•	—	•	•	•	•	—	—	•	•	—	—	•
TNFRSF19	—	—	•	—	—	—	—	—	—	•	—	—	—	•	—
TOR1AIP2	—	•	•	•	—	—	—	—	—	•	—	—	—	—	—
TP53I13	—	—	•	•	—	—	—	—	—	—	—	—	—	—	—
TREM2	•	—	•	•	—	•	•	•	—	•	—	—	•	—	•
TRPV2	—	—	—	•	—	•	—	—	—	—	—	—	—	•	—
TSPAN1	•	—	—	•	—	•	•	—	—	—	—	•	•	•	—
TYROBP	—	—	•	•	•	—	•	•	—	—	—	—	—	—	—
UNC93B1	•	•	•	•	—	—	—	—	•	—	—	•	—	—	—
UPK1A	—	—	—	•	—	—	—	—	—	—	—	—	—	—	—
VSIG4	—	—	•	•	—	•	•	•	•	—	—	—	—	—	—
ZDHHC12	—	—	•	•	—	—	—	—	—	—	—	•	—	—	—

•: means overexpression in a given tumor in at least one ONCOMINE study ($P < 0.01$).

also over expressed in breast tumors according to our analysis (Table S1).

4. Conclusions

The expression profiling generated in this work, together with an integrative analysis using other genomics information, allows some considerations. First, like in GBM [5], signaling through members of the TRAF family seems to be important in breast tumorigenesis. In particular the gene TNFRSF12A (also known as TWEAK receptor) seems to be critical as it was also detected as overexpressed in GBM and colorectal tumors samples [5]. We confirmed that this gene is significantly overexpressed in breast tumors and seems to be associated with local invasiveness [37]. In addition, MMP15, a metalloproteinase that was found over expressed in our samples, is also over expressed in samples with important clinical features such as higher grades, positive lymph nodes, and poor prognosis (Table 2). It is important to note that this study focus on expression of cell surface gene products thus, well-known cancer genes products localized at cytoplasm or nucleus were not detected in this dataset. In addition, we focused our analysis and discussion on genes that have been previously associated with tumorigenesis and

Table 2: Evaluation of breast cell surface overexpressed genes according to ONCOMINE studies of grade, stage, and prognosis in breast tumors.

	Grade[1]													Stage[2]									Prognosis								
	Bittner	Chin	Desmedt	Farmer	Finak	Ginestier	Hess	Kreike	Ma	Miller	Pollack	Sorlie	Sottiriou	Sottiriou	Zhao	Bittner	T Sorlie	Sorlie	Bittner	Hess	Sorlie	N Sorlie	Sottiriou	Turashvili	Yu	M Sorlie	Bild	Desmedt	Survival[3] Pawitan	Sorlie	VandeVijver	Ma	Disease-free survival[4] Wang	Wang	Van de Vijver	VandeVijver
SQLE	X	X	X	—	—	X	X	X	—	X	—	—	X	X	X	—	—	—	X	—	—	—	—	—	—	—	—	—	X	—	X	—	X	X	X	X
CNOT1	X	X	X	X	—	X	X	—	—	X	—	—	X	—	—	—	—	—	—	—	—	—	—	—	—	—	—	—	X	—	X	—	X	X	—	—
TMEM132A	X	—	X	X	—	X	X	—	—	X	—	—	X	—	—	—	—	—	—	—	—	—	—	—	—	—	—	—	X	—	X	X	—	X	X	—
PTDSS1	X	—	X	—	—	X	X	—	—	X	—	X	X	—	—	—	—	—	—	—	—	—	—	—	—	—	—	—	—	X	—	X	—	—	X	X
RPN2	X	—	X	X	X	X	X	—	—	X	—	—	—	—	—	—	—	—	—	—	—	—	—	—	—	—	—	—	—	—	—	X	—	—	X	X
SLC2A1	X	—	X	X	—	X	—	—	—	X	—	—	X	—	X	—	—	—	—	—	—	—	—	—	—	—	—	—	—	—	—	X	—	—	X	X
GPRI72A	X	—	X	X	—	X	X	—	—	X	—	—	X	—	—	—	—	—	—	—	—	—	—	—	—	—	—	—	X	—	—	X	—	—	X	X
MMP15	—	—	—	X	—	—	X	—	—	—	—	—	X	—	—	—	—	—	—	—	—	X	—	—	—	—	—	—	X	—	X	—	—	—	X	X
UNC93B1	X	—	—	—	—	X	—	—	—	—	—	—	X	—	X	—	—	—	—	—	—	—	—	—	—	—	—	—	—	—	X	—	—	—	X	X
C6orf129	X	—	—	—	—	X	—	—	X	—	—	—	—	—	X	—	—	—	—	—	—	—	—	—	—	—	—	—	X	—	—	—	—	—	—	—
NRM	X	—	—	—	—	X	—	—	X	—	—	—	—	—	—	—	—	—	—	—	—	—	—	—	—	—	—	—	—	—	X	—	—	X	—	—
SLC10A3	X	—	—	—	—	—	—	—	—	X	—	—	—	—	—	—	—	—	—	—	—	—	—	—	—	—	—	—	—	—	X	—	—	X	X	X
CD72	X	—	X	—	—	—	—	—	X	—	—	—	—	X	—	—	—	—	—	—	—	—	—	—	—	—	—	—	—	—	—	—	—	—	—	—
TNFRSF12A	X	—	—	—	—	X	—	—	—	X	—	—	—	—	—	—	—	—	—	—	—	X	—	—	—	—	—	—	—	—	—	—	—	—	—	—
IFI6	X	—	—	—	—	—	—	X	—	—	—	—	—	—	—	—	—	—	—	—	—	—	—	—	—	—	—	—	—	—	X	—	—	X	X	X
BRI3	X	—	—	—	—	—	—	—	—	—	—	—	—	—	X	—	—	—	—	—	—	—	—	—	—	—	—	—	—	—	X	—	—	X	—	X
SCARB1	X	—	—	—	—	—	—	—	—	—	—	—	—	—	—	—	—	—	—	—	—	—	—	—	—	—	—	—	—	—	X	—	—	X	X	X
PERLD1	—	X	—	—	—	—	X	—	—	X	—	—	X	—	—	—	—	—	—	—	—	—	—	—	—	—	—	—	—	—	—	—	—	—	—	—
TRPV2	—	—	—	—	—	X	—	—	—	—	—	—	—	—	—	—	—	—	—	—	—	—	—	—	—	—	—	—	—	—	X	—	—	X	—	—
ORMDL3	X	X	—	—	—	—	—	—	—	—	—	—	—	—	—	—	—	—	—	—	—	—	—	—	—	—	—	—	X	—	—	—	—	—	—	—
C19orf28	X	—	—	—	—	X	—	—	—	—	—	—	—	—	X	—	—	—	—	—	—	—	—	—	—	—	—	—	—	—	—	—	—	—	—	—
PAQR4	X	—	—	—	—	—	—	—	—	X	—	—	—	—	—	—	—	—	—	—	—	—	—	—	—	—	—	—	X	—	—	—	—	—	—	—
TM9SF1	—	—	—	X	—	—	—	—	—	—	—	—	—	—	—	—	—	—	X	—	—	—	—	—	—	—	—	—	X	—	—	—	—	—	—	—
MMP14	—	—	—	—	—	X	—	—	—	—	—	—	—	—	—	—	—	—	—	—	—	—	—	—	—	—	—	—	—	—	X	—	—	X	—	—
PTPRU	—	—	—	—	—	—	—	—	X	—	—	—	—	—	—	—	—	—	—	—	—	—	—	X	—	—	—	—	X	—	—	—	—	—	—	—
TMEM109	X	—	—	X	—	—	—	—	—	—	—	—	—	—	—	—	—	—	—	—	—	—	—	—	—	—	—	—	—	—	—	—	—	—	—	—
P2RY11	—	—	—	X	—	X	—	—	—	—	—	—	—	—	—	—	—	—	—	—	—	—	—	—	—	—	—	—	—	—	—	—	—	—	—	—
UPK1A	—	—	—	X	—	—	—	—	—	—	—	—	—	—	—	—	—	—	—	—	—	—	—	—	—	—	—	—	—	—	—	X	—	—	—	—
CADM4	—	—	—	—	—	X	—	—	—	—	—	—	—	—	—	—	—	—	—	—	—	—	—	—	—	—	—	—	X	—	—	—	—	—	—	—
TYROBP	—	—	—	—	—	—	—	—	—	—	—	X	—	—	—	—	—	—	—	—	—	—	—	—	—	X	—	—	—	—	—	—	—	—	—	—
FXYD5	—	—	—	—	—	—	—	—	—	—	—	—	—	—	—	—	—	—	—	—	—	—	—	—	X	—	—	—	—	—	X	—	—	—	—	—
SPINT2	—	—	—	—	—	—	—	—	—	—	—	—	—	—	—	—	—	—	—	—	—	—	—	—	—	—	—	—	—	—	—	—	—	—	X	X

Table 2: Continued.

	Grade[1]															Stage[2]														Prognosis									
																T					N				M		Survival[3]			Disease-free survival[4]									
	Bittner	Chin	Desmedt	Farmer	Finak	Ginestier	Hess	Kreike	Ma	Miller	Pollack	Sorlie	Sotiriou	Sotiriou	Zhao	Bittner	Sorlie	Sorlie	Bittner	Hess	Sorlie	Sorlie	Sotiriou	Turashvili	Yu	Sorlie	Bild	Desmedt	Pawitan	Sorlie	VandeVijver	Ma	Wang	Wang	Van de Vijver	VandeVijver
SYNGR2	—	—	—	—	—	—	—	—	—	—	—	—	—	—	—	—	—	—	—	—	—	—	—	—	—	—	—	—	—	—	—	—	—	X	X
TMPRSS4	—	—	—	—	—	—	—	—	—	—	—	—	—	—	—	—	—	—	—	—	—	—	—	—	—	—	—	—	—	—	—	—	—	X	X
ORAI1	X	—	—	—	—	—	—	—	—	—	—	—	—	—	—	—	—	—	—	—	—	—	—	—	—	—	—	—	—	—	—	—	—	—	—
ZDHHC12	X	—	—	—	—	—	—	—	—	—	—	—	—	—	—	—	—	—	—	—	—	—	—	—	—	—	—	—	—	—	—	—	—	—	—
SDC4	—	X	—	—	—	—	—	—	—	—	—	—	—	—	—	—	—	—	—	—	—	—	—	—	—	—	—	—	—	—	—	—	—	—	—
SDC3	—	—	—	—	—	X	—	—	—	—	—	—	—	—	—	—	—	—	—	—	—	—	—	—	—	—	—	—	—	—	—	—	—	—	—
TMEM184B	—	—	—	—	—	X	—	—	—	—	—	—	—	—	—	—	—	—	—	—	—	—	—	—	—	—	—	—	—	—	—	—	—	—	—
TOR1AIP2	—	—	—	—	—	—	—	—	X	—	—	—	—	—	—	—	—	—	—	—	—	—	—	—	—	—	—	—	—	—	—	—	—	—	—
TMEM147	—	—	—	—	—	—	—	—	—	—	—	—	—	—	X	—	—	—	—	—	—	—	—	—	—	—	—	—	—	—	—	—	—	—	—
TMED3	—	—	—	—	—	—	—	—	—	—	—	—	—	—	—	—	—	—	—	—	—	—	—	—	—	—	—	X	—	—	—	—	—	—	—
TREM2	—	—	—	—	—	—	—	—	—	—	—	—	—	—	—	—	—	—	—	—	—	—	—	—	—	—	—	—	X	—	—	—	—	—	—
SLC15A3	—	—	—	—	—	—	—	—	—	—	—	—	—	—	—	—	—	—	—	—	—	—	—	—	—	—	—	—	—	—	X	—	—	—	—
VSIG4	—	—	—	—	—	—	—	—	—	—	—	—	—	—	—	—	—	—	—	—	—	—	—	—	—	—	—	—	—	—	X	—	—	—	—
ANKH	—	—	—	—	—	—	—	—	—	—	—	—	—	—	—	—	—	—	—	—	—	—	—	—	—	—	—	—	—	—	—	X	—	—	—
ATP13A2	—	—	—	—	—	—	—	—	—	—	—	—	—	—	—	—	—	—	—	—	—	—	—	—	—	—	—	—	—	—	—	X	—	—	—
DEGS2	—	—	—	—	—	—	—	—	—	—	—	—	—	—	—	—	—	—	—	—	—	—	—	—	—	—	—	—	—	—	—	X	—	—	—
TNFRSF19	—	—	—	—	—	—	—	—	—	—	—	—	—	—	—	—	—	—	—	—	—	—	—	—	—	—	—	—	—	—	—	X	—	—	—
TMEM134	—	—	—	—	—	—	—	—	—	—	—	—	—	—	—	—	—	—	—	—	—	—	—	—	—	—	—	—	—	—	—	—	—	X	—	—

[1]Compares lower with higher grade samples.
[2]Compares samples derived from Tn with Tn + x (T); Nx with Nx + 1 (N); and Mx with Mx + 1 (M).
[3]Compares samples derived from live and dead patients within 5 years.
[4]Compares samples derived from patients without and with relapse/recurrence in 5 years.
X: means overexpression in a given study ($P < 0.01$).

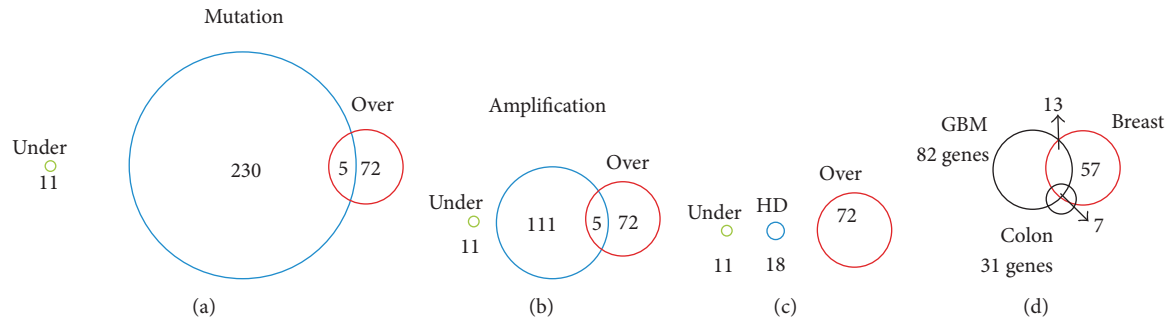

Figure 3: Comparison of over- and underexpressed genes in breast tumors with previous studies that identified genes with somatic mutation (a), chromosome amplification (b), or homozygous deletions (c) in breast tumors. (d) Comparison of surfaceome genes over-expressed in breast tumors with surfaceome genes over-expressed in GBM and colorectal tumors [5].

seem to have clinical relevance. Although presented evidence suggests that the overexpressed set of genes is enriched with genes important for breast tumorigenesis, additional studies are needed to establish any clinical applicability. Likewise, additional analyses are also required to uncover the function of the remaining genes that were not found to be associated with cancer and that were not explored in this work.

Abbreviations

GBM: Glioblastoma
MPSS: Massively Parallel Signature Sequencing
qPCR: Quantitative Real-Time Polymerase Chain Reaction
SAGE: Serial Analysis of Gene Expression
TM: Transmembrane.

Conflict of Interests

The authors declare that they have no conflict of interests.

Authors' Contribution

Lloyd J. Old and Sandro José de Souza designed research; Júlia Pinheiro Chagas da Cunha, Pedro Alexandre Favoretto Galante, Jorge Estefano Santana de Souza, and Martin Piepzyk performed research; Dirce Carraro contributed new reagents/analytic tools; Júlia Pinheiro Chagas da Cunha, Pedro Alexandre Favoretto Galante, Anamaria Aranha Camargo, and Sandro José de Souza analyzed data; and Júlia Pinheiro Chagas da Cunha, Anamaria Aranha Camargo, Lloyd J. Old, and Sandro José de Souza wrote the paper.

Acknowledgments

The authors are grateful to Paula Asprino, Gladis Wilner, Bruna Quevedo, Valéria Paixão, Ken Livak, and Min Lin for technical assistance. Júlia Pinheiro Chagas da Cunha was supported by a fellowship from FAPESP. This work was supported by intramural funds from the Ludwig Institute for Cancer Research and National Institutes of Health Fogarty International Center Grant 5D43TW007015-02.

References

[1] A. Jemal, R. Siegel, E. Ward et al., "Cancer statistics, 2008," *CA: A Cancer Journal for Clinicians*, vol. 58, no. 2, pp. 71–96, 2008.

[2] C. M. Perou, T. Sørile, M. B. Eisen et al., "Molecular portraits of human breast tumours," *Nature*, vol. 406, no. 6797, pp. 747–752, 2000.

[3] L. Harris, H. Fritsche, R. Mennel et al., "American Society of Clinical Oncology 2007 update of recommendations for the use of tumor markers in breast cancer," *Journal of Clinical Oncology*, vol. 25, no. 33, pp. 5287–5312, 2007.

[4] L. J. van't Veer, H. Dai, M. J. van de Vijver et al., "Gene expression profiling predicts clinical outcome of breast cancer," *Nature*, vol. 415, no. 6871, pp. 530–536, 2002.

[5] J. P. C. da Cunha, P. A. F. Galante, J. E. de Souza et al., "Bioinformatics construction of the human cell surfaceome," *Proceedings of the National Academy of Sciences of the United States of America*, vol. 106, no. 39, pp. 16752–16757, 2009.

[6] W. Xia, R. J. Mullin, B. R. Keith et al., "Anti-tumor activity of GW572016: a dual tyrosine kinase inhibitor blocks EGF activation of EGFR/erbB2 and downstream Erk1/2 and AKT pathways," *Oncogene*, vol. 21, no. 41, pp. 6255–6263, 2002.

[7] H. X. Chen, R. E. Gore-Langton, and B. D. Cheson, "Clinical trials referral resource: current clinical trials of the anti-VEGF monoclonal antibody bevacizumab," *Oncology*, vol. 15, no. 8, pp. 1017–1026, 2001.

[8] D. J. Slamon, G. M. Clark, S. G. Wong, W. J. Levin, A. Ullrich, and W. L. McGuire, "Human breast cancer: correlation of relapse and survival with amplification of the HER-2/neu oncogene," *Science*, vol. 235, no. 4785, pp. 182–191, 1987.

[9] M. A. Owens, B. C. Horten, and M. M. Da Silva, "HER2 amplification ratios by fluorescence in situ hybridization and correlation with immunohistochemistry in a cohort of 6556 breast cancer tissues," *Clinical Breast Cancer*, vol. 5, no. 1, pp. 63–69, 2004.

[10] T. Sjöblom, S. Jones, L. D. Wood et al., "The consensus coding sequences of human breast and colorectal cancers," *Science*, vol. 314, no. 5797, pp. 268–274, 2006.

[11] L. D. Wood, D. W. Parsons, S. Jones et al., "The genomic landscapes of human breast and colorectal cancers," *Science*, vol. 318, no. 5853, pp. 1108–1113, 2007.

[12] R. J. Leary, J. C. Lin, J. Cummins et al., "Integrated analysis of homozygous deletions, focal amplifications, and sequence alterations in breast and colorectal cancers," *Proceedings of the*

National Academy of Sciences of the United States of America, vol. 105, no. 42, pp. 16224–16229, 2008.

[13] A. C. Stamps, S. C. Davies, J. Burman, and M. J. O'Hare, "Analysis of proviral integration in human mammary epithelial cell lines immortalized by retroviral infection with a temperature-sensitive SV40 T- antigen construct," *International Journal of Cancer*, vol. 57, no. 6, pp. 865–874, 1994.

[14] K. J. Livak and T. D. Schmittgen, "Analysis of relative gene expression data using real-time quantitative PCR and the 2-ΔΔCT method," *Methods*, vol. 25, no. 4, pp. 402–408, 2001.

[15] J. Singh, L. Young, D. J. Handelsman, and Q. Dong, "Molecular cloning and characterization of a novel androgen repressible gene expressed in the prostate epithelium," *Gene*, vol. 348, no. 1-2, pp. 55–63, 2005.

[16] K. A. Egland, X. F. Liu, S. Squires et al., "High expression of a cytokeratin-associated protein in many cancers," *Proceedings of the National Academy of Sciences of the United States of America*, vol. 103, no. 15, pp. 5929–5934, 2006.

[17] A. W. Eckert, M. H. W. Lautner, H. Taubert, J. Schubert, and U. Bilkenroth, "Expression of Glut-1 is a prognostic marker for oral squamous cell carcinoma patients," *Oncology Reports*, vol. 20, no. 6, pp. 1381–1385, 2008.

[18] A. Ozcan, S. S. Shen, Q. Zhai, and L. D. Truong, "Expression of GLUT1 in primary renal tumors: morphologic and biologic implications," *American Journal of Clinical Pathology*, vol. 128, no. 2, pp. 245–254, 2007.

[19] M. Tsukioka, Y. Matsumoto, M. Noriyuki et al., "Expression of glucose transporters in epithelial ovarian carcinoma: correlation with clinical characteristics and tumor angiogenesis," *Oncology Reports*, vol. 18, no. 2, pp. 361–367, 2007.

[20] R. S. Haber, A. Rathan, K. R. Weiser et al., "GLUT1 glucose transporter expression in colorectal carcinoma: a marker for poor prognosis," *Cancer*, vol. 83, pp. 34–40, 1998.

[21] R. S. Haber, K. R. Weiser, A. Pritsker, I. Reder, and D. E. Burstein, "Glut1 glucose transporter expression in benign and malignant thyroid nodules," *Thyroid*, vol. 7, no. 3, pp. 363–667, 1997.

[22] W. K. Youn, Y.-K. Park, Y. Y. Tae, and M. L. Sang, "Expression of the GLUT1 glucose transporter in gallbladder carcinomas," *Hepato-Gastroenterology*, vol. 49, no. 46, pp. 907–911, 2002.

[23] P. W. Dempsey, S. E. Doyle, J. Q. He, and G. Cheng, "The signaling adaptors and pathways activated by TNF superfamily," *Cytokine and Growth Factor Reviews*, vol. 14, no. 3-4, pp. 193–209, 2003.

[24] S. Rudchenko, M. Scanlan, G. Kalantarov et al., "A human monoclonal autoantibody to breast cancer identifies the PDZ domain containing protein GIPC1 as a novel breast cancer-associated antigen," *BMC Cancer*, vol. 8, article 248, 2008.

[25] H. Kirikoshi and M. Katoh, "Expression of human GIPC1 in normal tissues, cancer cell lines, and primary tumors," *International Journal of Molecular Medicine*, vol. 9, no. 5, pp. 509–513, 2002.

[26] K. Lambaerts, S. A. Wilcox-Adelman, and P. Zimmermann, "The signaling mechanisms of syndecan heparan sulfate proteoglycans," *Current Opinion in Cell Biology*, vol. 21, no. 5, pp. 662–669, 2009.

[27] G. Orend, W. Huang, M. A. Olayioye, N. E. Hynes, and R. Chiquet-Ehrismann, "Tenascin-C blocks cell-cycle progression of anchorage-dependent fibroblasts on fibronectin through inhibition of syndecan-4," *Oncogene*, vol. 22, no. 25, pp. 3917–3926, 2003.

[28] B. T. MacDonald, K. Tamai, and X. He, "Wnt/β-catenin signaling: components, mechanisms, and diseases," *Developmental Cell*, vol. 17, no. 1, pp. 9–26, 2009.

[29] D. V. Rozanov, A. Y. Savinov, R. Williams et al., "Molecular signature of MT1-MMP: transactivation of the downstream universal gene network in cancer," *Cancer Research*, vol. 68, no. 11, pp. 4086–4096, 2008.

[30] Y. Tsunezuka, H. Kinoh, T. Takino et al., "Expression of membrane-type matrix metalloproteinase 1 (MT1-MMP) in tumor cells enhances pulmonary metastasis in an experimental metastasis assay," *Cancer Research*, vol. 56, no. 24, pp. 5678–5683, 1996.

[31] T.-H. Chun, F. Sabeh, I. Ota et al., "MT1-MMP-dependent neovessel formation within the confines of the three-dimensional extracellular matrix," *Journal of Cell Biology*, vol. 167, no. 4, pp. 757–767, 2004.

[32] H. Sato, T. Kinoshita, T. Takino, K. Nakayama, and M. Seiki, "Activation of a recombinant membrane type 1-matrix metalloproteinase (MT1-MMP) by furin and its interaction with tissue inhibitor of metalloproteinases (TIMP)-2," *FEBS Letters*, vol. 393, no. 1, pp. 101–104, 1996.

[33] K. Holmbeck, P. Bianco, J. Caterina et al., "MT1-MMP-deficient mice develop dwarfism, osteopenia, arthritis, and connective tissue disease due to inadequate collagen turnover," *Cell*, vol. 99, no. 1, pp. 81–92, 1999.

[34] L. Devy, L. Huang, L. Naa et al., "Selective inhibition of matrix metalloproteinase-14 blocks tumor growth, invasion, and angiogenesis," *Cancer Research*, vol. 69, no. 4, pp. 1517–1526, 2009.

[35] R. J. Leary, J. C. Lin, J. Cummins et al., "Integrated analysis of homozygous deletions, focal amplifications, and sequence alterations in breast and colorectal cancers," *Proceedings of the National Academy of Sciences of the United States of America*, vol. 105, no. 42, pp. 16224–16229, 2008.

[36] M. Katoh and M. Katoh, "MGC9753 gene, located within PPP1R1B-STARD3-ERBB2-GRB7 amplicon on human chromosome 17q12, encodes the seven-transmembrane receptor with extracellular six-cystein domain," *International Journal of Oncology*, vol. 22, no. 6, pp. 1369–1374, 2003.

[37] A. L. Willis, N. L. Tran, J. M. Chatigny et al., "The fibroblast growth factor-inducible 14 receptor is highly expressed in HER2-positive breast tumors and regulates breast cancer cell invasive capacity," *Molecular Cancer Research*, vol. 6, no. 5, pp. 725–734, 2008.

Hindawi Publishing Corporation
BioMed Research International
Volume 2013, Article ID 630683, 7 pages
http://dx.doi.org/10.1155/2013/630683

Research Article

Bovine Papillomavirus Clastogenic Effect Analyzed in Comet Assay

R. P. Araldi,[1,2] T. C. Melo,[1,2] N. Diniz,[1,3] J. Mazzuchelli-de-Souza,[1,3] R. F. Carvalho,[1] W. Beçak,[1,4] and R. C. Stocco[1,2]

[1] *Laboratório de Genética, Instituto Butantan, Avenida Vital Brasil, 1500, Butantã, 05503-900 São Paulo, SP, Brazil*
[2] *Programa de Pós-graduação Interunidades em Biotecnologia, Instituto de Ciências Biomédicas, Universidade de São Paulo, Avenida Prof. Lineu Prestes, 2415 Edifício ICB-III-Cidade Universitária, 05508-900 São Paulo, SP, Brazil*
[3] *Programa de Pós-graduação em Biologia Estrutural e Funcional, Universidade Federal de São Paulo, Rua Botucatu, 740, 04023-900 São Paulo, SP, Brazil*
[4] *Departamento de Biologia, Universidade Federal da Integração Latino-Americana (UNILA), Avenida Tancredo Neves, 6731 bloco 4, 85867-970 Foz do Iguaçú, PR, Brazil*

Correspondence should be addressed to R. C. Stocco; ritastocco@butantan.gov.br

Received 26 March 2013; Accepted 8 May 2013

Academic Editor: Franco Roperto

Bovine papillomavirus (BPV) is an oncogenic virus related to serious livestock diseases. Oncoproteins encoded by BPV are involved in several steps of cellular transformation and have been reported as presenting clastogenic effects in peripheral lymphocytes and primary culture cells. The aim of this study was to evaluate the clastogenic potential of BPV types 1, 2, and 4 by comet assay. Peripheral blood was collected from 37 bovines, 32 infected with different levels of papillomatosis (12 animals have no affection) and five calves, virus free (negative control). The viral identification showed presence of more than one virus type in 59.375% of the infected animals. Comet assay was performed according to alkaline technique. The Kruskal-Wallis test showed statistical difference between the negative control group and infected animals ($P = 0.0015$). The Dunn post hoc test showed difference comparing the infected animals with calves. Mann-Whitney U test verified no difference between animals infected with only one viral type and animals presenting more than one viral type. The comet assay is considered an efficient tool for assessment of damage in the host chromatin due to viral action, specifically highlighting viral activity in blood cells.

1. Introduction

Bovine papillomavirus (BPV) is a widespread oncogenic virus found worldwide belonging to the Papillomaviridae family, which displays tropism for squamous epithelial and mucosal tissues. These viruses are associated with benign and malignant epithelial lesions. Specifically, BPV presents a double-stranded circular DNA, not coiled, with approximately 8 kb, surrounded by an icosahedral capsid consisting of 360 copies of the L1 protein of 55 kDa, 72 capsomeres arranged in approximately 12 copies of the L2 protein, 39 kDa [1–8]. The papillomavirus genome is divided into three regions: early, late, and noncoding long control region (LCR), separated by two polyadenylation sites [3]. The early control region occupies 50% of the viral genome and encodes E1, E2, E3, E4, E5, E6, and E7 proteins. The late control region occupies 40% of the genome and contains the genes that codify L1 and L2 capsid proteins and LCR, which comprises 10% of the genome, with 850 bp. However, it also contains the origin of replication and the binding sites of multiple transcription factors [3]. Oncoproteins encoded by BPV are involved in several steps of the cell transformation [1, 9].

In cattle, the correlation between papillomavirus and cancer has been investigated in view of the economic costs generated by viral infection [1, 8, 10, 11]. BPV is the etiological agent of bovine papillomatosis, infectious disease, characterized by the presence of hyperproliferative skin lesions (papillomas), causing significant economic loss to livestock ranchers and can progress to cancer with the action of cofactors [8, 10, 12].

Currently, there are 13 BPV virus types described in the literature, although this number may be greater than twenty [7, 9]. The virus types are divided into three genres: *Deltapapillomavirus* (BPV-1, -2, and -13), *Epsilonpapillomavirus* (BPV-5 and -8), and *Xipapillomavirus* (BPV-3, -4, -6, -8, -9, -10, and -12), as well as the BPV-7 that remains not ranked in any genre [7]. Beside these, there are 16 new putative BPVs (BAA-1 to -4, BAPV-2 to -5, BAPV-7 to -10, BAPPV11MY and BPV/BR-UEL-2 to -5) [13]. According to Zhu et al. [13], BAA1 was detected in tongue epithelial papilloma, being designated BPV-12, and BPV/BR-UEL-4 described in ear cutaneous lesions was designated BPV-13 [9].

According to Stocco dos Santos et al. [1], papillomavirus can act on host chromatin causing cytogenetic alterations, such as changes in ploidy, chromatin gaps and breaks, dicentric chromosomes and rings. Significant increase of chromosomal aberrations was detected in animals infected with BPV, affecting genomic stability [4]. However, to date, there are no studies evaluating the BPV clastogenic potential in peripheral blood cells analyzed by comet assay.

Comet assay or single cell gel electrophoresis was introduced by Östling and Johanson [14] and later modified by Singh et al. [15]. The comet assay is a simple and versatile technique that requires few eukaryotic cells, as well as having a vast DNA damage spectrum detection capacity [16–19]. In the test, cells are engulfed by agarose gel and spread over the slide, and then subjected to an electric field that promotes free DNA fragment migration, with the appearance of a comet [15]. The nuclear region causes the head of the comet to fragment, and the length of the tail is directly related to the intensity of the damage.

The objective of this work was to evaluate the clastogenic potential of BPV types 1, 2, and 4 through comet assay in infected animals presenting cutaneous papillomatosis symptoms (hyperproliferative lesions-papillomas), asymptomatic (without papillomas) and calves, not infected, as negative control. The efficacy of the comet assay in clastogenic evaluations justifies this study.

2. Material and Methods

2.1. Ethics Statements. The protocols used in this study was approved by the Ethical Committee in Research of the Universidade Federal de São Paulo (Protocol number 1829/09) assigned by the President of this committee. All efforts were made to minimize any suffering in the animals.

2.2. BPV Diagnosis

2.2.1. Animal Selection. 37 bovines (*Bost aurus*) were selected: 32 adults, 12 asymptomatic (without visible cutaneous papillomas) and 20 symptomatic (with visible cutaneous papillomas) and 5 newborn calves that were separated from their mother after birth and did not receive breast milk. The presence of papillomas in others organs was not evaluated due the absence of clinical characteristics that suggest bladder and/or esophageal cancer. The farm does not have the presence of bracken fern *Pteridium aquilinum* that is involved in oncogenic and mutagenic processes in function of quercetin presence [20]. These calves were isolated in order to obtain virus negative controls. *Blood sample.* The peripheral blood samples were collected using the EDTA vacutainer. *Blood DNA extraction.* The extraction of DNA from peripheral blood cells was performed using the GenomicPrep Blood Mini Kit Illustra Spin (GE Healthcare, Buckinghamshire, UK), which uses enzymatic digestion method with protease K, according to the manufacturer. The quality of obtained DNA was verified using PCR by amplifying a bovine β-globin gene fragment [21].

2.2.2. Viral Identification. Viral identification was performed using specific primers for BPV-1 (forward: 5′-GGAGCGCCTGCTAACTATAGGA-3′ and reverse: 5′-ATCTGTTGTTTGGGTGGTGAC-3′), which amplifies the L1 gene, resulting in a 301 bp amplicon, BPV-2 (forward: 5′-GTTATACCACCCAAAGAAGACCCT-3′ and reverse: 5′-CTGGTTGCAAÇAGCTCTCTTTCTC-3′), which amplifies the L2 gene, resulting in a 164 amplicon, and BPV-4 (forward; 5′-GCTGACCTTCCAGTCTTAAT-3′ and reverse; 5′-CAGTTTCAATCTCCTCTTCA-3′), which amplifies the E7 gene, resulting in a 170 bp amplicon. We choose these primers because the virus types are often observed in Brazil and in function of the association with esophageal (BPV-4) and bladder cancer (BPV-1 and -2). In detail, the amplification reactions were performed in a Veriti 96-well thermal cycler (Applied Biosystems, Singapore), with Master Mix (Promega, Madison, USA), under the following conditions: 5 minutes at 95°C, followed by 35 cycles of 1 minute and 30 seconds at 98°C, 2 minutes at 52°C, and 1 minute and 30 seconds at 72°C and a final extension step of 5 minutes at 72°C, for β-globin and specific primers. The PCR products were analyzed in 2% agarose gel electrophoresis stained with GelRed in TAE buffer, visualized under UV light. The images were captured through the software Kodak 1D 3.6.5. Cloned BPV-1, -2 and -4 genomes in *Escherichia coli* D5Hα were used as positive controls. These clones form part of the biological collection of Genetic Laboratory of Butantan Institute. The fragments were purified using Illustra GFX PCR DNA and Gel Band Purification Kit (GE Healthcare, Buckinghamshire, UK). DNA concentration and purity were determined in a spectrophotometer BioPhotometer plus (Eppendorf, Hamburg, Germany) and submitted to sequencing reactions. *Sequencing.* The purified amplified products were sequenced in an ABI377 PRISM Genetic Analyzer. The quality of DNA sequences was checked, the overlapping fragments were assembled using the BioEdit package software BioEdit package 7.0.9.0 [22], and the nucleotide sequences were compared through BLAST (http://blast.ncbi.nlm.nih.gov/Blast.cgi).

2.3. Comet Assay. Comet assay was performed according to alkaline technique [15]. An aliquot of 10 μL (0.1×10^5 cells) was transferred to 0.2 mL polypropylene tubes and mixed with 75 μL of low-melting-point agarose (0.7% in PBS) at 37°C, LMA optimum concentration (≤0.8%), without affecting the DNA migration [17], which was spread onto 76 × 26 mm microscope slides precoated with

normal-melting-point agarose (1.5% in PBS) at 60°C and dried at 22°C overnight. After the agarose had solidified (4°C for 10 min), the coverslips were carefully removed, and the slides were immersed in lysis solution (2.5 M NaCl, 100 mM Na_2EDTA, 10 mM Tris-HCl; pH 10; 1% Triton X-100, and 10% DMSO) for 1 hour at 4°C and then placed into a horizontal electrophoresis apparatus filled with buffer (1 mM Na_2EDTA, 300 mM NaOH) at 4°C. The slides were incubated for 40 min in this buffer to unwind the DNA. The electrophoresis was run for 20 min at fixed voltage of 25 V (0.83 V/cm) and 300 mA. At the end of electrophoresis, the slides were washed three times with neutralization buffer (0.4 M Tris-HCl, pH 7.5) and once in 100% ethanol. All steps described above were carried out with the lights out to avoid DNA damage. The slides were stained with 20 μL of propidium iodide (4 μg/mL) and visualized in Carl Zeiss Axio Scope A1 fluorescent microscopy. Nucleoids were classified from 0 (without lesion) to 2 (major damage), and the number of nucleoids observed per class was multiplied to the class value, resulting in a comet score. *Statistical analysis.* The data were analyzed using the Kruskal-Wallis test, followed by post hoc Dunn test and Mann-Whitney *U* test, both with significance level of 5%, through BioEstat 5.3. software.

3. Results

3.1. Viral Genotyping. PCR using specific primers to β-globin revealed DNA quality enough for further PCR procedures: all samples resulted in a 450 bp amplicon. We selected the specific primers for BPV-1, -2, and -4 due to their prevalence in the herd, and we could detect the virus sequences in peripheral blood cells collected from the adult animals, with and without skin papillomas (Figure 1(a)). The resulting bands were purified and sequenced to confirm the genotyping of the amplification products. The sequences were aligned through the BioEdit 7.0.9.0, and the nucleotide comparison was done through the BLAST tool, confirming the specificity of the primers employed. Using these primers, coinfection was reported in 59.375% of the infected bovines—19 animals (Table 1(a)). The use of these primers did not detect the presence of BPV in calf peripheral blood samples, with this group being considered a negative control.

3.2. Comet Assay. The samples of peripheral blood cells collected from infected animals and calves (negative control) were evaluated through comet assay, counting 100 nucleoids per sample that were evaluated and classified as 0 (without damage), 1 (medium damage), and 2 (maximum damage) according to Figure 2. The nucleoid value per class was multiplied by the respective class value, resulting in the comet score (Table 1(a)).

Based on these data, a Kruskal-Wallis test was used, with 5% significance level, through BioEstat 5.3. software to compare the different groups (infected and not infected group). The test reveled statistical differences between the groups (H = 12.9714 and P value = 0.0015). The Dunn post hoc test showed difference in score values among calf and infected animals (asymptomatic and symptomatic)

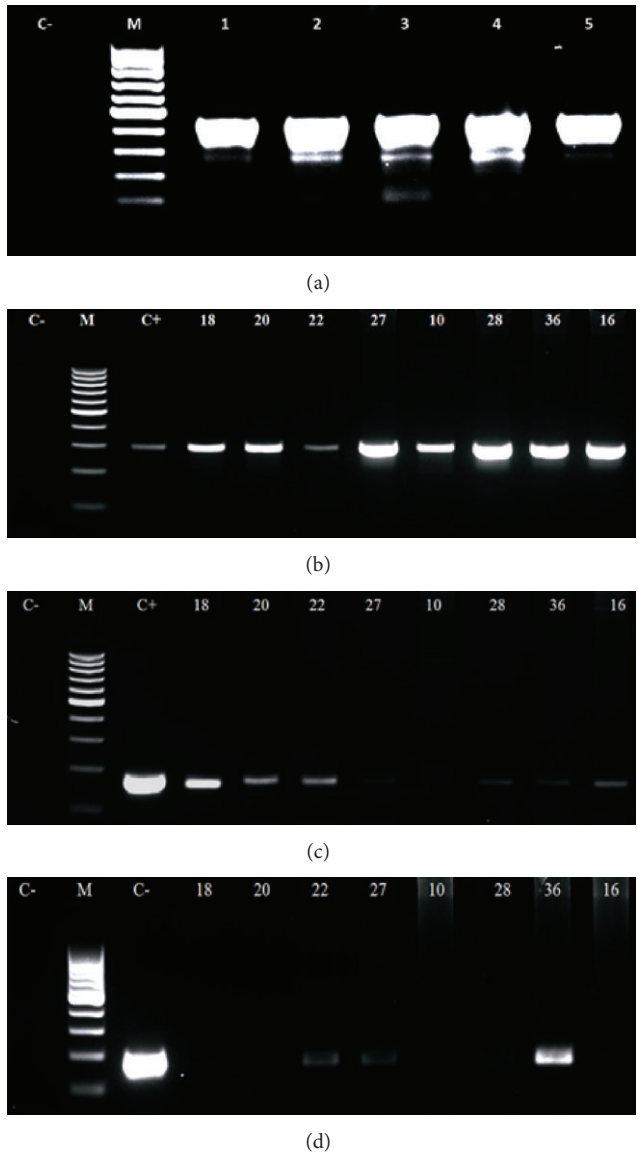

Figure 1: Electrophoresis's images of: (a) (β-globin amplification, resulting in an amplicon of 450 bp), (b) (amplification of L1 gene, using primer to BPV-1, showing an amplicon of 301 bp), (c) (amplification of L2 gene, using primer to BPV-2, showing an amplicon of 164 bp) and (d) (amplification of E7 gene, using primer to BPV-4, showing an amplicon of 170 bp), being C– (negative control) and C+ (positive control).

(Table 1(b)). Mann-Whitney *U* test was done using the same software to compare the level of clastogenicity between animals, which showed just one virus type, and coinfected cattle. The results did not reveal statistical differences between animals infected with only one viral type and animals presenting more than one viral type (Table 1(c)).

4. Discussion

The carcinogenic mechanisms related to BPV are not yet fully elucidated; however, it is known that the malignancy is caused

Table 1: (a) Results of molecular diagnosis of calves (negative control) and asymptomatic and symptomatic adult cattle, showing the BPV type, the frequency of nucleoids observed per class, and the comet score. (b) Kruskal-Wallis statistic to compare the clastogenicity among calves, asymptomatic and symptomatic cattle, from the comet score. (c) Comparison between comet score observed in monoinfected and coinfected bovines through Mann-Whitney U test.

(a)

Controls	Clinical	Virus type	Class of nucleoids			Score
			0	1	2	
1	Asymptomatic	—	93	4	3	10
2	Asymptomatic	—	92	5	3	11
3	Asymptomatic	—	96	1	3	7
4	Asymptomatic	—	90	8	2	12
5	Asymptomatic	—	95	3	2	7
Infected bovines						
6	Asymptomatic	BPV-1	15	60	25	110
7	Asymptomatic	BPV-2	57	36	7	50
8	Asymptomatic	BPV-1	75	19	6	31
9	Asymptomatic	BPV-1, -2	43	17	40	97
10	Asymptomatic	BPV-1	73	19	8	35
11	Asymptomatic	BPV-1, -2	47	26	27	80
12	Asymptomatic	BPV-1	38	26	36	98
13	Asymptomatic	BPV-1, -2	62	13	25	63
14	Asymptomatic	BPV-2	72	21	7	35
15	Asymptomatic	BPV-1, -2	63	12	25	62
16	Asymptomatic	BPV-1, -2	58	8	34	76
17	Asymptomatic	BPV-1, -2	40	42	18	78
18	Symptomatic	BPV-1, -2	61	30	9	48
19	Symptomatic	BPV-2	22	13	65	143
20	Symptomatic	BPV-1, -2	65	12	23	58
21	Symptomatic	BPV-1, -2	57	21	22	65
22	Symptomatic	BPV-1, -2, -4	31	31	38	107
23	Symptomatic	BPV-1	89	6	5	16
24	Symptomatic	BPV-1	92	2	6	14
25	Symptomatic	BPV-1	69	25	6	37
26	Symptomatic	BPV-1	41	10	49	108
27	Symptomatic	BPV-1, -2, -4	70	21	9	39
28	Symptomatic	BPV-1, -2, -4	65	26	9	44
29	Symptomatic	BPV-2	87	8	5	18
30	Symptomatic	BPV-1, -2	0	66	34	134
31	Symptomatic	BPV-1, -2	60	31	9	49
32	Symptomatic	BPV-2	52	23	25	73
33	Symptomatic	BPV-1, -2	72	9	19	47
34	Symptomatic	BPV-1, -2	91	7	2	11
35	Symptomatic	BPV-1, -2	74	15	11	37
36	Symptomatic	BPV1, -2, -4	82	13	5	23
37	Symptomatic	BPV-1, -2	36	22	42	106

(b)

Groups	Average post	Z calculated	P value
Calves and asymptomatic	3.300	3.5348	<0.05
Calves and symptomatic	23.666	3.1097	<0.05
Asymptomatic and symptomatic	20.125	0.8961	n.s.

$H = 12.9714$, $P = 0.0015$, R of calves = 16.5, R of asymptomatic = 284.0 and R of symptomatic = 402.5.

(c)

Monoinfected sample	Score	Coinfected sample	Score
6	110	9	97
7	50	11	80
8	31	13	63
10	35	15	62
12	98	16	76
14	35	17	78
19	143	18	48
23	16	20	20
24	14	21	21
25	37	22	22
26	108	27	39
29	18	28	44
32	74	30	134
—	—	31	49
—	—	33	47
—	—	34	11
—	—	35	37
—	—	36	23
—	—	37	106

Mann-Whitney U test results: $U = 102.5$, $Z(U) = 0.80$, P value = 0.21.

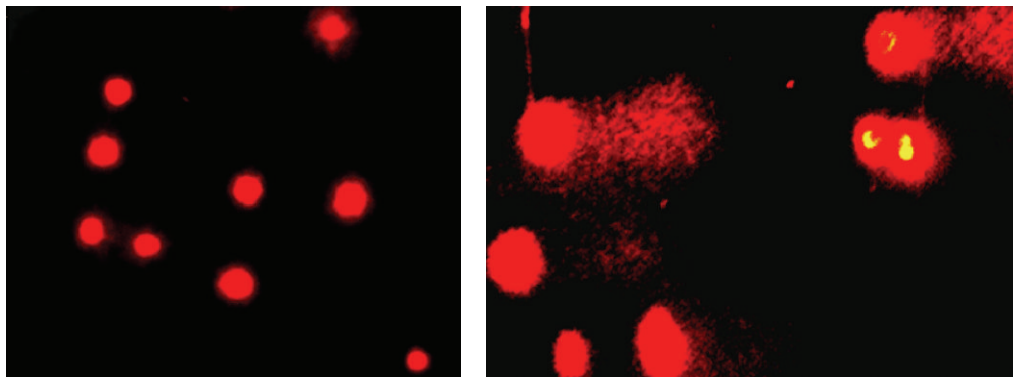

(a) (b)

Figure 2: (a) Images of class 0 nucleoids, observed in calves (negative control) and (b) class 2 nucleoids, observed in symptomatic adult bovine, showing DNA fragmentation that is indicative of clastogenicity.

by mutations induced by the virus, associated with the action of viral protein E6, which accelerates the degradation of p53 and E7, which degrades the tumor suppressor protein pRb. These processes change the transcriptional pathway through degradation of transcription factors, activating telomerase, affecting the DNA repair system, and leading to an increase of damage in host genetic material [6, 23–25]. According to You [6], the protein E7 interacts with microtubules in mitosis, causing defects in the alignment of chromosomes during pre-metaphase, resulting in cytogenetic alteration [1, 26]. Wade et al. [25] discussed that the BPV oncoproteins can act on the signal transduction, allowing the return of interphase spinous epithelial cells to synthesis phase, resulting in mutated cell proliferation. Oncoproteins E6 and E7 induce immortalization of transformed cells [3]. According to Primrose and Twyman [27], these oncoproteins are required in the process of viral replication and act in the process of oncogenic transformation of the host cell. Furthermore, the accelerated p53 proteasomal degradation has a prominent role in the carcinogenic action of the virus, since the p53 protein function is to check the integrity of the genome, preventing the proliferation of mutated cells. The p53 accumulates in the cell nucleus, keeping the mitotic cycle in early G1 phase by activating p21 gene, whose gene product inhibits the action of cycling-dependent kinases (CDKs) and activates genes related to repair system [28].

Melo et al. [26] analyzed peripheral blood lymphocytes obtained from clinically asymptomatic bovines and showed a high level of chromosomal aberrations, suggesting the BPV action in the host chromatin even before the clinical manifestation of papillomatosis. These data also indicate that the skin lesions (papillomas) represent visible clinical manifestations,

but the virus or its DNA sequences, detected in peripheral blood, can represent a potential risk to carcinogenesis.

In this study, we verified BPV clastogenic action by comet assay indicating chromatin instability. The comet assay results demonstrated that the BPV is able to induce severe DNA damages, which hinder the repair system, this is because the assay allows to evaluate the DNA double-strand breaks (DSBs) and critical lesions that are involved in genomic instability [29–31].

The DSB is associated with the homologous recombination from the formation of DNA simple strand that invades the template strand, originating a Holliday junction, which migrates to the resolution of heteroduplex [29, 31]. However, unrepaired DSBs leave to apoptosis or cell-cycle arrest, resulting in carcinogenesis [29]. There are lines of evidence that unrepaired DSBs could leave to telomeric breaks and fusion events, also associated with oncogenic process [29, 31].

The viral oncoproteins affect the repair system, allowing an accumulation of stochastic mutations and resulting in increased genomic instability [17]. According to Duensing and Münger [23], breaks in DNA affect the cell-cycle checkpoint that is associated with genomic instability, leading to hyper proliferation, featuring an oncogenic process. According to the European Study Group on Health's Biomarkers, cytogenetic findings, as a high frequency of chromosomal aberrations, including breaks in single or double-stranded, are associated to the carcinogenesis [32]. So, at the same time the presence of BPV is causing DSBs, the virus affects the repair system, favoring oncogenic process associated with unrepaired DSBs.

The virus presence in the blood can suggest one alternative pathway to infection, in which asymptomatic but infected cattle could turn symptomatic from a tissue injury, considering that a lesion causes an inflammatory process with lymphocyte infiltration [33]. The presence of BPV in leukocytes was demonstrated, had been observed the BPV presence in peripheral blood mononuclear cells [33] and the presence of L1 protein in CD4+ and CD8+ leukocytes, representing a potential infection sites to BPV-2 [34]. The possibility of the existence of endogenous pathway of infection has been discussed by Wobeser et al. [33], who suggested that the mononuclear cells act as a source of infection for inflammation sites, as inflamed areas become more susceptible to infection by BPV. Furthermore, it is known that lymphocytes express heparan sulfate, being cells susceptible to infection by papillomavirus [33]. Another observation that supports the possibility of infection was reported by Hartl et al. [35], who found that the spontaneous regression of papillomavirus in transient infections in humans and cattle is accompanied by an accumulation of active lymphocytes CD4+ and CD8+. So, in this pathway, the infiltration of BPV infected cell could develop a tumorigenic process from a clonal evolution started in a histologically normal tissue [35, 36].

5. Conclusion

This study presents direct evidence of DNA damage related to bovine papillomavirus in blood cells, indicating a viral activity in peripheral blood. The levels of damage were analyzed in order to verify if the presence of more than one viral type could increase the clastogenic viral action, but no significant differences could be detected. The results showed the same DNA damage both in presence or absence of cutaneous papillomas, indicating that the presence of bovine papillomatosis just represents clinical symptoms due the BPV presence; however, the BPV presence in peripheral blood leaves to double-stranded breaks, which is associated to carcinogenesis, affecting the healthy animal, as previously reported [1, 26]. Comet assay can be discussed as an interesting technique to evaluate DNA damage which, in this special situation, is related to viral action, demonstrating viral activity in different sites as blood cells.

Conflict of Interests

All the authors declare that there is no conflict of interests regarding the research, authorship, and/or publication of this paper. The authors inform that all materials and trademarks mentioned were used just as a part of experimental protocol and there are no financial gains or favoritism of business.

Acknowledgments

The authors thank the Ministério de Ciência, Tecnologia e Inovação/Conselho Nacional de Desenvolvimento Científico e Tecnológico (CNPq Proc. 402539/2011-7), Coordenação de Aperfeiçoamento Pessoal de Nível Superior (CAPES), Fundação do Desenvolvimento Administrativo (PAP-FUNDAP) for the financial support, Carolina da Paz Sabino for the editorial support, and Martin W. Breuer for all the efforts and structural support.

References

[1] R. C. Stocco dos Santos, C. J. Lindsey, O. P. Ferraz et al., "Bovine papillomavirus transmission and chromosomal aberrations: an experimental model," *Journal of General Virology*, vol. 79, no. 9, pp. 2127–2135, 1998.

[2] A. C. de Freitas, C. de Carvalho, O. Brunner et al., "Viral DNA sequences in peripheral blood and vertical transmission of the virus: a discussion about BPV-1," *Brazilian Journal of Microbiology*, vol. 34, no. 1, pp. 76–78, 2003.

[3] Z.-M. Zheng and C. C. Baker, "Papillomavirus genome structure, expression, and post-transcriptional regulation," *Frontiers in Bioscience*, vol. 11, no. 1, pp. 2286–2302, 2006.

[4] A. C. Freitas, M. A. R. Silva, C. C. R. Carvalho et al., "Papillomavirus DNAdetectionin non-epithelial tissue: adiscussion about bovine papillomavirus," in *Communicating Current Research and Educational Topics and Trends in Applied Microbiology*, pp. 697–704, 2007.

[5] S. Roperto, R. Brun, F. Paolini et al., "Detection of bovine papillomavirus type 2 in the peripheral blood of cattle with urinary bladder tumours: possible biological role," *Journal of General Virology*, vol. 89, no. 12, pp. 3027–3033, 2008.

[6] J. You, "Papillomavirus interaction with cellular chromatin," *Biochimica et Biophysica Acta*, vol. 1799, no. 3-4, pp. 192–199, 2010.

[7] A. C. Freitas, A. R. M. Silva, A. L. S. Jesus et al., "Recent insights into bovine papillomavirus," *African Journal of Microbiology Research*, vol. 5, no. 33, pp. 6004–6012, 2011.

[8] C. de Carvalho, A. C. de Freitas, O. Brunner et al., "Bovine papillomavirus type 2 in reproductive tract and gametes of slaughtered bovine females," *Brazilian Journal of Microbiology*, vol. 34, no. 1, pp. 82–84, 2003.

[9] M. Lunardi, A. A. Alfieri, R. A. A. Otonel et al., "Genetic characterization of a novel bovine papillomavirus member of the Deltapapillomavirus genus," *Veterinary Microbiology*, vol. 162, no. 1, pp. 207–213, 2013.

[10] J. DeMasi, M. C. Chao, A. S. Kumar, and P. M. Howley, "Bovine papillomavirus E7 oncoprotein inhibits anoikis," *Journal of Virology*, vol. 81, no. 17, pp. 9419–9425, 2007.

[11] C. J. Lindsey, M. E. Almeida, C. F. Vicari et al., "Bovine papillomavirus DNA in milk, blood, urine, semen, and spermatozoa of bovine papillomavirus-infected animals," *Genetics and Molecular Research*, vol. 8, no. 1, pp. 310–318, 2009.

[12] S. R. C. Campos, C. Trindade, O. P. Ferraz et al., "Can established cultured papilloma cells harbor bovine papillomavirus?" *Genetics and Molecular Research*, vol. 7, no. 4, pp. 1119–1126, 2008.

[13] W. Zhu, J. Dong, E. Shimizu et al., "Characterization of novel bovine papillomavirus type 12 (BPV-12) causing epithelial papilloma," *Archives of Virology*, vol. 157, no. 1, pp. 85–91, 2012.

[14] O. Östling and K. Johanson, "Microeletrophoretic study of radiation-induced DNA damages in individual mammalian cells," *Biochemical and Biophysical Research Communications*, vol. 123, pp. 291–298, 1984.

[15] N. P. Singh, M. T. McCoy, R. R. Tice, and E. L. Schneider, "A simple technique for quantitation of low levels of DNA damage in individual cells," *Experimental Cell Research*, vol. 175, no. 1, pp. 184–191, 1988.

[16] P. Escobar, "New applications of the Comet Assay in genetic toxicology testing," in *Proceedings of the Genetic Toxicology Association Meeting*, September 2008.

[17] S. A. S. Langie, K. M. Cameron, K. J. Waldron, K. P. R. Fletcher, T. von Zglinicki, and J. C. Mathers, "Measuring DNA repair incision activity of mouse tissue extracts towards singlet oxygen-induced DNA damage: a comet-based in vitro repair assay," *Mutagenesis*, vol. 26, no. 3, pp. 461–471, 2011.

[18] S. Khoei, S. Delfan, A. Neshasteh-Riz, and S. R. Mahdavi, "Evaluation of the combined effect of 2ME2 and ^{60}Co on the inducement of DNA damage by IUdR in a spheroid model of the U87MG glioblastoma cancer cell line using alkaline comet assay," *Cell Journal*, vol. 13, no. 2, pp. 83–90, 2011.

[19] R. Fabiani, P. Rosignoli, A. de Bartolomeo, R. Fuccelli, and G. Morozzi, "Genotoxicity of alkene epoxides in human peripheral blood mononuclear cells and HL60 leukaemia cells evaluated with the comet assay," *Mutation Research*, vol. 747, pp. 1–6, 2012.

[20] J. D. C. Dias, M. D. C. Sgnacchiti, P. G. G. Giuriato, L. C. Nunes, and O. S. Pereira-Júnior, "Detecção do papilomavírus bovino tipo 2 em bexigas de bovinos com hematúria enzoótica pela técnica de reação de cadeia de polimerase no Sul do Espírito Santo," *Revista Brasileira de Medicina Veterinária*, vol. 34, pp. 146–151, 2012.

[21] A. Yaguiu, M. L. Z. Dagli, E. H. Birgel Jr. et al., "Simultaneous presence of bovine papillomavirus and bovine leukemia virus in different bovine tissues: in situ hybridization and cytogenetic analysis," *Genetics and Molecular Research*, vol. 7, no. 2, pp. 487–497, 2008.

[22] T. A. Hall, "BioEdit: a user-friendly biological sequence alignment editor and analysis program for Windows 95/98/NT," *Nucleic Acids Symposium Series*, vol. 41, pp. 95–98, 1999.

[23] S. Duensing and K. Münger, "The human papillomavirus type 16 E6 and E7 oncoproteins independently induce numerical and structural chromosome instability," *Cancer Research*, vol. 62, no. 23, pp. 7075–7082, 2002.

[24] Y. Liu and J. D. Baleja, "Structure and function of the papillomavirus E6 protein and its interacting proteins," *Frontiers in Bioscience*, vol. 13, no. 1, pp. 121–134, 2008.

[25] R. Wade, N. Brimer, and S. Vande Pol, "Transformation by bovine papillomavirus type 1 E6 requires paxillin," *Journal of Virology*, vol. 82, no. 12, pp. 5962–5966, 2008.

[26] T. C. Melo, N. Diniz, S. R. C. Campos et al., "Cytogenetic studies in peripheral blood of bovines afflicted by papillomatosis," *Veterinary and Comparative Oncology*, vol. 9, no. 4, pp. 269–274, 2011.

[27] S. B. Primrose and R. M. Twyman, *Principles of Gene Manipulation and Genomics*, Blackwell Scientific Publications, Oxford, UK, 7th edition, 2006.

[28] G. B. Cavalcanti-Júnior, C. E. Klumb, and R. C. Maia, "p53 e as hemopatias malignas," *Revista Brasileira de Cancerologia*, vol. 48, pp. 419–442, 2002.

[29] M. O'Driscoll and P. A. Jeggo, "The role of double-strand break repair—insights from human genetics," *Nature Reviews Genetics*, vol. 7, no. 1, pp. 45–54, 2006.

[30] R. Kanaar, J. H. J. Hoeijmakers, and D. C. van Gent, "Molecular mechanisms of DNA double-strand break repair," *Trends in Cell Biology*, vol. 8, no. 12, pp. 483–489, 1998.

[31] M. Shrivastav, L. P. de Haro, and J. A. Nickoloff, "Regulation of DNA double-strand break repair pathway choice," *Cell Research*, vol. 18, no. 1, pp. 134–147, 2008.

[32] A. Collins, D. Anderson, E. Coskun et al., "Launch of the ComNet (Comet-Network) project on the comet assay in human population studies during the International Comet Assay Workshop Meeting in Kusadasi, Turkey (September 13–16, 2011)," *Mutagenesis*, vol. 27, pp. 385–386, 2012.

[33] B. K. Wobeser, J. E. Hill, M. L. Jackson et al., "Localization of Bovine papillomavirus in equine sarcoids and inflammatory skin conditions of horses using laser microdissection and two forms of DNA amplification," *Journal of Veterinary Diagnostic Investigation*, vol. 24, no. 1, pp. 32–41, 2012.

[34] S. Roperto, S. Comazzi, E. Ciusani et al., "PBMCS are additional sites of productive infection of bovine papillomavirus type 2," *Journal of General Virology*, vol. 92, no. 8, pp. 1787–1794, 2011.

[35] B. Hartl, E. K. Hainisch, S. Shafti-Keramat et al., "Inoculation of young horses with bovine papillomavirus type 1 virions leads to early infection of PBMCS prior to pseudo-sarcoid formation," *Journal of General Virology*, vol. 92, no. 10, pp. 2437–2445, 2011.

[36] C. T. Leung and J. S. Brugge, "Outgrowth of single oncogene-expressing cells from suppressive epithelial environments," *Nature*, vol. 482, no. 7385, pp. 410–413, 2012.

Hindawi Publishing Corporation
BioMed Research International
Volume 2013, Article ID 283985, 12 pages
http://dx.doi.org/10.1155/2013/283985

Research Article

Analysis of Activated Platelet-Derived Growth Factor β Receptor and Ras-MAP Kinase Pathway in Equine Sarcoid Fibroblasts

Gennaro Altamura,[1] Annunziata Corteggio,[1] Lubna Nasir,[2] Zheng Qiang Yuan,[3] Franco Roperto,[1] and Giuseppe Borzacchiello[1]

[1] *Department of Veterinary Medicine and Animal Production, University of Naples Federico II, Via Veterinaria, 180137 Napoli, Italy*
[2] *MRC-University of Glasgow Centre for Virus Research, Institute of Infection, Immunity and Inflammation, College of Medical, Veterinary and Life Sciences, Bearsden Road, Glasgow G61 1QH, UK*
[3] *University College London, Internal Medicine, Division of Medicine, Faculty of Medical Sciences, Gower Street, London WC1E 6BT, UK*

Correspondence should be addressed to Giuseppe Borzacchiello; borzacch@unina.it

Received 14 February 2013; Revised 3 June 2013; Accepted 18 June 2013

Academic Editor: Marcelo Palma Sircili

Equine sarcoids are skin tumours of fibroblastic origin affecting equids worldwide. Bovine papillomavirus type-1 (BPV-1) and, less commonly, type-2 are recognized as etiological factors of sarcoids. The transforming activity of BPV is related to the functions of its major oncoprotein E5 which binds to the platelet-derived growth factor β receptor (PDGFβR) causing its phosphorylation and activation. In this study, we demonstrate, by coimmunoprecipitation and immunoblotting, that in equine sarcoid derived cell lines PDGFβR is phosphorylated and binds downstream molecules related to Ras-mitogen-activated protein kinase-ERK pathway thus resulting in Ras activation. Imatinib mesylate is a tyrosine kinase receptors inhibitor which selectively inhibits the activation of PDGFβR in the treatment of several human and animal cancers. Here we show that imatinib inhibits receptor phosphorylation, and cell viability assays demonstrate that this drug decreases sarcoid fibroblasts viability in a dose-dependent manner. This study contributes to a better understanding of the molecular mechanisms involved in the pathology of sarcoids and paves the way to a new therapeutic approach for the treatment of this common equine skin neoplasm.

1. Introduction

Sarcoids are skin tumours of fibroblastic origin affecting equids and are considered to be the most common equine cutaneous neoplasm worldwide. These tumours are locally invasive, nonmetastatic, and very rarely regress. Sarcoids may exist as single or multiple lesions, most frequently arising from sites of previous injuries such as the skin of the head, ventral abdomen, and the paragenital region, with six clinical types recognized: occult, verrucous, nodular, fibroblastic, mixed, and malignant [1]. They are all histologically characterized by proliferation of spindle-shaped dermal fibroblasts forming whorls and by epidermal hyperplasia, hyperkeratosis, and rete peg formation [2, 3]. Although the pathology of this equine neoplasm is not completely understood, a role for bovine papillomavirus type-1 (BPV-1) and, less commonly, BPV-2 infection had been recognized in the etiology of sarcoids [4, 5]. BPV-1 and -2 are oncogenic double-stranded DNA viruses belonging to the genus of Delta papillomaviruses, which are able to infect both epithelial cells and fibroblasts in their natural host [6]. The oncogenic potential of BPV-1/-2 in bovids is known to be related to the expression of viral oncoproteins E5, E6, and E7 [7]; BPV genes have been found to be expressed in sarcoids, suggesting that the viral proteins also play a role in the development of this equine skin neoplasm [8–12].

E5 is the major oncoprotein encoded by BPVs [13]; it is mostly localized in the endomembrane compartments

of the Golgi apparatus (GA), endoplasmic reticulum, and plasma membrane of epithelial cells [14]; cytoplasmic and juxtanuclear expression of E5 has also been reported in sarcoid fibroblasts [11].

PDGFβR and other tyrosine kinase receptors are involved in human and animal papillomavirus-induced carcinogenesis since their physiological activity is impaired by E5 oncoproteins of PVs [13].

The major transforming activity of BPV-1 E5 is due to its ability to specifically bind and activate PDGFβR in a ligand independent manner, and, importantly, it does not activate other related receptors [15–18]. E5 binds to PDGFβR as a dimer thereby inducing receptor oligomerization, autophosphorylation, and thus activation [19–21]. PDGFβR is constitutively activated in transformed mouse cells expressing BPV-1 E5, and binding of BPV-1 E5 to PDGFβR induces its activation in mortal human fibroblasts [18, 22]. Importantly, this interaction also takes place *in vivo*, confirming the role of the E5-PDGFβR complex in carcinogenesis [15, 23]; additionally, PDGFβR has been found to be activated in BPV-E5 positive urinary bladder tumours and equine sarcoids [24, 25].

Activated tyrosine kinase receptors can stimulate intracellular-signalling pathways which regulate cell proliferation, such as the Ras-mitogen-activated protein kinase-ERK (Ras-MAPK-ERK) pathway [26, 27]; once phosphorylated, they recruit growth factor receptor bound protein 2 (GRB2) which is constitutively associated with Sos1 protein, a guanine nucleotide exchange factor of the small GTP-ase, Ras. When recruited to plasma membrane together with GRB2, Sos1 catalyses the switch of Ras from inactive GDP bound form (Ras-GDP) to a transductionally active GTP bound form (Ras-GTP). Ras-GTP binds to and stimulates downstream effectors (among these, Raf1), resulting in phosphorylation and activation of MEK and its downstream kinase ERK, which can regulate cell growth or differentiation [28]. In response to PDGFβR stimulation, GRB2 facilitates activation of the Ras-MAPK-ERK pathway [27] playing a role in brain cancer development [29]. BPV E5 induces recruitment of GRB2 to activated PDGFβR (pPDGFβR), contributing to cell transformation *in vitro* [22]; furthermore, pPDGFβR recruits GRB2-Sos1 which promote Ras activation in bovine urinary bladder cancer, suggesting a role of this pathway in BPV-induced carcinogenesis [25].

Imatinib mesylate is a tyrosine kinase receptor inhibitor formerly known as STI-571 or Gleevec; this small molecule, derived from 2-phenylaminopyrimidine, binds to the ATP-binding site, thus inhibiting the tyrosine kinase activity of the PDGFR (both α and β) and the downstream signals, including the Ras-MAPK-ERK cell proliferation pathway [30–32]. Imatinib has been largely studied in human solid tumours, where it has been shown to induce cell growth arrest [33–37]. Furthermore, imatinib selectively inhibits the Bcr-Abl tyrosine kinase in chronic myeloid leukemia and c-kit in several human cancers, resulting in either apoptosis or inhibition of proliferation [30, 31, 38–42]. Gleevec is used in veterinary medicine for the treatment of canine mast cells tumours (MCTs) [43–45] and has been proposed as therapy for several feline neoplasms, including vaccine associated sarcomas (VAS), in which the PDGFβR is selectively inhibited by the treatment [46, 47].

The aim of this study was to investigate the activation of PDGFβR, the Ras-MAPK-ERK pathway and to further evaluate the effects of imatinib mesylate on PDGFβR phosphorylation and cell viability in an equine sarcoid disease model.

2. Methods

2.1. Cells and Cell Culture. Equine sarcoid-derived cell lines EqS01 and EqS04b, expressing endogenous BPV-1 E5, EqS02a transfected with BPV-1 E5 (EqS02aE5) and EqS02a cells which do not express E5 and are not fully transformed, have all been described previously [48, 49]. Cells were cultured in Dulbecco's modified eagle medium (DMEM) supplemented with 10% fetal bovine serum (FBS) (Gibco) or in serum-deprived DMEM depending on the experiment, in a 37°C humidified atmosphere of 5% CO_2 in air.

2.2. Coimmunoprecipitation, Immunoprecipitation, and Immunoblotting. To prepare protein extracts for immunoprecipitation, 80% confluent monolayers in 150 mm dishes were washed three times in phosphate-buffered saline (PBS; pH 7.4, 0.1 M) and then lysed in ice-cold JS buffer (50 mM HEPES, PH 7.5, 150 mM NaCl, 1% glycerol, 1% Triton-X100, 150 μM $MgCl_2$, and 5 mM ethylene glycol tetra acetic acid) added with 20 mM sodium pyrophosphate, 0,1 mg mL^{-1} aprotinin, 2 mM phenylmethylsulfonyl fluoride, 10 mM disodium orthovanadate, and 50 mM sodium fluoride. Protein concentrations were determined by use of a protein assay kit (Bio-Rad Laboratories). Equal amounts of protein lysates (500 μg) were immunoprecipitated with 2 μg mL^{-1} rabbit anti-pPDGFβR antibody (Santa Cruz Biotechnology) overnight at 4°C. A-G/plus sepharose beads (Santa Cruz Biotechnology) (20 μL) were added to the samples, and the mixture was rotated for 1 h at 4°C. After 3 washings in lysis buffer, the immunoprecipitates were resuspended in Laemmli sample buffer [50] (sodium dodecyl sulphate (SDS), Tris-HCl pH 6.8, glycerol, bromophenol blue, and 2β-mercaptoethanol) and analyzed by SDS polyacrylamide gel electrophoresis (PAGE) and immunoblotting. Nitrocellulose membranes were blocked with 5% bovine serum albumin (BSA)-in-Tris-buffered saline (TBS: 12.5 mM TrisHCl pH 7.4; 125 mM NaCl) at room temperature (RT) and incubated O/N at 4°C with rabbit anti-pPDGFβR, mouse anti-GRB2 (Upstate Biotechnology) and rabbit anti-Sos1 (Santa Cruz Biotechnology) antibodies diluted 1 : 500, 1 : 1000, and 1 : 200, respectively. After 3 washing steps in TBS-Tween 0.1%, appropriate peroxidase-conjugated secondary antibodies (Amersham, Gel Health Care) were applied 1 h at RT at 1 : 1000 dilution. Membranes were washed again, and bound antibodies were visualized by enhanced chemiluminescence (ECL) (Western Blot Luminol Reagent, Santa Cruz Biotechnology). Protein levels were quantitatively estimated by densitometry using ChemiDoc gel scanner (Bio-Rad

Table 1: Primers sets used to amplify cDNA from exons 11–20 of PDGFβR in EqS cells.

Primers sets	Annealing position	Annealing T°	Fragments size
F1: ATCCTCATCATGCTCTGGCAG	F1: 2119	52°C	628 bp
R1: TCTCCTTTCATGTCCAGCATG	R1: 2747		
F1: ATCCTCATCATGCTCTGGCAG	F1: 2119	52°C	1226 bp
R3: TCGAGAAGCAGCACCAGCTG	R3: 3344		
F3: TGGCTACATGGACATGAGCAAG	F3: 2682	52°C	663 bp
R3: TCGAGAAGCAGCACCAGCTG	R3: 3344		
F3: TGGCTACATGGACATGAGCAAG	F3: 2682	52°C	593 bp
R2: ATCTCGTAGATCTCGTCGGAG	R2: 3275		

T°: temperature; F: forward; R: reverse; bp: base pairs.

Laboratories) equipped with a densitometric workstation (Image Lab software, Bio Rad Laboratories).

Similarly, protein extracts were immunoprecipitated for Sos1 (2 μg mL^{-1}) and analyzed by SDS-PAGE and immunoblotting with anti-GRB2 and anti-Sos1 antibodies. The reciprocal coimmunoprecipitation assay could not be performed since the anti-GRB2 antibody does not work for immunoprecipitation.

For evaluation of phosphorylation status of PDGFβR in starved serum-deprived cells, the same amount of protein lysates were immunoprecipitated with a rabbit anti-PDGFβR antibody (2 μg mL^{-1}) (Santa Cruz Biotechnology) and probed for PDGFβR presence, using the aforementioned antibody; the membranes were stripped and reprobed with a mouse antiphosphotyrosine (pTyr) antibody at 1 : 1000 dilution (Upstate Biotechnology). Bound antibodies were visualized as mention above.

For the evaluation of activation status of PDGFβR after treatment with imatinib mesylate, cell lysates were subjected to immunoprecipitation with rabbit anti-PDGFβR and immunoblotting. The membranes were incubated with mouse anti-pTyr antibody, washed, and probed with appropriate secondary antibody. After stripping, rabbit anti-PDGFβR antibody was applied and revealed as mentioned above.

Equal volumes (30 μL) of cell lysates were analyzed by immunoblotting for actin levels detection (see the following for details) before coimmunoprecipitation and immunoprecipitation assays to ensure equal amounts of protein loading and allow normalization.

2.3. Ras-Pull-Down Assay. To assess Ras activation status, a Ras-pull-down assay (Millipore) was performed according to manufacturer protocol with slight modifications. Briefly, cell lysates were incubated with GST-Raf1-RBD agarose beads for 15 minutes at 4°C with gentle agitation. Beads containing activated Ras were collected by centrifugation, washed with JS lysis buffer, and then prepared and analyzed for immunoblotting with a mouse monoclonal anti-Ras antibody provided by the kit. Raf1-RBD-Ras levels were normalized to total Ras levels and expressed as densitometric ratio. Total Ras expression levels were normalised to actin levels.

2.4. Immunoblotting on Whole Cell Lysates. For protein expression analysis on whole cell lysates, equal amounts of proteins were boiled in 2x Laemmli sample buffer [50], electrophoresed, and subjected to immunoblotting; after blocking in TBS-BSA 5%, rabbit anti-PDGFβR diluted 1 : 500, rabbit anti-pMEK antibody diluted 1 : 1000, and rabbit anti-pERK (pERK) antibody at 1 : 2000 dilution (Cell Signaling Technology) were applied O/N at 4°C. The membranes were washed and incubated with peroxidase-conjugated anti-rabbit IgG diluted 1 : 1000, 1 h at RT. Following further washing, bound antibodies were visualized as above. The membranes were stripped and reprobed with mouse anti-actin antibody (Calbiochem) at 1 : 5000 dilution to ensure equal amount of proteins for each sample. The protein concentrations were normalised to the actin levels.

2.5. RT-PCR and Sequencing of Exons 11–20 of PDGFβR Gene. Total RNA from 80% confluent cell monolayers in 60 mm dishes was extracted using RNeasy mini Kit (Qiagen). Following DNase I treatment, first-strand cDNA from PDGFβR gene was synthesized using SuperScript III First-Strand Synthesis System for RT-PCR (Invitrogen) according to manufacturer's protocol. cDNA was amplified using different primers sets, which amplified different regions of all sequences from exon 11 to exon 20. The primers sets, the annealing position, the size of amplified fragments, and the annealing temperatures are summarized in Table 1. PCR conditions were as follows: denaturation at 94°C for 20 s, followed by 28 cycles at 94°C for 20 s, 52°C for 30 s, and 68°C for 20 s, with a final extension at 68°C for 10 min. PCR products were separated by electrophoresis in 1% agarose gels with Tris borate ethylene diamine tetra acetic acid (EDTA) buffer (TBE; 89 mMTris base, 89 mM Boric acid, and 2 mM EDTA), stained with ethidium bromide, and visualised under ultraviolet light. Amplicons were purified using the Charge Switch PCR Clean-Up Kit (Invitrogen) following manufacturer's instructions. Cycle sequencing reactions were performed using Applied Biosystems BigDye Terminator Ready Reaction v3.1 Kit, followed by purification of sequence reactions and electrophoresing using ABI Prism 3130XL Genetic Analyser (Applied Biosystems). The sequences were aligned to *Equus caballus* wild type PDGFβR using Basic Local Alignment Search Tool (NCBI/BLAST).

2.6. Double Immunofluorescence and Confocal Microscopy. EqS cell lines were grown for 2 days on coverslips, washed with PBS, fixed in 4% paraformaldehyde for 20 min, and

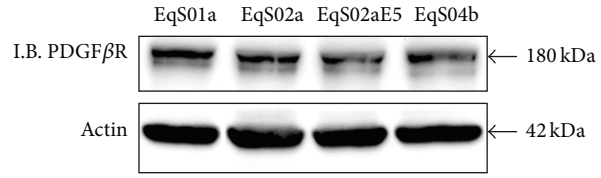

Figure 1: Immunoblotting (I.B.) analysis of PDFGβR expression in sarcoid-derived cell lines (EqS). PDFGβR was expressed at similar levels in all the analyzed cell lines. Actin protein levels confirmed equal amount of protein loading in each lane.

permeabilized with 0,1% triton X-100 in PBS 5 min. The slides were blocked with 2% BSA for 30 min. Sheep anti-E5 (a kind gift of Professor Maria Saveria Campo, University of Glasgow, Scotland [51, 52]) and rabbit anti-PDGFβR primary antibodies were applied O/N at 4°C in a humidified chamber at 1 : 50 dilution in PBS. The slides were washed three times with PBS, then incubated with Alexa Fluor 488 donkey anti-sheep and Alexa Fluor 546 goat anti-rabbit 30 min at RT (Molecular Probes) in a humidified chamber at 1 : 100 dilution. Finally, after washing with PBS, the slides were mounted in aqueous medium PBS : Glycerol 1 : 1 (Sigma). For scanning and photography, a confocal laser-scanning microscope LSM-510 (Zeiss) was used. Alexa Fluor 488/546 was irradiated at 488 nm and 543 nm and detected with a 505–530 nm and 506–615 nm bandpass filters, respectively.

2.7. Imatinib Mesylate, Inhibition of PDGFβR Activation, and Cell Viability Assay. Imatinib mesylate was provided by LC laboratories (Woburn, USA). For our studies, 50 mM stock solutions were prepared in DMSO and stored at −80°C. Dilutions of imatinib were made from the stock solutions in serum-free medium.

For the evaluation of activation status of PDGFβR after drug treatment, 80% confluent cells monolayers in 60 mm dishes were incubated in serum-free medium for 24 h and treated for 15 min with imatinib at the following concentrations: 0,01 μM, 0,1 μM, 1 μM, 5 μM, with or without 30 ng mL^{-1} of human recombinant PDGF-BB (PDGFβR natural ligand) (Sigma). Cells were then lysed and subjected to immunoprecipitation of PDGFβR and immunoblotting for pTyr and PDGFβR as described previously.

For cell viability assay, cells were plated in 96-well microtiter plates at 10000 cells/well and incubated in DMEM 10% FBS in standard conditions. After 24 h, the plates were washed, and serum-free medium containing various concentrations of imatinib with or without 30 ng mL^{-1} of human recombinant PDGF-BB was added. Each condition was replicated in five wells. Relative viable cell numbers were measured after 72 h using the Cell Titer 96 AQ$_{\text{ueous}}$ one solution assay (Promega), a colorimetric system based on the tetrazolium salt MTS, according to manufacturer's protocol. Absorbance at 490 nm was measured using a Sirio-S Reader (Seac and Radim Diagnostics) and Sirio-S v7.0 software.

3. Results

3.1. PDGFβR Activation and Its Binding to Downstream Molecules in Equine Sarcoid Fibroblasts. In order to investigate the activation of PDGFβR, we first assessed PDGFβR expression levels, which were very similar among all EqS cell lines (Figure 1), and then the interaction of activated receptor with its molecular substrates, GRB2 and Sos1. pPDGFβR immunoprecipitation followed by immunoblotting for pPDGFβR, GRB2, and Sos1-yielded the following results: pPDGFβR is immunoprecipitated in higher amounts in EqS02aE5 and EqS04b, both expressing higher levels of BPV-1 E5, and, to a lesser extent, in EqS01a, which expresses lower levels of the oncogene, when compared to EqS02a; the latter cell line harbours very few copies of viral genome, and E5 expression is not detectable [48, 49]; the levels of GRB2 and Sos1 co-immunoprecipitated with pPDGFβR were increased in EqS01a, EqS02aE5, and EqS04b correlating with pPDGFβR levels, when compared to EqS02a (Figure 2).

Since Sos1 could be recruited to activated PDGFβR via GRB2, we next analyzed the physical interaction between Sos1 and GRB2 by coimmunoprecipitation. GRB2 bound Sos1 in all the analyzed cell lines; however, the complex was found in larger amounts in EqS02aE5 and EqS04b (both highly expressing E5) (Figure 3).

3.2. Molecular Analysis of Ras-MAPK-ERK Pathway. To further analyze the downstream signalling molecules of pPDGFβR complexed with GRB2-Sos1, we investigated the activation of Ras using a pull-down assay. Firstly, immunoblotting on whole cell lysates collected before performing the pull-down assay showed similar Ras-expression levels in EqS02a, EqS02aE5 and EqS04b. Ras was found to be overexpressed and, consistently, activated at higher levels in EqS01a when compared to other cell lines. Raf1-RBD-Ras was also detected at higher levels in EqS02aE5 and EqS04b when compared to EqS02a (Figures 4(a) and 4(b)).

The phosphorylation status of ERK (pERK) and its upstream kinase MEK (pMEK) were also determined by immunoblotting using phosphospecific antibodies; however, no differences in expression levels were observed in EqS cell lines (Figure 4(c)).

3.3. Analysis of PDGFβR Activation in Serum-Starved EqS Cells. EqS cell lines were grown in serum-deprived medium to exclude the possibility that receptor activation could be due to growth factors from FBS. Immunoprecipitation assay, performed by using an anti-PDGFβR antibody followed by immunoblotting with anti-PDGFβR and anti-pTyr antibodies, revealed that PDGFβR is phosphorylated only in EqS02aE5 and EqS04b, both expressing high levels of E5 (Figure 5).

3.4. Sequence Analysis of Exons 11–20 of PDGFβR Gene. To further evaluate whether the sustained activation of PDGFβR in EqS cell lines might be caused by activating mutations in the transmembrane and/or cytosolic domain, cDNAs of exons 11–20 of PDGFβR were amplified by RT-PCR using

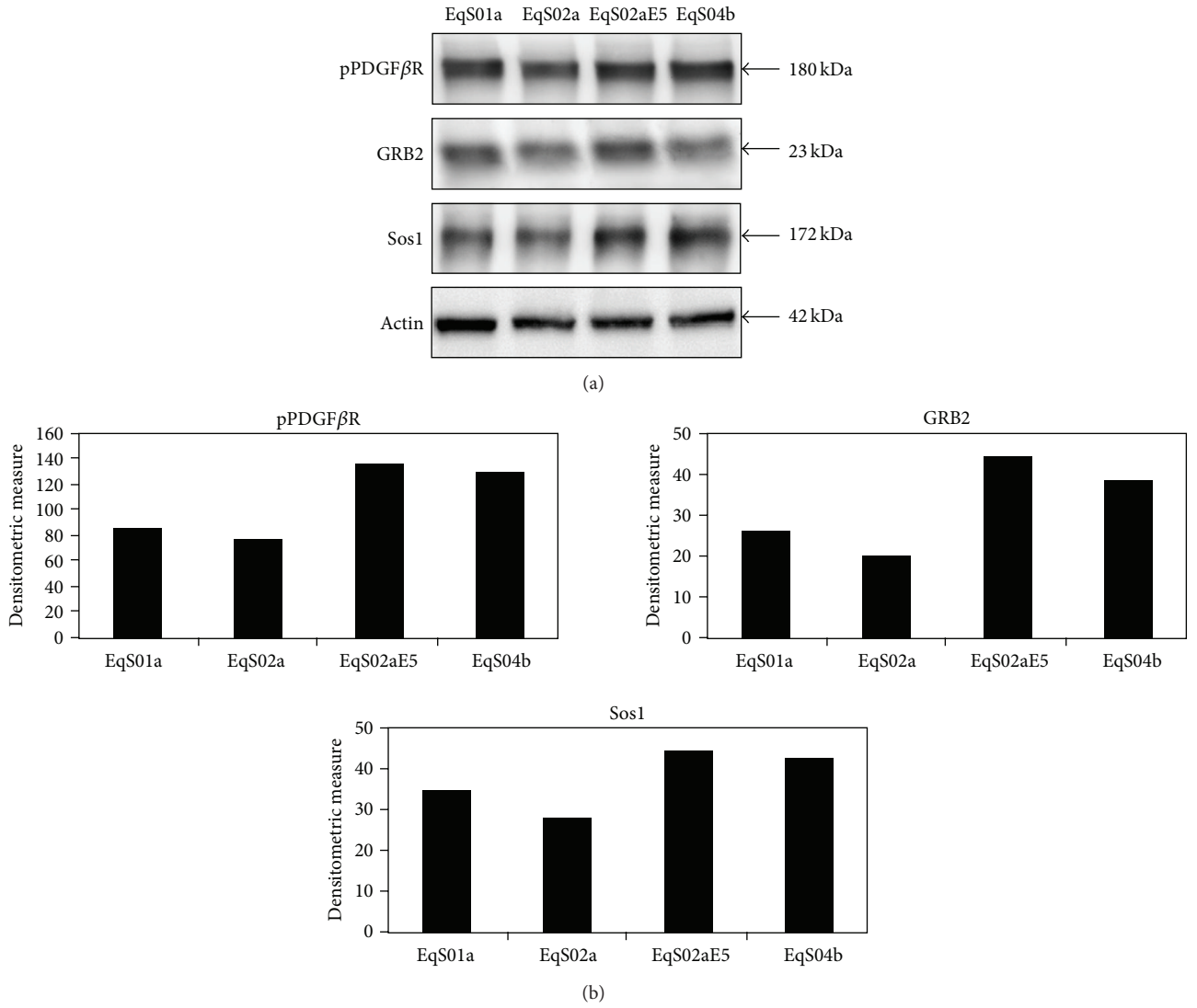

Figure 2: pPDFGβR-GRB2-Sos1 coimmunoprecipitation in EqS cell lines. (a) The presence of GRB2 and Sos1 was detected in pPDFGβR immunoprecipitates in higher amount in cell lines EqS01a, EqS02aE5, and EqS04b expressing BPV-1 E5 when compared to EqS02a which do not express the oncoprotein. Actin protein levels were detected on whole cell lysates before immunoprecipitation to ensure equal protein loading and allow normalization. (b) Quantitative densitometric analysis of the bands was performed with Image Lab software (ChemiDoc, Bio-Rad Laboratories).

different primers sets followed by sequencing. Sequence analysis and alignment with wild type sequence revealed that no mutations occurred in these exons in EqS cell lines (data not shown).

3.5. Colocalization of PDGFβR with BPV-1 E5. As gene mutations that may induce activation of PDGFβR have been excluded, we next sought to address whether the receptor c-localizes with BPV-1 E5. EqS cell lines were analyzed by double labelling immunofluorescence using rabbit anti-PDGFβR and sheep anti-E5 primary antibodies (green fluorescence for E5 and red fluorescence for PDGFβR). Interestingly, both proteins appeared to be mostly expressed in a juxtanuclear position in EqS02aE5, where they markedly colocalize as judged by the yellow fluorescence of merged images (Figure 6(a)). PDGFβR was found to be expressed also in the cytoplasm of EqS01a, EqS04b (data not shown), and EqS02a cells (Figure 6(b)); the latter cell line showed, as expected, no signal for E5 (Figure 6(b)). BPV-1 E5 staining was not recorded in EqS01a and EqS04b, which is probably due to undetectable expression levels of endogenous protein by immunofluorescence (expression of E5 in these cells has been shown previously by RT-PCR [48]).

3.6. Effects of Imatinib Mesylate on PDGFβR Phosphorylation and Cell Viability. Serum-starved cells were exposed to various concentration of imatinib with or without PDGF-BB in order to determine the effects of the drug on PDGFβR activation and cell viability in EqS cell lines. Protein extracts were subjected to immunoprecipitation of PDGFβR followed

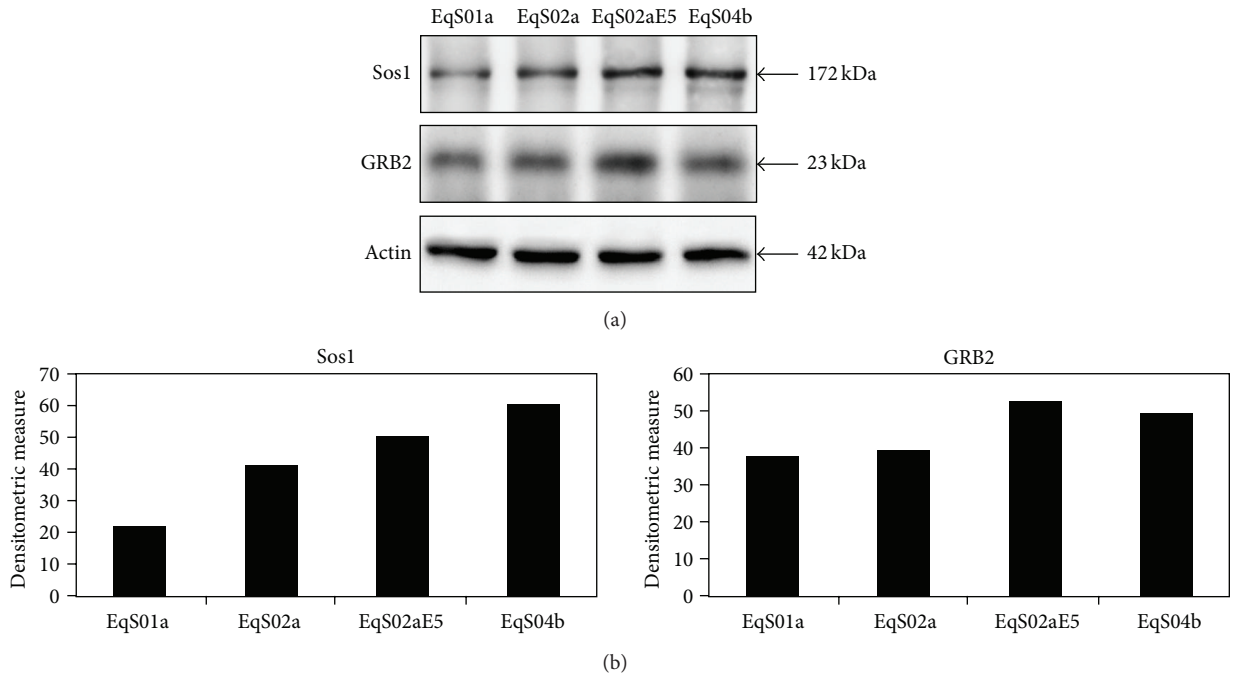

Figure 3: Sos1-GRB2 coimmunoprecipitation. (a) Binding of GRB2 to Sos1 was recorded in all EqS cell lines; the complex was coimmunoprecipitated in higher amount in EqS02aE5 and EqS04b, which express the highest levels of BPV-1 E5 among the analyzed cell lines. Actin protein levels were detected on whole cell lysates before immunoprecipitation to ensure equal protein loading and allow normalization. (b) Quantitative densitometric analysis of the bands was performed with Image Lab software (ChemiDoc, Bio-Rad Laboratories).

by immunoblotting with anti-pTyr and anti-PDGFβR antibodies. Figure 7 clearly shows that PDGF-BB was able to induce PDGFβR transphosphorylation, which indeed was not observed in the absence of ligand; furthermore imatinib is shown to inhibit PDGFβR autophosphorylation induced by PDGF-BB in a dose-dependent manner, with near complete inhibition at a concentration of 5 μM in all the cell lines. Additionally, PDGFβR expression levels decreased parallel to the increase of its phosphorylation degree, whereas they increased concomitantly with inhibition of phosphorylation by imatinib with a dose-dependent manner.

Similarly, cells were exposed to 10% FBS or various concentrations of imatinib with or without PDGF-BB and subjected to MTS-based cell viability assay. As shown in Figure 8, all the cell lines proliferated in the presence of both FBS and PDGF-BB, and imatinib at a concentration of 0.1 μM is already sufficient to severely reduce cell viability in EqS01a, EqS02aE5, and EqS04b; treatment with increasing doses of imatinib caused a further gradual decrease in cell viability levels. All these biological effects appear to be milder in EqS02a, in which no difference in cell viability can be observed at the highest doses of imatinib.

4. Discussion

E5 is the major oncoprotein encoded by BPV-1 and plays a key role in the tumorigenic process [13]; the main transforming activity of BPV E5 is due to its specifical binding to PDGFβR, causing receptor autophosphorylation and activation, which results in mitogenic signalling and neoplastic transformation [18, 20].

Among the downstream pathways of pPDGFβR, the Ras-MAPK-ERK signalling is known to regulate cell proliferation [26, 27]. In this study we investigated the activation of PDGFβR and Ras-MAPK-ERK pathway in equine sarcoid-derived cell lines EqS01a, EqS02a, EqS02aE5, and EqS04b [48, 49]. We found that PDGFβR was phosphorylated and bound its downstream partners GRB2-Sos1 in higher amounts in EqS02aE5 and EqS04b (both containing high levels of oncoproteins transcripts) and, to a lesser extent, in EqS01a when compared to EqS02a (which expresses low and not detectable levels of oncoproteins, resp.). Consistently, active Ras was expressed at higher levels in EqS cell lines expressing E5, suggesting that BPV-1 E5 may contribute to activation of this pathway and lead to sarcoid fibroblasts full transformation. Accordingly, PDGFβR was found to be constitutively activated in transformed mouse cells expressing BPV-1 E5, and pPDGFβR binds GRB2 in mortal human fibroblasts transfected with the oncoprotein [18, 22]; moreover, PDGFβR has been found to be activated *in vivo* in BPV-E5 positive equine sarcoids, and pPDGFβR recruits GRB2-Sos1 which enhance Ras activation in bovine urinary bladder cancer [24, 25]; our finding of total Ras overexpression in EqS01a cell line is in agreement with previous studies which reported an association between PV infection in bovids and activation of Ras gene [53]: these data may suggest a role of this pathway in BPV-induced carcinogenesis. In addition, Ras had been found to be activated in cultured fibroblasts also by Rhesus-PV E5, indicating that E5 genes may play a major role in the regulation of this transduction pathway [54].

Surprisingly, no differences were found in phosphorylation status of the downstream kinases of activated Ras,

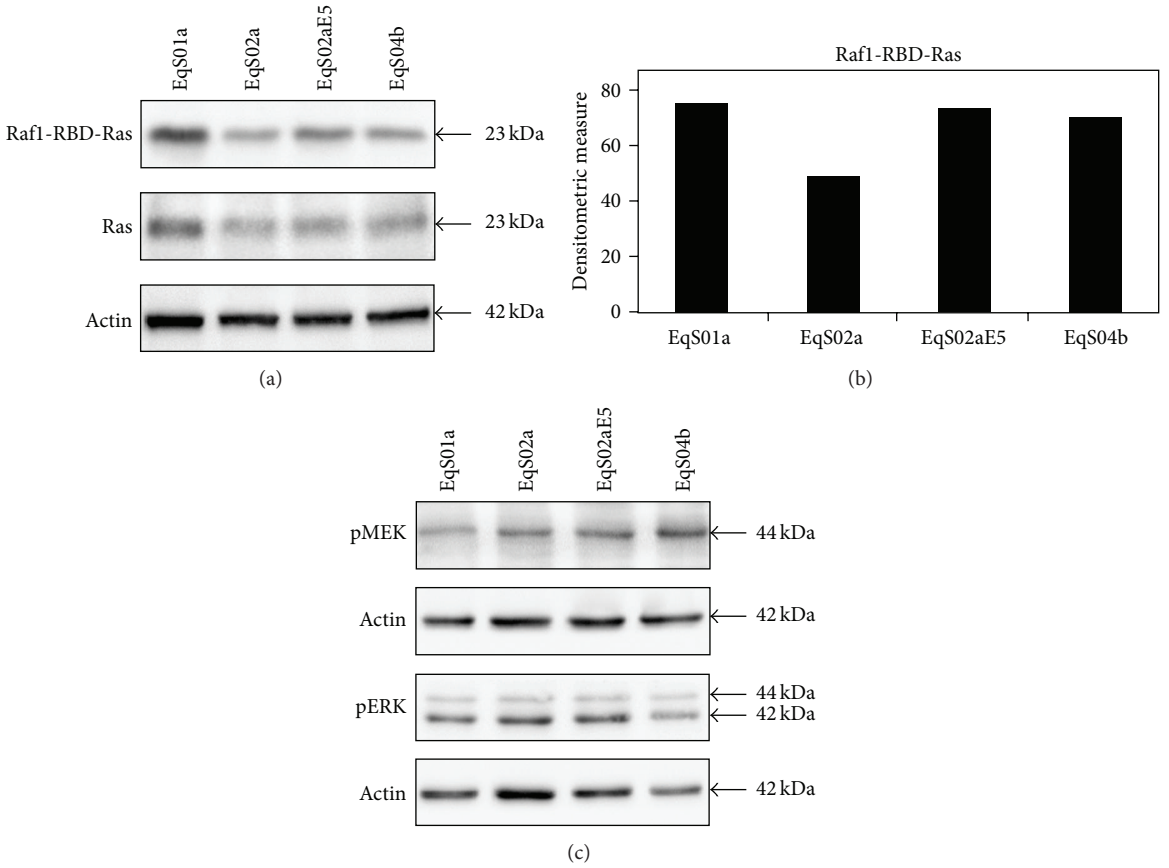

Figure 4: Analysis of Ras-mitogen-activated protein kinase-ERK pathway in sarcoid-derived cell lines (EqS). (a) Immunoblotting analysis of Ras in a pull-down assay of activated Ras (Raf1-RBD-Ras). Raf1-RBD-Ras was increased in cell lines EqS01a (to higher extent), EqS02aE5, and EqS04b when compared to EqS02a (not expressing E5). Total Ras levels were detected on whole cell lysates before pull-down assay to allow normalization of Raf1-RBD-Ras. Ras was overexpressed in EqS01a. Ras expression levels were normalized to actin levels. (b) Quantitative densitometric analysis of the bands was performed with Image Lab software (ChemiDoc, Bio-Rad Laboratories). (c) Immunoblotting analysis of pMEK and pERK expression. No differences in phosphorylation status of both MEK and ERK kinases were recorded. Actin protein levels were detected to ensure equal amounts of proteins for each lane.

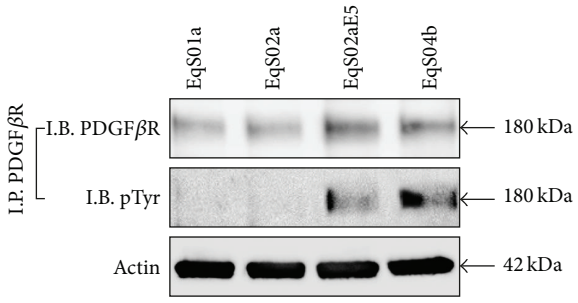

Figure 5: Activation of PDFGβR in serum-starved sarcoid-derived cell lines (EqS). The PDFGβR immunoprecipitated in serum-deprived cells is phosphorylated only in EqS02aE5 and EqS04b, which express the higher levels of BPV-1 E5 among the analyzed cell lines (I.P.: immunoprecipitation; I.B.: immunoblotting).

namely, pMEK and pERK. Previous studies showed that E5 does not promote any changes in ERK activity in cultured fibroblasts [22, 55] as well as in BPV-induced tumours *in vivo*: it is therefore possible that pPDGFβR activates GRB2, Sos1, and Ras which may deviate on phosphatidylinositol-3-kinase/AKT pathway (PI3 K/AKT). As matter of the fact, PI3 K/AKT pathway, rather than MEK-ERK signalling, had been found to be activated in BPV-induced tumours, thus contributing to neoplastic transformation [25, 56].

To further investigate the possible factors contributing to PDGFβR activation, we first assessed PDGFβR phosphorylation status on serum starved cells: the receptor was found to be phosphorylated only in EqS02aE5 and EqS04b, which express the highest levels of BPV-1 E5 among all cell lines, suggesting that its activation may be due to the interaction with the E5 oncoprotein rather than to the presence of growth factors added to the medium. Accordingly, Petti et al. demonstrated that BPV-1 E5 activates PDGFβR in a ligand-independent manner [18]. Taken together, all these findings may indicate that the extent of PDGFβR activation may correlate with E5 expression levels and the number of viral copies; direct association of viral load with impaired expression of tyrosine kinase receptors has been reported for human cervical tumours harboring human papillomavirus,

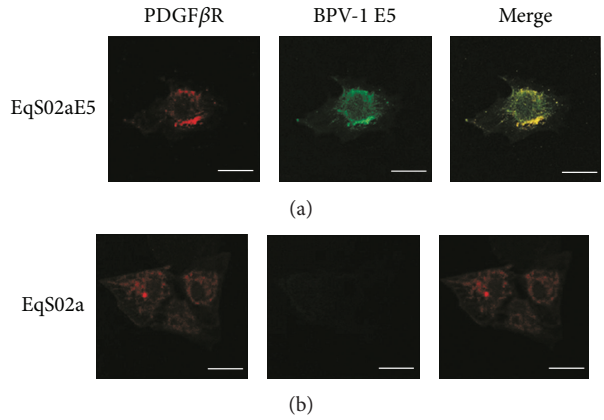

Figure 6: BPV-1E5-PDFGβR colocalization. (a) BPV-1 E5 (green fluorescence) and PDFGβR (red fluorescence) markedly colocalized (merged panel, yellow fluorescence) in a juxtanuclear Golgi-like position in sarcoid-derived EqS02a cells transfected with BPV-1 E5 (EqS02aE5). A representative image is shown. (b) EqS02a cells expressed PDFGβR in the cytoplasm and showed no green signal for E5. Bar = 20 μm.

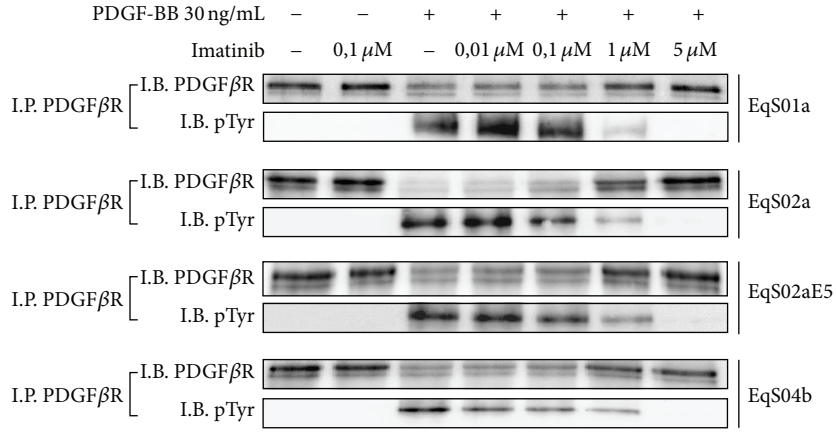

Figure 7: Dose-dependent inhibition of PDGF-BB-induced PDFGβR activation by imatinib mesylate. In sarcoid-derived cell lines (EqS) treated with increasing doses of imatinib with or without PDGF-BB, the drug inhibited PDFGβR autophosphorylation. PDGFβR downregulation was another measure of its activation induced by PDFG-BB, and, conversely, increasing of PDGFβR expression in cells treated with higher doses of imatinib confirmed the inhibition of receptor activation (I.P.: immunoprecipitation; I.B.: immunoblotting).

suggesting that the impairing of these cellular functions may depend on the viral load in PVs induced cancer [57].

PDGFR and other related tyrosine kinase receptors may be activated by mutations or genetic rearrangements causing tumours in both human and animal species, particularly in the transmembrane and cytosolic domains [58–64]. Sequence analysis of PDGFβR in our cell lines revealed that no mutations occurred along these domains, suggesting that the receptor is not activated by itself in our experimental model.

Furthermore, double labeling immunofluorescence showed that PDGFβR perfectly colocalized with BPV-1 E5 in EqS02aE5 where it was mostly expressed in a juxtanuclear position, consistently with the location of E5 in the Golgi apparatus (GA) [14, 65]. The intracellular colocalization of E5 and PDGFβR indicates that this protein interaction may take place in the GA and may be another proof of evidence of the possible receptor activation upon E5 interaction; juxtanuclear colocalization of E5 with PDGFβR was also reported in bovine urinary bladder cancer by this research group, suggesting that this finding could be common in BPV-induced tumours [15]. Many studies have reported the physical interaction between these two proteins and subsequent activation of PDGFβR both *in vitro* and *in vivo* [23, 66], thus we speculate that BPV-1 E5 may bind to PDGFβR also in our sarcoid-derived cell lines expressing E5, inducing its phosphorylation and activation of downstream pathways leading to transformation.

Although many therapeutical strategies have been proposed for treatment of sarcoid, no 100% effective therapy is available so far [1]. Many tyrosine kinase receptors inhibitors are used in veterinary medicine [67]; among these, imatinib mesylate (also known as STI-571 or Gleevec) has been shown to selectively inhibit PDGFβR activation in both human and animal tumours [33–36, 47]. In this study we showed that sarcoid fibroblasts proliferation was mostly dependent on

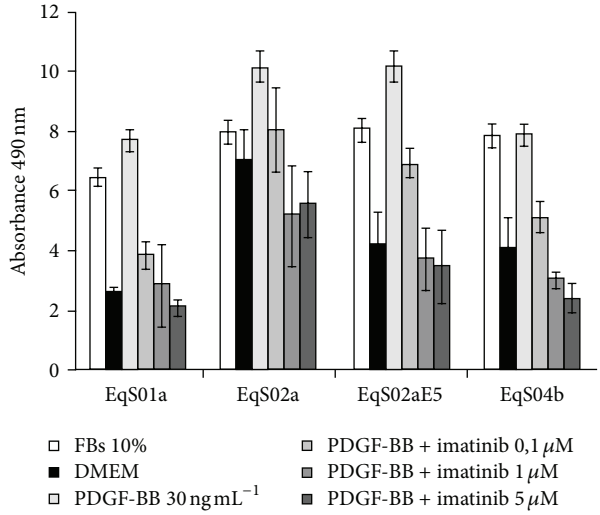

Figure 8: Effects of imatinib mesylate on PDGF-BB-stimulated sarcoids-derived cells (EqS) viability. MTS-based assay revealed that PDGF-BB stimulates cell growth as well as FBS and that imatinib decreases cell viability in all the analyzed cell lines in a dose-dependent manner, but with lower efficiency in EqS02a (not expressing E5). The data represent the mean of repeated independent experiments.

PDGFβR stimulation; furthermore, we demonstrated that imatinib inhibited PDGFβR phosphorylation in a dose-dependent manner. In this case no phosphorylation of PDGFβR could be observed in serum-free conditions, whilst the receptor was phosphorylated after 24 h of starvation, suggesting that longer times are needed to reach detectable levels of its activation. The finding of total PDGFβR down-regulation concomitant to the augmentation of its phosphorylation degree induced by PDGF-BB, was not surprising: for the PDGFβR and other tyrosine kinase receptors, ligand binding induces receptor phosphorylation and thus triggers its clustering in coated pits, followed by endocytosis and lysosomal degradation of receptor-ligand complexes [68, 69]. Thus the augmentation of PDGFβR expression levels at increasing doses of drug was another measure of the efficiency of treatment. Here we also demonstrated that imatinib was able to decrease sarcoid fibroblasts cell viability in a dose-dependent manner. However, lower effects were observed on cell viability in EqS02a by imatinib treatment at all the experimental doses; lacking E5 expression, this cell line may have lower levels of activated PDGFβR, thus the drug may have less access to the ATP-binding site and, as a consequence, milder biological effects when compared to other cell lines. These findings strengthen our hypothesis of a PDGFβR activation by E5 and suggest that imatinib may target more efficiently on fully transformed sarcoid fibroblasts.

5. Conclusions

Finally, our study demonstrates that PDGFβR is activated thus binding downstream molecular partners in sarcoid-derived cell lines expressing BPV-1 E5; this activation results in Ras activation but not major phosphorylation of MEK and ERK kinases, suggesting that this signalling cascade may possibly cross-talk with other transduction pathways which had been found to be activated in BPV-induced tumours. Further investigations are needed to clarify the specific roles of activated PDGFβR and downstream pathways in the pathology of equine sarcoid. Furthermore, the data obtained by treatment of sarcoid-derived fibroblasts with imatinib, suggest that this drug could be proposed for a clinical trial leading to therapy of sarcoid *in vivo*. We have developed a translational approach, and a clinical trial is ongoing to test on sarcoid-affected donkeys the therapeutic effects of a dermatological cream based on Imatinib mesylate (CESA protocol number 2012/0052665).

Authors' Contribution

Gennaro Altamura and Annunziata Corteggio have contributed equally to this work.

Acknowledgments

The authors wish to express their gratitude to Ph.D. student F. Bocaneti for her technical help. The authors are grateful to Professor Maria Saveria Campo (Emeritus Professor, Glasgow University) for her kind gift of sheep anti-E5 antibody and for her critical reading of the paper. This work was supported by grant from MIUR: PRIN 2009: L 'EMATURIA ENZOOTICA CRONICA NEL BOVINO. CUP E6J11000300001.

References

[1] G. Borzacchiello and A. Corteggio, "Equine sarcoid: state of the art," *Ippologia*, vol. 20, no. 4, pp. 7–14, 2009.

[2] A. Martens, A. De Moor, J. Demeulemeester, and R. Ducatelle, "Histopathological characteristics of five clinical types of equine sarcoid," *Research in Veterinary Science*, vol. 69, no. 3, pp. 295–300, 2000.

[3] D. W. Scott and W. H. Miller, "Equine dermatology," *Journal of Equine Veterinary Science*, vol. 23, no. 2, pp. 65–67, 2003.

[4] W. D. Lancaster, G. H. Theilen, and C. Olson, "Hybridization of bovine papilloma virus type 1 and type 2 DNA to DNA from virus-induced hamster tumors and naturally occurring equine tumors," *Intervirology*, vol. 11, no. 4, pp. 227–233, 1979.

[5] N. T. Gorman, "Equine sarcoid—time for optimism," *Equine Veterinary Journal*, vol. 17, no. 6, pp. 412–414, 1985.

[6] L. Nasir and M. S. Campo, "Bovine papillomaviruses: their role in the aetiology of cutaneous tumours of bovids and equids," *Veterinary Dermatology*, vol. 19, no. 5, pp. 243–254, 2008.

[7] G. Borzacchiello and F. Roperto, "Bovine papillomaviruses, papillomas and cancer in cattle," *Veterinary Research*, vol. 39, no. 5, article 45, 2008.

[8] L. Nasir and S. W. J. Reid, "Bovine papillomaviral gene expression in equine sarcoid tumours," *Virus Research*, vol. 61, no. 2, pp. 171–175, 1999.

[9] E. A. Carr, A. P. Théon, B. R. Madewell, M. E. Hitchcock, R. Schlegel, and J. T. Schiller, "Expression of a transforming gene (E5) of bovine papillomavirus in sarcoids obtained from

horses," *American Journal of Veterinary Research*, vol. 62, no. 8, pp. 1212–1217, 2001.

[10] G. Chambers, V. A. Ellsmore, P. M. O'Brien et al., "Sequence variants of bovine papillomavirus E5 detected in equine sarcoids," *Virus Research*, vol. 96, no. 1-2, pp. 141–145, 2003.

[11] G. Borzacchiello, V. Russo, L. Della Salda, S. Roperto, and F. Roperto, "Expression of platelet-derived growth factor-beta receptor and bovine papillomavirus E5 and E7 oncoproteins in equine sarcoid," *Journal of Comparative Pathology*, vol. 139, no. 4, pp. 231–237, 2008.

[12] A. Corteggio, G. Altamura, F. Roperto, and G. Borzacchiello, "Bovine papillomavirus E5 and E7 oncoproteins in naturally occurring tumors: are two better than one?" *Infectious Agents and Cancer*, vol. 8, article 1, 2013.

[13] A. Venuti, F. Paolini, L. Nasir et al., "Papillomavirus E5: the smallest oncoprotein with many functions," *Molecular Cancer*, vol. 10, article 140, 2011.

[14] W. D. Pennie, G. J. Grindlay, M. Cairney, and M. S. Campo, "Analysis of the transforming functions of bovine papillomavirus type 4," *Virology*, vol. 193, no. 2, pp. 614–620, 1993.

[15] G. Borzacchiello, V. Russo, F. Gentile et al., "Bovine papillomavirus E5 oncoprotein binds to the activated form of the platelet-derived growth factor β receptor in naturally occurring bovine urinary bladder tumours," *Oncogene*, vol. 25, no. 8, pp. 1251–1260, 2006.

[16] D. DiMaio and D. Mattoon, "Mechanisms of cell transformation by papillomavirus E5 proteins," *Oncogene*, vol. 20, no. 54, pp. 7866–7873, 2001.

[17] D. J. Goldstein, W. Li, L.-M. Wang et al., "The bovine papillomavirus type 1 E5 transforming protein specifically binds and activates the β-type receptor for the platelet-derived growth factor but not other related tyrosine kinase-containing receptors to induce cellular transformation," *Journal of Virology*, vol. 68, no. 7, pp. 4432–4441, 1994.

[18] L. Petti, L. A. Nilson, and D. DiMaio, "Activation of the platelet-derived growth factor receptor by the bovine papillomavirus E5 transforming protein," *The EMBO Journal*, vol. 10, no. 4, pp. 845–855, 1991.

[19] V. M. Nappi and L. M. Petti, "Multiple transmembrane amino acid requirements suggest a highly specific interaction between the bovine papillomavirus E5 oncoprotein and the platelet-derived growth factor beta receptor," *Journal of Virology*, vol. 76, no. 16, pp. 7976–7986, 2002.

[20] C.-C. Lai, C. Henningson, and D. Dimaio, "Bovine papillomavirus E5 protein induces oligomerization and transphosphorylation of the platelet-derived growth factor β receptor," *Proceedings of the National Academy of Sciences of the United States of America*, vol. 95, no. 26, pp. 15241–15246, 1998.

[21] O. Klein, D. Kegler-Ebo, J. Su, S. Smith, and D. DiMaio, "The bovine papillomavirus E5 protein requires a juxtamembrane negative charge for activation of the platelet-derived growth factor β receptor and transformation of C127 cells," *Journal of Virology*, vol. 73, no. 4, pp. 3264–3272, 1999.

[22] L. M. Petti, E. C. Ricciardi, H. J. Page, and K. A. Porter, "Transforming signals resulting from sustained activation of the PDGFβ receptor in mortal human fibroblasts," *Journal of Cell Science*, vol. 121, no. 8, pp. 1172–1182, 2008.

[23] S. Roperto, G. Borzacchiello, I. Esposito et al., "Productive infection of bovine papillomavirus type 2 in the placenta of pregnant cows affected with urinary bladder tumors," *PLoS ONE*, vol. 7, no. 3, Article ID e33569, 2012.

[24] G. Borzacchiello, S. Mogavero, G. De Vita, S. Roperto, L. Della Salda, and F. Roperto, "Activated platelet-derived growth factor β receptor expression, PI3K-AKT pathway molecular analysis, and transforming signals in equine sarcoids," *Veterinary Pathology*, vol. 46, no. 4, pp. 589–597, 2009.

[25] A. Corteggio, O. Di Geronimo, S. Roperto, F. Roperto, and G. Borzacchiello, "Activated platelet-derived growth factor β receptor and Ras-mitogen-activated protein kinase pathway in natural bovine urinary bladder carcinomas," *Veterinary Journal*, vol. 191, no. 3, pp. 393–395, 2012.

[26] A. Carnero, "The PKB/AKT pathway in cancer," *Current Pharmaceutical Design*, vol. 16, no. 1, pp. 34–44, 2010.

[27] S. J. Moeller, E. D. Head, and R. J. Sheaff, "p27Kip1 inhibition of GRB2-SOS formation can regulate Ras activation," *Molecular and Cellular Biology*, vol. 23, no. 11, pp. 3735–3752, 2003.

[28] M. Dance, A. Montagner, J.-P. Salles, A. Yart, and P. Raynal, "The molecular functions of Shp2 in the Ras/Mitogen-activated protein kinase (ERK1/2) pathway," *Cellular Signalling*, vol. 20, no. 3, pp. 453–459, 2008.

[29] N. A. Lokker, C. M. Sullivan, S. J. Hollenbach, M. A. Israel, and N. A. Giese, "Platelet-derived growth factor (PDGF) autocrine signaling regulates survival and mitogenic pathways in glioblastoma cells: evidence that the novel PDGF-C and PDGF-D ligands may play a role in the development of brain tumors," *Cancer Research*, vol. 62, no. 13, pp. 3729–3735, 2002.

[30] B. J. Druker, S. Tamura, E. Buchdunger et al., "Effects of a selective inhibitor of the Abl tyrosine kinase on the growth of Bcr-Abl positive cells," *Nature Medicine*, vol. 2, no. 5, pp. 561–566, 1996.

[31] E. Buchdunger, J. Zimmermann, H. Mett et al., "Inhibition of the Abl protein-tyrosine kinase in vitro and in vivo by a 2-phenylaminopyrimidine derivative," *Cancer Research*, vol. 56, no. 1, pp. 100–104, 1996.

[32] E. Buchdunger, C. L. Cioffi, N. Law et al., "Abl protein-tyrosine kinase inhibitor STI571 inhibits in vitro signal transduction mediated by c-Kit and platelet-derived growth factor receptors," *The Journal of Pharmacology and Experimental Therapeutics*, vol. 295, no. 1, pp. 139–145, 2000.

[33] T. Kilic, J. A. Alberta, P. R. Zdunek et al., "Intracranial inhibition of platelet-derived growth factor-mediated glioblastoma cell growth by an orally active kinase inhibitor of the 2-phenylaminopyrimidine class," *Cancer Research*, vol. 60, no. 18, pp. 5143–5150, 2000.

[34] B. P. Rubin, S. M. Schuetze, J. F. Eary et al., "Molecular targeting of platelet-derived growth factor B by imatinib mesylate in a patient with metastatic dermatofibrosarcoma protuberans," *Journal of Clinical Oncology*, vol. 20, no. 17, pp. 3586–3591, 2002.

[35] T. Sjöblom, A. Shimizu, K. P. O'Brien et al., "Growth inhibition of dermatofibrosarcoma protuberans tumors by the platelet-derived growth factor receptor antagonist STI571 through induction of apoptosis," *Cancer Research*, vol. 61, no. 15, pp. 5778–5783, 2001.

[36] E. C. McGary, K. Weber, L. Mills et al., "Inhibition of platelet-derived growth factor-mediated proliferation of osteosarcoma cells by the novel tyrosine kinase inhibitor STI571," *Clinical Cancer Research*, vol. 8, no. 11, pp. 3584–3591, 2002.

[37] R. E. Gilbert, D. J. Kelly, T. McKay et al., "PDGF signal transduction inhibition ameliorates experimental mesangial proliferative glomerulonephritis," *Kidney International*, vol. 59, no. 4, pp. 1324–1332, 2001.

[38] B. J. Druker and N. B. Lydon, "Lessons learned from the development of an Abl tyrosine kinase inhibitor for chronic

myelogenous leukemia," *The Journal of Clinical Investigation*, vol. 105, no. 1, pp. 3–7, 2000.

[39] M. J. Mauro, M. O'Dwyer, M. C. Heinrich, and B. J. Druker, "STI571: a paradigm of new agents for cancer therapeutics," *Journal of Clinical Oncology*, vol. 20, no. 1, pp. 325–334, 2002.

[40] G. W. Krystal, S. Honsawek, J. Litz, and E. Buchdunger, "The selective tyrosine kinase inhibitor STI571 inhibits small cell lung cancer growth," *Clinical Cancer Research*, vol. 6, no. 8, pp. 3319–3326, 2000.

[41] A. T. van Oosterom, I. Judson, J. Verweij et al., "Safety and efficacy of imatinib (STI571) in metastatic gastrointestinal stromal tumours: a phase I study," *The Lancet*, vol. 358, no. 9291, pp. 1421–1423, 2001.

[42] A. T. van Oosterom, I. R. Judson, J. Verweij et al., "Update of phase I study of imatinib (STI571) in advanced soft tissue sarcomas and gastrointestinal stromal tumors: a report of the EORTC Soft Tissue and Bone Sarcoma Group," *European Journal of Cancer*, vol. 38, supplement 5, pp. S83–S87, 2002.

[43] M. Isotani, N. Ishida, M. Tominaga et al., "Effect of tyrosine kinase inhibition by imatinib mesylate on mast cell tumors in dogs," *Journal of Veterinary Internal Medicine*, vol. 22, no. 4, pp. 985–988, 2008.

[44] L. Marconato, G. Bettini, C. Giacoboni et al., "Clinicopathological features and outcome for dogs with mast cell tumors and bone marrow involvement," *Journal of Veterinary Internal Medicine*, vol. 22, no. 4, pp. 1001–1007, 2008.

[45] O. Yamada, M. Kobayashi, O. Sugisaki et al., "Imatinib elicited a favorable response in a dog with a mast cell tumor carrying a c-kit c.1523A>T mutation via suppression of constitutive KIT activation," *Veterinary Immunology and Immunopathology*, vol. 142, no. 1-2, pp. 101–106, 2011.

[46] J. L. Lachowicz, G. S. Post, and E. Brodsky, "A phase I clinical trial evaluating imatinib mesylate (Gleevec) in tumor-bearing cats," *Journal of Veterinary Internal Medicine*, vol. 19, no. 6, pp. 860–864, 2005.

[47] R. Katayama, M. K. Huelsmeyer, A. K. Marr, I. D. Kurzman, D. H. Thamm, and D. M. Vail, "Imatinib mesylate inhibits platelet-derived growth factor activity and increases chemosensitivity in feline vaccine-associated sarcoma," *Cancer Chemotherapy and Pharmacology*, vol. 54, no. 1, pp. 25–33, 2004.

[48] Z. Q. Yuan, E. A. Gault, P. Gobeil, C. Nixon, M. S. Campo, and L. Nasir, "Establishment and characterization of equine fibroblast cell lines transformed in vivo and in vitro by BPV-1: Model systems for equine sarcoids," *Virology*, vol. 373, no. 2, pp. 352–361, 2008.

[49] Z. Yuan, E. A. Gault, M. Saveria Campo, and L. Nasir, "Different contribution of bovine papillomavirus type 1 oncoproteins to the transformation of equine fibroblasts," *The Journal of General Virology*, vol. 92, no. 4, pp. 773–783, 2011.

[50] U. K. Laemmli, "Cleavage of structural proteins during the assembly of the head of bacteriophage T4," *Nature*, vol. 227, no. 5259, pp. 680–685, 1970.

[51] G. Borzacchiello, V. Russo, C. Spoleto et al., "Bovine papillomavirus type-2 DNA and expression of E5 and E7 oncoproteins in vascular tumours of the urinary bladder in cattle," *Cancer Letters*, vol. 250, no. 1, pp. 82–91, 2007.

[52] M. A. Silva, G. Altamura, A. Corteggio et al., "Expression of connexin 26 and bovine papillomavirus E5 in cutaneous fibropapillomas of cattle," *The Veterinary Journal*, vol. 195, no. 3, pp. 337–343, 2013.

[53] M. S. Campo, R. E. McCaffery, I. Doherty, I. M. Kennedy, and W. F. H. Jarrett, "The Harvey ras 1 gene is activated in papillomavirus-associated carcinomas of the upper alimentary canal in cattle," *Oncogene*, vol. 5, no. 3, pp. 303–308, 1990.

[54] J. Ghai, R. S. Ostrow, J. Tolar et al., "The E5 gene product of rhesus papillomavirus is an activator of endogenous Ras and phosphatidylinositol-3′-kinase in NIH 3T3 cells," *Proceedings of the National Academy of Sciences of the United States of America*, vol. 93, no. 23, pp. 12879–12884, 1996.

[55] M. Zago, M. S. Campo, and V. O'Brien, "Cyclin A expression and growth in suspension can be uncoupled from p27 deregulation and extracellular signal-regulated kinase activity in cells transformed by bovine papillomavirus type 4 E5," *The Journal of General Virology*, vol. 85, no. 12, pp. 3585–3595, 2004.

[56] A. Corteggio, O. Di Geronimo, S. Roperto, F. Roperto, and G. Borzacchiello, "Bovine papillomavirus E7 oncoprotein binds to p600 in naturally occurring equine sarcoids," *The Journal of General Virology*, vol. 92, no. 2, pp. 378–382, 2011.

[57] S. H. Song, J. K. Lee, J. Y. Hur, I. Kim, H. S. Saw, and Y. K. Park, "The expression of epidermal growth factor receptor, vascular endothelial growth factor, matrix metalloproteinase-2, and cyclooxygenase-2 in relation to human papilloma viral load and persistence of human papillomavirus after conization with negative margins," *International Journal of Gynecological Cancer*, vol. 16, no. 6, pp. 2009–2017, 2006.

[58] T. R. Golub, G. F. Barker, M. Lovett, and D. Gary Gilliland, "Fusion of PDGF receptor β to a novel ets-like gene, tel, in chronic myelomonocytic leukemia with t(5;12) chromosomal translocation," *Cell*, vol. 77, no. 2, pp. 307–316, 1994.

[59] M. C. Heinrich, C. L. Corless, A. Duensing et al., "PDGFRA activating mutations in gastrointestinal stromal tumors," *Science*, vol. 299, no. 5607, pp. 708–710, 2003.

[60] S. Hirota, A. Ohashi, T. Nishida et al., "Gain-of-function mutations of platelet-derived growth factor receptor α gene in gastrointestinal stromal tumors," *Gastroenterology*, vol. 125, no. 3, pp. 660–667, 2003.

[61] S. Hirota, "Gain-of-function mutation of c-kit gene and molecular target therapy in GISTs," *Japanese Journal of Gastroenterology*, vol. 100, no. 1, pp. 13–20, 2003.

[62] N. Sirvent, G. Maire, and F. Pedeutour, "Genetics of dermatofibrosarcoma protuberans family of tumors: from ring chromosomes to tyrosine kinase inhibitor treatment," *Genes Chromosomes and Cancer*, vol. 37, no. 1, pp. 1–19, 2003.

[63] M. Giantin, M. Vascellari, E. M. Morello et al., "c-KIT messenger RNA and protein expression and mutations in canine cutaneous mast cell tumors: correlations with post-surgical prognosis," *Journal of Veterinary Diagnostic Investigation*, vol. 24, no. 1, pp. 116–126, 2012.

[64] I. Matsumura, M. Mizuki, and Y. Kanakura, "Roles for deregulated receptor tyrosine kinases and their downstream signaling molecules in hematologic malignancies," *Cancer Science*, vol. 29, no. 3, pp. 479–485, 2008.

[65] A. Burkhardt, M. Willingham, C. Gay, K.-T. Jeang, and R. Schlegel, "The E5 oncoprotein of bovine papillomavirus is oriented asymmetrically in Golgi and plasma membranes," *Virology*, vol. 170, no. 1, pp. 334–339, 1989.

[66] K. Talbert-Slagle and D. DiMaio, "The bovine papillomavirus E5 protein and the PDGF β receptor: it takes two to tango," *Virology*, vol. 384, no. 2, pp. 345–351, 2009.

[67] C. A. London, "Tyrosine kinase inhibitors in veterinary medicine," *Topics in Companion Animal Medicine*, vol. 24, no. 3, pp. 106–112, 2009.

[68] J. Nilsson, J. Thyberg, C. H. Heldin, B. Westermark, and A. Wasteson, "Surface binding and internalization of platelet-derived growth factor in human fibroblasts," *Proceedings of the National Academy of Sciences of the United States of America*, vol. 80, no. 181, pp. 5592–5596, 1983.

[69] J. L. Goldstein, M. S. Brown, R. G. Anderson, D. W. Russell, and W. J. Schneider, "Receptor-mediated endocytosis: concepts emerging from the LDL receptor system," *Annual Review of Cell Biology*, vol. 1, pp. 1–39, 1985.

Hindawi Publishing Corporation
BioMed Research International
Volume 2013, Article ID 421398, 9 pages
http://dx.doi.org/10.1155/2013/421398

Research Article

Expression and *In Silico* Analysis of the Recombinant Bovine Papillomavirus E6 Protein as a Model for Viral Oncoproteins Studies

J. Mazzuchelli-de-Souza,[1,2] R. F. Carvalho,[1,2] R. M. Ruiz,[1,2] T. C. Melo,[1,3] R. P. Araldi,[1,2] E. Carvalho,[4] C. E. Thompson,[5] M. P. Sircili,[1,2] W. Beçak,[1,6] and R. C. Stocco[1,2]

[1] *Laboratório de Genética, Instituto Butantan, Secretaria de Estado da Saúde, Avenida Vital Brasil, 1500 Butantã, 05503-900 São Paulo, SP, Brazil*
[2] *Programa de Pós-graduação Interunidades em Biotecnologia, Instituto de Ciências Biomédicas, Edifício ICB-III-Cidade Universitária, Universidade de São Paulo, Avenida Prof. Lineu Prestes, 2415 Butantã, 05508-900 São Paulo, SP, Brazil*
[3] *Programa de Pós-graduação em Biologia Estrutural e Funcional, Universidade Federal de São Paulo, Rua Botucatu 740, Vila Clementina, 04023-900 São Paulo, SP, Brazil*
[4] *Laboratório de Biotecnologia Molecular, Instituto Butantan, Secretaria de Estado da Saúde, Avenida Vital Brasil 1500, Butantã, 05503-900 São Paulo, SP, Brazil*
[5] *Laboratório Nacional de Computação Científica, Avenida Getúlio Vargas 333, Quitandinha, 25651-075 Petrópolis, RJ, Brazil*
[6] *Departamento de Biologia, Universidade Federal da Integração Latino-Americana (UNILA), Avenida Tancredo Neves 6731 bloco 4, 85867-970 Foz do Iguaçú, PR, Brazil*

Correspondence should be addressed to R. C. Stocco; ritastocco@butantan.gov.br

Received 2 April 2013; Accepted 16 May 2013

Academic Editor: Franco Roperto

Bovine papillomaviruses (BPVs) are recognized as the causal agents of economical relevant diseases in cattle, associated with the development of tumors in skin and mucosa. The oncogenesis process is mainly associated with different viral oncoprotein expressions, which are involved in cell transformation. The expression and characterization of recombinant viral oncoproteins represent an attractive strategy to obtain biotechnological products as antibodies and potential vaccines, Thus, the aim of this work was to clone and express the BPV-1 and BPV-2 E6 recombinant proteins and perform *in silico* analysis in order to develop a strategy for the systematic study of other papillomaviruses oncoproteins. The results demonstrated that BPV-1 and BPV-2 E6 recombinant proteins were expressed and purified from bacterial system as well as its *in silico* analysis was performed in order to explore and predict biological characteristics of these proteins.

1. Introduction

Different papillomaviruses (PVs) have been described as infectious agents of the vertebrates species, including domestic animals and human beings [1, 2]. The correlation between the papillomavirus infection and the cellular malignant progression is associated with the expression of viral oncoproteins. These proteins act on different aspects of the tumoral suppression cascades as well as on the ones that take part in the control of cell cycle and immune response. Viral oncoproteins can also interact with cellular DNA. Altogether, these actions can induce mutational changes in the host cell chromatin [3].

Currently, the *Papillomaviridae* family is divided into 16 genera according to their genomic organization [4, 5]. These small (55–60 nm), nonenveloped viruses have a genome of a double-stranded circular DNA molecule of approximately eight kilobases [6], codifying functional, early (E) proteins, and structural, late (L) proteins, expressed at different stages of the viral cycle. With at least eight potential open reading frames, the viral genome also consists of a noncoding region, the long control region (LCR), associated with the

viral transcriptional regulation. The E region encodes the replication and transcription regulatory proteins E1, E2, and the transforming proteins E5, E6, and E7, which are associated with uncontrolled cell proliferation and differentiation [7]. The E4 protein formed by alternative splicing of genes E1 and E1/E4 transcripts (E1–E4) is associated with the release of the virions through the disruption of the cytoskeleton structure [8–10]. It is also shown that actin cytoskeleton was altered in BPV-1 E6-transformed cells through E6 interaction with the focal adhesion protein paxillin [11]. On the other hand, the L region encodes structural proteins L1 and L2 that assemble into the capsid during the viral particle maturation [12]. Specifically, L1 is the most conserved gene within PV genome and has therefore been used for the identification of new PVs types [4].

The bovine papillomavirus (BPV) is recognized as the causal agent of benign and malignant tumors in cattle, such as cutaneous papillomas, urinary bladder, and esophagus cancer. This virus is distributed worldwide, being associated with severe economic losses in meat, milk, and leather production. Thirteen types of the BPVs are currently well characterized and classified into three distinct genera, Delta, Epsilon, and Xi, and have been characterized and associated with different histopathological lesions [13]. Specifically, the BPV-1 and 2 are classified as *Deltapapillomaviruses* [14, 15]. Characteristically, these types induce the appearance of fibropapillomas, associated with the recruitment of the subepithelial fibroblasts [16] and have the ability to infect different host species, not only bovines, causing the equine sarcoid [15]. Lately, the genome of a new Delta-BPV type (BPV-13) was fully sequenced [17].

The BPV-1 is commonly associated with lesions in the teats and udder [13, 18, 19]. BPV-1 can cause fibropapillomas of the penis, leading to necrosis and the loss of reproductive function [20]. BPV-2 is the causal agent of malignant tumors in the bladder [21]. Both types have also already been detected in peripheral blood and in tissues of the reproductive tract, and their vertical transmission has been suggested [16, 21–26].

The first evidence of the oncogenic properties of E6 protein came from studies on human tumors cell lineages derivate from uterine cervix where E6 was found expressed and maintained many years after the initial transformation events [27–29]. The E6 and E7 gene products are essential in the process of cell transformation and immortalization [28, 30]. Particularly, E6 protein has a central role as a carcinogen factor because it binds to p53, a major tumor suppressor protein, inducing its degradation [4]. Studies conducted with different cervical cancer cell lines infected with HPV-16 showed that the only expressed viral proteins were E6 and E7, leading to the speculation that they could be expressed like fusion proteins, an important indicator for the malignant progression [31]. It is also suggested that the genes E6 and E7 have a synergic action during the induction of genital human keratinocytes immortalization, although in some other cell types, like mammary epithelial cells, they may act separately [32].

Knowing the importance of E6 protein, the aim of this work was to clone and express the BPV-1 and BPV-2 E6 recombinant proteins enabling the development of antibodies and vaccines and to perform *in silico* analysis in order to develop a strategy for the systematic study of other papillomaviruses oncoproteins.

2. Material and Methods

2.1. E6-1 and E6-2 Gene Amplification. The following specific primers were designed: E6-1 sense primer, 5′-GAAAACCTG TATTTTCAGGGCTAGGACCTGAAACCTTTTGC-3′; and E6-1 antisense primer, 5′-GGC*CTCGAG*CTGCAGGTGAAT CATCCAAG-3′, E6-2 sense primer, 5′-GAAAACCTGTAT TTTCAGGGCATGGACCTGCAAAGTTTTTC-3′; and E6-2 antisense primer, 5′-GGC*CTCGAG*GAATCATCCAAG TTTCTA-3′. Underlined letters indicate the nucleotides for TEV protease site, and italic underlined letters indicate *Xho*I restriction site. The primers were designed based on complete genome sequences deposited in GenBank (accession numbers X02346 and M20219.1). These primers were used in a PCR reaction to amplify E6 gene, using the genomic DNA of BPV-1 or BPV-2 previously cloned in pAT153 vector as a template [33]. A Palm- Corbett Cycler Cobbert Research Version 2.1.7 (Uniscience) was used with the following amplification program: an initial denaturation step at 95°C for 4 min followed by 30 cycles at 95°C for 1 min, 50°C for 30 sec, 72°C for 1 min, and finally, 5 min elongation step at 72°C.

2.2. Cloning and Subcloning. The amplified PCR products were detected in a 1% agarose gel electrophoresis, excised from the gel, and purified with Invisorb Fragment Clean Up Kit (Invitek). The purified amplicons were cloned in pCR4-TOPO vector (Invitrogen). The resulting constructs were cloned in transformed *E. coli* DH5a competent cells, and positive clones were selected from plates supplemented with ampicillin. Plasmid DNA was prepared from overnight grown cultures with a WIZARD Mini Prep Purification Kit (Promega) following the manufacturer's recommendations. Plasmids were digested with *Eco*RI and *Xho*I to check the insert presence. Purified inserts were subcloned into the pET-28(+) vector (Merck), which was previously digested with the same enzymes. T4 DNA ligase (Invitrogen) was used for the ligation reaction. Recombinants pET-E61 and pET-E62 were then used to transform *E. coli* BL21 (DE3) competent cells cells by heat shock. Positive recombinant clones were selected on LB plates containing kanamycin, and the correct insertion of the E6 ORF into the cloning sites was verified by DNA sequencing.

2.3. Protein Expression. Transformed *E. coli* BL21 (DE) cells harboring the correct expression construct (pET-E61 and pET-E62) were grown in 1L LB broth containing kanamycin (50 μg/mL) at 37°C until the growth reached log phase (OD600 = 0.6). IPTG at a final concentration of 1 mM was added to the cultures to induce recombinant protein expression. Induced bacterial cultures were pelleted by centrifugation at 10,000 g for 30 min at 4°C.

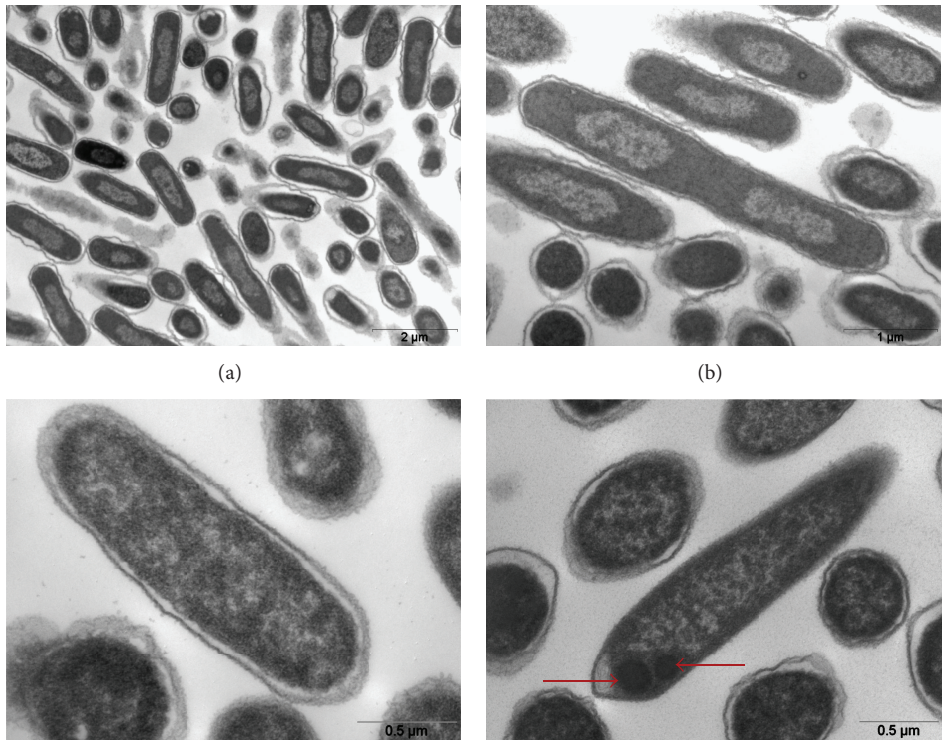

Figure 1: Electron microscopy *E. coli* BL21 (DE) not induced and induced by IPTG. (a) Transformed bacteria—plasmid pET-28a, without E6-1 not induced, 12.930X; (b) transformed bacteria—plasmid pET-28a, without E6-1 induced, 16.700X; (c) transformed bacteria—plasmid pET-28a, with E6-1 not induced, 35.970X; (d) transformed bacteria—plasmid pET-28a, with E6-1 induced 27.800X. Arrows: inclusion bodies. Transmission Microscopy LEO 906E, Laboratório de Biologia Celular do Instituto Butantan.

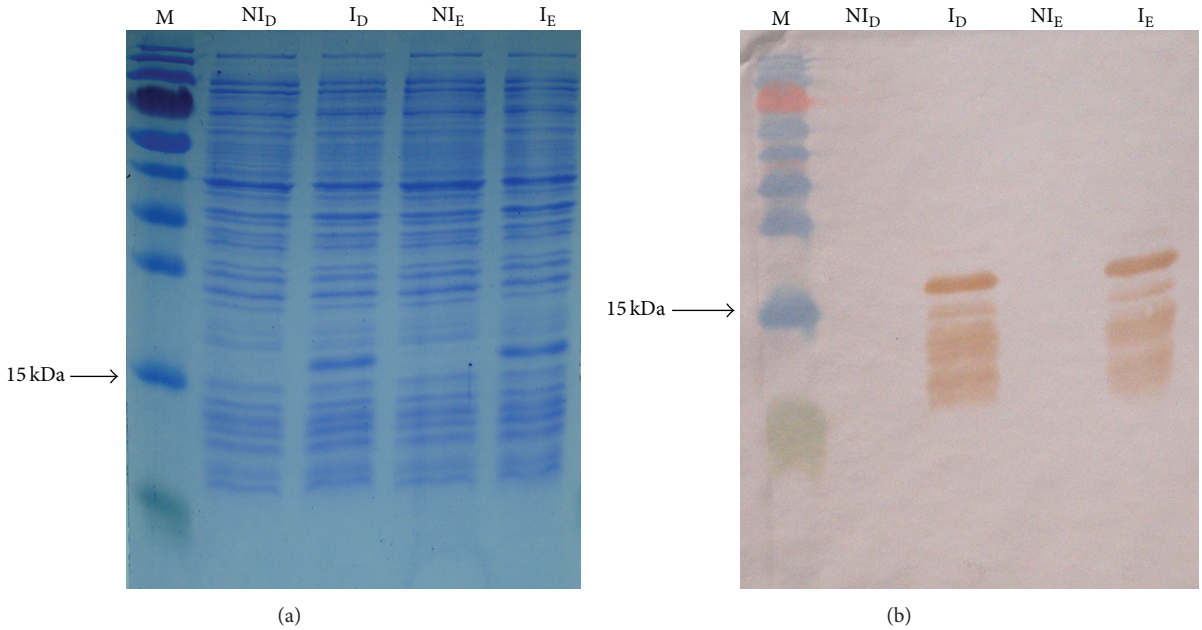

Figure 2: (a) Induction of E6-1 recombinant protein. M: molecular weight marker; NI_D: noninduced D colony; I_D: induced D colony; NI_E: noninduced E colony; I_E: induced E colony. SDS-PAGE 17% stained with Coomassie blue. (b)Western blotting of E6-1 recombinant protein induction. M: molecular weight marker; NI_D: noninduced D colony; I_D: induced D colony; NI_E: noninduced E colony; I_E: induced E colony.

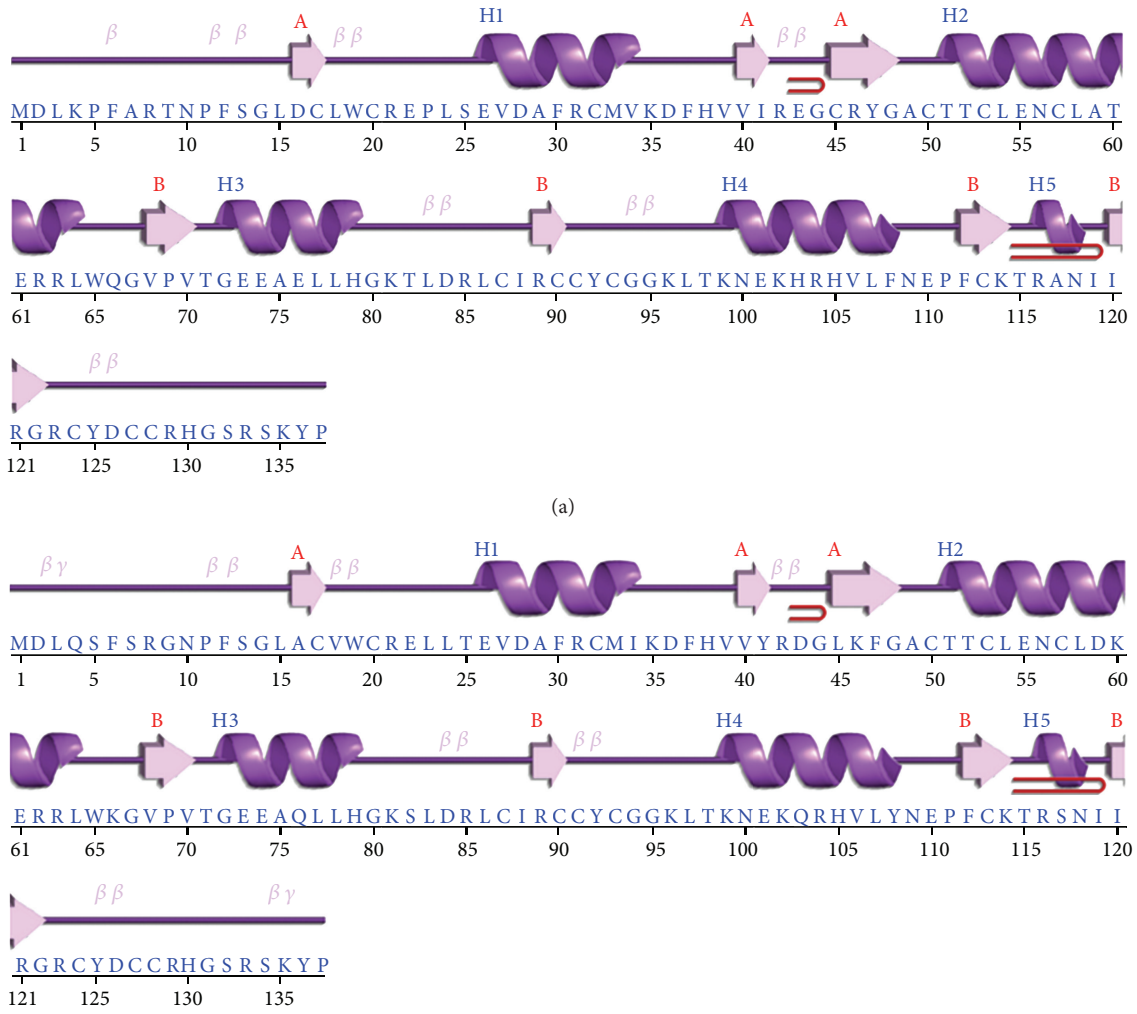

Figure 3: Topology diagram recombinants E6-1 and E6-2, respective sequences (a) E6-1 recombinant; (b) E6-2 recombinant.

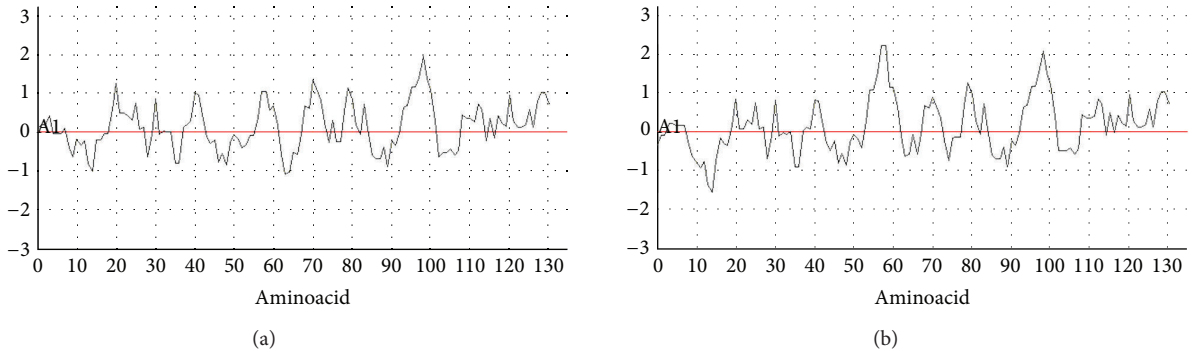

Figure 4: Antigenicity-recombinants E6-1 and E6-2, (a) E6-1 recombinant; (b) E6-2 recombinant.

2.4. Electron Microscopy. Samples of transformed *E. coli* BL21 cultured cells with the recombinant plasmid E6-1/pET-28a and with the empty pET-28a vector (negative control) were induced for recombinant protein expression. Fractions of these cultures were centrifuged and resuspended in approximately 1.0 mL of glutaraldehyde. These samples were sent to the Department of Cell Biology and Development at the Institute of Biomedical Sciences-ICB II to be prepared for electron

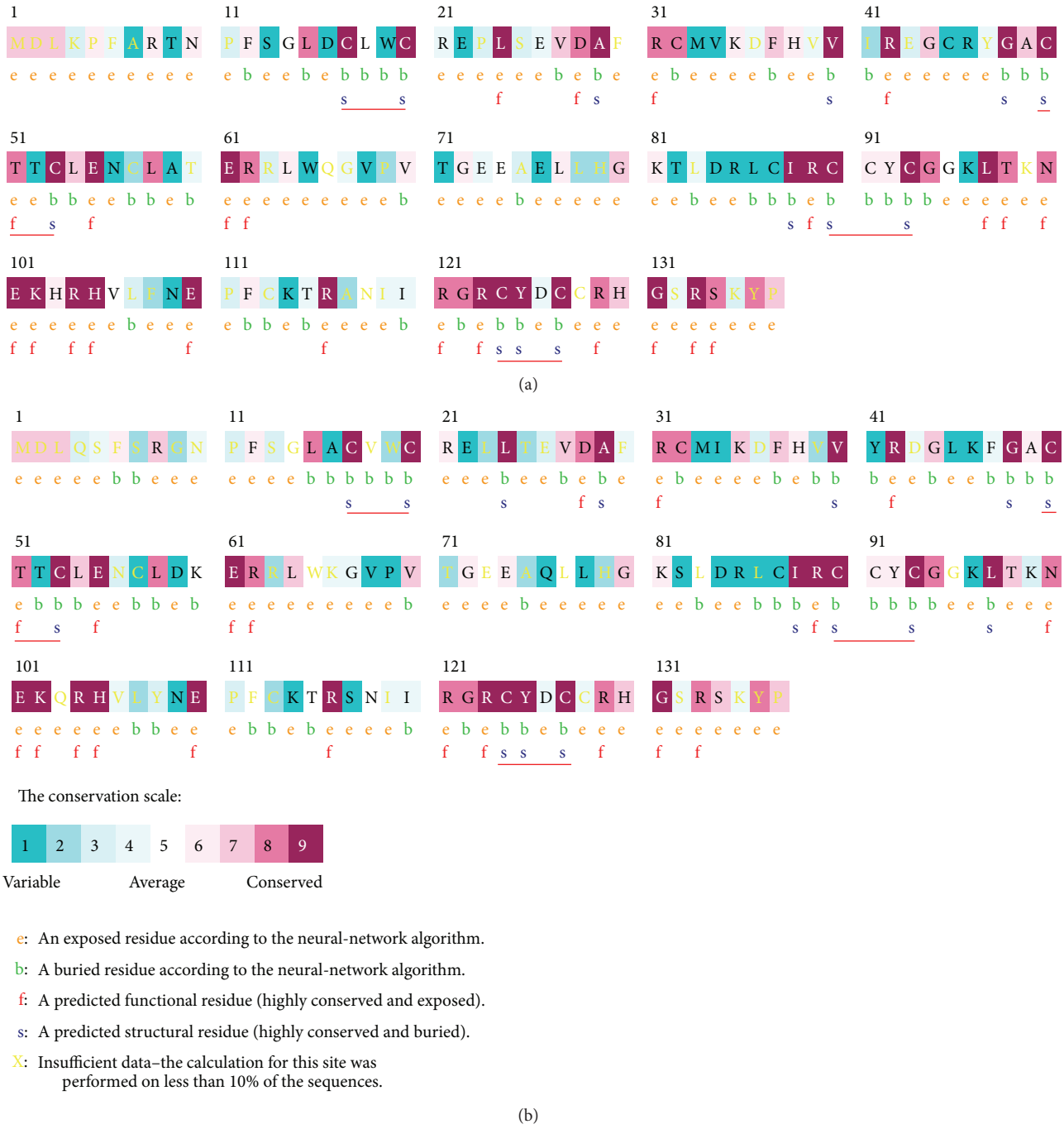

Figure 5: Protein sequences E6-1 e E6-2 conservation levels. (a) E6-1 recombinant; (b) E6-2 recombinant. CXXC red.

microscopy (ME) for the verification of the E6 recombinant expression through the observation of inclusion bodies. ME observations and image recording were performed at the Laboratory of Cellular Biology, Instituto Butantan, using a transmission electron microscope LEO 906E.*2.5.*

2.5. Protein Purification. In order to purify the E6 recombinant proteins, the bacterial pellets were resuspended in 20 mM TrisHCl, NaCl 500 mM, and pH 8.0, supplemented with protease inhibitor (PMSF at a final concentration of 2 mM), and lysed with a French Press. The cell lysates were centrifuged at 6000 g for 60 min at 4°C. The pellets were resuspended in 20 mM TrisHCl, 500 mM NaCl, 8 M ureia, 50 mM imidazole, pH 8.0, and final volume 25 mL. Aliquots of the clarified suspension were collected and analyzed in 17% SDS-PAGE. These tagged recombinant proteins were purified by Ni Sepharose 6 Fast Flow (GE Health Care): the clarified supernatants were passed through columns of charged resin and subsequently washed with 20 mM Tris-HCl, pH 8.0, 500 mM NaCl, 6 M urea, and 50 mM imidazole.

The recombinant proteins were then eluted with 500 mM imidazole in the same buffer. The proteins quantification was determined by the Bradford method [34]. Purified recombinant proteins were separated by 17% SDS-PAGE and transferred to nitrocellulose membranes. Membranes were blocked with 5% powdered nonfat dry milk in phosphate buffered saline containing 0.05% Tween 20 (PBST) and incubated for 2 h using anti-his monoclonal antibody (GE) (1 : 3000). Blots were then submitted to three 5 min washes with TBST and incubated with Goat Anti-Mouse IgG Horseradish Peroxidase (1 : 2000) for 1 h at room temperature. Bands were visualized by chemiluminescence reaction in the presence of H_2O_2 and using diaminobenzidine (DAB). The reaction was stopped with distilled water.

2.6. Bioinformatics. The nucleotide sequences generated by sequencing of E6-1 and E6-2 cloned genes were translated into amino acids with the BioEdit 7.1.3.0 [35]. The obtained nucleotide and amino acids sequences were aligned with sequences deposited in Nucleotide Collection and Protein Data Bank using BLASTN and BLASTP algorithms (http://blast.ncbi.nlm.nih.gov/Blast.cgi). Sequence alignments were also performed using the BioEdit software, and the identity matrix was calculated. The topology diagrams of the recombinant proteins was generated with the PDBsum software [36].

The analysis of conserved regions of the proteins E6-1 to E6-2 recombinants were performed by comparing all E6 protein sequences of other PVs already deposited using ConSurf server [37]. The degree of conservation for each amino acid was pointed out in a linear sequence.

In addition, the analysis of the antigenicity properties was performed using the JaMBW Edition 1.1 software [38].

3. Results and Discussion

3.1. E6-1 and E6-2 Gene Amplification and Cloning. E6-1 and E6-2 gene PCR products showed bands in the gel with approximately 500pb. E6-1/TOPO and E6-2/TOPO were successfully cloned in *E. coli* DH5a competent cells as indicated with double digestion of the recombinant TOPO vectors. Subsequently, E6-1/pET and E6-2/pET were subcloned in *E. coli* BL21 competent cells as indicated by double digestion and sequencing. DNA sequencing showed that the cloned genes were inserted in the correct frame of pET-28a (+). The primers sets were also effective for DNA sequencing.

3.2. Electron Microscopy. In regard to electronic microscopy (EM), both induced and noninduced cultured bacteria used as negative control (transformed with pET-28a, but without E6 insert) showed no inclusion corpuscles (Figures 1(a) and 1(b)). On the other hand, EM of the cultured, induced *E. coli* BL21 cells transformed with E6-1/pET-28a revealed the presence of inclusion bodies (Figure 1(d)), suggesting the presence of recombinant protein expression. As before, these were not observed in noninduced E6-1/pET-28a bacteria (Figure 1(c)). Papillomavirus E6 proteins are notoriously difficult to express and purify and unfused E6 proteins form insoluble aggregates upon bacterial overexpression [39].

Table 1: Mutations in nucleotide and aminoacid sequences of BPV1 E6 (bold).

E6 BPV-1										
Nucleotide				Codon			Amino acid			
Position	Ref.		Rec.	Ref.		Rec.	Ref.		Rec.	Position
48	T	→	C	GA**U**	→	GA**C**	D	=	D	16
73	A	→	T	**A**CA	→	**U**CA	T	≠	**S**	25
78	A	→	G	GA**A**	→	GA**G**	C	=	C	26
155	T	→	C	A**U**U	→	A**C**U	I	≠	**T**	52

Ref.: reference sequences (accession number X02346 and PDB codes 3PY7); Rec.: recombinant sequences obtained in this study.

However, in this study, the feasibility of E6-1 and E6-2 purifications from a bacterial expression system was demonstrated.

3.3. E6 Recombinant Protein Expression and Purification. Cloning and expression of different papillomavirus oncoproteins in bacterial vectors have already been done, enabling structural studies [40]. In the present work, the E6 gene of both BPV-1 and BPV-2 was cloned in a bacterial expression system, with the respective recombinant proteins being purified.

SDS-PAGE and Western blotting analysis using an anti-his tag antibody demonstrated that the large majority of detected fusion proteins migrated predominantly as a single band with an approximate expected molecular mass of 16 kDa (Figure 2(a)). However, Western blotting showed other bands also, indicating the possible occurrence of protein dimerization (Figure 2(b)). The purified recombinant eluted proteins were also examined by SDS-PAGE and Western blotting as before, with observed bands being approximately 16 kDa.

3.4. Bioinformatics Analysis

3.4.1. Alignment and Identity Matrix. The identity matrix showed 0.99 of similarity between E6-1 recombinant and reference (X02346) sequences of nucleotides. The amino acid sequence of the E6-1 recombinant protein showed 0.99 of identity with PDB codes 3PY7 sequence which has been considered as the protein sequence reference.

It was observed that, when translated into amino acids, two mutations (A78G and T48C) were silent, that is, no change in the amino acids was generated. The other two mutations (A73T and T155C) generated different amino acids (Table 1).

Differences between recombinant cloned E6-2 and deposited corresponding sequences were also observed. The identity matrix showed 0.99 of similarity between E6-2 recombinant and reference (M20219.1) sequences of nucleotides. Amino acid sequence of the E6-2 recombinant protein showed 0.98 of identity with UniProtKB/Swiss-Prot codes P11302.1 sequence which has been considered as the protein sequence reference. It was observed that, when translated into amino acids, all three mutations (T68C, T45G, and A405C) generated different amino acids (Table 2).

Table 2: Mutations in nucleotide and aminoacid sequences of BPV2 E6 (bold).

E6 BPV-2										
Nucleotide				Codon			Amino acid			
Position	Ref.		Rec.	Ref.		Rec.	Ref.		Rec.	Position
68	C	→	T	C**C**U	→	C**U**U	P	≠	**L**	23
134	G	→	T	**G**UG	→	**U**UG	V	≠	**L**	45
405	C	→	A	AA**C**	→	AA**A**	N	≠	**K**	135

Ref.: reference sequences (accession number M20219.1 and UniProtKB/Swiss-Prot codes P11302.1); Rec.: recombinant sequences obtained in this study.

3.4.2. Topology. Topology diagram of recombinant proteins, E6-1 and E6-1 was generated. The presence of seven β-sheets and five α-helices was observed in both diagrams (Figures 3(a) and 3(b)).

3.4.3. Antigenicity Prediction. According to the antigenicity graph, E6-1 recombinant protein sequence showed one peak near amino acids 90 and 100 (CCYCGGKLTKNEKHR), and E6-2 recombinant protein showed two peaks near amino acids 50 and 60 (CTTCLENCLDKE), and amino acids 90 and 100 (CCYCGGKLTKNEKQR) were predicted as especially immunogenic (Figures 4(a) and 4(b)). Interestingly, these potential immunogenic, mapped regions could represent targets for the development of new designed antibodies.

3.4.4. Conserved Regions. In silico prediction identified conserved regions between E6-1 to E6-2 proteins as well as from other papillomaviruses species. CXXC motifs were localized at regions associated with the binding of zinc atoms (Figures 5(a) and 5(b)).

Usually, papillomavirus E6 proteins share a common architecture consisting of two zinc-binding domains (E6-N and E6-C). These structural features indicated that E6 can interact directly with DNA molecule, acting as a transcriptional activator [41–43]. Both BPV-1 and BPV-2 encode an E6 protein of 137 amino acids that acts as a transcriptional activator, p53 and paxillin ligand, presenting also telomerase activity. Here, the primary amino acid sequences of these recombinant proteins were analyzed *in silico* for comparison with virtual protein sequences deposited in GenBank. The presence of divergences which may represent functional differences were observed. It is emphasized that the DNA sequencing in our laboratory was redundant in order to cover the entire E6 gene sequence for at least three times.

Among papillomaviruses oncoproteins, conserved regions were maintained in regard to the structure and function of these proteins. For example, E7 protein has 127 amino acids and a zinc finger domain [44]. Recombinant E7 protein with mutated regions showed lower efficiency in transforming activity [45]. On the other hand, several studies indicated that the hydrophobic nature of the BPV E5 protein has a crucial importance in conferring the transforming activity [46]. These essential amino acid residues are highly conserved among papillomaviruses as previously reported [47].

4. Conclusions

The cloning and recombinant protein expression of E6-1 and E6-2 in bacterial system proved to be a feasible methodological approach. For the first time, BPV-2 E6 protein is expressed and purified in a bacterial system. The purification of E6 BPV recombinant protein as well its structural and antigenicity analyses could allow the production of biotechnology material such as antibodies and vaccines candidates. This work could be also employed as a model for the obtainment of other papillomaviruses recombinant oncoproteins.

Acknowledgments

The authors would like to thank the *Ministério de Ciência, Tecnologia e Inovação/Conselho Nacional de Desenvolvimento Científico e Tecnológico* (CNPq Proc. 554816/2006-7 and 402539/2011-7), FAPESP (Proc. 2006/02439-6), and Coordenação de Aperfeiçoamento Pessoal de Nível Superior (CAPES) for the financial support and Carolina da Paz Sabino for her editorial support.

References

[1] H. zur Hausen, "Papillomavirus infections—a major cause of human cancers," *Biochimica et Biophysica Acta*, vol. 1288, no. 2, pp. F55–F78, 1996.

[2] J. Carr and T. Gyorfi, "Human papillomavirus: epidemiology, transmission, and pathogenesis," *Clinics in Laboratory Medicine*, vol. 20, no. 2, pp. 235–255, 2000.

[3] N. Stewart and S. Bacchetti, "Expression of SV40 large T antigen, but not small t antigen, is required for the induction of chromosomal aberrations in transformed human cells," *Virology*, vol. 180, no. 1, pp. 49–57, 1991.

[4] S.-Y. Chan, H. Delius, A. L. Halpern, and H.-U. Bernard, "Analysis of genomic sequences of 95 papillomavirus types: uniting typing, phylogeny, and taxonomy," *Journal of Virology*, vol. 69, no. 5, pp. 3074–3083, 1995.

[5] E.-M. de Villiers, C. Fauquet, T. R. Broker, H.-U. Bernard, and H. zur Hausen, "Classification of papillomaviruses," *Virology*, vol. 324, no. 1, pp. 17–27, 2004.

[6] M. S. Campo, "Papillomavirus and disease in humans and animals," *Veterinary and Comparative Oncology*, vol. 1, no. 1, pp. 3–14, 2003.

[7] M. Gottschling, A. Köhler, E. Stockfleth, and I. Nindl, "Phylogenetic analysis of beta-papillomaviruses as inferred from nucleotide and amino acid sequence data," *Molecular Phylogenetics and Evolution*, vol. 42, no. 1, pp. 213–222, 2007.

[8] J. Doorbar, S. Ely, J. Sterling, C. McLean, and L. Crawford, "Specific interaction between HPV-16 E1-E4 and cytokeratins results in collapse of the epithelial cell intermediate filament network," *Nature*, vol. 352, no. 6338, pp. 824–827, 1991.

[9] S. Roberts, I. Ashmole, S. M. Rookes, and P. H. Gallimore, "Mutational analysis of the human papillomavirus type 16 E1ΛE4 protein shows that the C terminus is dispensable for keratin cytoskeleton association but is involved in inducing disruption of the keratin filaments," *Journal of Virology*, vol. 71, no. 5, pp. 3554–3562, 1997.

[10] J. Doorbar, A. Parton, K. Hartley et al., "Detection of novel splicing patterns in a HPV16-containing keratinocyte cell line," *Virology*, vol. 178, no. 1, pp. 254–262, 1990.

[11] X. Tong and P. M. Howley, "The bovine papillomavirus E6 oncoprotein interacts with paxillin and disrupts the actin cytoskeleton," *Proceedings of the National Academy of Sciences of the United States of America*, vol. 94, no. 9, pp. 4412–4417, 1997.

[12] J. Doorbar, "The papillomavirus life cycle," *Journal of Clinical Virology*, vol. 32, pp. S7–S15, 2005.

[13] G. Borzacchiello and F. Roperto, "Bovine papillomaviruses, papillomas and cancer in cattle," *Veterinary Research*, vol. 39, no. 5, article 45, 2008.

[14] M. S. Campo, W. F. H. Jarrett, R. Barron, B. W. O'Neil, and K. T. Smith, "Association of bovine papillomavirus type 2 and bracken fern with bladder cancer in cattle," *Cancer Research*, vol. 52, no. 24, pp. 6898–6904, 1992.

[15] L. Nasir and M. S. Campo, "Bovine papillomaviruses: their role in the aetiology of cutaneous tumours of bovids and equids," *Veterinary Dermatology*, vol. 19, no. 5, pp. 243–254, 2008.

[16] F. Jelínek and R. Tachezy, "Cutaneous papillomatosis in cattle," *Journal of Comparative Pathology*, vol. 132, no. 1, pp. 70–81, 2005.

[17] M. Lunardi, A. A. Alfieri, R. A. Otonel et al., "Genetic characterization of a novel bovine papillomavirus member of the Deltapapillomavirus genus," *Veterinary Microbiology*, vol. 162, pp. 378–1135, 2013.

[18] W. F. H. Jarrett, K. T. Smith, B. W. O'Neil et al., "Studies on vaccination against papillomaviruses: prophylactic and therapeutic vaccination with recombinant structural proteins," *Virology*, vol. 184, no. 1, pp. 33–42, 1991.

[19] M. S. Campo, "Animal models of papillomavirus pathogenesis," *Virus Research*, vol. 89, no. 2, pp. 249–261, 2002.

[20] D. W. Gardiner, J. P. Teifke, B. K. Podell, and D. A. Kamstock, "Fibropapilloma of the glans penis in a horse," *Journal of Veterinary Diagnostic Investigation*, vol. 20, no. 6, pp. 816–819, 2008.

[21] S. R. Wosiacki, M. A. B. Barreiro, A. F. Alfieri, and A. A. Alfieri, "Semi-nested PCR for detection and typing of bovine Papillomavirus type 2 in urinary bladder and whole blood from cattle with enzootic haematuria," *Journal of Virological Methods*, vol. 126, no. 1-2, pp. 215–219, 2005.

[22] A. C. de Freitas, C. de Carvalho, O. Brunner et al., "Viral DNA sequences in peripheral blood and vertical transmission of the virus: a discussion about BPV-1," *Brazilian Journal of Microbiology*, vol. 34, no. 1, pp. 76–78, 2003.

[23] R. C. Stocco dos Santos, C. J. Lindsey, O. P. Ferraz et al., "Bovine papillomavirus transmission and chromosomal aberrations: an experimental model," *Journal of General Virology*, vol. 79, no. 9, pp. 2127–2135, 1998.

[24] C. de Carvalho, A. C. de Freitas, O. Brunner et al., "Bovine papillomavirus type 2 in reproductive tract and gametes of slaughtered bovine females," *Brazilian Journal of Microbiology*, vol. 34, no. 1, pp. 82–84, 2003.

[25] S. Roperto, R. Brun, F. Paolini et al., "Detection of bovine papillomavirus type 2 in the peripheral blood of cattle with urinary bladder tumours: possible biological role," *Journal of General Virology*, vol. 89, no. 12, pp. 3027–3033, 2008.

[26] C. J. Lindsey, M. E. Almeida, C. F. Vicari et al., "Bovine papillomavirus DNA in milk, blood, urine, semen, and spermatozoa of bovine papillomavirus-infected animals," *Genetics and Molecular Research*, vol. 8, no. 1, pp. 310–318, 2009.

[27] E. Schwarz, U. K. Freese, L. Gissmann et al., "Structure and transcription of human papillomavirus sequences in cervical carcinoma cells," *Nature*, vol. 314, no. 6006, pp. 111–114, 1985.

[28] E. J. Androphy, N. L. Hubbert, J. T. Schiller, and D. R. Lowy, "Identification of the HPV-16 E6 protein from transformed mouse cells and human cervical carcinoma cell lines," *EMBO Journal*, vol. 6, no. 4, pp. 989–992, 1987.

[29] L. Banks, P. Spence, E. Androphy et al., "Identification of human papillomavirus type 18 E6 polypeptide in cells derived from human cervical carcinomas," *Journal of General Virology*, vol. 68, no. 5, pp. 1351–1359, 1987.

[30] W. A. Rivoire, E. Capp, H. E. Corleta, and I. S. B. Silva, "Bases biomoleculares da oncogênese cervical," *Revista Brasileira de Cancerologia*, vol. 47, pp. 179–184, 2001.

[31] C. C. Baker, W. C. Phelps, V. Lindgren, M. J. Braun, M. A. Gonda, and P. M. Howley, "Structural and transcriptional analysis of human papillomavirus type 16 sequences in cervical carcinoma cell lines," *Journal of Virology*, vol. 61, no. 4, pp. 962–971, 1987.

[32] D. E. Wazer, X.-L. Liu, Q. Chu, Q. Gao, and V. Band, "Immortalization of distinct human mammary epithelial cell types by human papilloma virus 16 E6 or E7," *Proceedings of the National Academy of Sciences of the United States of America*, vol. 92, no. 9, pp. 3687–3691, 1995.

[33] M. S. Campo and L. W. Coggins, "Molecular cloning of bovine papillomavirus genomes and comparison of their sequence homologies by heteroduplex mapping," *Journal of General Virology*, vol. 63, no. 2, pp. 255–264, 1982.

[34] M. M. Bradford, "A rapid and sensitive method for the quantitation of microgram quantities of protein utilizing the principle of protein dye binding," *Analytical Biochemistry*, vol. 72, no. 1-2, pp. 248–254, 1976.

[35] T. A. Hall, "BioEdit: a user-friendly biological sequence alignment editor and analysis program for Windows 95/98/NT," *Nucleic Acids Symposium Series*, vol. 41, pp. 95–98, 1999.

[36] R. A. Laskowski, M. W. McArthur, D. S. Moss, and J. M. Thornton, "PROCHECK: a program to check the stereochemical quality of protein structures," *Journal of Applied Crystallography*, vol. 26, pp. 283–291, 1993.

[37] H. Ashkenazy, E. Erez, E. Martz, T. Pupko, and N. Ben-Tal, "ConSurf 2010: calculating evolutionary conservation in sequence and structure of proteins and nucleic acids," *Nucleic Acids Research*, vol. 38, no. 2, pp. 529–533, 2010.

[38] I. G. Toldo, JaMBW: JaMBW, the Java based Molecular Biologist's Workbench, coordinated by Luca Toldo, 1997, http://www.bioinformatics.org/JaMBW/.

[39] A. O. M. O. Sidi, K. O. Babah, N. Brimer et al., "Strategies for bacterial expression of protein-peptide complexes: application to solubilization of papillomavirus E6," *Protein Expression and Purification*, vol. 80, no. 1, pp. 8–16, 2011.

[40] G. Pahel, A. Aulabaugh, S. A. Short et al., "Structural and functional characterization of the HPV16 E7 protein expressed in bacteria," *Journal of Biological Chemistry*, vol. 268, no. 34, pp. 26018–26025, 1993.

[41] M. Lusky, L. Berg, H. Weiher, and M. Botchan, "Bovine papilloma virus contains an activator of gene expression at the distal end of the early transcription unit," *Molecular and Cellular Biology*, vol. 3, no. 6, pp. 1108–1122, 1983.

[42] M. E. Jackson and M. S. Campo, "Positive and negative E2-independent regulatory elements in the long control region of bovine papillomavirus type 4," *Journal of General Virology*, vol. 72, no. 4, pp. 877–883, 1991.

[43] D. E. Groff and W. D. Lancaster, "Genetic analysis of the 3' early region transformation and replication functions of bovine

papillomavirus type 1," *Virology*, vol. 150, no. 1, pp. 221–230, 1986.

[44] J. Bohl, K. Das, B. Dasgupta, and S. B. Vande Pol, "Competitive binding to a charged leucine motif represses transformation by a papillomavirus E6 oncoprotein," *Virology*, vol. 271, no. 1, pp. 163–170, 2000.

[45] N. Sarver, M. S. Rabson, Y. C. Yang, J. C. Byrne, and P. M. Howley, "Localization and analysis of bovine papillomavirus type 1 transforming functions," *Journal of Virology*, vol. 52, no. 2, pp. 377–388, 1984.

[46] B. H. Horwitz, A. L. Burkhardt, R. Schlegel, and D. DiMaio, "44-amino-acid E5 transforming protein of bovine papillomavirus requires a hydrophobic core and specific carboxyl-terminal amino acids," *Molecular and Cellular Biology*, vol. 8, no. 10, pp. 4071–4078, 1988.

[47] R. Kulke, B. H. Horwitz, T. Zibello, and D. DiMaio, "The central hydrophobic domain of the bovine papillomavirus E5 transforming protein can be functionally replaced by many hydrophobic amino acid sequences containing a glutamine," *Journal of Virology*, vol. 66, no. 1, pp. 505–511, 1992.

Hindawi Publishing Corporation
BioMed Research International
Volume 2013, Article ID 297692, 14 pages
http://dx.doi.org/10.1155/2013/297692

Research Article

Interference with RUNX1/ETO Leukemogenic Function by Cell-Penetrating Peptides Targeting the NHR2 Oligomerization Domain

Yvonne Bartel,[1,2] Manuel Grez,[1] and Christian Wichmann[1,3]

[1] *Institute for Biomedical Research, Georg-Speyer-Haus, 60596 Frankfurt, Germany*
[2] *Institute for Molecular Medicine, Goethe-University, 60590 Frankfurt, Germany*
[3] *Department of Transfusion Medicine, Cell Therapy and Haemostasis, Ludwig-Maximilian University Hospital, 81377 Munich, Germany*

Correspondence should be addressed to Christian Wichmann; christian.wichmann@med.uni-muenchen.de

Received 22 February 2013; Revised 9 June 2013; Accepted 10 June 2013

Academic Editor: Lubna Nasir

The leukemia-associated fusion protein RUNX1/ETO is generated by the chromosomal translocation t(8;21) which appears in about 12% of all *de novo* acute myeloid leukemias (AMLs). Essential for the oncogenic potential of RUNX1/ETO is the oligomerization of the chimeric fusion protein through the nervy homology region 2 (NHR2) within ETO. In previous studies, we have shown that the intracellular expression of peptides containing the NHR2 domain inhibits RUNX1/ETO oligomerization, thereby preventing cell proliferation and inducing differentiation of RUNX1/ETO transformed cells. Here, we show that introduction of a recombinant TAT-NHR2 fusion polypeptide into the RUNX1/ETO growth-dependent myeloid cell line Kasumi-1 results in decreased cell proliferation and increased numbers of apoptotic cells. This effect was highly specific and mediated by binding the TAT-NHR2 peptide to ETO sequences, as TAT-polypeptides containing the oligomerization domain of BCR did not affect cell proliferation or apoptosis in Kasumi-1 cells. Thus, the selective interference with NHR2-mediated oligomerization by peptides represents a challenging but promising strategy for the inhibition of the leukemogenic potential of RUNX1/ETO in t(8;21)-positive leukemia.

1. Introduction

Acute myeloid leukemia (AML) is the most common form of myeloid leukemia. In half of all patient-derived AML blasts, chromosomal translocations can be detected leading to the expression of aberrant fusion proteins which are generally not found in normal cells of healthy individuals [1]. Most often, the affected proteins are transcription factors regulating critical steps during hematopoiesis [2]. Their altered function results in the block of cellular differentiation, a general feature of AML.

The chromosomal translocation t(8;21) generates the chimeric protein RUNX1/ETO which is expressed in 12% of all *de novo* AML with 40% of them belonging to the M2 subtype of the FAB (French-American-British) classification [3]. The hematopoietic transcription factor RUNX1 (also known as AML1, CBFα2, or PEBP2αB) belongs to the family of core-binding transcription factors and is a key regulator of myeloid cell differentiation [4]. As a consequence of the translocation, the DNA-binding domain of RUNX1 (RUNT homology domain, RHD) is fused to almost the entire ETO protein (alternatively named MTG8 or RUNX1T1) which functions mainly as a transcriptional repressor protein [5, 6]. Thus, most RUNX1 target genes are transcriptionally repressed in t(8;21)-positive blasts. Likewise, RUNX1/ETO can act as a positive regulator of gene expression, depending on cofactor recruitment and epigenetic modifications [7]. Expression of RUNX1/ETO in primitive hematopoietic cells leads to increased cell survival, proliferation, and a delay in myelo-erythroid differentiation which certainly contributes to the onset of leukemia development [8]. However, additional genetic alterations are necessary for overt transformation from an initial preleukemic clone [9, 10].

The ETO protein is characterized by four nervy homology regions (NHR1-4) that mediate the interaction with diverse

cellular factors such as the nuclear corepressors N-CoR, SMRT, mSIN3A, and histone deacetylases (HDACs) [11, 12]. The NHR2 domain is responsible for the binding to the ETO family members MTGR1 and ETO-2 as well as for homooligomerization [13]. Thereby, RUNX1/ETO generates high molecular weight protein complexes that are critical for the oncogenic potential of the fusion protein [14]. Recent studies suggest the NHR2 domain as one essential ETO domain crucial for RUNX1/ETO-associated leukemogenesis [15, 16]. The crystal structure of a recombinant NHR2 protein revealed an α-helical structure with the capacity to build tetramers with a total interaction area of nearly 10,000 Å^2 [17]. Mutations inside the NHR2 domain that abrogate the formation of oligomers resulted in a complete loss of the oncogenic potential of RUNX1/ETO. We recently demonstrated that a dimeric mutant of RUNX1/ETO, generated by alanine substitution of 5 essential amino acids within the NHR2 domain, is no longer able to transform hematopoietic progenitor cells [18]. Consequently, the selective interference with tetramerization could be a promising strategy to inhibit the oncogenic properties of this fusion protein.

Previously, we have shown that the lentiviral overexpression of a protein containing the entire NHR2 domain efficiently inhibits RUNX1/ETO oligomerization and restores expression of RUNX1 target genes [19]. Proliferation of RUNX1/ETO-dependent cell lines was reduced and the block of differentiation was reverted after expression of the NHR2-only protein, thus allowing for myeloid maturation of blast cells. Furthermore, an increase in apoptosis was measured in treated cells, indicating that the leukemic potential of RUNX1/ETO was efficiently blocked.

Here, we investigated the use of cell penetrating proteins as an alternative approach to deliver the NHR2 domain into RUNX1/ETO-transformed myeloid cells. A TAT-NHR2 polypeptide, TN122, was successfully internalized by human cells and interacted specifically with the ETO protein. In a RUNX1/ETO-dependent myeloid cell line, the consecutive treatment with TN122 inhibited proliferation and increased the rate of apoptotic cells.

2. Materials and Methods

2.1. Plasmid Construction. Truncated versions of the previously described N89 sequence [19] were generated by PCR and cloned into the SacII sites of the lentiviral vector SiEW. A codon optimized N89 construct was generated by Geneart and also cloned via SacII into the SiEW expression vector.

The TAT fusion constructs were generated by using the bacterial expression vector pSW5 [20], kindly provided by Professor Dr. Winfried Wels (Georg-Speyer-Haus, Frankfurt, Germany). The plasmid contains an N-terminal HIV-1 TAT protein transduction domain and a C-terminal myc- and His(6)-tag. The NLS-containing protein sequences of the NHR2 domain (aa 482-548 in RUNX1/ETO), or the oligomerization domain of BCR (aa 1-72) as a control, were cloned into the vector by PCR using the Kpn I and Hind III cleavage sites. The two cysteines present in the NHR2 sequence were substituted by serine using site-directed mutagenesis (Stratagene kit, Stratagene, La Jolla, CA). A TAT- and NLS-free NHR2 protein was generated using the Nde I/Hind III cleavage sites of the vector. For protein localization studies, a fluorescent protein was generated in which eGFP was inserted into the construct downstream of the NHR2 domain.

2.2. Protein Expression and Purification. *E. coli* BL21-CodonPlus (DE3) competent cells were transformed with the expression plasmids. A single clone was used to inoculate an overnight preculture containing ampicillin (100 μg/mL) and glucose (0.8% w/v) in LB medium. The next day, fresh culture medium was inoculated at a ratio of 1 : 10, and the bacteria were grown at 37°C until an OD_{600} of 0.7 was reached. Expression of the proteins was induced with 250 μM IPTG, and the culture was incubated for 4 hours at 30°C. To purify the recombinant proteins, the pelleted bacteria were resuspended in IMAC buffer (20 mM Tris-HCl, 500 mM NaCl, 10% glycerine, 20 mM imidazole, pH 8.0) containing a protease inhibitor cocktail (P8849, Sigma-Aldrich, Taufkirchen, Germany). The cells were lysed by addition of lysozyme (1 mg/mL) and subsequent sonification. For affinity purification of the His-tagged proteins, a HisTrap HP column (GE Healthcare, Uppsala, Sweden) was used. The TAT- and NLS-free NHR2 protein was additionally purified by anion exchange chromatography. The IMAC eluate was diluted 1 : 20 in IEQ running buffer (20 mM Tris-HCl, 3% glycerine, pH 8.0) and purified with a HiTrap HP column (GE Healthcare). The buffer of all protein samples was subsequently exchanged to PBS by using a HiTrap Desalting column (GE Healthcare), and aliquots were stored at −80°C until use.

2.3. CD Spectroscopy. CD spectroscopy of the NHR2-containing protein was performed on a Jasco CD spectrometer in a 0.1 cm path-length cuvette using a protein concentration of 50 μM and a temperature of 25°C. The spectrum presented is a cumulative spectrum of three individual scans from 195–250 nm wavelength in increments of 0.1 nm.

2.4. Protein Crosslinking. Crosslinking was used to demonstrate the oligomerization status of the recombinant NHR2 proteins as was described before for the BCR oligomerization domain [21]. Briefly, 20 μM of the protein sample diluted in PBS was incubated at room temperature for various time periods with 0.01% glutaraldehyde. The reaction was stopped by addition of SDS-containing 2x Laemmli buffer, and 40 μL of the sample was separated on a SDS-PAGE and stained with coomassie brilliant blue.

2.5. Cell Culture and Protein Transduction into Human Cell Lines. 293T cells were maintained in DMEM+10% FCS, and Kasumi-1 cells were cultured in RPMI 1640+20% FCS. The TAT fusion proteins were added directly to the cell culture medium of subconfluent 293T cells at a final concentration of 1–5 μM. Optionally, chloroquine and/or heparin were also added. To perform protein transduction into hematopoietic Kasumi-1 cells, the culture medium was exchanged to serum-free X-Vivo 10 medium. In some experiments, the cells were preincubated with dextran sulfate (0.1 or 1 mg/mL) for 3 hours at 37°C and extensively washed with PBS. Cells were then

seeded at a density of 4×10^5 cells in 500 μL into a 24-well plate, and the cell-penetrating proteins were added to the medium at a final concentration of 2–8 μM. In some experiments, a TAT-HA2 peptide (5 μM) was cotransfected with TN122 to improve peptide uptake. All cells were treated with trypsin for 10 minutes at 37°C and extensively washed before further analysis.

2.6. Peptide Synthesis. The TAT-HA2 peptide was ordered from BioLux (Stuttgart, Germany) in retroinverso sequence as described before [22]. To increase peptide stability, D-enantiomers were incorporated for the last two amino acids on both termini.

2.7. Coimmunoprecipitation and Western Blot Analysis. Binding of the different NHR2 constructs to ETO protein was analyzed by cotransfection of 293T cells with vectors coding for the respective proteins. After two days, cells were lysed in NP40-containing buffer. NHR2-containing proteins were immunoprecipitated using an antibody directed against the Flag-tag of the proteins (anti-Flag M2, Santa Cruz, CA). The immune complexes were bound to protein A/G-agarose (Santa Cruz) and washed extensively. The coprecipitated ETO protein was then analyzed by western blotting using a polyclonal antibody for ETO (C-20, Santa Cruz). EGFP was detected to check for the transfection levels. Secondary HRP-coupled antibodies were obtained from Santa Cruz, and western blots were developed using the Pico ECL reagent (Thermo Scientific, MA).

The TAT-NHR2 fusion protein TN122 was added twice (0 and 24 h) in a final concentration of 5 μM and in the presence of 20 μM chloroquine to a 293T cell line stably expressing the NHR2-containing protein NC128 [19]. 14 hours later, the cells were treated with trypsin, washed, and lysed in NP40-containing buffer. Immunoprecipitation of the intracellularly expressed NC128 protein was performed using an antibody directed against the Flag-tag of the protein. The immune complexes were analyzed by western blotting using an antibody directed against the myc-tag of TN122 (anti-myc 9E10, Santa Cruz) or against eGFP (Roche, Mannheim, Germany) and actin (I-19, Santa Cruz) as a control.

2.8. Confocal Laser Scanning Microscopy. For localization studies, an eGFP-containing TN122 protein was used and added to 293T cells in a final concentration of 2 μM in the presence of 20 μM chloroquine. 24 hours later, a trypsin digestion was performed, the cells were extensively washed, and the cellular membrane was stained by a rhodamine-conjugated wheat germ agglutinin (W-849, Molecular Probes, Invitrogen, Darmstadt, Germany) for 30 minutes at 37°C. The sample was covered with ProLong Gold (SigmaAldrich), and the living cells were analyzed with a confocal laser scanning microscope (TCS-SL, Leica, Wetzlar, Germany) using the 63x oil immersion objective.

2.9. Flow Cytometry. The percentage of transduced Kasumi-1 cells was determined by the expression of the marker gene eGFP. For flow cytometry, cells were washed, resuspended in PBS, and analyzed on a FACS-Calibur (Becton Dickinson, Heidelberg, Germany). To investigate levels of CD34 expression, transduced Kasumi-1 cells were stained with an APC-conjugated CD34-antibody (BD Biosciences) for 20 minutes at room temperature in the dark prior to flow cytometry analysis. 10,000 cells were measured and analyzed using the CellQuest Pro software.

The percentage of eGFP-stained cells after addition of cell penetrating NHR2-eGFP proteins was also analyzed by flow cytometry. 7-amino-actinomycin D (7AAD) and allophycocyanin (APC)-conjugated Annexin V (both from BD Biosciences) were used to determine the percentage of dead cells.

3. Results

3.1. Definition of the Minimal NHR2 Sequence Required for RUNX1/ETO Inhibitory Function. In order to define the minimal length of the NHR2 proteins required for optimal inhibition of RUNX1/ETO, we generated mutants of the previously described inhibitory protein N89 [19] by deleting the C-terminal flanking region of the NHR2 domain (N74) and the NLS sequence (N68) (Figure 1(a)). A control protein contained the oligomerization domain of the breakpoint cluster region (BCR) protein (aa 1-72) instead of the NHR2 domain. These constructs were then cloned into the lentiviral vector SiEW. Proper expression of the proteins was verified in lysates from transfected 293T cells by western blotting (Figure 1(b)). Next, binding of the polypeptides to ETO protein was investigated by immunoprecipitation of the Flag-tagged proteins from co-transfected 293T cells. All three NHR2-containing proteins were able to interact with the ETO protein (Figure 1(c)), while the BCR control failed. For analyzing the inhibitory potential of the deletion mutants on RUNX1/ETO function, Kasumi-1 cells were transduced with viral vectors and the growth of transduced (i.e., eGFP expressing) cells investigated by flow cytometry analysis. The expression of each of the three NHR2-containing proteins led to a decrease in the relative amount of transduced cells over time as indicated by expression of the marker protein eGFP (Figure 1(d)). This was due to an inhibition of cellular growth of transduced Kasumi-1 (Figure 1(e)), while the nontransduced cells in the culture were not affected in their growth kinetics. Contrary to this, cells transduced with the BCR control construct did not show any signs of growth inhibition. Furthermore, in contrast to the BCR control peptide, expression of the NHR2-containing constructs in Kasumi-1 cells induced a decrease in the expression of the progenitor cell marker CD34 over time (Figure 1(f)). This indicates that expression of the NHR2 sequence was, at least in part, able to overcome the differentiation block mediated by RUNX1/ETO. Although, in general, all three NHR2-containing constructs displayed inhibitory potential, N89-expressing Kasumi-1 cells showed a slightly faster decrease in the amount of transduced cells (Figure 1(d)) as well as a faster and even stronger decrease in the percentage of CD34 positive cells (Figure 1(f)) arguing for a stronger inhibitory potential of N89 in comparison to the deletion mutants N74 and N68. Further shortening of the NHR2 core amino acids, the seven alpha-helical loops, led to instability of the polypeptides N49 and N52 (Figure 1(g)). To demonstrate

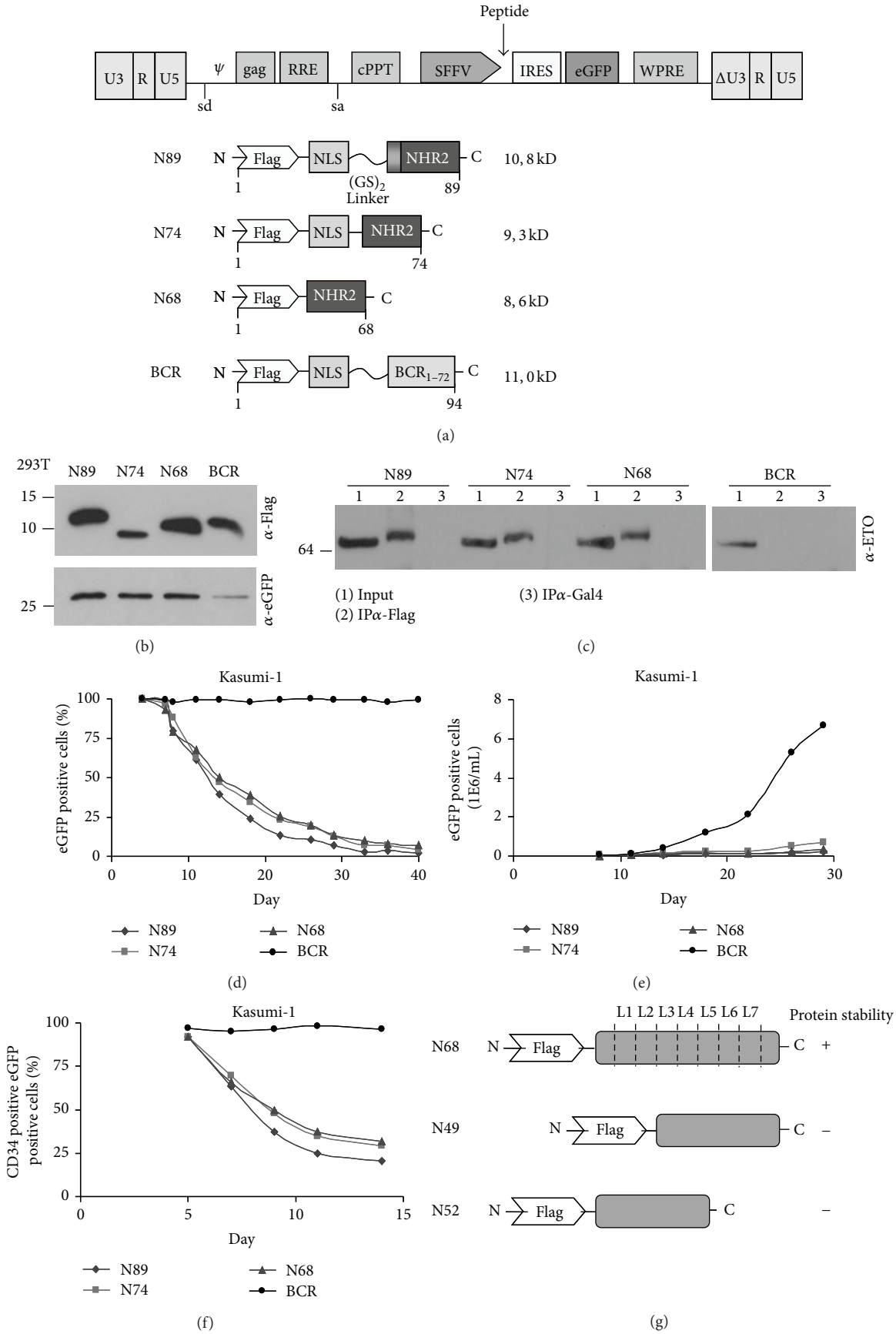

Figure 1: Continued.

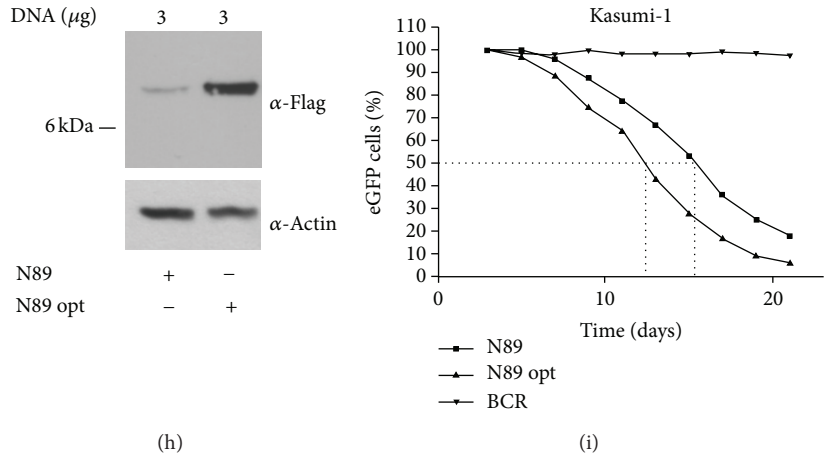

Figure 1: Definition of the minimal NHR2 sequence required for RUNX1/ETO inhibitory function. (a) Lentiviral vector SiEW and tested NHR2-containing constructs. (b) Overexpression of the individual proteins in 293T cells and detection of the Flag-tagged constructs by Western blotting. The marker protein eGFP serves as a loading control. (c) Binding of all NHR2-containing proteins to ETO. Co-transfection of 293T cells with the respective constructs together with a plasmid coding for the ETO protein. Immunoprecipitation of the individual protein complexes was performed with an anti-Flag antibody. (d–f) Cellular effects following lentiviral expression of the different NHR2 constructs in Kasumi-1 cells. Time course of the percentage of eGFP-positive cells (d), growth curve of the transduced cells (e), and time course of the expression of the progenitor cell marker CD34 for transduced Kasumi-1 cells (f). (g) Scheme of N68 based NHR2 deletion forms. Indication of the 7 alpha-helical loops L1-L7 of the NHR2 domain. (h) Comparison of N89 and codon-optimized N89 expression levels by western blotting. (i) Percentage of transduced cells in cocultures expressing N89 and the codon-optimized version thereof.

a dose-dependent effect of inhibitor peptide expression, we compared N89 with a codon-optimized version with increased intracellular peptide levels (Figure 1(h)). Indeed higher N89 expression correlated to a faster net decrease of transduced cells arguing for a dose dependency of NHR2 inhibitor peptides (Figure 1(i)).

3.2. Design of Constructs, Expression, Purification, and Analysis of Recombinant Proteins. Cell-penetrating polypeptides were generated by linking the protein transduction domain of the HIV-1 TAT protein (YGRKKRRQRRR) to the N-terminus of the polypeptides used in this study. The results obtained with the NHR2-deletion mutants (Figure 1) and our previous results [19] indicate that the complete NHR2 domain is required for an effective inhibitory function of NHR2 peptides. Although a construct lacking the NLS also does inhibit cell growth of RUNX1/ETO-dependent Kasumi-1 cells (Figure 1), the NLS domain was included in all constructs for maximal effects. Therefore, the NHR2 polypeptides were based on the N89 sequence containing a nuclear localization signal (NLS) from SV40, a flexible GSGS linker, and the complete NHR2 domain (aa 482–548 in RUNX1/ETO). In addition, a myc- and a histidine-tag were included at the C-terminus for detection and purification of the recombinant polypeptides, respectively, resulting in the TAT-NHR2 polypeptide TN122 (Figure 2(a)). For cellular localization studies, a TN122-eGFP fusion construct was also generated. As a control polypeptide, the oligomerization domain of BCR was used to substitute for the NHR2 domain in the TN122 construct. The proteins were expressed in *E. coli* and purified from the bacterial lysates under native conditions by immobilized metal ion affinity chromatography (IMAC). After optimization of the protocol, a relatively pure protein fraction of TN122 was obtained (Figure 2(b)).

Before testing the recombinant polypeptides in cell culture, we analyzed the structural properties of the NHR2 domain within the NHR2 containing polypeptides. This was necessary since deviation from the expected α-helical structure could affect the biological properties of the fusion polypeptides. For these studies, we used a protein that lacked the TAT and NLS sequences and consisted by two thirds of the NHR2 domain (NHR2-mH). This recombinant protein was selected because of its high purity after ion exchange chromatography, as determined by analytical ultracentrifugation (purity of >90%, data not shown). The secondary structure of NHR2-mH was investigated by CD spectroscopy revealing the typical curve shape of an α-helical protein (Figure 2(c)). From ellipticity measurements at 222 nm, the helical content of the protein was calculated [23] and revealed a value of 64%. Assuming that the myc- and the histidine-tag are unstructured, this value indicates that the NHR2-mH polypeptide was properly folded. It has been previously described that the isolated NHR2 domain forms tetramers [17]. To investigate the oligomerization state of the recombinant NHR2-mH polypeptide, crosslinking experiments were performed using glutaraldehyde as a crosslinker to preserve the rigidity of the protein structure after denaturation. Analysis of the crosslinked sample on SDS-PAGE revealed the existence of monomers, dimers, and tetramers (Figure 2(d)). With prolonged incubation times, the proportion of tetramers increased at the expense of the lower oligomer forms. This observation verifies that the recombinant NHR2 polypeptides retained their ability to form tetramers *in vitro*.

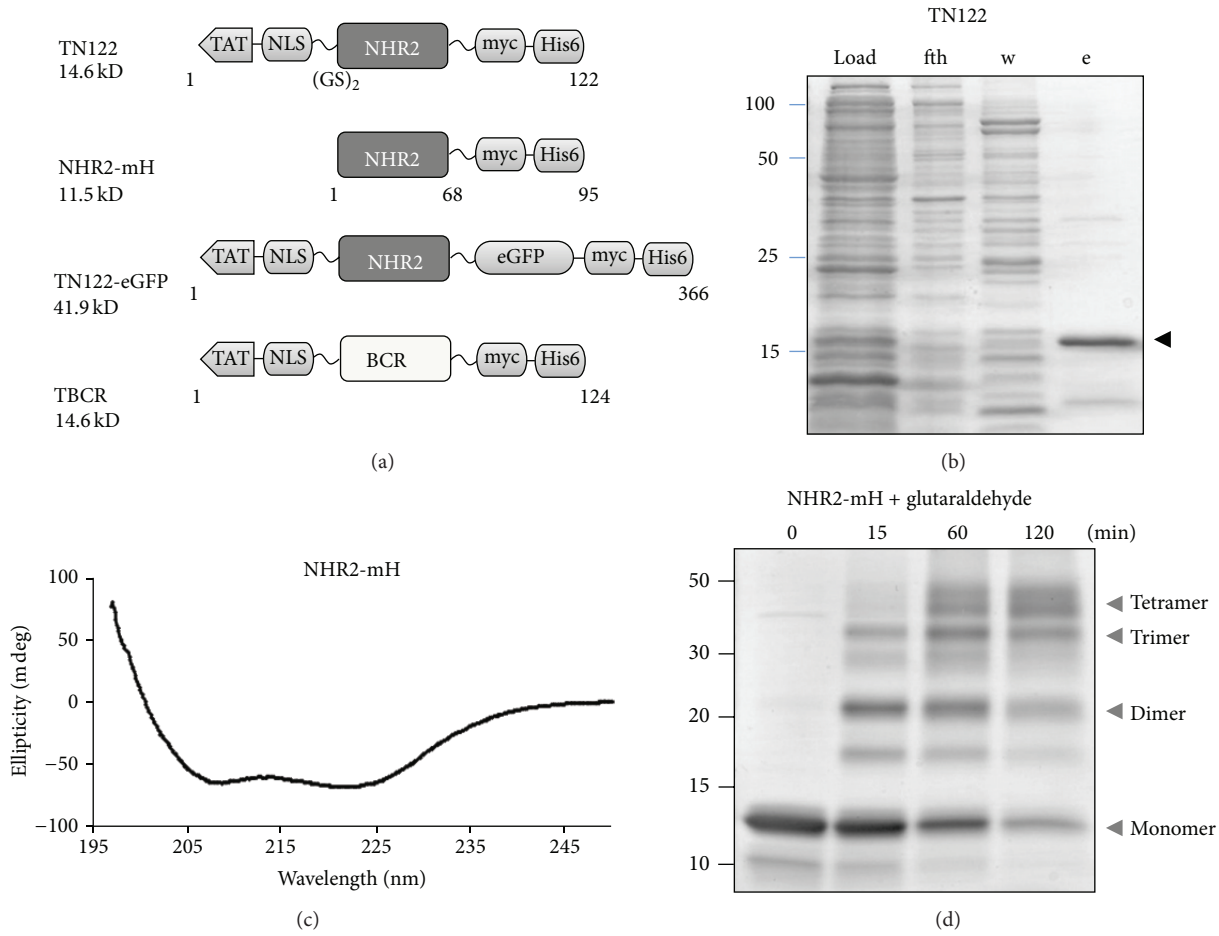

Figure 2: Purification and analysis of recombinant NHR2 containing polypeptides. (a) Schematic representation of the constructs used in this study. *TAT*, protein transduction domain of HIV-1 TAT protein; *NLS*, nuclear localization signal of SV40. (b) Purification of the recombinant NHR2 containing polypeptide TN122 by nickel affinity chromatography. SDS-PAGE and coomassie brilliant blue staining of the bacterial lysate (load), the flow through (fth), the washing fraction (w), and the eluate (e). The arrow indicates the purified TN122 protein. (c) CD spectroscopy of the NHR2 protein (NHR2-mH) at 25°C in PBS reveals an α-helical structure. (d) Glutaraldehyde crosslinking of the NHR2 protein for the indicated incubation times at room temperature and subsequent SDS-PAGE analysis. The arrows indicate the different oligomerization states of the crosslinked NHR2 proteins.

3.3. Cell-Penetrating NHR2 Proteins Transduce Mammalian Cells and Bind to ETO Protein Sequences. The transduction potential of TN122 was investigated by adding the recombinant TN122-eGFP protein to the culture medium of 293T cells followed by flow cytometry for the assessment of eGFP positive cells. To guarantee that only successfully internalized proteins were detected, a digestion with trypsin was performed before FACS analysis to cleave all TAT-proteins bound to the outer side of the plasma membrane. After an incubation time of 24 hours, almost 50% of the cells showed the presence of the eGFP marker protein (Figure 3(a)). The addition of chloroquine, an inhibitor of endosome acidification and lysosomal protein degradation, to the cell culture medium at a concentration of 100 μM increased the uptake and intracellular stability of the TN122 polypeptide resulting in a 100% of the cells expressing eGFP at 24 hours after addition of the polypeptide. Therefore, it can be assumed that, initially, all of the adherent cells were successfully transduced with TN122-eGFP but in the absence of chloroquine, the protein was slowly degraded by lysosomes leading to a decrease in the content of eGFP positive cells over time. To further control for a TAT-mediated uptake of TN122-eGFP, heparin was added to the cell culture medium resulting in a complete block in uptake as described previously [24]. The TAT domain attaches to the cells mainly by binding to heparan sulfate proteoglycan (HSPG) on the outer surface of the cells [25]. An excess of soluble heparin competes with HSPG for binding to the TAT domain and thus inhibits the TAT-mediated cellular internalization of proteins. Kinetic studies on the stability of TN122 showed that the polypeptide was stable for at least 8 hours in the cell culture medium at 37°C and could be detected even at 24 hours after the initial addition (Figure 3(b)). Western blotting experiments revealed that successful protein transduction was only achieved with the TN122 construct, while an NHR2 protein lacking the TAT-PTD was not able to transduce the cells even when high

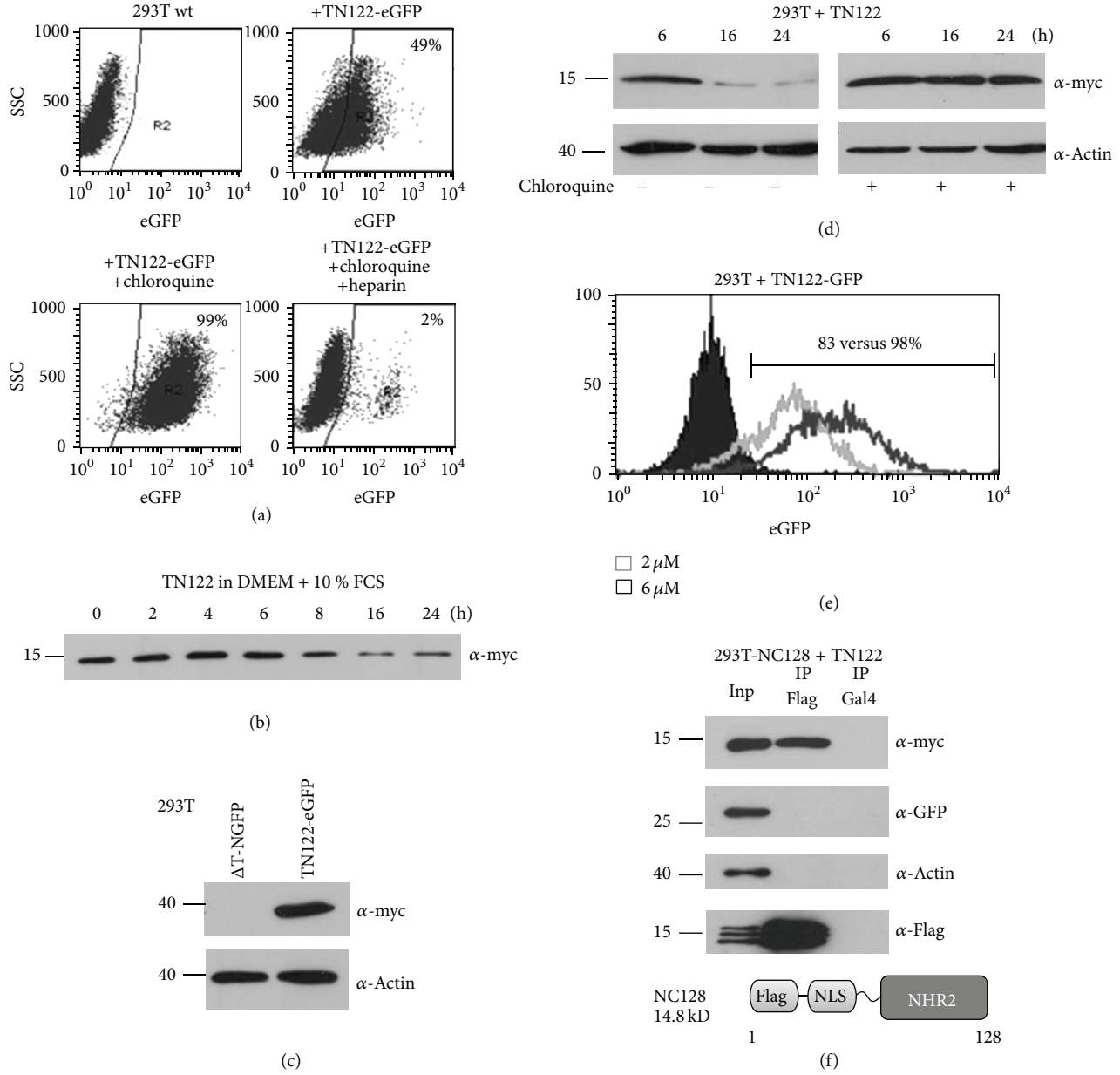

Figure 3: Protein transduction into 293T cells and interaction of recombinant TN122 with the NHR2 domain. (a) Protein transduction of 1 μM TN122-eGFP into 293T cells in the presence or absence of 100 μM chloroquine and addition of 10 μM heparin. After 24 h, the cells were treated with trypsin (10 min, 37°C) and analyzed for the percentage of eGFP positive cells by flow cytometry. (b) Incubation of 1 μM TN122 for various times in serum-containing medium at 37°C and analysis of the stability of the protein by western blotting. (c) TAT-mediated protein transduction. Incubation of 293T cells with either 10 μM ΔT-NGFP or 2 μM TN122-eGFP in the presence of 100 μM chloroquine for 4 h. Thereafter trypsin treatment and western blot analysis of the myc-tagged proteins. (d) Influence of chloroquine on protein transduction. The 293T cells were incubated with 1 μM TN122 in the presence or absence of 20 μM chloroquine for the indicated time, treated with trypsin, and analyzed for the myc-tagged TN122 protein by western blotting. (e) Concentration dependency of protein transduction. Incubation of 293T cells with 2 μM (light gray) or 6 μM (dark gray) TN122-eGFP for 3 h and trypsin treatment followed by flow cytometry. The content of eGFP positive cells is indicated. (f) Binding of the recombinant cell-penetrating NHR2 polypeptide to ETO protein sequences. Protein transduction of 2 × 5 μM TN122 (at 0 and 24 h) in the presence of 20 μM chloroquine into 293T cells that stably express the NHR2-containing polypeptide NC128. The cells were treated with trypsin 14 hours after the last addition of the protein. The Flag-tagged NC128 was immunoprecipitated and the co-precipitated TN122 detected by western blotting. The blot was also stained for eGFP and actin to verify the specificity of the interaction.

concentrations were used (Figure 3(c)). Internalized TN122 was detected for at least 24 hours in cell lysates prepared from transduced 293T cells in the presence of chloroquine, while no TN122 was detectable 16 hours after protein transduction in the absence of chloroquine (Figure 3(d)). For the intracellular stabilization of the transduced protein, a minimal concentration of 20 μM chloroquine was necessary as determined by titration experiments (data not shown). By using increasing concentrations of TN122-eGFP, the efficiency of protein transduction measured by flow cytometry could be enhanced (Figure 3(e)).

We also investigated whether TN122, upon protein transduction, was able to interact with ETO inside the cells. For this purpose, we used a 293T cell line stably expressing the Flag-tagged NHR2 polypeptide NC128 [19]. NC128 expressing cells were incubated twice with 5 μM TN122 in the presence of chloroquine. Coimmunoprecipitation experiments revealed that TN122 was indeed able to interact with NC128 (Figure 3(f)). This binding was specific since neither the highly expressed eGFP protein nor actin was co-precipitated with NC128. Also, no unspecific binding to the antibody was detected when cellular extracts from wild type 293T were used in this assay (data not shown).

3.4. Requirements for TAT-Mediated Protein Transduction into Myeloid Kasumi-1 Cells. Based on the successful transduction of TN122 into mammalian 293T cells, we next investigated the cell culture conditions required for an efficient transduction of the TAT fusion proteins into hematopoietic cell lines. In contrast to the results obtained with the adherent cell line, uptake of TN122 by the RUNX1/ETO-expressing Kasumi-1 cell line could only be observed in the absence of serum (Figure 4(a)). The preincubation of the cells with dextran sulfate could further enhance the efficiency of TN122 internalization in a dose-dependent manner as determined by increased amounts of TN122 detectable in cellular lysates prepared from transduced Kasumi-1 cells (Figure 4(a)). Dextran sulfate is a structural analogue of HSPG and is able to act as an artificial attachment receptor for TAT proteins in cell lines that express low levels of HSPG [26]. However, serum-free RPMI medium as well as prolonged incubation times with dextran sulfate had a negative effect on the viability of Kasumi-1 cells (data not shown) and were therefore not used for further experiments. As an alternative, X-Vivo 10 medium was used, and the concentration of TN122 was increased to compensate for the poor uptake of the TAT proteins by the myeloid cell line. Flow cytometry analysis of cells treated with the TN122-eGFP protein revealed that the efficiency of protein transduction into Kasumi-1 cells, as determined by the percentage of eGFP positive cells under optimal conditions, was lower than that observed for 293T cells (compare Figures 3(a) and 4(b)). At a concentration of 6 μM TN122-eGFP and an incubation time of 3 hours, eGFP fluorescence was detected in 43% of the cells.

In order to investigate the localization of the internalized TAT fusion proteins, Kasumi-1 cells were incubated with TN122-eGFP and analyzed by confocal laser scanning microscopy (CLSM) 24 hours after transduction. The fluorescent protein was detected exclusively in vesicular structures (Figure 4(c)). Assuming that the TN122-eGFP proteins enter the cells by endocytosis [27], these vesicles were most likely endosomes. To verify this observation, protein localization studies were also performed using 293T cells. 24 hours after protein transduction in the presence of chloroquine, TN122-eGFP was found to localize mainly to large vesicles, confirming the observations made in Kasumi-1 cells. Only a minor fraction of TN122-eGFP was localized to the cytosol under these conditions (Figure 4(d)). The use of similar cell culture conditions for Kasumi-1 cells revealed that a concentration of 20 μM chloroquine was toxic for Kasumi-1 cells and therefore not suitable for long-term experiments (Figure 4(e)). With the intention to increase the intracellular stability of the transduced proteins in Kasumi-1 cells, we tested a fusion peptide derived from the influenza virus protein hemagglutinin-2 (HA2). The HA2 peptide has been shown to destabilize the lipid membrane of endosomes upon acidification, thereby enabling the release of molecules from endosomes into the cytoplasm [28]. Therefore, the HA2 sequence was fused to the TAT domain of HIV-1 to generate a cell-penetrating endosomolytic peptide that could be used to release internalized TAT proteins from the endosomes [22]. Consequently, the co-treatment of Kasumi-1 cells with TN122 and TAT-HA2 resulted in an intracellular stabilization of the internalized TN122 as reflected by the high amount of polypeptide detected in western blots 5 hours after treatment of the cells. In contrast, the amount of TN122 in cellular lysates of Kasumi-1 cells was significantly decreased 5 hours after the addition of the protein in the absence of TAT-HA2, presumably because the majority of TN122 was retained within the endosomes and thus subjected to protein degradation via the lysosomal route (Figure 4(f)). This result indicates that the HA2 peptide was effective in releasing TN122 from the endosomes and could be used as an alternative to chloroquine to perform functional studies of TN122 in Kasumi-1 cells.

3.5. TN122 Negatively Affects Proliferation of Kasumi-1 Cells and Decreases Cellular Viability. The effects of the cell-penetrating NHR2 protein TN122 on Kasumi-1 cells were investigated after daily administration of 8 μM TN122 plus 5 μM TAT-HA2 to the cells over a period of 7 days (Figure 5). To demonstrate the specificity of the cellular effects mediated by TN122 on the RUNX1/ETO growth-dependent cell line, we used in parallel a cell-penetrating peptide containing the oligomerization domain of BCR (TBCR) as a control protein. The successful internalization of TN122 and TBCR by Kasumi-1 cells was demonstrated by western blotting (Figure 5(a)). Under the influence of TN122, Kasumi-1 cells showed a strongly decreased proliferation rate which was evident three days after start of the protein treatment (Figure 5(b)). Although a negative effect of the buffer itself on cell proliferation became evident during these experiments, the strong reduction in proliferation rate observed with TN122 cannot be explained by the influence of the buffer alone as the reduction in cell proliferation in the presence of TN122 was highly significant. In contrast to TN122, the BCR containing polypeptide did not affect proliferation of Kasumi-1 cells beyond the effect caused by the buffer

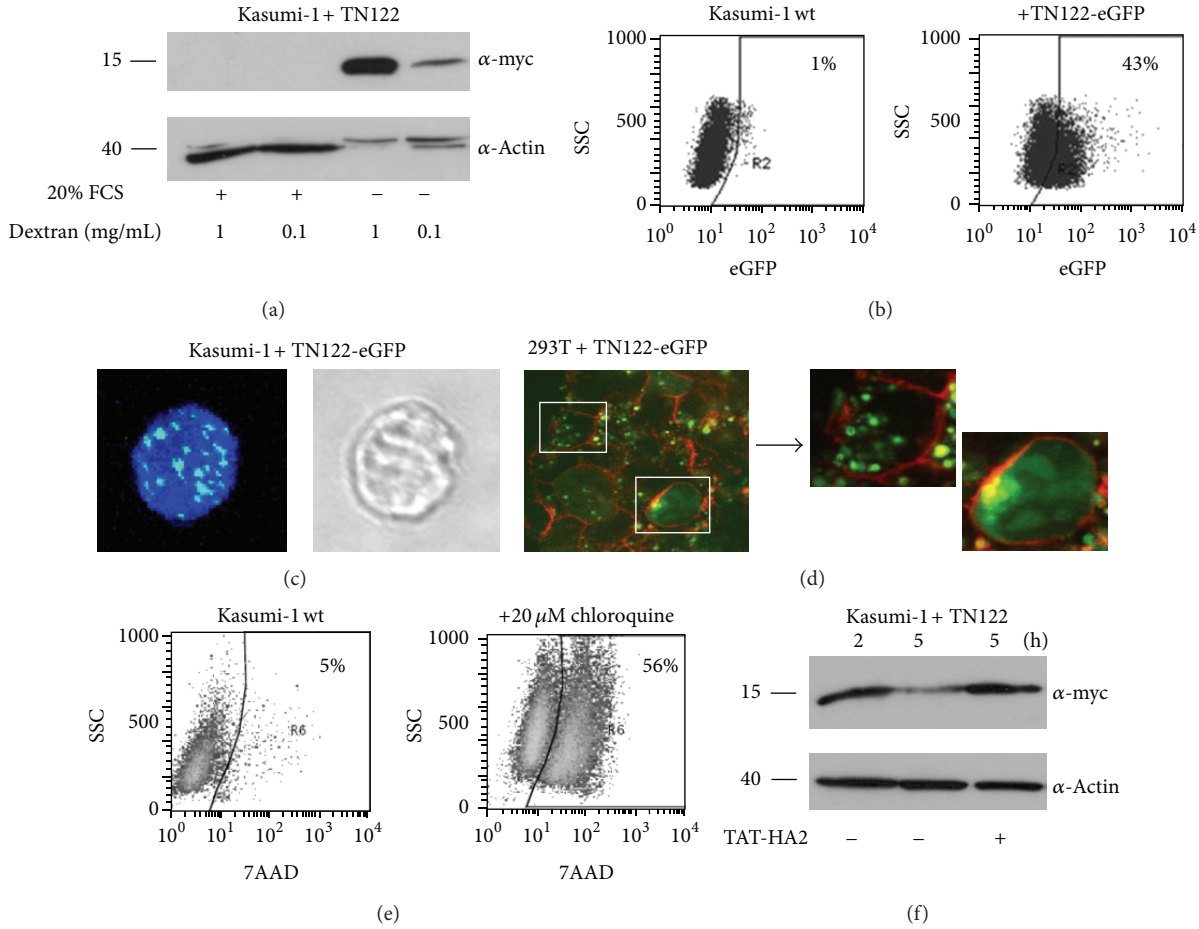

Figure 4: Cell-penetrating NHR2-containing polypeptides transduce myeloid Kasumi-1 cells. (a) Effect of serum and dextran on protein transduction efficiency into hematopoietic cells. Preincubation of Kasumi-1 cells for 3 hours in dextran (0.1 or 1 mg/mL) containing medium, extensive washing of the cells and incubation with 2 μM TN122 for 4 hours in the presence or absence of 20% FCS. Successfully transduced protein was detected by Western blotting after trypsin treatment of the cells. (b) Incubation of Kasumi-1 cells with 6 μM TN122-eGFP in serum-free X-Vivo 10 medium for 3 h, trypsin treatment and flow cytometry analysis to determine the efficiency of protein transduction. Percentages correspond to the percentage of eGFP positive cells. (c) Intracellular localization of TN122-eGFP in Kasumi-1 cells. Incubation of the cells with 4 μM TN122-eGFP in X-Vivo 10 medium for 1 h, trypsin treatment, fixation and permeabilization, DNA staining with Toto3, and subsequent CLSM analysis (63x magnification). (d) TN122-eGFP is captured inside endosomes upon protein transduction. Incubation of 293T cells with 2 μM TN122-eGFP in the presence of 20 μM chloroquine for 24 h, trypsin treatment, staining of the unfixed cells with a rhodamine-coupled wheat germ agglutinin (red), and CLSM analysis. (e) Cytotoxicity of 20 μM chloroquine on Kasumi-1 cells. The percentage of dead cells was measured by flow cytometry using 7-amino-actinomycin D (7AAD) after a 24 hours incubation of the cells in chloroquine-containing medium. (f) Endosomolytic TAT-HA2 increases the intracellular stability of transduced proteins. Cotreatment of Kasumi-1 cells with 3 μM TN122 in the presence or absence of 5 μM TAT-HA2 for different times, trypsin treatment and detection of the myc-tagged TN122 in the cellular lysates.

alone (Figure 5(b)). The negative effect of the cell-penetrating NHR2 protein on the cellular viability was further analyzed via flow cytometry by measuring the percentage of apoptotic cells. At day seven after start of TN122 treatment, a significant increase in the percentage of Annexin V and 7AAD double positive Kasumi-1 cells was detected. This effect was clearly caused by TN122, as the apoptotic effect mediated by the control polypeptide TBCR was 3-fold lower than that observed with TN122, indicating that induction of apoptosis by the cell-penetrating NHR2 polypeptide on RUNX1/ETO-dependent Kasumi-1 cells was specific (Figure 5(c)).

4. Discussion

The current treatment of acute myeloid leukemia with t(8;21) translocation is based mainly on the use of cytotoxic drugs, especially anthracyclines and cytarabine, with a median survival time from first diagnosis of 2-3 years and a 5-year overall survival of less than 40% [29, 30]. Due to the lack of specificity and selectivity, this treatment is in most cases associated with severe side effects that can be fatal particularly for older patients. An alternative strategy that specifically targets the leukemic cells is therefore highly desirable. Consequently,

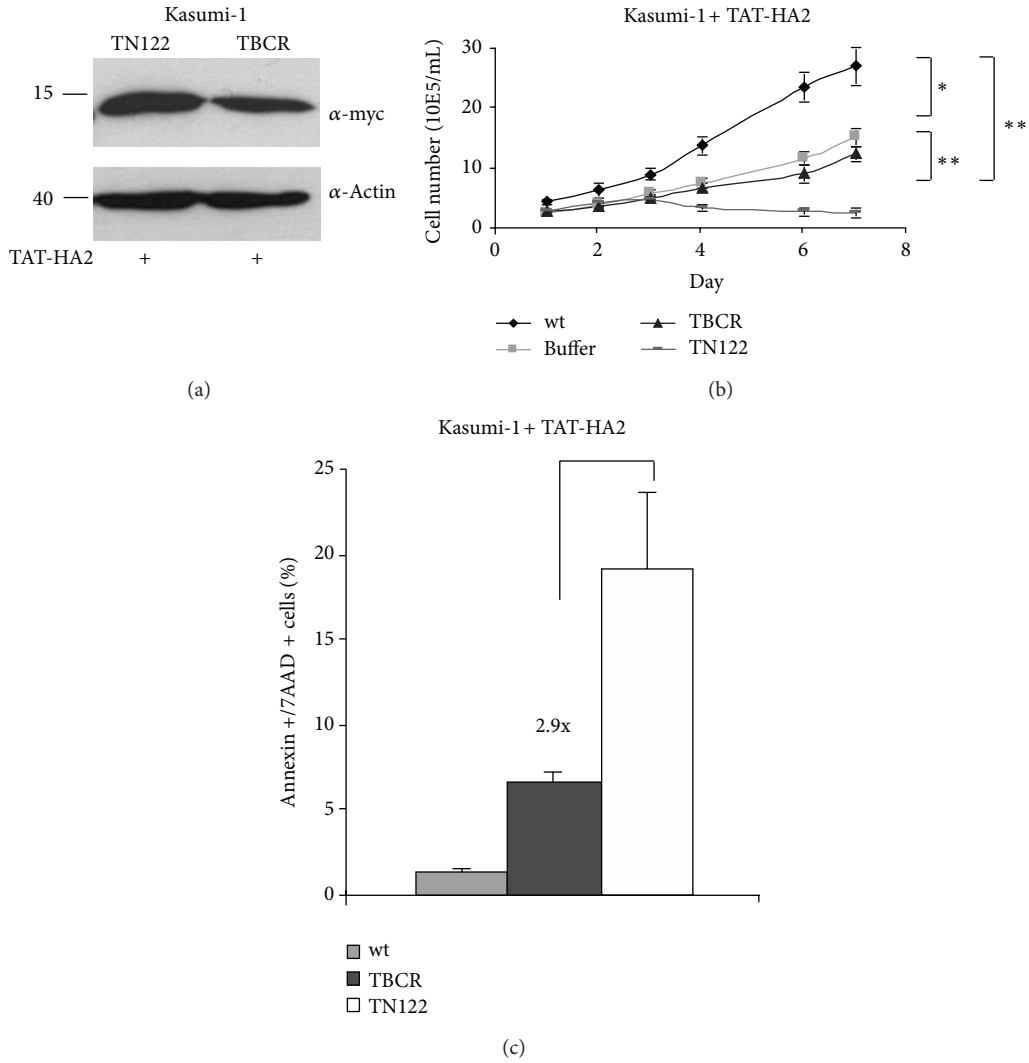

Figure 5: Cellular effects of TN122 on the proliferation and viability of Kasumi-1 cells. Incubation of Kasumi-1 cells for 7 days in X-Vivo 10 medium with daily cotreatment of the cells with 8 μM TN122 or TBCR as a control protein and 5 μM TAT-HA2. (a) Western blot detection of both cell-penetrating proteins in the cellular lysates 5 hours after the last addition of the proteins. (b) Analysis of the proliferation rates of treated Kasumi-1 cells. At day 0, 2×10^5 c/mL were seeded, and cell numbers were measured daily by trypan blue staining. The values are mean values with the corresponding standard deviation of the experiment carried out in triplicates. Data were statistically analyzed using two-tailed student's t test for unpaired samples; $P < 0.05$ was considered significant ($*$) and $P < 0.01$ highly significant ($**$). (c) Analysis of the percentage of apoptotic cells by flow cytometry at day 7. Shown is the percentage of cells that are double positive for Annexin V and 7AAD. The values are mean values with the corresponding standard deviation of the experiment carried out in duplicates.

numerous studies have concentrated on the development of molecular therapies targeted at tumor-relevant functions of leukemia-specific oncoproteins [31, 32]. Whereas the clinical relevance of inhibitors of histone deacetylases and demethylating agents to revert the block of myeloid differentiation seems to be limited [33], better results were achieved using tyrosine kinase inhibitors such as gleevec to decelerate the enhanced proliferation of the blast cells. Originally developed for the treatment of BCR/ABL positive chronic myeloid leukemia, gleevec is also effective for several constitutively active mutations of c-kit found in numerous t(8;21) positive patients [34]. However, under the influence of kinase inhibitors, the development of escape mutations in the kinase domain leading to drug resistance has been reported repeatedly [35]. Obviously, novel specific therapies are still required.

Leukemias with t(8;21) are addicted to the permanent expression of the RUNX1/ETO fusion protein [19, 36]. In order to eliminate the transformed cells, inhibition of crucial protein-protein interactions could therefore be a suitable strategy for a targeted therapy against RUNX1/ETO. We have previously shown that the leukemogenic potential of RUNX1/ETO can be inhibited by interference with tetramerization of the chimeric protein using proteins containing the NHR2 oligomerization domain, which were expressed intracellularly in leukemic cells [19]. However, for a therapeutic approach, the application of viral vectors *in vivo* is

difficult due to the lack of efficient targeting. As an alternative delivery strategy, we therefore investigated whether the protein transduction technology could be utilized to directly deliver the inhibitory polypeptides to the leukemic cells. Several studies have demonstrated the feasibility of this approach also for hematopoietic cells. For example, a truncated mutant of nucleophosmin coupled to the TAT domain was found to inhibit proliferation and induce apoptosis in preleukemic stem cells [37]. Another group could show that cell-penetrating peptides derived from AF4 were able to specifically induce necrosis in cells expressing the ALL-associated fusion protein MLL/AF4 [38]. More recently, it was demonstrated that a constitutively active mutant of the transcription factor FOXO3 fused to the TAT domain induced apoptosis in leukemic cell lines and reduced viability of primary chronic lymphoid leukemia (CLL) cells [39]. In another promising approach, the coiled-coil domain of BCR was used to generate the cell-penetrating peptide TAT-CC in order to interrupt BCR/ABL oligomerization [40]. The authors could show that the peptide interacted with BCR/ABL endogenously expressed in leukemic cell lines and, as a consequence, led to a decrease in cell growth and induction of apoptotic death specifically in cells expressing the leukemia-associated fusion protein. For RUNX1/ETO, Racanicchi et al. used protein fragments derived from the RUNX1/ETO corepressor N-CoR to disrupt this essential protein-corepressor interaction. As a result, expression of RUNX1/ETO repressed genes was restored leading to myeloid differentiation of leukemic cell lines [41]. As N-CoR has multiple functions in development, homeostasis and prevention of disease, N-CoR-derived peptides may interfere with essential cellular functions of the protein, and thus, their therapeutic application must be taken with caution. Furthermore, recent studies have shown that an alternatively spliced isoform of RUNX1/ETO lacking the C-terminal N-CoR binding domain coexists with full length RUNX1/ETO in patients and strongly induces leukemia development in mice [42]. Consequently, peptides targeted to the N-CoR-RUNX1/ETO interaction domain may not be fully effective in t(8;21) leukemias expressing the truncated form of RUNX1/ETO. We therefore propose that targeting the oligomerization domain of RUNX1/ETO, which is crucial for the activity of both, the full-length as well as the truncated protein, could be a more valuable approach.

Here, we show that by fusion to the TAT protein transduction domain, recombinant NHR2 polypeptides could successfully be internalized by mammalian cells. As reported elsewhere for TAT mediated protein transfer [22], uptake of TAT-NHR2 polypeptides occurred most likely by macropinocytosis, a specialized form of endocytosis, because they were found to localize to endosome-like vesicles throughout the cytoplasm. We do not expect the eGFP-tag used for intracellular localization studies to influence cellular traffic since in our previous studies, an NHR2-eGFP fusion construct had the same antiproliferative effect on Kasumi-1 cells compared to an NHR2-only protein [19]. Moreover, successful protein transduction and biologic activity has been demonstrated with much larger proteins like β-galactosidase [43]. However, the size of the proteins does influence the time required for protein transduction [44]. The trapping of TAT fusion proteins in endosomes is a common observation made by several groups [45], and the escape of these proteins to the cytosol seems to be the rate limiting step in the protein transduction process that has to be optimized to fully exploit this methodology [46]. Chloroquine treatment effectively inhibited degradation of the proteins, thereby increasing their intracellular stability. The occurrence of large vesicular structures in which the internalized proteins are trapped is also attributed to the usage of chloroquine that induces lysosomal dilatation. It is believed that a high concentration of the TAT domain in the vesicles is able to destabilize the endosomal membrane, thus allowing a certain amount of the protein to escape from the endosomes and carry out its therapeutical function in the cell [47]. In agreement with this, the successfully internalized TN122 interacted with ETO protein sequences inside the cells.

In comparison to the adherent cell line, the amount of internalized TN122 that was detected in the hematopoietic Kasumi-1 cells was significantly lower. The poorer protein transduction efficiency of the suspension cell line is most likely related to different expression levels of HSPG at the cell surface that serves as a binding molecule for the TAT domain. Whereas HSPG is expressed at high levels on most adherent cells, only low amounts are found on hematopoietic cells [48]. Although it has been reported that myeloid cells from healthy donors do not express HSPG [49], a low but clear expression of HSPG was detected in myeloid leukemia cell lines as well as in leukemic blasts of AML patients [50]. However, for efficient *in vivo* targeting, a tumor-associated antigen fused to TAT-NHR2 may be required, as was successfully demonstrated for a TAT-p53-derived protein targeting cells overexpressing the CXCR4 receptor [51].

Other studies have reported the use of chloroquine to successfully inhibit lysosomal degradation of internalized cell membrane-penetrating proteins [20, 52]. However, in these cases, cells were generally treated for short time periods, most likely to avoid cytotoxic reactions associated with chloroquine that is known to inhibit cellular growth and viability by blocking lysosomal hydolases, arresting autophagy, activating the p53 pathway, and inducing apoptosis. Thus, in order to perform repetitive protein transduction of TN122 into Kasumi-1 cells over an extended time period, we used the TAT-HA2 peptide as an alternative to chloroquine. Coadministration of TAT-HA2 and TN122 to the cells resulted in a prolonged detection of internalized TN122, most likely mediated by increased endosomal escape of TAT-NHR2 proteins that consequently were no longer subjected to lysosomal degradation. The internalized TN122 polypeptides were found to bind to ETO as well as to inhibit proliferation and increase apoptosis in RUNX1/ETO positive cells, resembling the effects observed after lentiviral-mediated expression of NHR2 peptides in Kasumi-1 cells [19]. In order to control the specificity of these effects, we made use of the BCR tetramerization domain which has a very similar structure to that of the NHR2 domain with its four α-helical monomers building the tetramer. With the lentiviral vector system, the utilization of BCR as a proper control could be demonstrated (Figure 1 and [19]). Contrary to this, a monomeric mutant

of the NHR2 domain (m7) introduced by the Bushweller group [17] disrupts protein stability and could therefore not be used as a control because its expression and purification as a cell-penetrating protein failed. The influence of TN122 on Kasumi-1 cells was specific since a similar polypeptide containing the BCR oligomerization domain did not affect cell growth and vitality beyond the effects observed with the buffer alone. The buffer used for purification of the cell-penetrating proteins includes imidazole that has toxic effects on cells. It cannot be ruled out that small amounts are still present in the buffer after dialysis against PBS causing the growth inhibitory and apoptotic effects observed with both, the buffer alone and the BCR control. However, the potency of the TN122 effects was reduced compared to that observed after lentiviral transduction and expression of NHR2-containing polypeptides. These observations are not surprising as the confocal microscopic analysis of protein-transduced cells revealed that the majority of the internalized TN122 protein was localized in vesicles, and only a small proportion was able to escape to the cytosol. Obviously, the amount of NHR2 polypeptides released from the endosomes after internalization was not sufficient to completely abolish the leukemogenic potential of RUNX1/ETO. Since the efficiency of protein transduction dependents on the concentrations is used, we tested different concentrations of TN122 for growth inhibition in Kasumi-1 cells. While the effects with 1 μM TN122 were modest, 5 to 10 μM were found to be optimal leading to a significant reduction in cell growth. Higher protein concentrations did have an unspecific toxicity due to impurities present in the solvent as mentioned before and therefore were not further used.

The efficiency of protein transduction into hematopoietic cells strongly depends on the cell line used. Racanicchi et al. reported that a TAT fusion protein designed to interfere with the binding of PML/RARα to the corepressor molecule N-CoR in PML/RARα-expressing NB4 cells was able to induce full myeloid differentiation in the presence of vitamin D3. In contrast, a similar fusion protein designed to block the binding of RUNX1/ETO to N-CoR merely led to a partial induction of differentiation in the RUNX1/ETO positive cell line SKNO-1 [41]. Besides considerations on the uptake efficiency of cell-penetrating peptides by different cell types, the cellular localization of the TAT fusion proteins may also have a profound influence on the biological effects of the transduced proteins. RUNX1/ETO tetramers are found in high molecular weight protein complexes of >2 MDa that are stabilized by several protein-protein interactions. Thus, it is doubtful that these complexes can be destroyed efficiently by the NHR2 polypetides in the nucleus. More likely, the NHR2 polypeptides interfere during the synthesis of new RUNX1/ETO molecules by competing with the full-length protein for the assembly into RUNX1/ETO tetramers. Probably, high concentrations of the inhibitory polypeptides will be required inside leukemic cells to efficiently interfere with RUNX1/ETO complex assembly and oncogenic activity.

Because the size of the construct has a critical influence on efficiency of protein transduction [53], we tested several truncated versions of the previously described NC128 protein [19] and chose N89 as the shortest protein with the full inhibitory potential. Further deletions of the construct that could increase transduction efficiency were not as efficient in its inhibitory function as N89. When using the TAT-PTD an additional NLS sequence might be dispensable [54], and the tags included for purification and western blot detection are not required to achieve biological efficiency of the protein. However, our data indicate that the entire NHR2 domain is necessary for the full inhibitory potential since the deletion of only seven amino acids inhibits the binding of the construct to RUNX1/ETO [19]. Recently, we were able to show that five amino acids in the NHR2 sequence are critical for tetramerization of the leukemic protein and are involved in its oncogenic potential [18]. Because these hot spots for tetramer formation are located at the outer edges of the NHR2 sequence, it is mandatory to include the whole 59 amino acids of the NHR2 domain.

Altogether, the functional effect of TN122 is limited. However, this strategy serves as a proof of principle and indeed is the first report showing that a peptide-based protein domain interference strategy can be regarded as a potential way to interfere with RUNX1/ETO tetramerization and oncogene function. Current limitations of the protein transduction approach are mainly in terms of efficiency and specificity. In order to increase the intracellular stability of the proteins, usage of D-amino acids is possible that would, however, require chemical synthesis of the peptides. Transduction efficiency of the proteins is mainly hampered by their improper release from endosomes. To overcome this hurdle, several different endosomolytic peptides of viral or bacterial origin have been described with the capacity to destabilize endosomal membranes [55]. Specificity of the therapeutic protein for the cancer cells might be achieved by the incorporation of tumor-associated targeting peptides. Of course, also a combination therapy of the cell-penetrating peptides with inducers of differentiation like vitamin D3 and/or valproic acid is possible. As an alternative to protein transduction, NHR2-containing proteins might be administered by liposomes or other nanoparticles [56]. However, further approaches will concentrate on the development of peptide mimetica and small molecular weight inhibitors with increased cellular uptake and efficiency that are able to interfere with NHR2 tetramer formation. As we recently described, indeed disruption of tetramers into dimmers is sufficient to block RUNX1/ETO oncogenic function [18].

Our results indicate that the NHR2 domain of RUNX1/ETO is a challenging but promising target for a molecular intervention in t(8;21)-positive leukemia. Since oligomerization of chimeric proteins seems to be essential for their leukemogenic activity [57], we further propose that interference with oligomerization could be a general principle towards a targeted therapy in leukemia. Indeed, the value of this approach has already been demonstrated for the BCR/ABL fusion protein using a BCR-derived TAT-coiled-coil peptide [40]. Likewise, it should also provide an attractive treatment option for RUNX1/ETO-mediated leukemia.

Conflict of Interests

The authors certify that there is no conflict of interests with any financial organization regarding the material discussed in the paper.

Authors' Contribution

Manuel Grez and Christian Wichmann contributed equally to this work.

Acknowledgments

The authors are supported by research Grants from the NGFN Cancer Network (grant 01GS0450, TP-10), the LOEWE OSF (TP-C3), the LOEWE CGT (startup grant, CW), and the José Carreras Leukemia Foundation (DJCLS R 12/28, CW). The Georg-Speyer-Haus is supported by the Bundesministerium für Gesundheit and the Hessisches Ministerium für Wissenschaft und Kunst.

References

[1] K. Döhner and H. Döhner, "Molecular characterization of acute myeloid leukemia," *Haematologica*, vol. 93, no. 7, pp. 976–982, 2008.

[2] F. Rosenbauer and D. G. Tenen, "Transcription factors in myeloid development: balancing differentiation with transformation," *Nature Reviews Immunology*, vol. 7, no. 2, pp. 105–117, 2007.

[3] A. T. Look, "Oncogenic transcription factors in the human acute leukemias," *Science*, vol. 278, no. 5340, pp. 1059–1064, 1997.

[4] K. A. Link, F.-S. Chou, and J. C. Mulloy, "Core binding factor at the crossroads: determining the fate of the HSC," *Journal of Cellular Physiology*, vol. 222, no. 1, pp. 50–56, 2010.

[5] A. M. Melnick, J. J. Westendorf, A. Polinger et al., "The ETO protein disrupted in t(8;21)-associated acute myeloid leukemia is a corepressor for the promyelocytic leukemia zinc finger protein," *Molecular and Cellular Biology*, vol. 20, no. 6, pp. 2075–2086, 2000.

[6] L. F. Peterson and D.-E. Zhang, "The 8;21 translocation in leukemogenesis," *Oncogene*, vol. 23, no. 24, pp. 4255–4262, 2004.

[7] L. Wang, A. Gural, X.-J. Sun et al., "The leukemogenicity of AML1-ETO is dependent on site-specific lysine acetylation," *Science*, vol. 333, no. 6043, pp. 765–769, 2011.

[8] B. Niebuhr, M. Fischer, M. Täger, J. Cammenga, and C. Stocking, "Gatekeeper function of the RUNX1 transcription factor in acute leukemia," *Blood Cells, Molecules, and Diseases*, vol. 40, no. 2, pp. 211–218, 2008.

[9] N. Boissel, H. Leroy, B. Brethon et al., "Incidence and prognostic impact of c-Kit, FLT3, and Ras gene mutations in core binding factor acute myeloid leukemia (CBF-AML)," *Leukemia*, vol. 20, no. 6, pp. 965–970, 2006.

[10] P. Paschka, G. Marcucci, A. S. Ruppert et al., "Adverse prognostic significance of KIT mutations in adult acute myeloid leukemia with inv(16) and t(8;21): a Cancer and Leukemia Group B study," *Journal of Clinical Oncology*, vol. 24, no. 24, pp. 3904–3911, 2006.

[11] D. Hildebrand, J. Tiefenbach, T. Heinzel, M. Grez, and A. B. Maurer, "Multiple regions of ETO cooperate in transcriptional repression," *Journal of Biological Chemistry*, vol. 276, no. 13, pp. 9889–9895, 2001.

[12] B. Lutterbach, J. J. Westendorf, B. Linggi et al., "ETO, a target of t(8;21) in acute leukemia, interacts with the N-CoR and mSin3 corepressors," *Molecular and Cellular Biology*, vol. 18, no. 12, pp. 7176–7184, 1998.

[13] B. Lutterbach, D. Sun, J. Schuetz, and S. W. Hiebert, "The MYND motif is required for repression of basal transcription from the multidrug resistance 1 promoter by the t(8;21) fusion protein," *Molecular and Cellular Biology*, vol. 18, no. 6, pp. 3604–3611, 1998.

[14] J. Zhang, B. A. Hug, E. Y. Huang et al., "Oligomerization of ETO is obligatory for corepressor interaction," *Molecular and Cellular Biology*, vol. 21, no. 1, pp. 156–163, 2001.

[15] M. Yan, E.-Y. Ahn, S. W. Hiebert, and D.-E. Zhang, "RUNX1/AML1 DNA-binding domain and ETO/MTG8 NHR2-dimerization domain are critical to AML1-ETO9a leukemogenesis," *Blood*, vol. 113, no. 4, pp. 883–886, 2009.

[16] C. Kwok, B. B. Zeisig, J. Qiu, S. Dong, and C. W. So, "Transforming activity of AML1-ETO is independent of CBFβ3 and ETO interaction but requires formation of homo-oligomeric complexes," *Proceedings of the National Academy of Sciences of the United States of America*, vol. 106, no. 8, pp. 2853–2858, 2009.

[17] Y. Liu, M. D. Cheney, J. J. Gaudet et al., "The tetramer structure of the Nervy homology two domain, NHR2, is critical for AML1/ETO's activity," *Cancer Cell*, vol. 9, no. 4, pp. 249–260, 2006.

[18] C. Wichmann, Y. Becker, L. Chen-Wichmann et al., "Dimer-tetramer transition controls RUNX1/ETO leukemogenic activity," *Blood*, vol. 116, no. 4, pp. 603–613, 2010.

[19] C. Wichmann, L. Chen, M. Heinrich et al., "Targeting the oligomerization domain of ETO interferes with RUNX1/ETO oncogenic activity in t(8;21)-positive leukemic cells," *Cancer Research*, vol. 67, no. 5, pp. 2280–2289, 2007.

[20] A. Sloots and W. S. Wels, "Recombinant derivatives of the human high-mobility group protein HMGB2 mediate efficient nonviral gene delivery," *FEBS Journal*, vol. 272, no. 16, pp. 4221–4236, 2005.

[21] J. R. McWhirter, D. L. Galasso, and J. Y. J. Wang, "A coiled-coil oligomerization domain of Bcr is essential for the transforming function of Bcr-Abl oncoproteins," *Molecular and Cellular Biology*, vol. 13, no. 12, pp. 7587–7595, 1993.

[22] J. S. Wadia, R. V. Stan, and S. F. Dowdy, "Transducible TAT-HA fusogenic peptide enhances escape of TAT-fusion proteins after lipid raft macropinocytosis," *Nature Medicine*, vol. 10, no. 3, pp. 310–315, 2004.

[23] C. A. Rohl and R. L. Baldwin, "Comparison of nh exchange and circular dichroism as techniques for measuring the parameters of the helix-coil transition in peptides," *Biochemistry*, vol. 36, no. 28, pp. 8435–8442, 1997.

[24] D. A. Mann and A. D. Frankel, "Endocytosis and targeting of exogenous HIV-1 Tat protein," *The EMBO Journal*, vol. 10, no. 7, pp. 1733–1739, 1991.

[25] M. Tyagi, M. Rusnati, M. Presta, and M. Giacca, "Internalization of HIV-1 Tat requires cell surface heparan sulfate proteoglycans," *Journal of Biological Chemistry*, vol. 276, no. 5, pp. 3254–3261, 2001.

[26] J. C. Mai, H. Shen, S. C. Watkins, T. Cheng, and P. D. Robbins, "Efficiency of protein transduction is cell type-dependent and is enhanced by dextran sulfate," *Journal of Biological Chemistry*, vol. 277, no. 33, pp. 30208–30218, 2002.

[27] J. P. Richard, K. Melikov, E. Vives et al., "Cell-penetrating peptides: a reevaluation of the mechanism of cellular uptake,"

Journal of Biological Chemistry, vol. 278, no. 1, pp. 585–590, 2003.

[28] C. Plank, B. Oberhauser, K. Mechtler, C. Koch, and E. Wagner, "The influence of endosome-disruptive peptides on gene transfer using synthetic virus-like gene transfer systems," *Journal of Biological Chemistry*, vol. 269, no. 17, pp. 12918–12924, 1994.

[29] M. S. Tallman, D. G. Gilliland, and J. M. Rowe, "Drug therapy for acute myeloid leukemia," *Blood*, vol. 106, no. 4, pp. 1154–1163, 2005.

[30] J. M. Rowe and M. S. Tallman, "How I treat acute myeloid leukemia," *Blood*, vol. 116, no. 17, pp. 3147–3156, 2010.

[31] S. Durual, A. Rideau, S. Ruault-Jungblut et al., "Lentiviral PU.1 overexpression restores differentiation in myeloid leukemic blasts," *Leukemia*, vol. 21, no. 5, pp. 1050–1059, 2007.

[32] J. Dunne, C. Cullmann, M. Ritter et al., "siRNA-mediated AML1/MTG8 depletion affects differentiation and proliferation-associated gene expression in t(8;21)-positive cell lines and primary AML blasts," *Oncogene*, vol. 25, no. 45, pp. 6067–6078, 2006.

[33] T. Haferlach, "Molecular genetic pathways as therapeutic targets in acute myeloid leukemia," *American Society of Hematology Education Program*, pp. 400–411, 2008.

[34] J. Cammenga, S. Horn, U. Bergholz et al., "Extracellular KIT receptor mutants, commonly found in core binding factor AML, are constitutively active and respond to imatinib mesylate," *Blood*, vol. 106, no. 12, pp. 3958–3961, 2005.

[35] M. E. Gorre, M. Mohammed, K. Ellwood et al., "Clinical resistance to STI-571 cancer therapy caused by BCR-ABL gene mutation or amplification," *Science*, vol. 293, no. 5531, pp. 876–880, 2001.

[36] O. Heidenreich, J. Krauter, H. Riehle et al., "AML1/MTG8 oncogene suppression by small interfering RNAs supports myeloid differentiation of t(8;21)-positive leukemic cells," *Blood*, vol. 101, no. 8, pp. 3157–3163, 2003.

[37] Y. Zhou, W. Du, T. Koretsky, G. C. Bagby, and Q. Pang, "TAT-mediated intracellular delivery of NPM-derived peptide induces apoptosis in leukemic cells and suppresses leukemogenesis in mice," *Blood*, vol. 112, no. 6, pp. 2474–2483, 2008.

[38] C. M. Palermo, C. A. Bennett, A. C. Winters, and C. S. Hemenway, "The AF4-mimetic peptide, PFWT, induces necrotic cell death in MV4-11 leukemia cells," *Leukemia Research*, vol. 32, no. 4, pp. 633–642, 2008.

[39] M. Essafi, A. D. Baudot, X. Mouska, J.-P. Cassuto, M. Ticchioni, and M. Deckert, "Cell-penetrating TAT-FOXO3 fusion proteins induce apoptotic cell death in leukemic cells," *Molecular Cancer Therapeutics*, vol. 10, no. 1, pp. 37–46, 2011.

[40] Z. Huang, M. Ji, Z. Peng et al., "Purification of TAT-CC-HA protein under native condition, and its transduction analysis and biological effects on BCR-ABL positive cells," *Biomedicine and Pharmacotherapy*, vol. 65, no. 3, pp. 183–192, 2011.

[41] S. Racanicchi, C. Maccherani, C. Liberatore et al., "Targeting fusion protein/corepressor contact restores differentiation response in leukemia cells," *The EMBO Journal*, vol. 24, no. 6, pp. 1232–1242, 2005.

[42] M. Yan, E. Kanbe, L. F. Peterson et al., "A previously unidentified alternatively spliced isoform of t(8;21) transcript promotes leukemogenesis," *Nature Medicine*, vol. 12, no. 8, pp. 945–949, 2006.

[43] S. R. Schwarze, A. Ho, A. Vocero-Akbani, and S. F. Dowdy, "In vivo protein transduction: delivery of a biologically active protein into the mouse," *Science*, vol. 285, no. 5433, pp. 1569–1572, 1999.

[44] M. Zorko and Ü. Langel, "Cell-penetrating peptides: mechanism and kinetics of cargo delivery," *Advanced Drug Delivery Reviews*, vol. 57, no. 4, pp. 529–545, 2005.

[45] C. Pan, B. Lu, H. Chen, and C. E. Bishop, "Reprogramming human fibroblasts using HIV-1 TAT recombinant proteins OCT4, SOX2, KLF4 and c-MYC," *Molecular Biology Reports*, vol. 37, no. 4, pp. 2117–2124, 2010.

[46] J. M. Gump and S. F. Dowdy, "TAT transduction: the molecular mechanism and therapeutic prospects," *Trends in Molecular Medicine*, vol. 13, no. 10, pp. 443–448, 2007.

[47] C. Foerg, U. Ziegler, J. Fernandez-Carneado et al., "Decoding the entry of two novel cell-penetrating peptides in HeLa cells: lipid raft-mediated endocytosis and endosomal escape," *Biochemistry*, vol. 44, no. 1, pp. 72–81, 2005.

[48] W. Shi and J. S. Bartlett, "RGD inclusion in VP3 provides adeno-associated virus type 2 (AAV2)-based vectors with a heparan sulfate-independent cell entry mechanism," *Molecular Therapy*, vol. 7, no. 4, pp. 515–525, 2003.

[49] Z. Drzeniek, G. Stöcker, B. Siebertz et al., "Heparan sulfate proteoglycan expression is induced during early erythroid differentiation of multipotent hematopoietic stem cells," *Blood*, vol. 93, no. 9, pp. 2884–2897, 1999.

[50] P. Vongchan and R. J. Linhardt, "Expression of human liver HSPGs on acute myeloid leukemia," *Clinical Immunology*, vol. 122, no. 2, pp. 194–206, 2007.

[51] E. L. Snyder, C. C. Saenz, C. Denicourt et al., "Enhanced targeting and killing of tumor cells expressing the CXC chemokine receptor 4 by transducible anticancer peptides," *Cancer Research*, vol. 65, no. 23, pp. 10646–10650, 2005.

[52] N. J. Caron, S. P. Quenneville, and J. P. Tremblay, "Endosome disruption enhances the functional nuclear delivery of Tat-fusion proteins," *Biochemical and Biophysical Research Communications*, vol. 319, no. 1, pp. 12–20, 2004.

[53] G. Tünnemann, R. M. Martin, S. Haupt, C. Patsch, F. Edenhofer, and M. C. Cardoso, "Cargo-dependent mode of uptake and bioavailability of TAT-containing proteins and peptides in living cells," *The FASEB Journal*, vol. 20, no. 11, pp. 1775–1784, 2006.

[54] E. Vivès, P. Brodin, and B. Lebleu, "A truncated HIV-1 Tat protein basic domain rapidly translocates through the plasma membrane and accumulates in the cell nucleus," *Journal of Biological Chemistry*, vol. 272, no. 25, pp. 16010–16017, 1997.

[55] C. Plank, W. Zauner, and E. Wagner, "Application of membrane-active peptides for drug and gene delivery across cellular membranes," *Advanced Drug Delivery Reviews*, vol. 34, no. 1, pp. 21–35, 1998.

[56] C. Borghouts, C. Kunz, and B. Groner, "Current strategies for the development of peptide-based anti-cancer therapeutics," *Journal of Peptide Science*, vol. 11, no. 11, pp. 713–726, 2005.

[57] C. W. So and M. L. Cleary, "Dimerization: a versatile switch for oncogenesis," *Blood*, vol. 104, no. 4, pp. 919–922, 2004.

Hindawi Publishing Corporation
BioMed Research International
Volume 2013, Article ID 270898, 7 pages
http://dx.doi.org/10.1155/2013/270898

Research Article

Bovine Papillomavirus in Brazil: Detection of Coinfection of Unusual Types by a PCR-RFLP Method

R. F. Carvalho,[1] S. T. Sakata,[1,2] D. N. S. Giovanni,[1] E. Mori,[2] P. E. Brandão,[2] L. J. Richtzenhain,[2] C. R. Pozzi,[3] J. R. P. Arcaro,[3] M. S. Miranda,[3] J. Mazzuchelli-de-Souza,[1,4] T. C. Melo,[1,5] G. Comenale,[1] S. L. M. R. Assaf,[1] W. Beçak,[1,6] and R. C. Stocco[1,4]

[1] *Laboratório de Genética, Instituto Butantan, Secretária de Estado da Saúde, Avenida Vital Brasil 1500, Butantan, 05503-900 São Paulo, SP, Brazil*
[2] *Laboratório de Biologia Molecular Aplicada e Sorologia, Departamento de Medicina Veterinária Preventiva e Saúde Animal, Faculdade de Medicina Veterinária, e Zootecnia da Universidade de São Paulo, Avenida Prof. Dr. Orlando Marques de Paiva, 87 Cidade Universitária, Butantan, 05508-270 São Paulo, SP, Brazil*
[3] *Centro de Pesquisa em Pecuária do Leite, Instituto de Zootecnia, Agencia Paulista de Tecnologia dos Agronegócios, CAPTA Bovinos Leiteiros, Rodovia Luiz de Queiroz km 129, 13460-000 Nova Odessa, SP, Brazil*
[4] *Programa de Pós-Graduação Interunidades em Biotecnologia, Instituto de Ciências Biomédicas, Edifício ICB-III, Universidade de São Paulo, Avenida Prof. Lineu Prestes, 2415 Cidade Universitária, Butantan, 05508-900 São Paulo, SP, Brazil*
[5] *Programa de Pós-Graduação em Biologia Estrutural e Funcional, Universidade Federal de São Paulo, Rua Botucatu, 740 Vila Clementino, 04023-900 São Paulo, SP, Brazil*
[6] *Departamento de Biologia, Universidade Federal da Integração Latino-Americana (UNILA), Avenida Tancredo Neves 6731, Bloco 4, 85867-970 Foz do Iguaçú, PR, Brazil*

Correspondence should be addressed to R. F. Carvalho; rodsfc@uol.com.br

Received 26 March 2013; Accepted 16 May 2013

Academic Editor: Lubna Nasir

Bovine papillomavirus (BPV) is recognized as a causal agent of benign and malignant tumors in cattle. Thirteen types of BPV are currently characterized and classified into three distinct genera, associated with different pathological outcomes. The described BPV types as well as other putative ones have been demonstrated by molecular biology methods, mainly by the employment of degenerated PCR primers. Specifically, divergences in the nucleotide sequence of the L1 gene are useful for the identification and classification of new papillomavirus types. On the present work, a method based on the PCR-RFLP technique and DNA sequencing was evaluated as a screening tool, allowing for the detection of two relatively rare types of BPV in lesions samples from a six-year-old Holstein dairy cow, chronically affected with cutaneous papillomatosis. These findings point to the dissemination of BPVs with unclear pathogenic potential, since two relatively rare, new described BPV types, which were first characterized in Japan, were also detected in Brazil.

1. Introduction

The Bovine papillomavirus (BPV) is recognized as the causal agent of benign and malignant tumors in cattle, such as cutaneous papillomas, benign fibroplasias, urinary bladder, and esophagus cancer, causing significant economic losses. This oncogenic virus has a double-stranded circular DNA genome of approximately eight kilobases [1].

Currently, the *Papillomaviridae* family is divided into 16 genera according to their genomic organization [2, 3]. The papillomavirus (PV) genome codified functional, early (E) proteins and structural, late (L) proteins, expressed at different stages of the viral cycle. The L1 is the most conserved gene within a PV genome and has therefore been used for the identification of new PVs: one PV isolate is recognized as a new type if the complete genome has been cloned and the

DNA sequence of L1 differs by more than 10% from the closest known PV type. Differences between 2% and 10% define a subtype and less than 2%, a variant [3]. Thirteen types of BPVs are currently well characterized and classified into three distinct genera—Delta, Epsilon, and Xi—each one associated with epithelia lesions of specific histological nature [4].

The BPVs-1 and -2 are classified as *Delta papillomaviruses* [5]. Characteristically, these types induce the appearance of fibropapillomas, associated with the recruitment of the subepithelial fibroblasts [6]. As far as concerned, both types are also unique in their ability to infect different host species, not only bovines, causing the equine sarcoid [7]. Lately, the genome of a new Delta-BPV type (BPV-13) was fully sequenced [8].

A larger number of BPV types (-3, -4, -6, -9, -10, -11 and -12) belong to the *Xipapillomavirus* genus. These viruses are considered exclusively epitheliotropic, inducing the formation of "true papillomas," without the involvement of fibroblasts [9–11]. On the other hand, the BPVs-5 and -8 have the potential to induce both fibropapillomas and true papillomas in the course of their infectious cycle, being classified into a third genus, *Epsilonpapillomavirus* [12, 13]. The BPV-7 represents an exception and is classified separately (unsigned genus). This virus was first isolated from a cutaneous papilloma lesion and also from healthy teat skin samples [14].

The thirteen described BPV types as well as other putative ones have been demonstrated by molecular biology methods, since papillomaviruses are not prone to be replicated or recovered in cell cultures [15–19]. According to the guidelines outlined by the Papil omavirus Nomenclature Committee (14th International Papillomavirus Conference, Quebec City, QC, Canada), it has been specified that the amplified sequences isolated from novel papillomaviruses isolates could indicate only putative new PV types—instead of PV types—since the PCR amplicons represent only part of the L1 gene [15].

The use of PCR assays with degenerated primers, followed by sequencing has allowed the identification of several PV types in human and other animal hosts [15, 20]. The PCR primer FAP set was designed from two relatively conserved regions found in the L1 gene and has been shown to amplify PVs DNA from both papillomas and healthy tissue of many animal species, including BPVs in bovines [15, 16, 20].

Brazil has a cattle herd of approximately 210 million, being a major exporter of meat, milk and leather. BPVs have been previously detected in Brazil [21], but the extent of the impact of BPVs associated diseases, both in dairy and cattle herds, needs further studies. Available reports in different regions of the country indicate a significant diversity of viral types among the Brazilian herd, implying an evident disease burden [18, 22–25]. Thus, the improvement of knowledge concerning the diagnosis and related clinical aspects of different BPV types among the Brazilian herd should be considered in the development of new sanitary measures, aiming to the prevention of BPV infection and its consequences.

Unfortunately, BPV epidemiological surveys are still limited by the availability of high-throughput diagnostic techniques that could discriminate different BPV sequences at the same time in co infected samples [16, 26]. In this context, the present work represents an effort to identify BPV types employing an alternative screening method based on the PCR-RFLP technique and correlating the histological data of the analyzed lesions with the diagnosed viral type.

2. Material and Methods

In silico generation of RFLPs: the L1 FAP segment digestion profiles of the BPVs-1 to -13 could be generated with NEB cutter 2.0 [27] from all L1 complete nucleotide sequences available in Genbank (http://www.ncbi.nlm.nih.gov/genbank/). The restriction enzymes sites were chosen both by its presence (or absence) as well as the generated digestion fragments sizes, in order to differentiate those thirteen different BPV types. *Histopathological analysis*: wart biopsies were obtained from the trunk of a six-year-old Holstein dairy cow chronically affected with cutaneous papillomatosis. Samples from three different lesions were submitted to macroscopic, histological (hematoxylin and Eosin staining) and molecular analyses. *DNA extraction and PCR*: DNA was extracted from warts for viral typing (Illustra tissue and cells genomic Prep Mini Spin GE Healthcare) and an approximately 470, base-pairs L1 gene segment was amplified using the following primer sequences: forward: FAP59 (5′-TAA CWG TIG GIC AYC CWT ATT-3′) reverse: FAP64 (5′-CCWATATCWVHCATITCICCATC-3′). The PCR, were performed with slight modifications of a previously described protocol [16]. In detail the amplification reactions were performed in a Corbett CG1-96 thermocycler (Corbett Life Science, Sydney, Australia), with GoTaq Master Mix (Promega, Madison, USA), under the following conditions: 5 min at 95°C, followed by 35 cycles of 1 min and 30s at 95°C, 2 min at 52°C and 1 min and 30s at 72°C and a final extension step of 5 min at 72°C. *Restriction analysis*: an aliquot of PCR fragments were submitted to digestion reactions for RFLP analysis with four different restriction enzymes (*Dde*I, *Hinf* I, *Hind*III, *MsL*I), following manufacturer's instructions (New England Biolabs, Ipswich, USA). Cloned BPV-1 and BPV-2 genomes as well as a known typed clinical sample (Mg-19, BPV-2 typed) were used as positive controls. PCR-RFLP products were analyzed in 2.0% agarose gel electrophoresis stained with ethidium bromide (0.5 μg/mL) in TAE buffer and visualized under UV light. *Sequencing*: An aliquot of all generated PCR fragments were purified with extraction columns (Illustra GFX PCR DNA and Gel Band Purification Kit GE Healthcare). DNA concentration and purity were determined in a spectrophotometer (Eppendorf BioPhotometer, Hamburg, Germany) and submitted to sequencing reactions: three independent sequencing reactions were done for each PCR fragment in an ABI377 PRISM Genetic Analyzer (Life Applied Biosystems, USA). The quality of DNA sequences was checked and overlapping fragments were assembled using the BioEdit package 7.0.9.0 [28]. Assembled sequences with high quality were aligned using ClustalW 1.83 [29] with default gap penalties. Homology analyses were performed with the NCBI database and BLAST [30]. BioEdit software was used to identify the equivalent amino acid sequences. The sequence alignments were performed using

Table 1: L1 FAP segment digestion profiles of the BPVs-1 to -13 for *Dde* I, *Hinf* I, *MsL* I and *Hind*III.

	L1 FAP Fragment	*Dde*I	*Hinf*I	*MsL*I	*Hind*III
BPV-1	475 bp	264 159 52	329 146	301 174	475
BPV-2	475 bp	316 159	329 146	475	475
BPV-3	473 bp	319 154	473	373 87 13	473
BPV-4	469 bp	324 145	469	469	230 182 87
BPV-5	469 bp	469	254 145 70	469	469
BPV-6	472 bp	321 151	384 88	373 99	472
BPV-7	484 bp	403 81	271 119 94	484	484
BPV-8	469 bp	469	317 152	469	322 147
BPV-9	469 bp	316 153	344 125	469	469
BPV-10	472 bp	319 90 63	381 91	373 99	472
BPV-11	475 bp	420 55	407 68	370 105	475
BPV-12	469 bp	351 118	317 152	469	469
BPV-13	475 bp	316 109 50	329 146	475	475

Reference Sequences:
BPV-1_NC_001522.1, BPV-1_X02346.1, BPV-2_M20219.1, BPV-2_X01768.1, BPV-3_AF486184.1, BPV-3_AJ620207.1, BPV-3_NC_004197.1, BPV-4_X05817.1, BPV-5_AF457465.1, BPV-5_NC_004195.1, BPV-6_AJ620208.1, BPV-7_DQ217793.1, BPV-7_NC_007612.1, BPV-8_EB_DQ098917.1, BPV-8_NC_009752.1, BPV-9_AB331650.1, BPV-10_AB331651.1, BPV-11_AB543507, BPV-12_JF834523, BPV-13_JQ798171.

the MEGA 5.0 software [31], using full alignment and 2000 total replications on the bootstrap, in order to ensure a higher level of confidence to our analysis [32]. *Phylogenetic Analysis*: phylogenetic relationship comparing nucleotide sequences was performed with MEGA. Neighbor-joining trees were drawn using TreeView version 1.6.6 [33]. Nucleotide and amino acid sequences from other BPV types and of a HPV-16 were retrieved from the GenBank (http://www.ncbi.nlm.nih.gov/) for comparison with the obtained sequences here.

Ethics Statement. The protocols used in this study were approved by the Ethical Committee for Animal Experimentation of the Instituto de Zootecnia (Protocol no. 109, on July 06th, 2009) assigned by the President of this Committee. All efforts were made to minimize animal suffering.

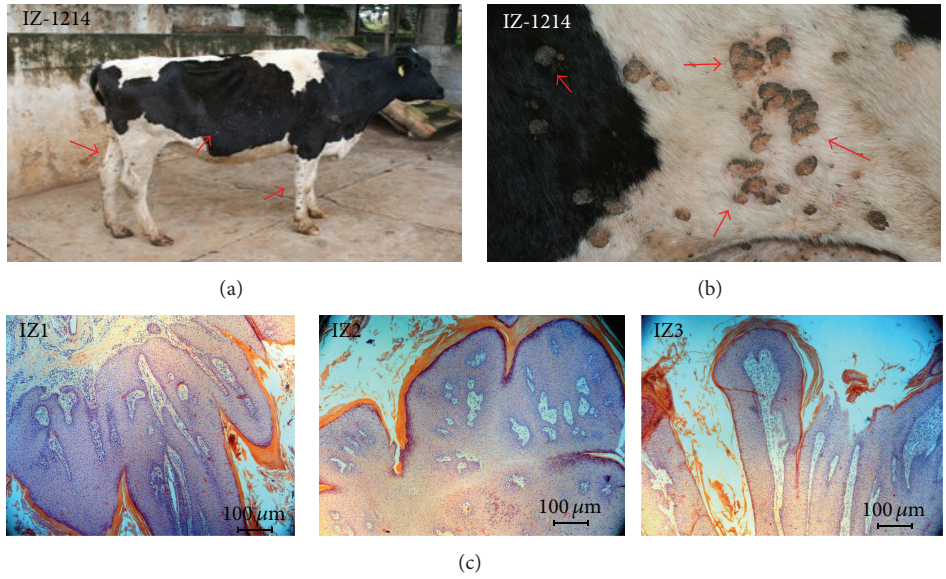

Figure 1: (a) Analyzed animal IZ-1214 with disseminated cutaneous papillomatosis. (b) Gross aspect of the papilloma lesions with a cauliflower-like appearance. (c) Histological preparation (hematoxylin and eosin staining, or HE) of the collected lesions (IZ1, IZ2, and IZ3) indicating characteristic hyperkeratosis, acanthosis, and papillomatosis with dermis proliferation in HE preparation (100x).

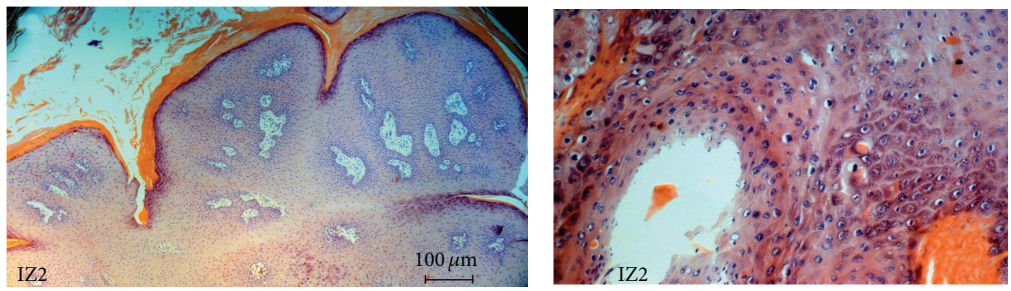

Figure 2: (a) Histopathology of a wart biopsy: detailed aspect of the IZ2 lesion exhibiting characteristic hyperkeratosis, acanthosis and dermal proliferation, indicated by arrows (100x). (b) Presence of koilocytosis.

3. Results

In silico analyses of the restrictionsites in FAP L1 fragments of 20 deposited BPVs sequences (from BPV-1 to BPV-13) revealed no intratype variation associated with the relative cut positions for the four enzymes employed (Table 1). Macroscopic and histological evaluations identified the collected lesions as cutaneous fibrous papillomas (Figures 1 and 2). From all the three lesions studied, two- (IZ1 and IZ3) RFLP profiling suggests the presence of BPV-11. On the other hand, IZ2 sample gene rated a profile which could not match with any of the thirteen characterized viral types (Figure 3, Table 1). In accordance with these results, DNA sequencing and BLAST analysis of IZ2 indicated a rare putative type (BAPV-3), originally described in Japan [16]. Furthermore, the DNA sequencing of other two samples confirms them as the recently described BPV-11 [10]. These sequences were deposited in GenBank (access numbers: HQ435675 and HQ612180). The phylogenetic reconstruction using this partial genomic sequence allowed its comparison with other sequences of *Papillomaviridae* family members (Figure 4).

4. Discussion

Originally, the recently characterized BPV-11 was described with the employment of a *Xipapillomavirus* consensus primer [10]. Here, the same type using the FAP generic primer could be detected, indicating this set as an effective alternative for the identification of BPVs. Other than that, we described the simultaneous presence of two BPV types in three different wart samples, obtained from a chronically affected animal with disseminated papillomatosis.

The typed BPV-11 and BAPV-3 samples have a fibrous aspect, with a similar fibropapilloma histology that is not commonly associated with the exclusive infection of the keratinocytes, commonly attributed to the Xi BPVs. In a previous report [10], Hatama and others discussed the "uncertain nature of BPV-11 tumorigenicity" since BPV-11 was first diagnosed in a fibropapilloma lesion in which the BPV-1 was

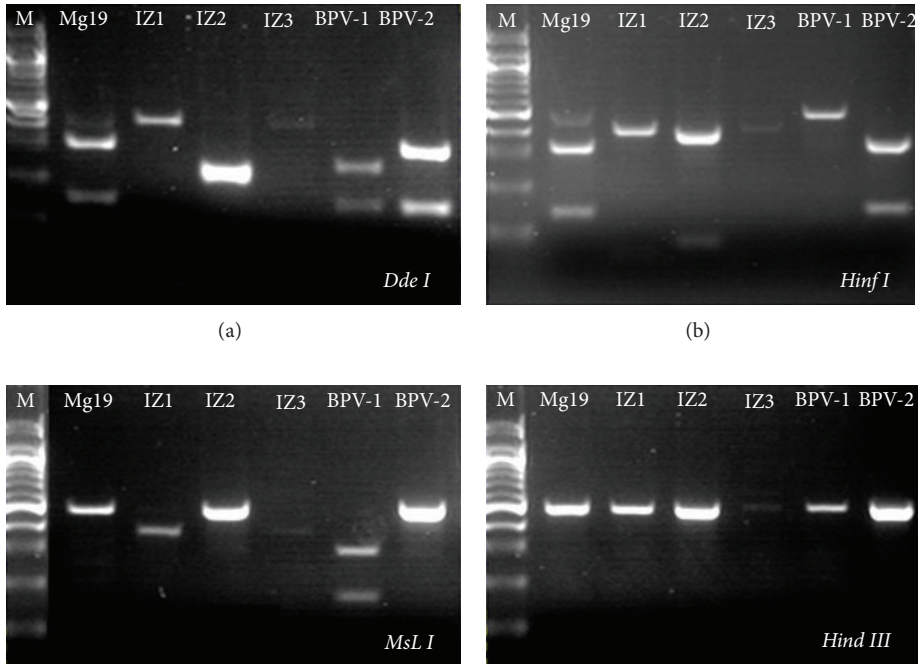

Figure 3: RFLP performed for restriction enzymes *Dde*I, *Hinf* I, *MsL*I, and *Hind*III. As BPV-1 and BPV-2 are the commonly associated with fibropapillomas, their L1 FAP amplicons were generated and digested as positive controls. IZ1, IZ2, IZ3 amplicons are from three different lesions of the same animal (IZ-1214). Mg-19 sample is from another bovine, clinically affected with cutaneous papillomatosis. Molecular marker: 100 bp ladder (New England Biolabs, Ipswich, UK).

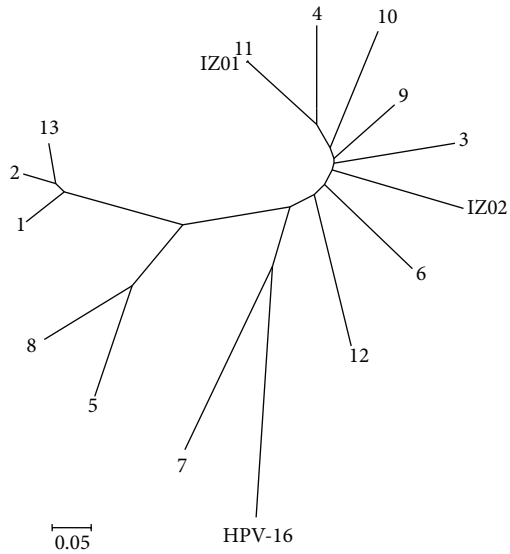

Figure 4: Neighbor-joining phylogenic tree constructed with 2000 bootstrap replications, using partial L1 nucleotide sequences, indicating the putative type BAPV-3 in IZ2 sample, originally described in Japan (accession: AY300819). The analysis of the other two samples, IZ1 and IZ3, demonstrated the presence of an identical sequence in both lesions, sharing 99% percent of similarity with the recently described BPV-11 type (accession: AB543507.1). As IZ3 sequence is identical to IZ1, it will not be shown here.

also detected. Despite the eventual limitations of the diagnostic methods employed, we could detect the same viral type in at least two different cauliflower-like lesions, with a suggestive fibrous core. In addition to Hatama's report, our data also link the BPV-11 with cutaneous papillomas, indicating it as a pathogenic type. Furthermore, the putative type BAPV-3, described by Ogawa and others [16], was detected just once from a skin papilloma sample, without histological description, being genetically associated with the BPV-3, -4, and -6, or Xi BPVs.

The L1 gene has taxonomical relevance due to its high degree of conservation, which can be accessed with the use of generic primer sets. In accordance with this, the restriction sites located in FAP fragments appears to be maintained, without intratype variations for the restriction enzymes employed, indicating that phylogenetic studies comparing BPVs and other members of the *Papillomaviridae* family are possible using a relatively short DNA sequence.

Since the early nineties, methods based on PCR-RFLP analysis within the L1 gene of the human papillomavirus (HPV) have been used for viral typing and infection diagnosis from a variety of sources, including cervical samples, fresh and paraffin-embedded tissues [34, 35]. Particularly, the PCR-RFLP method is useful to identify coinfections due to its sensitivity and specificity [36].

5. Conclusion

As an easy, rapid, and cost-effective assay, the PCR-RFLP represents a less-laborious approach than DNA cloning and sequencing, being an alternative as a first-line screening test, both for the diagnosis of an already classified virus type as to indicating the needing of DNA sequencing due to mixed and/or unknown digestion profiles. In a previous survey in Paraná State, Brazil, Claus and others [26] suggest that the occurrence of multiple or mixed BPVs infection may be widespread throughout Brazilian cattle herds and may occur in other Brazilian geographical regions. In agreement, our findings support these results and reinforce the notion that multiple papillomaviruses infections, with a significant pathogenic potential, can be as frequent in cattle as in human hosts [26].

To the best of our knowledge, the restriction map employed here is the first to be produced specifically for the screening and typing of BPVs. Our findings also point to the ubiquity of BPVs dissemination since two relatively rare, new described BPV types, which were first characterized in Japan, were also detected in Brazil.

Acknowledgments

The authors thank the *Ministério de Ciência, Tecnologia e Inovação/Conselho Nacional de Desenvolvimento Científico e Tecnológico* (CNPq Proc. 402539/2011-7), Coordenação de Aperfeiçoamento Pessoal de Nível Superior (CAPES), and Fundação do Desenvolvimento Administrativo (PAP-FUNDAP) for the financial support and Nadia Jorge Berriel, Carolina da Paz Sabino, and Jim Hesson (http://www.AcademicEnglishSolutions.com/) for the editorial support.

References

[1] M. S. Campo, "Papillomavirus and disease in humans and animals," *Veterinary and Comparative Oncology*, vol. 1, pp. 3–14, 2003.

[2] S.-Y. Chan, H. Delius, A. L. Halpern, and H.-U. Bernard, "Analysis of genomic sequences of 95 papillomavirus types: uniting typing, phylogeny, and taxonomy," *Journal of Virology*, vol. 69, no. 5, pp. 3074–3083, 1995.

[3] E.-M. de Villiers, C. Fauquet, T. R. Broker, H.-U. Bernard, and H. Zur Hausen, "Classification of papillomaviruses," *Virology*, vol. 324, no. 1, pp. 17–27, 2004.

[4] G. Borzacchiello and F. Roperto, "Bovine papillomaviruses, papillomas and cancer in cattle," *Veterinary Research*, vol. 39, no. 5, article 45, 2008.

[5] M. S. Campo, W. F. H. Jarrett, R. Barron, B. W. O'Neil, and K. T. Smith, "Association of bovine papillomavirus type 2 and bracken fern with bladder cancer in cattle," *Cancer Research*, vol. 52, no. 24, pp. 6898–6904, 1992.

[6] F. Jelínek and R. Tachezy, "Cutaneous papillomatosis in cattle," *Journal of Comparative Pathology*, vol. 132, no. 1, pp. 70–81, 2005.

[7] L. Nasir and M. S. Campo, "Bovine papillomaviruses: their role in the aetiology of cutaneous tumours of bovids and equids," *Veterinary Dermatology*, vol. 19, no. 5, pp. 243–254, 2008.

[8] M. Lunardi, A. A. Alfieri, R. A. Otonel et al., "Genetic characterization of a novel bovine papillomavirus member of the *Deltapapillomavirus genus*," *Veterinary Microbiology*, vol. 162, no. 1, pp. 207–213, 2012.

[9] W. F. H. Jarrett, M. S. Campo, B. W. O'Neil, H. M. Laird, and L. W. Coggins, "A novel bovine papillomavirus (BPV-6) causing true epithelial papillomas of the mammary gland skin: a member of a proposed new BPV subgroup," *Virology*, vol. 136, no. 2, pp. 255–264, 1984.

[10] S. Hatama, R. Ishihara, Y. Ueda, T. Kanno, and I. Uchida, "Detection of a novel bovine papillomavirus type 11 (BPV-11) using *Xipapillomavirus* consensus polymerase chain reaction primers," *Archives of Virology*, vol. 156, no. 7, pp. 1281–1285, 2011.

[11] W. Zhu, J. Dong, E. Shimizu et al., "Characterization of novel bovine papillomavirus type 12 (BPV-12) causing epithelial papilloma," *Archives of Virology*, vol. 157, no. 1, pp. 85–91, 2012.

[12] N. Bloch, R. H. Sutton, and P. B. Spradbrow, "Bovine cutaneous papillomas associated with bovine papillomavirus type 5," *Archives of Virology*, vol. 138, no. 3-4, pp. 373–377, 1994.

[13] Y. Tomita, I. Literak, T. Ogawa, Z. Jin, and H. Shirasawa, "Complete genomes and phylogenetic positions of bovine papillomavirus type 8 and a variant type from a European bison," *Virus Genes*, vol. 35, no. 2, pp. 243–249, 2007.

[14] T. Ogawa, Y. Tomita, M. Okada, and H. Shirasawa, "Complete genome and phylogenetic position of bovine papillomavirus type 7," *Journal of General Virology*, vol. 88, no. 7, pp. 1934–1938, 2007.

[15] A. Antonsson and B. G. Hansson, "Healthy skin of many animal species harbors papillomaviruses which are closely related to their human counterparts," *Journal of Virology*, vol. 76, no. 24, pp. 12537–12542, 2002.

[16] T. Ogawa, Y. Tomita, M. Okada et al., "Broad-spectrum detection of papillomaviruses in bovine teat papillomas and healthy teat skin," *Journal of General Virology*, vol. 85, no. 8, pp. 2191–2197, 2004.

[17] Y. Maeda, T. Shibahara, Y. Wada et al., "An outbreak of teat papillomatosis in cattle caused by bovine papilloma virus (BPV) type 6 and unclassified BPVs," *Veterinary Microbiology*, vol. 121, no. 3-4, pp. 242–248, 2007.

[18] M. P. Claus, M. Lunardi, A. F. Alfieri, L. M. Ferracin, M. H. P. Fungaro, and A. A. Alfieri, "Identification of unreported putative new bovine papillomavirus types in Brazilian cattle herds," *Veterinary Microbiology*, vol. 132, no. 3-4, pp. 396–401, 2008.

[19] S. Hatama, K. Nobumoto, and T. Kanno, "Genomic and phylogenetic analysis of two novel bovine papillomaviruses, BPV-9 and BPV-10," *Journal of General Virology*, vol. 89, no. 1, pp. 158–163, 2008.

[20] O. Forslund, A. Antonsson, P. Nordin, B. Stenquist, and B. G. Hansson, "A broad range of human papillomavirus types detected with a general PCR method suitable for analysis of cutaneous tumours and normal skin," *Journal of General Virology*, vol. 80, no. 9, pp. 2437–2443, 1999.

[21] R. C. Stocco Dos Santos, C. J. Lindsey, O. P. Ferraz et al., "Bovine papillomavirus transmission and chromosomal aberrations: an experimental model," *Journal of General Virology*, vol. 79, no. 9, pp. 2127–2135, 1998.

[22] S. R. Wosiacki, M. P. Claus, A. F. Alfieri, and A. A. Alfieri, "Bovine papillomavirus type 2 detection in the urinary bladder of cattle with chronic enzootic haematuria," *Memorias do Instituto Oswaldo Cruz*, vol. 101, no. 6, pp. 635–638, 2006.

[23] A. Yaguiu, C. Carvalho, A. C. Freitas et al., "Papillomatosis in cattle: in situ detection of Bovine Papillomavirus DNA sequences in reproductive tissues," *Brazilian Journal of Morphological Sciences*, vol. 23, no. 3, pp. 129–136, 2006.

[24] N. Diniz, T. C. Melo, J. F. Santos et al., "Simultaneous presence of bovine papillomavirus in blood and in short-term lymphocyte cultures from dairy cattle in Pernambuco, Brazil," *Genetics and Molecular Research*, vol. 8, no. 4, pp. 1474–1480, 2009.

[25] M. Lunardi, M. P. Claus, A. A. Alfieri, and M. H. P. Fungaro, "Phylogenetic position of an uncharacterized Brazilian strain of bovine papillomavirus in the genus *Xipapillomavirus* based on sequencing of the L1 open reading frame," *Genetics and Molecular Biology*, vol. 33, no. 4, pp. 745–749, 2010.

[26] M. P. Claus, M. Lunardi, A. A. Alfieri et al., "Multiple bovine papillomavirus infections associated with cutaneous papillomatosis in Brazilian cattle herds," *Brazilian Archives of Biology and Technology*, vol. 52, pp. 93–98, 2009.

[27] T. Vincze, J. Posfai, and R. J. Roberts, "NEBcutter: a program to cleave DNA with restriction enzymes," *Nucleic Acids Research*, vol. 31, no. 13, pp. 3688–3691, 2003.

[28] T. A. Hall, "BioEdit: a user-friendly biological sequence alignment editor and analysis program for Windows 95/98/NT," *Nucleic Acid Symposium Series*, vol. 41, pp. 95–98, 1999.

[29] J. D. Thompson, D. G. Higgins, and T. J. Gibson, "CLUSTAL W: improving the sensitivity of progressive multiple sequence alignment through sequence weighting, position-specific gap penalties and weight matrix choice," *Nucleic Acids Research*, vol. 22, no. 22, pp. 4673–4680, 1994.

[30] S. F. Altschul, T. L. Madden, A. A. Schäffer et al., "Gapped BLAST and PSI-BLAST: a new generation of protein database search programs," *Nucleic Acids Research*, vol. 25, no. 17, pp. 3389–3402, 1997.

[31] K. Tamura, D. Peterson, N. Peterson, G. Stecher, M. Nei, and S. Kumar, "MEGA5: molecular evolutionary genetics analysis using maximum likelihood, evolutionary distance, and maximum parsimony methods," *Molecular Biology and Evolution*, vol. 28, no. 10, pp. 2731–2739, 2011.

[32] B. Efron, E. Halloran, and S. Holmes, "Bootstrap confidence levels for phylogenetic trees," *Proceedings of the National Academy of Sciences of the United States of America*, vol. 93, no. 23, pp. 13429–13434, 1996.

[33] R. D.m.page, "TreeView: an application to display phylogenetic trees on personal computers," *Computer Applications in the Biosciences*, vol. 12, no. 4, pp. 357–358, 1996.

[34] O. Lungu, T. C. Wright Jr., and S. Silverstein, "Typing of human papillomaviruses by polymerase chain reaction amplification with L1 consensus primers and RFLP analysis," *Molecular and Cellular Probes*, vol. 6, no. 2, pp. 145–152, 1992.

[35] G. Astori, A. Arzese, C. Pipan, E.-M. De Villiers, and G. A. Botta, "Characterization of a putative new HPV genomic sequence from a cervical lesion using L1 consensus primers and restriction fragment length polymorphism," *Virus Research*, vol. 50, no. 1, pp. 57–63, 1997.

[36] R. J. Nobre, L. P. de Almeida, and T. C. Martins, "Complete genotyping of mucosal human papillomavirus using a restriction fragment length polymorphism analysis and an original typing algorithm," *Journal of Clinical Virology*, vol. 42, no. 1, pp. 13–21, 2008.

Hindawi Publishing Corporation
BioMed Research International
Volume 2013, Article ID 546354, 7 pages
http://dx.doi.org/10.1155/2013/546354

Research Article

Prevalence and Genetic Variability in Capsid L1 Gene of Rare Human Papillomaviruses (HPV) Found in Cervical Lesions of Women from North-East Brazil

Ana Pavla Almeida Diniz Gurgel,[1] Bárbara Simas Chagas,[1] Carolina Maria Medeiros do Amaral,[1] Eugênia Maria Bezerra Albuquerque,[2] Ivi Gonçalves Soares Santos Serra,[3] Jacinto da Costa Silva Neto,[4] Maria Tereza Cartaxo Muniz,[5] and Antonio Carlos de Freitas[1,6]

[1] *Department of Genetics, Federal University of Pernambuco, Brazil*
[2] *Gynaecological Unit, University Hospital Oswaldo Cruz, Brazil*
[3] *Gynaecological Unit, Integrated Medicine Center, Brazil*
[4] *Department of Histology and Embryology, Federal University of Pernambuco, Brazil*
[5] *Molecular Biology Laboratory, Pediatric Oncohematology Center, University of Pernambuco, Brazil*
[6] *Cidade Universitária, 50670-901, Recife, PE, Brazil*

Correspondence should be addressed to Antonio Carlos de Freitas; acf_ufpe@yahoo.com.br

Received 20 February 2013; Revised 30 April 2013; Accepted 9 May 2013

Academic Editor: Franco Roperto

The aim of this study was to examine the prevalence and genetic variability of the capsid L1 gene of rare HPV genotypes that were found in the cervical lesions of women from North-East Brazil. A total number of 263 patients were included in this study. HPV detection was performed using PCR followed by direct sequencing of MY09/11, as well as type-specific PCR to detect the Alpha-9 species. Epitope prediction was performed to determine whether or not the genetic variants are inserted in B-cell and T-cell epitopes. The prevalence of rare HPV types in cervical lesions was found to be 9.47%. The rare HPV genotypes that were detected were HPV-53, 54, 56, 61, 62, 66, 70, and 81. The genetic variability in the L1 gene of rare HPV types involved thirty nucleotide changes, eight of which were detected for the first time in this study. Moreover, some of these variants are embedded in B-cell or T-cell epitope regions. The results of this research suggest that rare HPV types might be involved in cervical lesions and some of these variants can be found in B-cell and T-cell epitopes. Data on the prevalence and variability of rare HPV types will assist in clarifying the role of these viruses in carcinogenesis.

1. Introduction

Cervical cancer is ranked as the third major cause of female cancer worldwide, with an estimate of more than 529,000 new cases diagnosed and 275,000 deaths in 2008 [1]. In developing countries, cervical cancer comprises 85% of the total number of cases [1] and in Brazil, cervical cancer is the third most common cancer among women [2].

Persistent infections caused by Human Papillomavirus (HPV) can result in cervical lesions and cervical cancer [3]. HPV is a nonenveloped virus with a circular double-stranded DNA [4]. This virus group belongs to the Papillomaviridae family, which comprises 29 genera and 189 Papillomaviruses (PV) [5]. To date, more than 120 HPV types have been identified and these can be divided into five genera: *Alphapapillomavirus* (Alpha), *Betapapillomavirus* (Beta), *Gammapapillomavirus* (Gamma), *Mupapillomavirus* (Mu), and *Nupapillomavirus* (Nu) [5, 6]. Among these, 40 HPV types infect the genital tract, 15 of which are considered to be High-Risk (HR) HPV (16, 18, 31, 33, 35, 39, 45, 51, 52, 56, 58, 59, 68, 73, and 82); six species are considered Low-Risk (LR) HPV (6, 11, 42, 44, 51, 81, and 83) and three species are considered Intermediate Risk (IR) HPV (26, 53, 66) [7]. The International

Table 1: Primer sequence used to detect HPV-16, 31, 33, and 58 genotypes.

HPV genotype (LCR)	Sequence primer	Amplicon size (base pairs)
HPV-16	F: 5′-TTCTGCAGACCTAGATCAGTTTC-3′ F: 5′-GTGCATAACTGTGGTAACTTTCTGG-3′	1057 bp
HPV-31	F: 5′-TTAGATCAGTTTCCACTGGGTCG-3′ F: 5′-TTAGTTCATGCAATTTCCGAGGTC-3′	1152 bp
HPV-33	F: 5′-TACCTCCAAAGGAAAAGGAAGACCC-3′ F: 5′-TTGGCACAAATCATGCAATGTTCG-3′	1184 bp
HPV-58	5′ CATGTTCTATGTCCTTGTCAG 3′ 5′ TGA CCC AAA ACG GTT AGT CC 3′	1000 bp

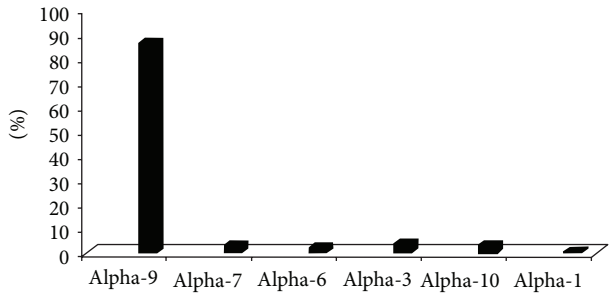

Figure 1: Percentage of *Alphapapillomavirus* species in cervical lesions of women from Pernambuco and Sergipe States, Northeast Brazil. The figure shows the high frequency of A9 species (86.46%), followed by A3 (4.2%), A10 (3.4%), A7 (3.4%), A6 (2.5%), and Alpha-1 (0.8%) HPV genotypes.

Agency for Research on Cancer (IARC) recognizes the HPV-16, 18, 31, 33, 35, 39, 45, 51, 56, 58, 59, and 68 as carcinogenic or probably carcinogenic groups [8]. Moreover, HPV that have a phylogenetic relationship with other carcinogenic HPV are regarded as possibly carcinogenic groups, called Alpha-5, Alpha-6, Alpha-7, Alpha-9, and Alpha-11 species [7].

Recently, epidemiological data on the worldwide incidence of HPV have shown that Alpha-9 and Alpha-7 species cause 91% of invasive cervical cancer [9]. HPV-16, 18, and 45 are responsible for 75% of squamous cell carcinoma and 74% of the adenocarcinoma cases [9]. Despite the high prevalence of Alpha-9 and Alpha-7 species, other Alpha species are involved in cervical cancer, though only to a very limited degree. For instance, in 2010 it was reported that 2.25% of total invasive cervical cancer were caused by rare HPV types [9].

There have been several studies that describe the prevalence and genetic variability of the HPV-16, HPV-18, HPV-31, and HPV-58 genotypes [9–21]. However, few studies have shown the extent of the prevalence and variability of rare HPV types in infected women [9, 16, 22, 23]. Rare HPV types might be involved in cervical cancer due to the genetic variability, especially when these changes are found in linear B-cell or T-cell epitopes, which theoretically allow the escape recognition by the innate immune system. Furthermore, it is still unknown what role they play in the single infections or coinfections that result in cervical lesions and cervical cancer.

Thus, the aim of this study was to investigate the prevalence of rare HPV types, as well as the genetic variability of the capsid L1 gene of these viruses, in cervical lesions of women from North-East Brazil.

2. Material and Methods

2.1. Population. Cervical cells were collected from November 2010 to August 2011. The samples were obtained from women during their medical consultations at the Gynaecological Unit of the Integrated Medicine Center, in Sergipe State and the Oswaldo Cruz University Hospital, in Pernambuco State, North-East Brazil. A total number of 263 women agreed to participate in the study and signed the consent form. The study included patients with Cervical intraepithelial Neoplasia (CIN) (Grade - I, II, III) and cervical invasive cancer. All the patients were sexually active and their average age was 38.02 (with ages ranging from 16 to 77). This study was approved by the Ethics Committee of the University of Pernambuco (HUOC/PROCAPE 64/2010) and the Ethics Committee of the Federal University of Sergipe (CEP/CCS/UFPE N° 491/11).

2.2. DNA Extraction and HPV Genotyping. The collected cells were placed in polyethylene tubes containing phosphate-buffered saline and then stored at −20°C until analysis. DNA was extracted by using the DNeasy Blood and Tissue Kit 135 (Qiagen) in accordance with the manufacturer's instructions.

HPV DNA detection was performed by using polymerase chain reaction (PCR) with degenerate primers MY09/11 [24], which amplify fragments containing 450 bp from the L1 gene of a wide spectrum of HPV types. In addition, a possible coinfection caused by HPV-16, 31, 33, and HPV-58 was detected through type-specific PCR using primers that target the long control region (LCR), which only allow amplification of the 1000 bp of LCR of each of the above-mentioned HPV genotypes (the primer sequences are described in Table 1) (Figure 1). The reactions were performed with a final volume of 25 μL containing 100 ng of DNA, 1.5 mM of $MgCl_2$, 50 μM of each dNTP, 20 pmol of each primer, and 1 unit of Taq DNA Polymerase and 1x buffer. The PCR cycling conditions were as follows: initial denaturation at 95°C for 5 minutes, 35 cycles of denaturation at 95°C for 30 seconds, annealing at 55°C for 1 minute, elongation at 72°C for 2 minutes, and a final extension at 72°C for 10 minutes. The PCR products were run on the agarose gel (1%).

The positive samples were purified with the Invisorb Fragment Cleanup (Invitek) kit and sequenced (in duplicate) by using ABI PRISM BigDye Terminator Cycle Sequencing v 3.1 Ready Reaction (Applied Biosystems) to obtain both the forward and reverse sequences.

Table 2: Rare HPV type found in cervical intraepithelial neoplasia grades I, II, III and invasive cervical cancer.

Rare HPV type	Histopathological grade
HPV-53	CIN III
HPV-54	CIN I
HPV-56	CIN I
HPV-61	CIN II
HPV-62	CIN III
HPV-66	CIN I
HPV-70	CIN I/Adenocarcinoma
HPV-81	CIN I

The sequences obtained were assembled into contigs using the Staden package [25]. They were then evaluated to determine the nucleotide divergence relative to the L1 nucleotide sequences of HPV-53 (NC_001593.1), HPV-54 (NC_001676.1), HPV-56 (X74483.1), HPV-61 (U31793.1), HPV-62 (AY395706), HPV-70 (U21941.1), and HPV-81 (AJ620209). Sequence comparisons were performed using the Basic Local Alignment Search Tool (BLAST) and multiple alignments were carried out by CLUSTALW (Mega 5, Beta version) program [26].

New variants were submitted to GeneBank with the following accession numbers: HPV-53-JX912952; HPV-54-JX912948; HPV-56-JX912947; HPV-62-JX912951; HPV-70-JX912950 and HPV-81-JX912949.

2.3. B-Cell and T-Cell Epitope Prediction. The putative impact of variability in L1 gene of rare HPV types was estimated in silico by predicting the B-cell and T-cell epitopes. In this study, it was assumed that changes in amino acid sequences of L1 proteins within B-cell and T-cell epitope regions could affect the binding affinities of the neutralizing antibodies and did not initiate an epitope-specific immune response, respectively. Thus, the B-cell epitope of prototype sequences was predicted by using the BcePred server, which is available from URL: http://www.imtech.res.in/raghava/bcepred/. The prediction was carried out with the aid of physico-chemical parameters, such as hydrophilicity, flexibility/mobility, accessibility, polarity, exposed surface, turns, and antigenic propensity [27].

The T-cell epitope predictions were performed by using ProPred and ProPred I servers. ProPred I server (available from URL: http://www.imtech.res.in/raghava/propred1/) was used to predict MHC Class-I binding regions [28], while the ProPred server (available from URL: http://www.imtech.res.in/raghava/propred/) was used to predict MHC Class-II binding peptide [29].

3. Results

3.1. Characteristics of the Population. A total of 263 cervical smear tests were carried out to detect HPV DNA. Of these, 95 cervical smears were submitted to variability studies because they were positive to HPV and also for histopathological findings (CIN I, II, III and invasive cervical cancer). These samples were genotyped and the results showed the presence of HPV-6, 11, 16, 18, 31, 33, 45, and 58 genotypes. With regard to rare HPV types, the following genotypes were detected: HPV-53, 54, 56, 61, 62, 66, 70, and 81 (Table 2). Among these, 9.47% were infected with rare HPV types, while 7.37% of the samples were infected with rare HPV types but without coinfection with other Alpha-9 species.

Twenty-seven cervical samples were coinfected, out of which eleven were infected with the HPV-16/31 genotype, two infected with HPV-16/18, six samples with HPV-31/58, two samples with HPV-16/33, and the remaining samples infected with the following genotypes: HPV-16/58, HPV-16/6, HPV-16/33, HPV-31/33, HPV-16/54, and HPV-16/58/33.

With regard to the Alpha species, it was found that 86.46% of the positive HPV DNA samples were infected with Alpha-9, followed by Alpha-3 (4.2%), Alpha-7 (3.4%), Alpha-10 (3.4%), Alpha-6 (2.5%), and Alpha-1 (0.8%) species (Figure 1).

3.2. Analysis of Variability. HPV-53 was obtained from patients with HSIL but without coinfection with HPV-16, 18, 31, 33, and 58 types. The analysis of the variability of the L1 gene revealed single nucleotide exchanges in six positions, when compared with the reference sequence. Among these, the mutation point C6942T led to amino acid changes involving P430S in the protein sequence of the L1 (Table 3(a)). Furthermore, the epitope predictions of the HPV-53 L1 protein sequence enabled us to observe that the P430S variation is embedded in the T-cell and B-cell epitope binding regions (Table 3(a)) (Tables 4 and 5).

The patient infected with HPV-54 was coinfected with the HPV-16 type. The L1 genetic variability showed single nucleotide exchanges in five positions when compared with the reference sequence. The A6622T and T6625C mutations have never been described until now. These two mutation points lead to Q313H and S333T amino acid changes in the L1 protein sequence, respectively (Table 3(b)). An analysis of peptide prediction showed that Q313H and T333S variations were found within the T-cell and B-cell epitope binding regions (Table 3(b)) (Tables 4 and 5).

HPV-81 was detected in one sample with CIN I but without coinfection with HPV-16, 18, 31, 33, and 58 genotypes. An analysis of the genetic variability of L1 showed a new synonymous mutation at the A7148G position (Table 6(a)). The sample infected with HPV-56 was observed without coinfection with other Alpha-9 species (Table 6(b)). Two synonymous mutations were observed in HPV-56 A6666G and A6987G. Moreover, HPV-61 and HPV-66 showed no nucleotide sequence divergence in the L1 gene when compared with the reference sequence.

The analysis of the L1 of HPV-70 was detected in two cervical samples with histopathological findings of adenocarcinoma and CIN I, but without coinfection with HPV-16, 18, 31, 33, and 58 genotypes. The sequence variation of these viruses showed five mutation points, one of which was a nonsynonymous variant. A6886G variation leads to a change in the amino acid (T433A). Furthermore, the T433A mutation is embedded in the T-cell and B-cell epitope binding regions (Table 6(c)) (Tables 4 and 5).

Table 3: Nucleotide sequence variation in the L1 gene of HPV-53 and HPV-54. The vertical numbers indicate the position of the nucleotide variations. HG: Histopathological grade. (*) Substitutions not previously reported.

(a)

HPV-53 L1 gene variability	6 6 8 6	6 7 0 6	6 7 4 4	6 9 1 3	6 9 4 7	7 0 0 3	HG
Prototype (NC_001593.1)	C	C	A	G	C	G	
6 SE	T	T	G	A	T	A	CIN III
Protein						P430S	
Hydropathic index						Hydrophobic/ Hydrophilic	
Biological functions altered						MHC Class-I/ B-cell	

(b)

HPV-54 L1 gene variability	6 5 5 2	6 5 7 9	6 6 2 2	6 6 2 4	6 6 2 5	6 9 7 5	HG
Prototype (NC_001676.1)	A	G	A	A	T	C	
233 PE	T	A	T*	T	C*	T	CIN I
Protein	Q313H		**T337S**	**T337S**			
Hydropathic index	Hydrophilic/ Hydrophilic		Hydrophilic	Hydrophilic			
Biological functions altered	MHC Class-I/ MHC Class-II/ B-cell		MHC Class-I/ MHC Class-II/ B-cell	MHC Class-I/ MHC Class-II/ B-cell			

Table 4: Amino acid residue changes mapped into T-cell epitopes. The amino acids in bold and italic are the positions of change in the predicted T-cell epitopes.

L1 epitopes prediction for T-cell epitopes	Amino acid change insered in epitope sequence
QKDQ***P***PPEKQDPL	P430S
YWL***Q***RAQGQNNGI	Q313H
TTRSTNL***T***LCATAST	T337S
NGICWFN***E***LFVTVVDTT	E329D
FTICTASTAAA***E***YKATNFR	A351T, E354D
FDLQFIFQLCKI***Q***LTPEIMAY	Q328R
HYLQSRAI***T***CQKGA	T427A
IACQKDAP***T***PEKKDPY	T433A

Table 5: Amino acid residue changes mapped into B-cell epitopes. The amino acids in bold and italic are the positions of change in the predicted B-cell epitopes.

L1 epitopes prediction for B-cell	Amino acid change insered in epitope sequence
TCQKDQ***P***PPEKQDPLSKYKFWEV	P430S
EYQIFNKPYWL***Q***RAQGQNNGI	Q313H
VDTTRSTNL***T***	T337S
N***E***LFVTVVDTT	E329D
A***E***YKATNFREFLRHTEEFDLQ	E354D
LQFIFQLCKI***Q***LTPE	Q382R
CQKDAP***T***PEKKDPYDDLKF	T433A

The genetic variability in L1 protein of HPV-62 showed nine nucleotide exchanges, five of which are nonsynonymous mutations. Among these, two new mutations were found at 6838C and A6921G, which led to E354D and Q382R changes in amino acid, respectively (Table 7). With regard to the altered biological functions, some of these mutation points are included in the T-cell and B-cell epitope binding regions (Table 7) (Tables 4 and 5).

4. Discussion

This study described the presence of rare HPV genotypes in CIN I, III and invasive cancer in women from North-East Brazil. The results of this study showed thirty nucleotide changes, nine of which were reported for the first time. Moreover, this study showed the predominance of Alpha-9 and a low frequency of Alpha-7 species in cervical lesions. These correspond to epidemiological data from the rest of the world, which have shown that Alpha-9 is the main species

Table 6: Nucleotide sequence variation in the L1 gene of HPV-56, HPV-70, and HPV-81. The vertical numbers indicate the position of the nucleotide variations. HG: Histopathological grade. (*) Substitutions not previously reported. (.) Similar to the prototype sequence.

(a)

HPV-81 L1 gene variability	7 1 4 8	7 2 4 9	HG
Prototype (AJ620209.1)	A	T	CIN I
106 PE	G*	A*	

(b)

HPV-56 L1 gene variability	6 6 6 6	6 9 8 7	HG
Prototype (X74483.1)	A	A	CIN I
35 SE	G	G	

(c)

HPV-70 L1 gene variability	6 6 3 3	6 7 4 1	6 8 0 1	6 8 7 3	6 8 8 6	HG
Prototype (HPU21941)	G	T	A	A	A	
41 PE	A	·	·	·	·	CIN I
42 PE	A	A	C*	G*	G*	Adenocarcinoma
Protein					T433A	
Hydropathic index					Hydrophilic/ Hydrophobic	
Biological functions altered					MHC Class-I B-cell	

Table 7: Nucleotide sequence variation in the L1 gene of HPV-62. The vertical numbers indicate the position of the nucleotide variations. HG: Histopathological grade. (*) Substitutions not previously reported.

HPV-62 L1 gene variability	6 7 6 3	6 8 2 7	6 8 3 8	6 8 4 7	6 9 2 1	6 9 2 5	7 0 5 5	7 1 1 4	7 1 5 9	HG
Prototype (AY395706)	A	G	A	T	A	A	A	A	C	
165 PE	C	A	C*	C	G*	G	G	C	T	CIN III
Protein	E329D	A351T	E354D		Q382R		T427A			
Hydropathic index	Hydrophilic/ Hydrophobic	Hydrophobic/ Hydrophilic	Hydrophobic/ Hydrophobic		Hydrophilic/ Hydrophilic		Hydrophilic/ Hydrophobic			
Biological functions altered	MHC Class-I/ MHC Class-II/ B-cell epitopes	MHC Class-I/ MHC Class-II	MHC Class-II/ B-cell epitopes		MHC Class-I/ MHC Class-II/ B-cell epitopes		MHC Class-I/ MHC Class-II			

involved in cervical cancer [9]. Furthermore, this study found low frequencies of Alpha-6, Alpha-10, Alpha-3, and Alpha-1 species in cervical lesions or cervical cancer.

Recently, epidemiological data on the worldwide incidence of HPV have provided evidence that 2.25% of total invasive cervical cancer was caused by rare HPV types [9, 30]. This study showed that 9.47% of cervical samples were infected with rare HPV types, while 7.37% were infected with rare HPV but without coinfection with other Alpha-9 species. Despite the low frequency of these viruses on an individual basis, when all the prevalence data were collated, it was confirmed that rare HPV types are the second most

common groups of viruses in cervical lesions of women from North-East Brazil. In addition, recent biological studies have reported that all HPV within Alpha-5, 6, 7, 9, and 11 species contain E6 oncoprotein that degrades p53 [31, 32]. This evidence suggests that rare HPV types play a putative role in carcinogenesis.

The use of PCR with MY09/11 degenerate primers followed by direct sequencing allows other Alpha species to be detected, apart from the Alpha-9 virus group. This study reported rare HPV types, including new variants that were occasionally characterized as single infections. Rare HPV types have also been detected as a single infection in invasive cancer in other studies [9].

Some of the rare HPV types found in cervical lesions or cervical cancer in this study are not considered as carcinogenic viruses [8]. Hence, we speculate that the abovementioned genetic variations in rare HPV types might be involved in carcinogenesis due to their higher infection ability. The genetic variations reported in this study could reduce the neutralizing effect of antibodies or make more efficient the interaction between virus and cellular membrane, thus allowing a more effective infection. However, further studies should be performed to demonstrate whether these rare HPV types and their variants can be regarded as carcinogenic.

In conclusion, this study found a predominance of Alpha-9 species in CIN I, III and invasive cancer in infected women from North-East Brazil. Moreover, genetic variability in L1 genes showed several synonymous and nonsynonymous mutations, which can lead to an altered immune response. Further investigation of the prevalence and variability of rare HPV types can clarify the role of this virus in infections and carcinogenesis.

Conflict of Interests

The authors declare that there is no conflict of interests.

Authors' Contribution

Ana Pavla Almeida Diniz Gurgel carried out all the experiments and wrote the paper; Maria Tereza C. Muniz and Jacinto da Costa Silva Neto were responsible for the data collection; Bárbara Simas Chagas, Carolina Maria Medeiros do Amaral and participated in some of the experiments; Eugenia M. B. Albuquerque and Ivi Gonçalves G. S. Serra are Gynecologists and were involved in the collection of the samples; Antonio Carlosde Freitas is the supervisor of this study and reviewed the final draft of this paper.

Acknowledgments

This research was supported by the Coordenação de Aperfeiçoamento de Pessoal de Nível Superior (CAPES), Conselho Nacional de Desenvolvimento Científico e Tecnológico (CNPq), and Fundação de Amparo à Ciência e Tecnologia do Estado de Pernambuco (FACEPE).

References

[1] A. Jemal, F. Bray, M. M. Center, J. Ferlay, E. Ward, and D. Forman, "Global cancer statistics," *CA Cancer Journal for Clinicians*, vol. 61, no. 2, pp. 69–90, 2011.

[2] A. C. De Freitas, "Vaccine strategies against human papillomavirus: a discussion focused on developing countries," *Journal of Clinical & Cellular Immunology*, vol. 1, no. S4, 2012.

[3] H. Zur Hausen, "Papillomavirus infections—a major cause of human cancers," *Biochimica et Biophysica Acta*, vol. 1288, no. 2, pp. F55–F78, 1996.

[4] A. C. De Freitas, A. P. A. D. Gurgel, B. S. Chagas, E. C. Coimbra, and C. M. M. Do Amaral, "Susceptibility to cervical cancer: an overview," *Gynecologic Oncology*, vol. 126, no. 2, pp. 304–311, 2012.

[5] H. U. Bernard, R. D. Burk, Z. Chen, K. van Doorslaer, H. Z. Hausen, and E. M. de Villiers, "Classification of papillomaviruses (PVs) based on 189 PV types and proposal of taxonomic amendments," *Virology*, vol. 401, no. 1, pp. 70–79, 2010.

[6] E. M. De Villiers, C. Fauquet, T. R. Broker, H. U. Bernard, and H. Zur Hausen, "Classification of papillomaviruses," *Virology*, vol. 324, no. 1, pp. 17–27, 2004.

[7] H. Zur Hausen, "Papillomaviruses and cancer: from basic studies to clinical application," *Nature Review Cancer*, vol. 2, no. 5, pp. 342–350, 2002.

[8] M. Schiffman, G. Clifford, and F. M. Buonaguro, "Classification of weakly carcinogenic human papillomavirus types: addressing the limits of epidemiology at the borderline," *Infectious Agents and Cancer*, vol. 4, no. 1, article 8, 2009.

[9] S. de Sanjose, W. G. V. Quint, L. Alemany et al., "Human papillomavirus genotype attribution in invasive cervical cancer: a retrospective cross-sectional worldwide study," *The Lancet Oncology*, vol. 11, no. 11, pp. 1048–1056, 2010.

[10] M. F. P. T. Baldez Da Silva, B. S. Chagas, V. Guimarães et al., "HPV31 and HPV33 incidence in cervical samples from women in Recife, Brazil," *Genetics and Molecular Research*, vol. 8, no. 4, pp. 1437–1443, 2009.

[11] B. S. Chagas, M. V. A. Batista, V. Guimarães, V. Q. Balbino, S. Crovella, and A. C. Freitas, "New variants of E6 and E7 oncogenes of human papillomavirus type 31 identified in Northeastern Brazil," *Gynecologic Oncology*, vol. 123, no. 2, pp. 284–288, 2011.

[12] M. R. Pillai, R. Hariharan, J. M. Babu et al., "Molecular variants of HPV-16 associated with cervical cancer in Indian population," *International Journal of Cancer*, vol. 125, no. 1, pp. 91–103, 2009.

[13] T. R. Alencar, D. M. Cerqueira, M. R. D. Cruz, P. S. Wyant, E. D. Ramalho, and C. R. F. Martins, "New HPV-16 European and non-European variants in Central Brazil," *Virus Genes*, vol. 35, no. 1, pp. 1–4, 2007.

[14] D. M. Cerqueira, T. Raiol, N. M. C. Véras et al., "New variants of human papillomavirus type 18 identified in central Brazil," *Virus Genes*, vol. 37, no. 2, pp. 282–287, 2008.

[15] T. Raiol, P. S. Wyant, R. M. S. De Amorim et al., "Genetic variability and phylogeny of the high-risk HPV-31, -33, -35, -52, and -58 in Central Brazil," *Journal of Medical Virology*, vol. 81, no. 4, pp. 685–692, 2009.

[16] M. M. Castro, I. P. Farias, C. M. Borborema-Santos, G. Correia, and S. Astolfi-Filho, "Prevalence of human papillomavirus (HPV) type 16 variants and rare HPV types in the central Amazon region.," *Genetics and Molecular Research*, vol. 10, no. 1, pp. 186–196, 2011.

[17] S. Pande, N. Jain, B. K. Prusty et al., "Human papillomavirus type 16 variant analysis of E6, E7, and L1 genes and long control region in biopsy samples from cervical cancer patients in North India," *Journal of Clinical Microbiology*, vol. 46, no. 3, pp. 1060–1066, 2008.

[18] I. E. Calleja-Macias, L. L. Villa, J. C. Prado et al., "Worldwide genomic diversity of the high-risk human papillomavirus types 31, 35, 52, and 58, four close relatives of human papillomavirus type 16," *Journal of Virology*, vol. 79, no. 21, pp. 13630–13640, 2005.

[19] I. E. Calleja-Macias, M. Kalantari, J. Huh et al., "Genomic diversity of human papillomavirus-16, 18, 31, and 35 isolates in a Mexican population and relationship to European, African, and Native American variants," *Virology*, vol. 319, no. 2, pp. 315–323, 2004.

[20] G. Cornut, S. Gagnon, C. Hankins et al., "Polymorphism of the capsid L1 gene of human papillomavirus types 31, 33, and 35," *Journal of Medical Virology*, vol. 82, no. 7, pp. 1168–1178, 2010.

[21] H. Arias-Pulido, C. L. Peyton, N. Torrez-Martínez, D. N. Anderson, and C. M. Wheeler, "Human papillomavirus type 18 variant lineages in United States populations characterized by sequence analysis of LCR-E6, E2, and L1regions," *Virology*, vol. 338, no. 1, pp. 22–34, 2005.

[22] J. C. Prado, I. E. Calleja-Macias, H. U. Bernard et al., "Worldwide genomic diversity of the human papillomaviruses-53, 56, and 66, a group of high-risk HPVs unrelated to HPV-16 and HPV-18," *Virology*, vol. 340, no. 1, pp. 95–104, 2005.

[23] V. Cento, N. Rahmatalla, M. Ciccozzi, A. Lo Presti, C. F. Perno, and M. Ciotti, "Human Papillomaviruses 53 and 66: clinical aspects and genetic analysis," *Virus Research*, vol. 163, no. 1, pp. 212–222, 2012.

[24] F. Karlsen, M. Kalantari, A. Jenkins et al., "Use of multiple PCR primer sets for optimal detection of human papillomavirus," *Journal of Clinical Microbiology*, vol. 34, no. 9, pp. 2095–2100, 1996.

[25] R. Staden, "The staden sequence analysis package," *Applied Biochemistry and Biotechnology B*, vol. 5, no. 3, pp. 233–241, 1996.

[26] K. Tamura, D. Peterson, N. Peterson, G. Stecher, M. Nei, and S. Kumar, "MEGA5: molecular evolutionary genetics analysis using maximum likelihood, evolutionary distance, and maximum parsimony methods," *Molecular Biologica Land Evolution*, vol. 28, no. 10, pp. 2731–2739, 2011.

[27] S. Saha and G. P. S. Raghava, "BcePred: prediction of continuous B-cell epitopes in antigenic sequences using physico-chemical properties," in *Proceedings of the 3rd International Conference on Artificial Immune Systems (ICARIS '04)*, G. Nicosia, V. Cutello, P. J. Bentley, and J. Timis, Eds., vol. 3239 of *LNCS*, pp. 197–204, Springer, 2004.

[28] H. Singh and G. P. S. Raghava, "ProPred1: prediction of promiscuous MHC Class-I binding sites," *Bioinformatics*, vol. 19, no. 8, pp. 1009–1014, 2003.

[29] H. Singh and G. P. Raghava, "ProPred: prediction of HLA-DR binding sites," *Bioinformatics*, vol. 17, no. 12, pp. 1236–1237, 2001.

[30] D. Geraets, L. Alemany, N. Guimera et al., "Detection of rare and possibly carcinogenic Human Papillomavirus genotypes as single infections in invasive cervical cancer," *The Journal of Pathology*, vol. 228, no. 4, pp. 534–543, 2012.

[31] L. Fu, K. van Doorslaer, Z. Chen et al., "Degradation of p53 by human Alphapapillomavirus E6 proteins shows a stronger correlation with phylogeny than oncogenicity," *PLoS ONE*, vol. 5, no. 9, Article ID e12816, pp. 1–8, 2010.

[32] T. Mesplède, D. Gagnon, F. Bergeron-Labrecque et al., "p53 degradation activity, expression, and subcellular localization of E6 proteins from 29 human papillomavirus genotypes," *Journal of Virology*, vol. 86, no. 1, pp. 94–107, 2012.

Hindawi Publishing Corporation
BioMed Research International
Volume 2013, Article ID 740187, 10 pages
http://dx.doi.org/10.1155/2013/740187

Research Article

TrkAIII Promotes Microtubule Nucleation and Assembly at the Centrosome in SH-SY5Y Neuroblastoma Cells, Contributing to an Undifferentiated Anaplastic Phenotype

Antonietta R. Farina,[1] Natalia Di Ianni,[1] Lucia Cappabianca,[1] Pierdomenico Ruggeri,[1] Marzia Ragone,[1] Giulia Ianni,[1] Alberto Gulino,[2] and Andrew R. Mackay[1]

[1] *Department of Applied Clinical and Biotechnological Sciences, University of L'Aquila, Via Vetoio, Coppito 2, 67100 L'Aquila, Italy*
[2] *Department of Experimental Medicine, University of Rome "La Sapienza," 00185 Rome, Italy*

Correspondence should be addressed to Andrew R. Mackay; andrewreay.mackay@univaq.it

Received 20 March 2013; Accepted 18 May 2013

Academic Editor: Rita de Cassia Stocco

The alternative TrkAIII splice variant is expressed by advanced stage human neuroblastomas (NBs) and exhibits oncogenic activity in NB models. In the present study, employing stable transfected cell lines and assays of indirect immunofluorescence, immunoprecipitation, Western blotting, microtubule regrowth, tubulin kinase, and tubulin polymerisation, we report that TrkAIII binds α-tubulin and promotes MT nucleation and assembly at the centrosome. This effect depends upon spontaneous TrkAIII activity, TrkAIII localisation to the centrosome and pericentrosomal area, and the capacity of TrkAIII to bind, phosphorylate, and polymerise tubulin. We propose that this novel role for TrkAIII contributes to MT involvement in the promotion and maintenance of an undifferentiated anaplastic NB cell morphology by restricting and augmenting MT nucleation and assembly at the centrosomal MTOC.

1. Introduction

TrkAIII is a developmentally regulated alternative splice variant of the NGF receptor tropomyosin-related kinase TrkA that is expressed by advanced stage human neuroblastomas (NBs), characterised by exon 6-7 skipping and exon 9 omission, and exhibits oncogenic activity in NB models [1–5]. TrkAIII oncogenic activity depends upon omission of the extracellular D4 Ig-like domain and several N-glycosylation sites, encoded within exons 6-7, important for receptor cell surface expression and prevention of ligand-independent activation [6, 7]. As a consequence and in contrast to fully spliced cell surface TrkA, TrkAIII exhibits intracellular expression and spontaneous, ligand-independent activation that is restricted to interphase within the intracellular membrane compartment. This results in chronic signalling through IP3k/Akt but not Ras/MAPK and promotes a more aggressive proliferating, undifferentiated stress-resistant, angiogenic, and tumourigenic stem cell-like NB cell phenotype, which is in stark contrast to ligand-activated cell surface TrkA, which signals through IP3k/Akt and Ras/MAPK and promotes a less aggressive phenotype characterised by neuronal differentiation associated with the inhibition of proliferation [1, 5, 8–10].

Microtubules (MTs) are dynamic polymers of α- and β-tubulins that play a central role in cellular differentiation [11–14]. In undifferentiated cells, MTs nucleate and assemble at the centrosome MT organising centre (MTOC), forming arrays of relatively short MTs that radiate outwards from the centrosome [11–15]. In differentiated cells, MTs differ in MTOC usage and nucleate also at cytoplasmic and/or perinuclear/Golgi-associated extracentrosomal MTOCs, resulting in the formation of more diffuse cytoplasmic MT mats and coils, and during neuronal differentiation, the formation of long MTs organised at the cell periphery is required for neuritogenesis and axon genesis [11–21].

Tyrosine kinases have been implicated in the regulation of MT nucleation, assembly, and stability. Src family tyrosine

kinases Fyn and Lyn phosphorylate tubulin and reorganise MTs during monocyte differentiation [15]; Fyn and Syk kinases regulate MT organisation in mast cells [22]; Src recruits γ-tubulin ring structures to the centrosome and promotes MT nucleation and assembly through MAPK/Erk [23, 24]; c-Fes binds and phosphorylates α-tubulin and promotes tubulin polymerisation during myeloid hematopoietic cell and neuron differentiations [25]; insulin receptor tyrosine kinase phosphorylates tubulin and promotes interaction between PI3k and γ-tubulin required for insulin-induced MT reorganisation [26, 27]; and JAK mediates growth hormone-induced MT assembly [28]. TrkA has also been implicated in MT reorganisation. The neurotrophins NGF and NT-3 activate cell surface TrkA, which responds by recruiting MTs to detergent-resistant cell surface lipid rafts and reorganising the assembly of MTs required for neuritogenesis, axon genesis, and growth cone formation, resulting in neuronal differentiation [29–31]. Tyrosine-phosphorylated TrkA colocalizes with α-tubulin positive MTs during mitosis [32], interacts with and modifies α-tubulin [33], and moves along MTs during retrograde transport via an interaction with dynein [34].

We have previously reported that tyrosine-phosphorylated TrkAIII binds γ-tubulin and localises to the centrosome in human SH-SY5Y NB cells [4]. Here, we report that TrkAIII interacts with α-tubulin and promotes tubulin polymerisation, contributing to MT involvement in promoting and maintaining a proliferating, undifferentiated, and anaplastic NB cell phenotype by restricting and augmenting MT nucleation and assembly at the interphase centrosome.

2. Materials and Methods

2.1. Cell Lines and Reagents. Empty pcDNA control, TrkAI, TrkAIII, and Y670/674/675F kinase dead mutant TrkAIII (kd-TrkAIII) stable transfected SH-SY5Y NB cell lines have been described previously [1, 3, 4]. All cell lines were grown in recommended medium (RPMI or DMEM), supplemented with appropriate antibiotics (Zeocin for stable transfectants, penicillin, and streptomycin) and 10% foetal calf serum. Nocodazole was purchased from Sigma-Aldrich (St. Louis, MO), and the pan Trk inhibitor CEP-701 [35] was kindly supplied by Cephalon Inc. (West Chester, PA). Rhodamine-conjugated α-tubulin, microtubule polymerisation buffers, and associated reagents were purchased from Cytoskeleton (Denver, CO). VectorMount mounting medium for immunofluorescence (IF) was purchased from Vector Laboratories (Burlingame, CA). Monoclonal α-tubulin, polyclonal anti-carboxyl terminal TrkA (C14), and monoclonal anti-phosphotyrosine (pY99) antibodies were purchased from Santa Cruz (Santa Cruz, CA). Polyclonal antibodies against γ-tubulin and TrkA phosphoY490 were from Sigma-Aldrich (St. Louis, MO). FITC and Texas red-conjugated secondary anti-mouse and anti-rabbit IgG antibodies were from Jackson Immune Research (Bar Harbor, Maine).

2.2. Indirect IF. Cells grown on Nunc glass chamber slides (Sigma-Aldrich) were washed in PBS, fixed in 96% ethanol-3% glacial acetic acid, and processed for indirect IF. Fixed slides were incubated for 1 h in blocking solution (1% bovine serum albumin in PBS-0.03% Triton X-100) and then for 2 to 16 h with primary antibody in blocking solution at room temperature. Slides were then washed three times in PBS-0.03% Triton X-100, incubated with secondary fluorochrome-conjugated antibody diluted in blocking solution for 1 hour at room temperature, washed in PBS-0.03% Triton X-100, and mounted using VectorMount. IF images were obtained using a Zeiss "Axioplan-2" fluorescence microscope, fitted with a digital camera, and images were processed using Leica M500 Image Manager software.

Nuclear lobulation was studied by fluorescent DAPI (Vector Labs) staining of nuclear chromatin.

2.3. Microtubule Regrowth Assay. Microtubule regrowth assays were performed as previously described [23]. Briefly, subconfluent (80%) cell cultures grown on Nunc glass chamber slides (Sigma-Aldrich) were treated for 2 hours at 4°C with 10 μg/mL nocodazole (Calbiochem) to depolymerise microtubules. Cells were then washed with cold PBS to remove nocodazole and subsequent microtubule regrowth assessed upon replacement of culture medium at 0, 5, and 15 minutes, at 37°C. Where stipulated, 100 nM CEP-701 was added during the last 30 minutes of nocodazole treatment and in regrowth medium.

To visualise microtubules, cells were permeabilized for 30 seconds in 80 mM Pipes, pH 6.8, 5 mM EGTA, pH 8.0, 1 mM $MgCl_2$, and 0.5% Triton X-100, fixed for 10 minutes in the same buffer containing 5% glutaraldehyde, and incubated for 7 minutes in 1% sodium borohydride in PBS. Cells were then stained with antibodies against α-tubulin (Santa Cruz) and γ-tubulin (Sigma-Aldrich) and washed in PBS prior to incubation with appropriate anti-mouse Texas-red conjugated and anti-rabbit FITC-conjugated secondary antibodies (Jackson Immune Research). Nuclear chromatin was counterstained with DAPI (Vector Labs). IF images were obtained at a constant exposure time to limit overexposure, and α-tubulin IF signals radiating from γ-tubulin positive centrosomes were measured in two separate concentric circles centred at the centrosome with radii of 1 and 2 μm, with background fluorescence subtracted using circles of corresponding sizes, using IF Jpeg images and ImageJ software [36]. MT regrowth areas and centrosome sizes were quantified by measuring respective α- and γ-tubulin IF areas calculated from outlined areas, using ImageJ software [36].

2.4. Immunoprecipitation and Western Blots. Cells were extracted in lysis buffer (PBS containing 0.5% sodium deoxycholate, 1% NP40, 0.1% SDS, 1 mM sodium orthovanadate, 1 mM PMSF, 1 μg/mL of pepstatin A, and Aprotinin) and protein concentrations calculated by Bradford protein concentration assay (Sigma-Aldrich). Prior to immunoprecipitation, extract aliquots (200–500 μg) were precleared with 1 μg of preimmune IgG (1 hour at 4°C) and 20 μL of Protein A Sepharose (Fast Flow, Sigma), for 20 minutes at 4°C. For immunoprecipitation, 200–500 μg of extract was incubated with antibody at a concentration range of 0.1–1.0 μg/500 μg total protein for 2–16 hours at 4°C. Following incubation, 20 μL of Protein A Sepharose (Fast flow, Sigma-Aldrich) in lysis buffer was added and reactions incubated for 30 minutes

at 4°C. Protein Sepharose/IgG conjugates were collected by centrifugation (10,000 ×g for 5 minutes), washed 3 times in lysis buffer, resuspended in SDS-PAGE sample buffer, and subjected to reducing SDS-PAGE/Western blotting. Briefly, proteins were transblotted by electrophoresis onto Hybond C+ nitrocellulose membranes (Amersham Int. UK) and air-dried. Nonspecific binding sites on membranes were blocked by incubation for 2 hours in 5% nonfat milk in TBS prior to incubation with primary antibodies at recommended dilutions for 2–16 hours at 4°C, washed in TBS, and then incubated with secondary HRP-conjugated antibodies diluted in blocking solution. Immunoreactive species were detected by chemiluminescence reaction as directed (Amersham Int., Bedford, UK).

2.5. α-Tubulin Kinase and Polymerisation Assays. Tubulin polymerisation assays were performed as previously described [25]. Control, TrkAI, and TrkAIII immunoprecipitates were prepared from respective SH-SY5Y transfectants by incubating total cell extracts (400 μg) with 1 μg of anti-TrkA (C-14) antibody for 2 hours at 4°C, followed by incubation with 20 μL of Protein A Sepharose suspension (Fast flow, Sigma-Aldrich). Protein A immunoprecipitates were recovered by centrifugation at 15,000 rpm in a microfuge at 4°C and washed 3 times in RIPA buffer and 2 times in 50 mM Tris-HCl (pH 7.5). Two vials were prepared each containing a 9 : 1 ratio of unlabelled (9 parts) bovine brain α/β-tubulins and rhodamine-labelled (1 part) bovine brain α-tubulin (Cytoskeleton Inc.), resuspended in general tubulin buffer (80 mM Pipes (pH.6.8), 1 mM $MgCl_2$, and 1 mM EGTA) containing 1 mM GTP (Sigma-Aldrich). To the first vial, 20 μL of general tubulin buffer containing 2 mM GTP and ATP was added to a final concentration of 100 μM. The second vial received 23 μL of general tubulin buffer containing 2 mM GTP but not ATP. Washed Protein A Sepharose immunoprecipitates were resuspended in either 15 μL of non-labelled tubulin/rhodamine α-tubulin (9 : 1) in the presence or absence of ATP and incubated for 1 hour at 37°C. Reaction samples (3–5 μL) were subsequently removed and either (a) mixed with reducing SDS-PAGE sample buffer for Western blotting to examine α-tubulin tyrosine phosphorylation or (b) mixed with an equal volume of general tubulin buffer containing 60% v/v glycerol on ice, spread onto glass slides, covered with a glass coverslip, and examined by fluorescent microscopy for the presence of rhodamine-labelled tubulin polymers.

3. Results

3.1. TrkAIII Promotes MT Nucleation and Assembly at the Centrosome. Indirect IF detected intense arrays of α-tubulin positive MTs in TrkAIII SH-SY5Y transfectants, radiating outwards from a perinuclear focal point consistent with a centrosomal MTOC origin during interphase. This pattern of MT assembly exhibited marked overlap with intracellular TrkAIII, which was concentrated to the pericentrosomal region but was not detected throughout the cytoplasm or at the cell periphery (Figure 1(a)). Significant overlap between TrkAIII and α-tubulin positive MTs was not detected during mitosis (Figure 1(b)). This pattern of α-tubulin positive MTs was markedly altered following overnight treatment with 100 nM CEP-701, which was also associated with a reduction in TrkAIII overlap with α-tubulin (Figure 2(a)).

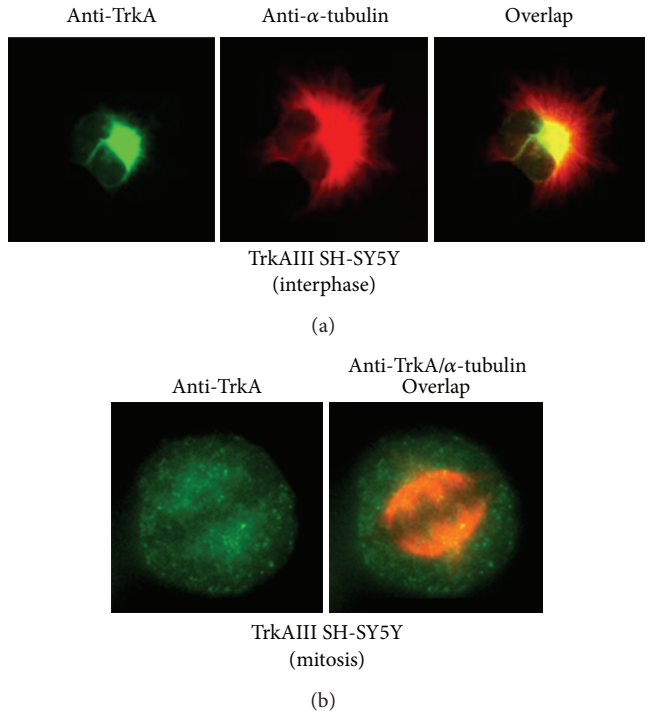

Figure 1: Representative IF images illustrating the typical pattern of TrkAIII expression (green), α-tubulin positive MTs (red), and overlap (yellow/orange) in interphase (a) and mitotic (b) TrkAIII SH-SY5Y transfectants.

In contrast to TrkAIII transfectants, neither kinase dead kd-TrkAIII, TrkAI, nor control SH-SY5Y transfectants exhibited this pattern of α-tubulin positive MT assembly, with all three cell lines characterised by less intense, more diffuse cytoplasmic MT distribution, which was less focalised at the centrosome (Figure 2(a)). CEP-701 inhibited TrkA-associated tyrosine phosphorylation, used as a surrogate for TrkAIII tyrosine kinase activity, at the dose employed in this study (Figures 2(b) and 4(b)).

3.2. MT Regrowth Assays. The centrosomal origin of α-tubulin positive MT arrays in TrkAIII transfectants was confirmed by contemporary α-tubulin and γ-tubulin IF (Figure 3(a)).

In MT regrowth assays, TrkAIII transfectants exhibited significantly more rapid MT regrowth at 5 and 15 minutes following nocodazole washout, in terms of both recovery of pericentrosomal α-tubulin IF intensity initiating at the γ-tubulin positive centrosome (Figures 3(a) and 3(b)) and total MT regrowth area (Figures 3(c) and 3(d)), when compared to untreated control and TrkAI transfectants and CEP-701-treated TrkAIII transfectants (100 nM, 30 minutes before treatment and for the duration of assay). When compared to untreated TrkAIII transfectants normalised to an arbitrary value of 100%, CEP-701-treated TrkAIII transfectants

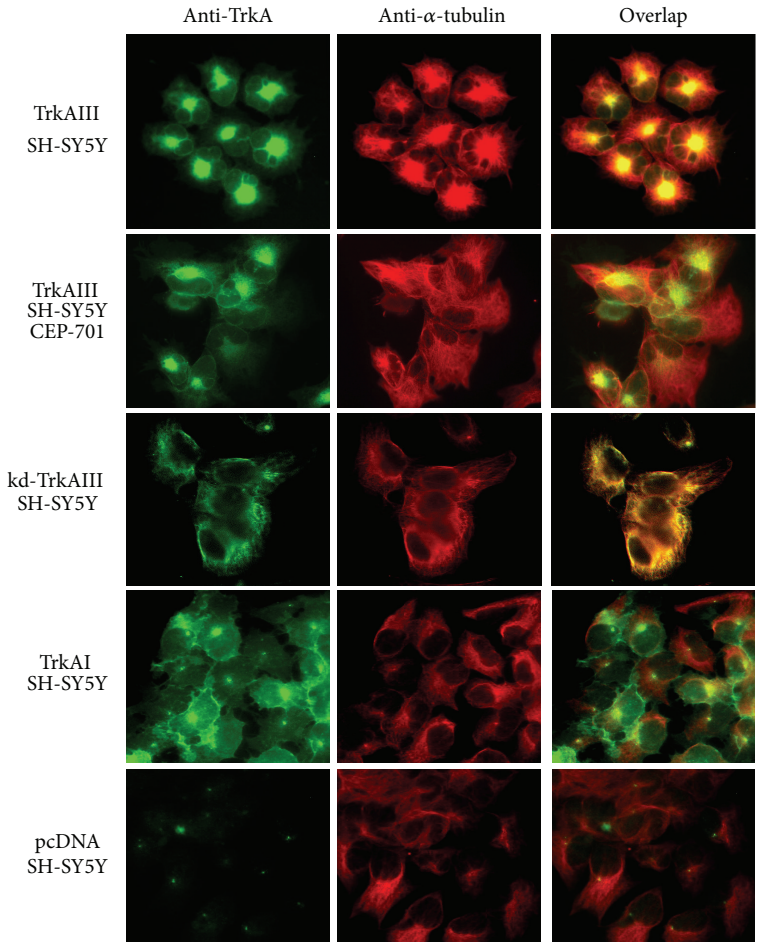

FIGURE 2: (a) Representative IF images comparing TrkA variant expression (green), α-tubulin positive MTs (red), and the overlap (yellow/orange) in untreated and CEP-701-treated (100 ng overnight) TrkAIII SH-SY5Y transfectants and in untreated kd-TrkAIII, TrkAI, and control pcDNA SH-SY5Y transfectants. (b) Representative IF images comparing the pattern of TrkAIII expression (green), TrkAIII-associated tyrosine phosphorylation (red), and overlap (yellow/orange) in untreated and CEP-701-treated (100 nM, overnight) TrkAIII SH-SY5Y transfectants.

exhibited a significant 78% reduction ($P \leq 0.002$, $n = 50$) in pericentrosomal α-tubulin IF intensity, 65% reduction ($P \leq 0.003$, $n = 50$) in total MT regrowth area at 5 minutes, a significant 40% reduction ($P \leq 0.027$, $n = 50$) in pericentrosomal α-tubulin IF intensity, and 41% reduction in total MT regrowth area ($P \leq 0.032$, $n = 50$) at 15 minutes, after nocodazole washout (Figures 3(b) and 3(d)); TrkAI transfectants exhibited a significant 82% reduction ($P \leq 0.0001$, $n = 50$) in pericentrosomal α-tubulin IF intensity, 78% reduction ($P \leq 0.0001$, $n = 50$) in total MT regrowth area at 5 minutes, a significant 41% reduction ($P \leq 0.026$, $n = 50$) in pericentrosomal α-tubulin IF intensity,

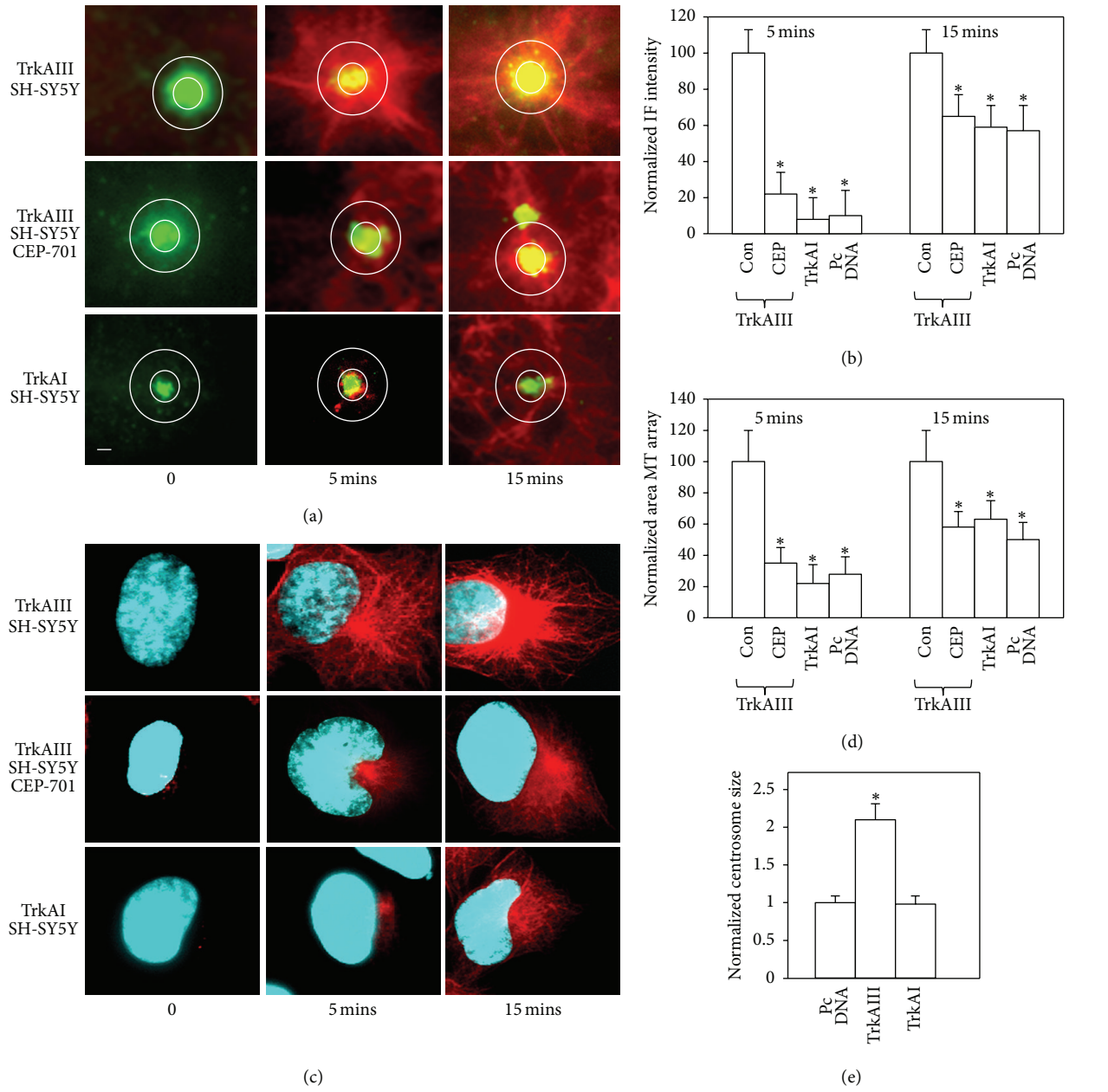

Figure 3: Representative IF images and histograms of MT regrowth assays, demonstrating (a) indirect IF changes in α-tubulin positive MT regrowth (red) from the γ-tubulin positive centrosome (green) in untreated and CEP-701-treated (100 nM) TrkAIII SH-SY5Y transfectants and in untreated TrkAI SH-SY5Y transfectants at 0, 5, and 15 minutes after nocodazole washout. (b) Histogram demonstrating the differences in mean (±S.E.) α-tubulin IF intensity in untreated and CEP-701-treated (100 nM for 1 hour) TrkAIII SH-SY5Y transfectants and in untreated TrkAI and control pcDNA SH-SY5Y transfectants at 0, 5, and 15 minutes after nocodazole washout, normalised with respect to untreated TrkAIII transfectants (arbitrary value 100%; $n = 50$ per group; * = statistical significance). (c) Indirect IF demonstrating differences in α-tubulin positive MT regrowth area (red) in untreated and CEP-701-treated (100 nM) TrkAIII SH-SY5Y transfectants and in untreated TrkAI SH-SY5Y transfectants at 0, 5, and 15 minutes after nocodazole washout. (d) Histogram demonstrating differences in α-tubulin positive MT regrowth area in untreated and CEP-701-treated (100 nM) TrkAIII SH-SY5Y transfectants and in untreated TrkAI and control pcDNA SH-SY5Y transfectants at 0, 5, and 15 minutes after nocodazole washout, normalised with respect to untreated TrkAIII transfectants (arbitrary value of 100%; $n = 50$ per group; * = statistical significance). (e) Histogram demonstrating the differences in γ-tubulin positive centrosome size in untreated control, TrkAI, and TrkAIII SH-SY5Y transfectants, normalised with respect to untreated control transfectants given the arbitrary value of 1 ($n = 50$ per group; * = statistical significance).

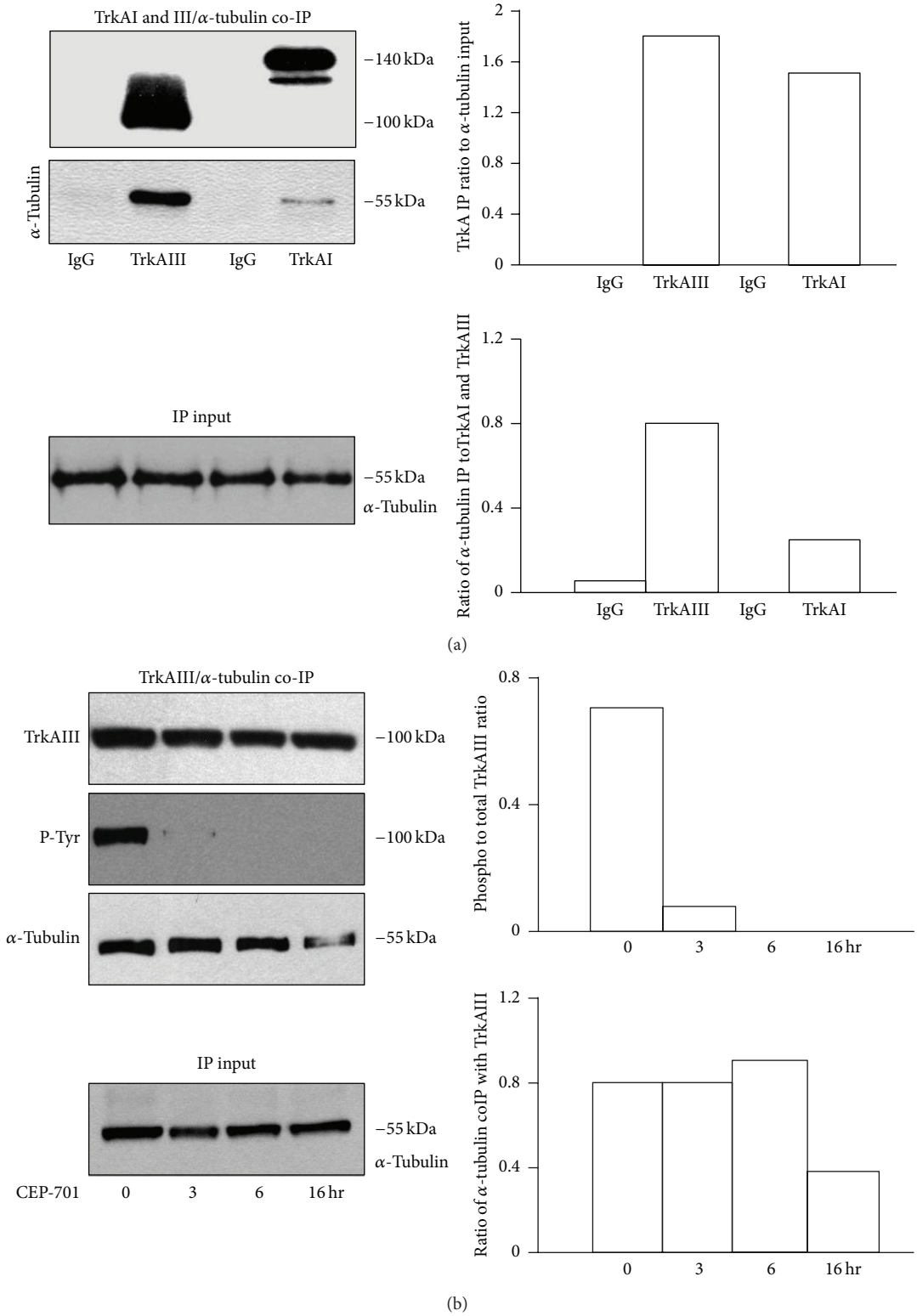

Figure 4: (a) IP/Western blots demonstrating differences in α-tubulin levels pulled down by TrkAIII and TrkAI immunoprecipitates from respective SH-SY5Y transfectants, plus histograms displaying densitometric analysis of the adjacent blots, demonstrating the presence of similar levels of TrkAI and TrkAIII immunoprecipitates, normalised to input α-tubulin levels, plus the difference in α-tubulin levels pulled down as a densitometric ratio to TrkAI and TrkAIII. (b) IP/Western blots demonstrating the effect of CEP-701 (100 nM for 0–16 hours) on TrkAIII tyrosine phosphorylation (P-Tyr) and α-tubulin levels pulled down in coimmunoprecipitation assays, plus histograms displaying densitometric analysis of the adjacent blots, demonstrating CEP-701-induced loss of TrkAIII tyrosine phosphorylation from 3 hr onwards, associated with reduced α-tubulin binding at 16 hours only.

and 37% reduction in total MT regrowth area ($P \leq 0.038$, $n = 50$) at 15 minutes, after nocodazole washout (Figures 3(b) and 3(d)); and control transfectants exhibited significant 78% reduction ($P \leq 0.006$, $n = 50$) in pericentrosomal α-tubulin IF intensity, 72% reduction ($P \leq 0.0001$, $n = 50$) in total MT regrowth area at 5 minutes, significant 43% reduction ($P \leq 0.027$, $n = 50$) in pericentrosomal α-tubulin IF intensity, and 50% reduction in total MT regrowth area ($P \leq 0.005$, $n = 50$) at 15 minutes, after nocodazole washout (Figures 3(b) and 3(d)).

Measurement of the area of γ-tubulin IF, as an estimate of relative centrosome size, revealed that centrosomes in TrkAIII transfectants were significantly ($P \leq 0.001$, $n = 50$) 2.1 ± 0.14-fold larger than centrosomes in control transfectants (normalised to an arbitrary value of 1.0 ± 0.07, $n = 50$) and TrkAI transfectants, which were not significantly different in size to control centrosomes (0.98 ± 0.12, $n = 50$, $P \leq 0.89$ NS) (Figure 3(d)).

3.3. TrkAIII Binds and Phosphorylates α-Tubulin and Promotes MT Assembly In Vitro. In coimmunoprecipitation assays, TrkAIII pulled down a greater quantity of α-tubulin when compared to an equivalent amount of immunoprecipitated TrkAI, normalised to α-tubulin levels in input extracts (Figure 4(a)). CEP-701 (100 nM) inhibited TrkAIII tyrosine phosphorylation at times from 3 hours onward (Figure 4(b)) and caused a moderate reduction in α-tubulin/TrkAIII coimmunoprecipitation at 16 hours but not before (Figure 4(b)).

In tubulin polymerisation assays, TrkAIII but not an equivalent amount of TrkAI immunoprecipitate induced low but detectable tyrosine phosphorylation of exogenous α-tubulin (Figure 5(a)) and promoted the polymerisation of tubulin *in vitro*, in the presence but not in the absence of ATP (Figure 5(b)).

3.4. TrkAIII Promotes Nuclear Lobulation. TrkAIII but not TrkAI or control SH-SY5Y transfectants exhibited a highly lobular nuclear morphology (Figure 6(a)). Nuclear lobulation was detected during interphase, lost during prophase in association with MT depolymerization (not shown), and inhibited by both CEP-701 (100 nM for 16 hours) and nocodazole (10 μg/mL for 2 hours) (Figure 6(a)). Human U251 glioblastoma cells, which express endogenous TrkAIII that localises to the centrosome [4], also exhibited a highly lobulated nuclear morphology (Figure 6(b)) that was inhibited by both CEP-701 (100 nM for 16 hours) and nocodazole (10 μg/mL for 2 hours), in association with the rearrangement of α-tubulin positive MTs (Figure 6(b)).

4. Discussion

In this study, we identify a novel role for TrkAIII in promoting the nucleation and assembly of MTs at the centrosome in human SH-SY5Y NB cells. We propose that this function depends upon spontaneous intracellular TrkAIII activation and the capacity of TrkAIII to bind α- and γ-tubulins, to localise to the centrosome, and to promote tubulin polymerisation, contributing to MT involvement in the promotion

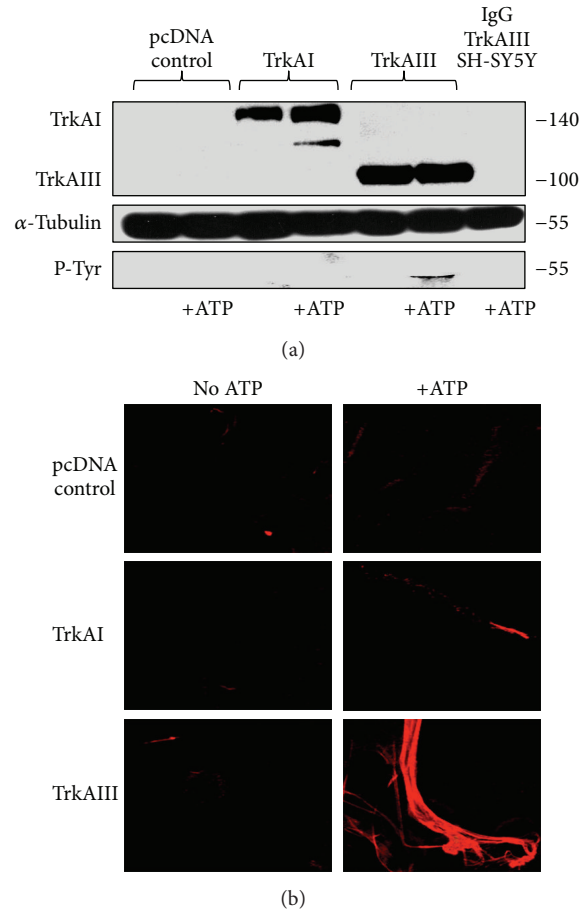

Figure 5: (a) Western blots demonstrating the relative levels of TrkAI, TrkAIII, and total tyrosine phosphorylated α-tubulins in a representative α-tubulin phosphorylation assay; (b) IF images demonstrating the difference in tubulin polymerisation induced by TrkAIII but not control or TrkAI immunoprecipitates in a representative tubulin polymerisation assay, in the presence but not in the absence of ATP.

and maintenance of a proliferating, undifferentiated, and anaplastic NB cell phenotype by restricting and augmenting MT nucleation and assembly at the centrosomal MTOC.

The striking difference in α-tubulin positive MT assembly exhibited by TrkAIII but not control or TrkAI transfectants, characterised by relatively short intense MT arrays radiating outwards from the centrosome, suggests a role for TrkAIII tyrosine kinase activity in MT assembly. This possibility is supported by the observations that (a) MT assembly and nucleation at the centrosome in TrkAIII transfectants were reduced by CEP-701 at TrkAIII inhibitory concentrations; (b) kd-TrkAIII SH-SY5Y transfectants did not exhibit this pattern of MT nucleation and assembly; and (c) TrkAIII SH-SY5Y transfectants exhibited significantly more rapid MT regrowth from the centrosome, when compared to control, TrkAI, and CEP-701-treated TrkAIII transfectants.

The formation of relatively short MT arrays in TrkAIII transfectants, radiating outward from the γ-tubulin positive centrosome, bears close similarity to MT assembly in undifferentiated cells [11–15], suggesting that TrkAIII promotion

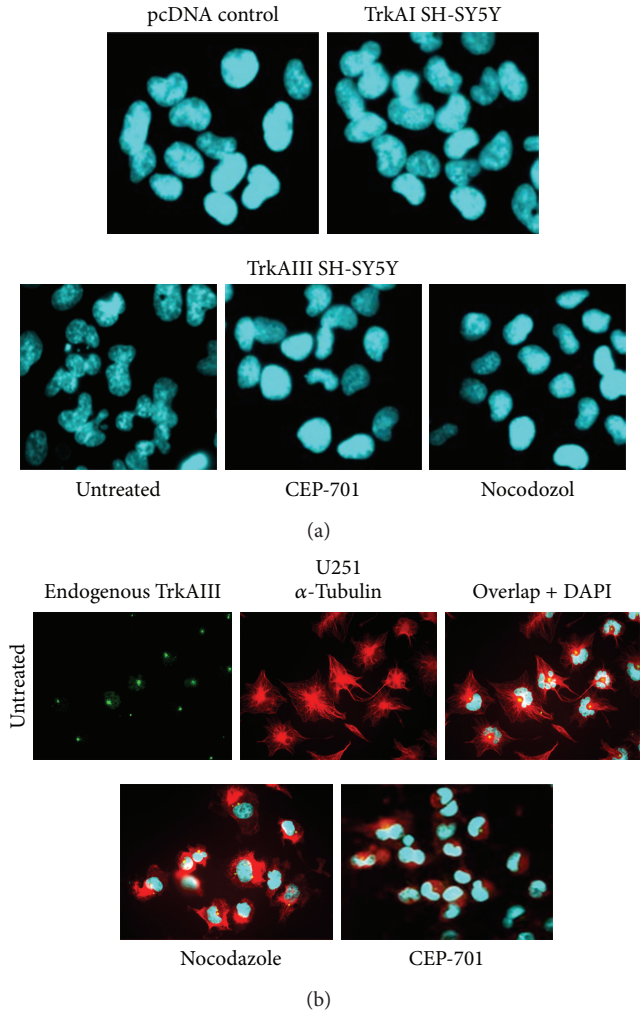

Figure 6: (a) Representative IF images demonstrating the difference in the regular oval nuclear morphology exhibited by pcDNA control and TrkAI SH-SY5Y transfectants, compared to the lobulated nuclei in TrkAIII SH-SY5Y transfectants, plus the inhibition of nuclear lobulation in TrkAIII SH-Sy5Y transfectants following incubation with CEP-701 (100 nM for 16 hours) and nocodazole (10 μg/mL for 2 hours). (b) Representative IF images demonstrating the intracellular distribution of endogenous TrkAIII (green), α-tubulin positive MTs (red), TrkAIII/α-tubulin overlap (yellow/orange), and DAPI-stained nuclei (blue) in human U251 cells, plus IF images demonstrating the capacity of nocodazole (10 μg/mL for 2 hours) and CEP-701 (100 nM for 16 hours) to inhibit nuclear lobulation in U251 cells.

and maintenance of an undifferentiated NB phenotype may depend, at least in part, upon the restriction and augmentation of MT nucleation and assembly at the centrosomal MTOC. This differs from MT reorganisation, nucleation, and assembly associated with neuronal differentiation induced either by neurotrophin-activated cell surface TrkA or cytoplasmic Fes, which is characterised by the formation of long MT processes required for neuritogenesis, growth cone formation, and axon genesis, which nucleate also from non-centrosomal MTOCs and are reorganised at the cell periphery [11, 21, 25, 29–32]. This difference may be explained by tyrosine kinase localisation, since TrkAIII exhibits spontaneous intracellular activation in the pericentrosomal region and at the centrosome [4], whereas neurotrophins activate fully spliced TrkA at the cell surface [1, 29–31], and c-Fes is activated throughout the cytoplasm [25]. Furthermore, the centralized location exhibited by activated TrkAIII (this study and [4]) may also help to explain the pericentrosomal overlap exhibited by TrkAIII and MTs, which did not extend throughout the cytoplasm, as reported for activated Fes [25], nor to the cell periphery, as reported for the interaction between MTs and TrkA within lipid rafts [21].

TrkAIII promotion of MT nucleation and assembly at the centrosome bears close similarity to the influence of c-Src upon MT nucleation and assembly, which has been reported to depend upon the recruitment of γ-tubulin ring structures to the centrosome [23, 24]. TrkAIII binds γ-tubulin [4] and may also interact with c-Src [37], suggesting that TrkAIII could also import γ-tubulin ring structures to the centrosome either directly or indirectly. In support of this, γ-tubulin positive centrosomes in TrkAIII transfectants were significantly larger than centrosomes in control or TrkAI transfectants. We are currently investigating potential c-Src involvement in this observation. Alternatively, TrkAIII may bind and not import γ-tubulin to the centrosome, limiting its potential influence to MT assembly after nucleation.

Spontaneous TrkAIII activation is restricted to interphase in SH-SY5Y cells [3–5], indicating that TrkAIII influence upon MT assembly may also be restricted to interphase. This is supported by the observation that TrkAIII expression did not inhibit proliferation, as occurs with terminal differentiation, indicating that MT remodelling required for cell cycle progression was not compromised [11, 14] and also explaining why we did not detect TrkAIII association with the mitotic spindle, as previously reported for tyrosine phosphorylated TrkA [32].

The capacity of TrkAIII to bind α-tubulin adds to its capacity to bind γ-tubulin [4]. TrkAIII tyrosine kinase involvement in α-tubulin binding is supported by the relatively low level of α-tubulin binding exhibited by TrkAI and the modest reduction in α-tubulin binding by TrkAIII following overnight treatment with CEP-701 and is corroborated by reports that phosphorylated TrkA colocalises with α-tubulin [32], activated TrkA interacts with and modifies α-tubulin [33], neurotrophin activated TrkA recruits and reorganises MTs in lipid rafts during neuron differentiation [21, 29, 30], and retrograde transport of activated TrkA is mediated by dynein/MT interaction [34]. Whether TrkAIII interacts directly with α-tubulin or indirectly via dynein [34], c-Src [23, 37], and/or perhaps FRS-3 [38] remains to be elucidated. However, the fact that TrkAIII contemporarily binds α and γ-tubulin (this study and [4]) suggests that TrkAIII may independently recruit α and γ-tubulin to the centrosome for MT nucleation and assembly.

TrkAIII promotion of MT assembly *in vivo,* exemplified by the exaggerated pattern of MT assembly in TrkAIII transfectants and confirmed in MT regrowth assays, was further supported in tubulin polymerisation assays *in vitro*, which unveiled the capacity of TrkAIII but not TrkAI or control immunoprecipitates to induce low but detectable tyrosine

phosphorylation of exogenous α-tubulin and to promote tubulin polymerisation. Whether this results directly from TrkAIII tyrosine kinase activity or TrkAIII-associated tyrosine kinases, such as c-Src [23, 35], remains to be elucidated. However, it is clear that spontaneously active TrkAIII acts in a manner analogous to neurotrophin-activated cell surface TrkA in its capacity to reorganise and promote MT assembly *in vivo* but does so at the centrosome rather than cell periphery, resulting in the promotion and maintenance of a proliferating, undifferentiated NB cell phenotype rather than inducing neuronal differentiation, which results from cell surface TrkA activation (this study [1, 8–10]).

The undifferentiated phenotype exhibited by TrkAIII SH-SY5Y transfectants was also accompanied by a lobular nuclear morphology. TrkAIII tyrosine kinase and MT involvement in nuclear lobulation was confirmed using CEP-701 and nocodazole, both of which inhibited nuclear lobulation. Human U251 glioblastoma cells, which express endogenous TrkAIII that localises to the centrosome [4], also exhibited a highly lobular nuclear morphology similar to that of TrkAIII SH-SY5Y transfectants, associated with intense MT arrays, radiating outward from the centrosome and overlapping pericentrosomal and centrosomal endogenous TrkAIII. As for TrkAIII SH-SY5Y transfectants, nuclear lobulation in U251 cells was inhibited by both CEP-701 and nocodazole, confirming close similarity between exogenous and endogenous TrkAIII.

5. Conclusions

In conclusion, we propose that spontaneous intracellular pericentrosomal TrkAIII activation contributes to MT involvement in the promotion and maintenance of a proliferating, undifferentiated, and anaplastic NB cell phenotype by restricting and augmenting MT nucleation and assembly to the centrosomal MTOC. This function depends upon TrkAIII capacity to bind α- and γ-tubulin, to localise to the centrosome, and to promote tubulin polymerisation.

Conflicts of Interests

The authors declare that there was no conflict of interests for the research presented in this paper.

Acknowledgments

Antonietta R. Farina and Natalia Di Ianni contributed equally to this paper. This work was supported by grants from AIRC, PRIN, and the Maugeri Foundation.

References

[1] A. Tacconelli, A. R. Farina, L. Cappabianca et al., "TrkA alternative splicing: a regulated tumor-promoting switch in human neuroblastoma," *Cancer Cell*, vol. 6, no. 4, pp. 347–360, 2004.

[2] A. Tacconelli, A. R. Farina, L. Cappabianca et al., "TrkAIII expression in the thymus," *Journal of Neuroimmunology*, vol. 183, no. 1-2, pp. 151–161, 2007.

[3] A. R. Farina, A. Tacconelli, L. Cappabianca et al., "The neuroblastoma tumour-suppressor trkAI and its oncogenic alternative trkAIII splice variant exhibit geldanamycin-sensitive interactions with Hsp90 in human neuroblastoma cells," *Oncogene*, vol. 28, no. 46, pp. 4075–4094, 2009.

[4] A. R. Farina, A. Tacconelli, L. Cappabianca et al., "The alternative TrkAIII splice variant targets the centrosome and promotes genetic instability," *Molecular and Cellular Biology*, vol. 29, no. 17, pp. 4812–4830, 2009.

[5] A. R. Farina, L. Cappabianca, P. Ruggeri et al., "Alternative TrkA splicing and neuroblastoma," in *Neuroblastoma Present and Future*, H. Shimada, Ed., pp. 111–136, Intech, Croatia, 2012.

[6] J. C. Arevalo, B. Conde, B. L. Hempstead, M. V. Chao, D. Martin-Zanca, and P. Perez, "TrkA Immunoglobulin-like ligand binding domains inhibit spontaneous activation of the receptor," *Molecular and Cellular Biology*, vol. 20, no. 16, pp. 5908–5916, 2000.

[7] F. L. Watson, M. A. Porcionatto, A. Bhattacharyya, C. D. Stiles, and R. A. Segal, "TrkA glycosylation regulates receptor localisation and activity," *Journal of Neurobiology*, vol. 39, pp. 323–336, 1999.

[8] E. Lavenius, C. Gestblom, I. Johansson, E. Nånberg, and S. Påhlman, "Transfection of TRK-A into human neuroblastoma cells restores their ability to differentiate in response to nerve growth factor," *Cell Growth and Differentiation*, vol. 6, no. 6, pp. 727–736, 1995.

[9] E. Lucarelli, D. Kaplan, and C. J. Thiele, "Activation of trk-A but not trk-B signal transduction pathway inhibits growth of neuroblastoma cells," *European Journal of Cancer*, vol. 33, no. 12, pp. 2068–2070, 1997.

[10] A. M. Simpson, R. Iyer, J. L. Mangino et al., "TrkAIII isoform expression upregulates stem cell markers and correlates with worse outcome in neuroblastomas (NBs)," in *Proceedings of the Advances in Neuroblastoma Research*, POT055, p. 164, 2012.

[11] M. Kuijpers and C. C. Hoogenraad, "Centrosomes, microtubules and neuronal development," *Molecular and Cellular Neuroscience*, vol. 48, no. 4, pp. 349–358, 2011.

[12] M. Bornens, "Centrosome composition and microtubule anchoring mechanisms," *Current Opinion in Cell Biology*, vol. 14, no. 1, pp. 25–34, 2002.

[13] J. Lüders, U. K. Patel, and T. Stearns, "GCP-WD is a γ-tubulin targeting factor required for centrosomal and chromatin-mediated microtubule nucleation," *Nature Cell Biology*, vol. 8, no. 2, pp. 137–147, 2006.

[14] J. Lüders and T. Stearns, "Microtubule-organizing centers: a reevaluation," *Nature Reviews Molecular Cell Biology*, vol. 8, pp. 161–167, 2007.

[15] K. Katagiri, T. Katagiri, K. Kajiyama, T. Yamamoto, and T. Yoshida, "Tyrosine-phosphorylation of tubulin during monocytic differentiation of HL-60 cells," *Journal of Immunology*, vol. 150, no. 2, pp. 585–593, 1993.

[16] Y. A. Komarova, A. S. Akhmanova, S. Kojima, N. Galjart, and G. G. Borisy, "Cytoplasmic linker proteins promote microtubule rescue in vivo," *Journal of Cell Biology*, vol. 159, no. 4, pp. 589–599, 2002.

[17] A.-M. Tassin, B. Maro, and M. Bornens, "Fate of microtubule-organizing centers during myogenesis in vitro," *Journal of Cell Biology*, vol. 100, no. 1, pp. 35–46, 1985.

[18] A. M. Tassin, M. Paintrand, E. G. Berger, and M. Bornens, "The Golgi apparatus remains associated with microtubule organizing centers during myogenesis," *Journal of Cell Biology*, vol. 101, no. 2, pp. 630–638, 1985.

[19] L. Lewis, Y. Barrandon, H. Green, and G. Albrecht-Buehler, "The reorganization of microtubules and microfilaments in differentiating keratinocytes," *Differentiation*, vol. 36, no. 3, pp. 228–233, 1987.

[20] K. J. M. Zaal, E. Reid, K. Mousavi et al., "Who needs microtubules? myogenic reorganization of MTOC, golgi complex and er exit sites persists despite lack of normal microtubule tracks," *PLoS ONE*, vol. 6, no. 12, Article ID e29057, 2011.

[21] S. Pryor, G. McCaffrey, L. R. Young, and M. L. Grimes, "NGF causes TrKA to specifically attract microtubules to lipid rafts," *PLoS ONE*, vol. 7, no. 4, Article ID e35163, 2012.

[22] V. Sulimenko, E. Dráberová, T. Sulimenko et al., "Regulation of microtubule formation in activated mast cells by complexes of γ-tubulin with Fyn and Syk kinases," *Journal of Immunology*, vol. 176, no. 12, pp. 7243–7253, 2006.

[23] D. Colello, C. G. Reverte, R. Ward et al., "Androgen and Src signaling regulate centrosome activity," *Journal of Cell Science*, vol. 123, no. 12, pp. 2094–2102, 2010.

[24] D. Colello, S. Mathew, R. Ward, K. Pumiglia, and S. E. LaFlamme, "Integrins regulate microtubule nucleating activity of centrosome through mitogen-activated protein kinase/extracellular signal-regulated kinase kinase/extracellular signal-regulated kinase (MEK/ERK) signaling," *Journal of Biological Chemistry*, vol. 287, no. 4, pp. 2520–2530, 2012.

[25] C. E. Laurent, F. J. Delfino, H. Y. Cheng, and T. E. Smithgall, "The human c-Fes tyrosine kinase binds tubulin and microtubules through separate domains and promotes microtubule assembly," *Molecular and Cellular Biology*, vol. 24, no. 21, pp. 9351–9358, 2004.

[26] T. Kadowaki, Y. Fujita-Yamaguchi, and E. Nishida, "Phosphorylation of tubulin and microtubule-associated proteins by the purified insulin receptor kinase," *Journal of Biological Chemistry*, vol. 260, no. 7, pp. 4016–4020, 1985.

[27] R. Kapeller, A. Toker, L. C. Cantley, and C. L. Carpenter, "Phosphoinositide 3-kinase binds constitutively to α/β-tubulin and binds to γ-tubulin in response to insulin," *Journal of Biological Chemistry*, vol. 270, no. 43, pp. 25985–25991, 1995.

[28] E. L. K. Goh, T. J. Pircher, and P. E. Lobie, "Growth hormone promotion of tubulin polymerization stabilizes the microtubule network and protects against colchicine-induced apoptosis," *Endocrinology*, vol. 139, no. 10, pp. 4364–4372, 1998.

[29] D. G. Drubin, S. C. Feinstein, E. M. Shooter, and M. W. Kirschner, "Nerve growth factor-induced neurite outgrowth in PC12 cells involves the coordinate induction of microtubule assembly and assembly-promoting factors," *Journal of Cell Biology*, vol. 101, no. 5 I, pp. 1799–1807, 1985.

[30] F. Zhou, J. Zhou, S. Dedhar, Y. Wu, and W. D. Snider, "NGF-induced axon growth is mediated by localized inactivation of GSK-3β and functions of the microtubule plus end binding protein APC," *Neuron*, vol. 42, no. 6, pp. 897–912, 2004.

[31] G. Morfini, M. C. DiTella, F. Feiguin, N. Carri, and A. Caceres, "Neurotrophin-3 enhances neurite outgrowth in cultured hippocampal pyramidal neurons," *Journal of Neuroscience Research*, vol. 39, no. 2, pp. 219–232, 1994.

[32] Z. Zhang, Y. Yang, A. Gong, C. Wang, Y. Liang, and Y. Chen, "Localization of NGF and TrkA at mitotic apparatus in human glioma cell line U251," *Biochemical and Biophysical Research Communications*, vol. 337, no. 1, pp. 68–74, 2005.

[33] E. J. Jung, S. Y. Lee, and C. W. Kim, "Proteomic analysis of novel targets associated with TrkA-mediated tyrosine phosphorylation signaling pathways in SK-N-MC neuroblastoma cells," *Proteomics*, vol. 13, pp. 355–367, 2013.

[34] H. Yano, F. S. Lee, H. Kong et al., "Association of Trk neurotrophin receptors with components of the cytoplasmic dynein motor," *The Journal of Neuroscience*, vol. 21, no. 3, article RC125, 2001.

[35] A. M. Camoratto, J. P. Jani, T. S. Angeles et al., "CEP-751 inhibits Trk receptor tyrosine kinase activity in vitro and exhibits antitumor activity," *International Journal of Cancer*, vol. 72, pp. 673–679, 1997.

[36] W. S. Rasband, "ImageJ," U. S. National Institutes of Health, Bethesda, Md, USA, 1997–2012, http://imagej.nih.gov/ij/.

[37] P. A. Bromann, H. Korkaya, and S. A. Courtneidge, "The interplay between Src family kinases and receptor tyrosine kinases," *Oncogene*, vol. 23, no. 48, pp. 7957–7968, 2004.

[38] S. J. Dixon, J. I. S. MacDonald, K. N. Robinson, C. J. Kubu, and S. O. Meakin, "Trk receptor binding and neurotrophin/fibroblast growth factor (FGF)-dependent activation of the FGF receptor substrate (FRS)-3," *Biochimica et Biophysica Acta*, vol. 1763, no. 4, pp. 366–380, 2006.

Hindawi Publishing Corporation
BioMed Research International
Volume 2013, Article ID 814635, 9 pages
http://dx.doi.org/10.1155/2013/814635

Research Article

Bovine Papillomavirus Type 2 Infection and a Series of Mesenchymal Tumors of the Urinary Bladder in Cattle

Manuela Martano,[1] Franco Roperto,[2] Rita de Cassia Stocco,[3] Valeria Russo,[1] Giuseppe Borzacchiello,[1] Orlando Paciello,[1] Valentina Iovane,[1] Leonardo Leonardi,[4] Paola Maiolino,[1] Brunella Restucci,[1] Serenella Papparella,[1] and Sante Roperto[1]

[1] *Department of Veterinary Medicine and Animal Productions, Naples University Federico II, Via F. Delpino, 80137 Naples, Italy*
[2] *Department of Biology, Naples University Federico II, Via Mezzocannone 16, 80134 Naples, Italy*
[3] *Instituto Butantan, Laboratório de Genética, Avenida Vital Brazil 1500, 05503-900 São Paulo, Brazil*
[4] *Department of Biopathological Sciences and Hygiene of Animal and Alimentary Productions, University of Perugia, Faculty of Veterinary Medicine, Via San Costanza, 4-06126 Perugia, Italy*

Correspondence should be addressed to Valeria Russo; valeria.russo@unina.it

Received 28 March 2013; Accepted 16 May 2013

Academic Editor: Lubna Nasir

This report describes the histopathology of two hundred and fifty-three mesenchymal tumors of the urinary bladder in cattle grazing on lands rich in bracken fern. Approximately 80% were hemangiomas and angiosarcomas. Hemangioma (capillary, cavernous, and large vessels) was the most frequent mesenchymal tumor and was more common than angiosarcoma. Although the appearance of endothelial cells can vary remarkably, epithelioid angiosarcomas, often containing multinucleated cells, were the most frequent malignant vascular tumors. Hemangiopericytoma and tumors of muscle and soft connective tissue origin, alone and/or in association with tumor-like lesions, were less frequently seen. Furthermore, forty-five cases of intravascular papillary endothelial hyperplasia (IPEH), a lesion not previously reported in the urinary bladder of cattle, were also described. Bovine papillomavirus type-2 DNA was amplified in tumor samples. Forty vascular tumors were investigated by dual-labeling immunofluorescence, and, for the first time, a coexpression of E5 and platelet-derived growth factor β receptor (PDGFβR) was shown to occur. The results show that the BPV-2 E5 oncoprotein binds to the activated form of the PDGFβ receptor thus playing an important role in mesenchymal as well as epithelial carcinogenesis of the urinary bladder. Furthermore, these findings demonstrate that BPV-2 infects both epithelial and mesenchymal cells.

1. Introduction

Tumors of the urinary bladder are quite rare in cattle, representing approximately 0.01% of all malignant tumors [1]. However, their incidence increases greatly (>90%) in adult cattle, reared in geographic regions rich in bracken fern (*Pteridium* spp.) [2–4]. Prolonged ingestion of bracken fern produces a clinical syndrome known as chronic enzootic hematuria (CEH), being characterized by hematuria and anemia. In over 90% of cases, hematuria originates from tumors of the urinary bladder [1, 5]. It is well known that this plant plays an important role in causing bladder tumors in cattle, either directly and/or indirectly. Toxic principles of bracken fern are known to be immunosuppressive, mutagenic, clastogenic, and carcinogenic [6, 7]; the most important carcinogen appears to be a sesquiterpenoid named ptaquiloside (PT) [8]. It has been suggested that PT targets both the stroma and the urothelium of urinary bladder [9]. PT is responsible for alkylation of the codon 61 of H-ras gene thus leading to an uncontrolled urothelial cell proliferation and urothelial cell dysplasia [9–11].

A strong synergism between bovine papillomavirus type 2 (BPV-2) and bracken fern has been shown in experimental bladder carcinogenesis [12], as well as in naturally occurring bovine bladder tumors [2, 4, 13, 14]. It is well known that PT can cause toxicity to the immune system, which could

contribute to the activation of a latent and/or subclinical urothelial BPV-2 infection resulting in neoplasia [13]. PT is a powerful immune suppressor that is genotoxic for lymphocytes [11, 15–17] and depresses NK cell activities [18].

Papillomavirus-associated bladder tumors are mainly urothelial in origin [4, 5, 19]. Numerous molecular pathways by which BPVs are able to transform urothelial cells are known to occur *in vivo*. It has been shown that BPV-2 is responsible for neoplastic transformation of urothelial cells via the activation of platelet-derived growth factor β receptor (PDGFβR) and/or of a tissue-specific protein named Calpain 3 [20, 21]. Mixed tumors (urothelial and mesenchymal) are frequently found in cattle grazing on fern-infested lands. In a recent survey, 331 out of 870 urinary bladder tumors (38%) showed a mesenchymal histogenesis and were found in cattle suffering from bovine enzootic hematuria [5]. Viral oncoproteins were found to be expressed also in vascular tumors of the bovine urinary bladder [22].

The purpose of this paper was to report some histologic features of the mesenchymal neoplastic lesions of the urinary bladder of cattle naturally exposed to bracken fern and infected with BPV-2.

2. Material and Methods

2.1. Tumor Samples. From 1999 to 2012, six hundred and fifty tumor samples of the urinary bladder were collected at public slaughterhouses from 4- to 30-year-old cattle that had suffered from chronic enzootic hematuria for several years. All the animals were known to graze on hilly/mountain pasturelands rich in bracken fern. For morphological investigations, the samples were fixed in 10% neutral buffered formalin and embedded in paraffin wax. Two hundred and fifty-three mesenchymal tumors were diagnosed on 4 μm-ticked sections that were stained with hematoxylin and eosin. The neoplastic lesions were classified according to criteria given in the 2004 World Health Organization (WHO) Blue Book on the pathology and genetics of tumors of the human urinary system as well as in more recent surveys about the soft tissue tumors of the urinary bladder [23–26].

2.2. Immunofluorescence and Confocal Laser-Scanning Microscopy. Two-color immunofluorescence staining was performed on forty vascular tumors (hemangiomas), to assess the expression of E5 and PDGF β receptors.

The sections were deparaffinized, rinsed in PBS, and heated in a microwave oven in citrate buffer to allow antigen unmasking. Slides were then preincubated with normal donkey serum diluted at 1 : 20 in PBS for 30 min and overlaid with polyclonal sheep anti-BPV-2 E5 diluted at 1 : 25 in PBS at 4°C, overnight, in a humid chamber. Then, a polyclonal goat anti-p-PDGFβ receptor antibody (Santa Cruz Biotechnology) diluted at 1 : 25 in PBS was applied overnight. A secondary antibody Alexa Fluor 488 donkey anti-sheep (green) (Invitrogen, Molecular Probes) and a secondary antibody Alexa Fluor 546 donkey anti-goat (red) (Invitrogen, Molecular Probes), diluted at 1 : 50 in PBS, were applied for 2 h at room temperature. The slides were washed three times with PBS and mounted under aqueous medium (Sigma-Aldrich). For observation and photography, a laser-scanning confocal microscope (LSM-510; Zeiss) was used.

Table 1: Histopathological types and number of mesenchymal tumors and tumor-like lesions in the bovine urinary bladder.

Details of tumors	No.	Percentage (%)
Tumors of vascular origin	*204*	*~81%*
Hemangioma	143	57%
Hemangioendothelioma	2	0.8%
Angiosarcoma	57	23%
Lymphangioma	2	0.8%
Hemangiopericytoma	9	3.6%
Glomus tumor	1	0.4%
Tumors of muscle origin	*16*	*~6%*
Leiomyoma	5	2%
Leiomyosarcoma	8	3.2%
Rhabdomyosarcoma	3	1.2
Miscellaneous mesenchymal neoplastic lesions	*23*	*9%*
Fibroma and stromal fibrous reaction	5	2%
Myxoma and stromal myxomatous reaction	13	5.2%
Fibrosarcoma	2	0.8%
Malignant lymphoma	3	*~1%*
Total	253	100%

3. Results

Two hundred and fifty-three out of six hundred and fifty bladder tumors were mesenchymal tumors (40%). Frequently, several different patterns of mesenchymal neoplasms coexisted. The size and location of neoplastic lesions varied greatly. In a few cases neoplasia was localized to a single site, but most tumors were shown to occur as multifocal lesions. Benign tumors (67%) were more common than malignant ones (33%). Mesenchymal tumors of the bladder are summarized in Table 1.

3.1. Tumor-Like Lesions and Tumors of Vascular Origin. Vascular tumors were seen in 204/253 cases accounting approximately for 81% of all bladder tumors.

3.1.1. Intravascular Papillary Endothelial Hyperplasia (IPEH). First described by Masson as "vegetant intravascular hemangioendothelioma" [27], it is a benign, florid proliferation of endothelial cells [28]. Very likely it does not represent a true tumor; it is believed to be an exuberant organization and recanalization of a thrombus [29] and is a rare lesion of the bladder in humans [30]. To our knowledge, the only one case of IPEH in veterinary medicine has been reported in the conjunctiva of a horse [31]. In the urinary bladder of cattle, this lesion is commonly observed. Both the *de novo*

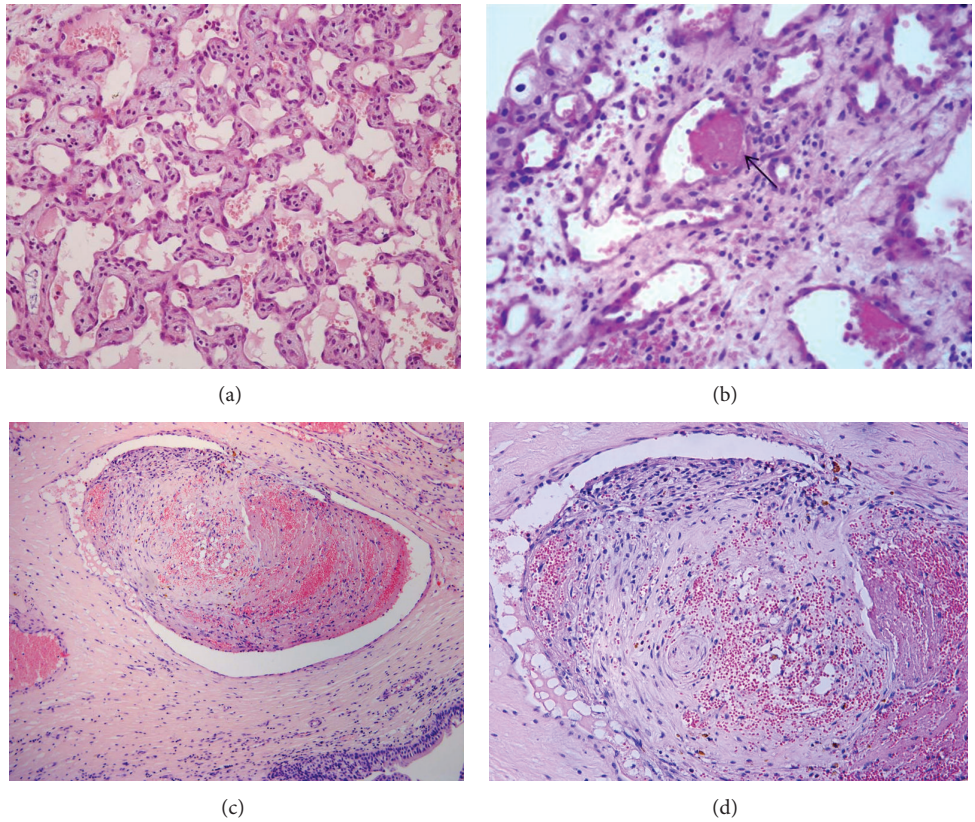

Figure 1: Intravascular papillary endothelial hyperplasia (IPEH). (a) Papillary structures within a vascular space, lined by monolayer and nonatypical endothelial cells, characterized this lesion (H&E, objective 20x). (b) Several intravascular fibrin deposits are seen (arrows) (H&E, objective 40x). (c) An exuberant, partly organized, and recanalyzed thrombus is shown (H&E, objective 10x). (d) As in (c) at higher magnification (H&E, objective 20x).

"pure" form and, more frequently, the mixed type associated with benign and malignant vascular and urothelial tumors were seen. The exclusively intravascular nature of the process, the lack of atypical cells and aberrant mitoses, and the hyaline appearance of the papillae covered by monolayered cells are characteristic features of the lesions in cattle as well as in humans (Figure 1(a)). Intravascular deposits of fibrin were present (Figure 1(b)), and, in some cases, there were exuberant, partly organized, and recanalized thrombi (Figures 1(c) and 1(d)).

3.1.2. Hemangioma. Hemangiomas in the present series were usually multiple and occurred anywhere in the bladder wall. The most common type of hemangioma was the *cavernous type*, which consisted of vascular lacunas, covered with endothelium, containing erythrocytes, and organized thrombi in the lumen (Figure 2(a)). Cavernous hemangioma has been observed alone or in association with the *capillary type*, consisting predominantly of closely packed aggregations of capillaries, usually of normal caliber, and separated by scant connective stroma (Figure 2(b)). Large-vessel hemangiomas were the less-common tumors and were generally composed of a combination of veins and arteries (*arteriovenous hemangiomas*) (Figure 2(c)).

In humans, bladder hemangioma is a rare benign lesion and is generally considered as a congenital anomaly, not infrequently associated with the Klippel-Trenaunay or Sturge-Weber syndromes [32, 33]. Hemangiomas are rare in animals as well [1]. On the contrary, in cattle with bovine enzootic hematuria, this was the most common soft tissue neoplasm of the urinary bladder (143/253 cases, 57% of all mesenchymal tumors). As in humans [29], cattle hemangioma can be classified according to the caliber of vessels in capillary, cavernous, and large-vessel hemangiomas.

3.1.3. Lymphangioma. This tumor occurred rarely in our survey (2/253 cases, 0.8%) and consisted of bundles of plump smooth muscle cells proliferating in and around lymphatic channels.

3.1.4. Angiosarcoma. Angiosarcoma consists of anastomosing vascular channels lined by endothelial cells with marked atypia and prominent nucleoli. Few cases of angiosarcoma in the urinary bladder have been reported in humans. On the contrary, these tumors were identified in approximately 23% of the cattle in the present series (57/253 cases). Most of these tumors have an *epithelioid pattern* and were composed

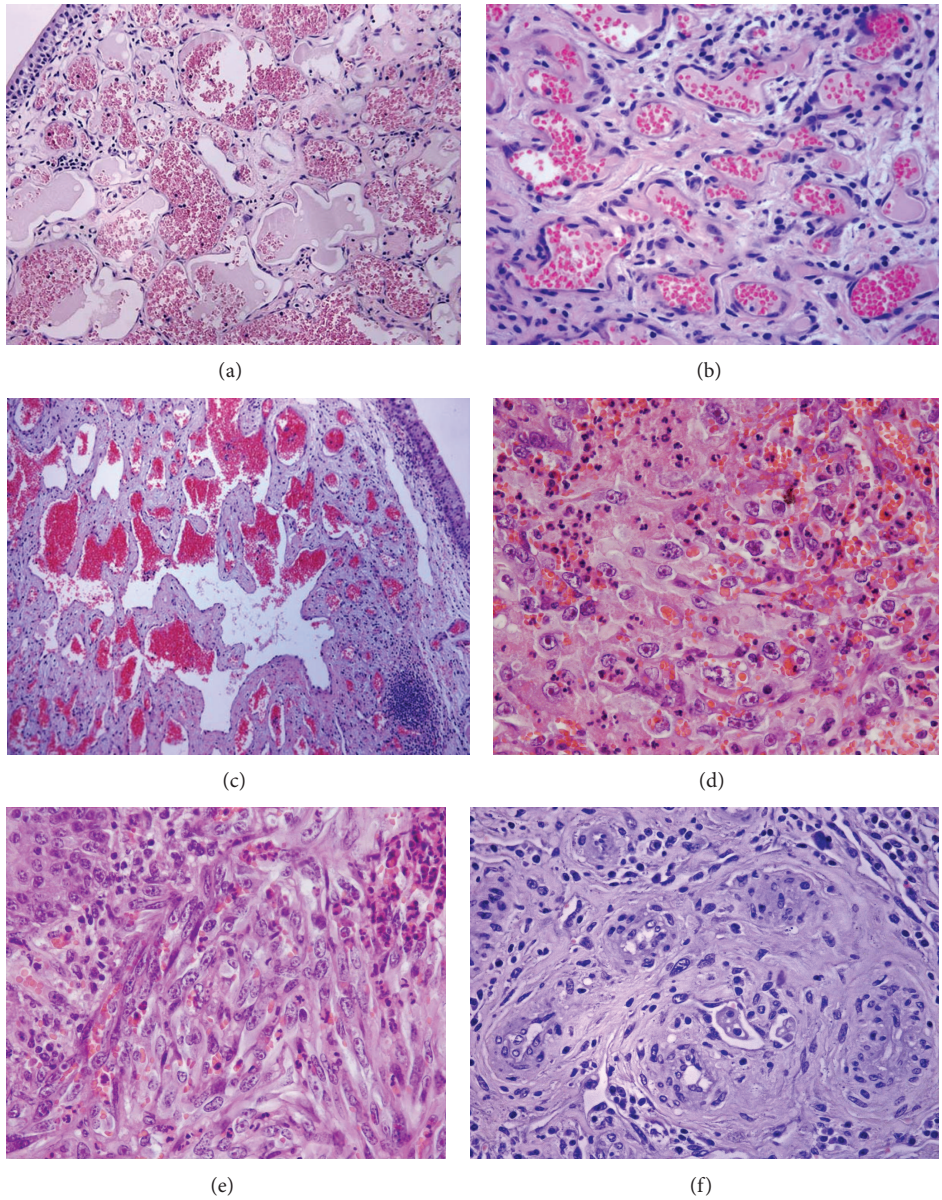

FIGURE 2: Tumors of vascular origin. (a) Cavernous haemangioma composed of vessels varying in size and shape (H&E, objective 20x). (b) Capillary hemangioma composed of small, rather uniform vessels (H&E, objective 20x). (c) Large-vessel hemangioma composed of intercommunicating vascular structures (H&E, objective 20x). (d) Epithelioid angiosarcoma characterized by round cells with vesicular nuclei with prominent nucleoli (H&E, objective 40x). (e) Kaposi-like hemangioendothelioma composed of spindle cells around vascular structures (H&E, objective 40x). (f) A particular staghorn appearance of the haemangiopericytoma (H&E, objective 40x).

of cords or nests of endothelial cells with an epithelioid morphology that formed small vascular structures (Figure 2(d)). Aberrant and multinucleated cells were seen in some of them. However, despite the fact that they often appear to be composed of marked atypical cells, they rarely metastasize. We found only one angiosarcoma that had metastasized to distant organs. Recently four epithelioid hemangiosarcomas were described in the urinary bladder of cows with severe enzootic haematuria. Neoplastic cells, like endothelial cells, were immunohistochemically positive to factor-VIII-related antigen and ultrastructurally often contained cytoplasmic intermediate filaments, resembling epithelial cells [34].

3.1.5. Hemangioendotelioma. The morphology of this tumor appears to be in a category between hemangioma and hemangiosarcoma and could arise in several organ systems, skin, and soft tissue. There are few reported cases arising primarily in the bladder [35].

We reported two cases of hemangioendotheliomas (0.8%) of the urinary bladder of cattle suffering from chronic

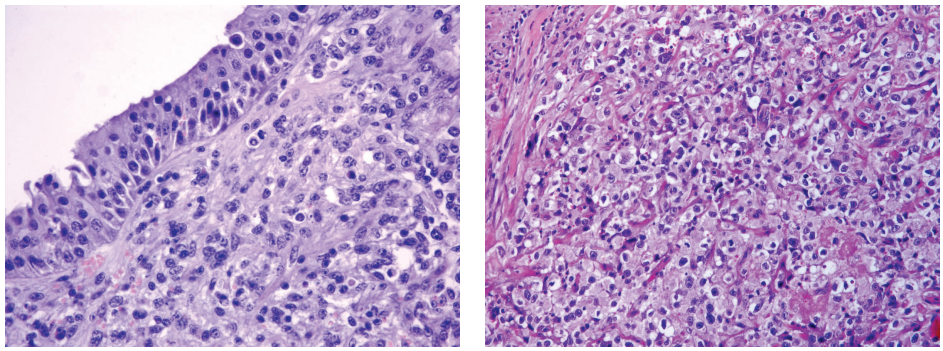

(a) (b)

Figure 3: Rhabdomyosarcoma: (a) suburothelial (cambium layer) proliferation of round cells with scant cytoplasm, vesicular nuclei, and prominent nucleoli (H&E, objective 40x); (b) rhabdomyosarcoma characterized by small round and spindle cells, some of which showing a deeply acidophilic cytoplasm (H&E, objective 20x).

enzootic haematuria. They were classified as Kaposi-like hemangioendotheliomas since they were characterized by a proliferation of fusiform tumor cells with eosinophilic cytoplasm and elongated nuclei, showing moderate atypia, associated to features of capillary hemangioma (Figure 2(e)). Kaposi-like hemangioendothelioma is extremely rare, and it has recently been described in the urinary bladder in a cow [36].

3.1.6. Hemangiopericytoma. Histologically this neoplasm appears to be composed of polygonal or spindle-shaped cells packed around branching vascular channels, with staghorn configuration (Figure 2(f)). Nine cases (3.6%) were reported in the cattle of the present series (Table 1). A similar percentage has been reported by other authors [5]. Unlike cattle, hemangiopericytoma of the urinary bladder is exceptionally rare in man. A review of the literature revealed rare cases arising primarily in the urinary bladder [26].

3.1.7. Glomus Tumor. Glomus tumor is composed of a proliferation of sharply demarcated modified smooth muscle cells, which are often arranged around dilated staghorn vessels. The cells contain a round nucleus and pale cytoplasm and generally low mitotic activity. The only case of multiple glomous tumor which has been reported in the present series was previously described by Roperto et al. [37].

3.2. Tumors of Muscle Origin

3.2.1. Leiomyoma, Leiomyosarcoma, and Rhabdomyosarcoma. In man, both benign and malignant tumors of smooth muscle origin are the most common mesenchymal tumors of the bladder [35]. Rhabdomyosarcoma of the bladder is relatively rare; however, the urinary bladder is believed to be the most common location for this type of tumor in the pediatric population since 90% of rhabdomyosarcomas in children are seen in the bladder [35]. Of the three types of rhabdomyosarcomas (embryonal, alveolar, and pleomorphic) by far the most common is the embryonal type [35, 38].

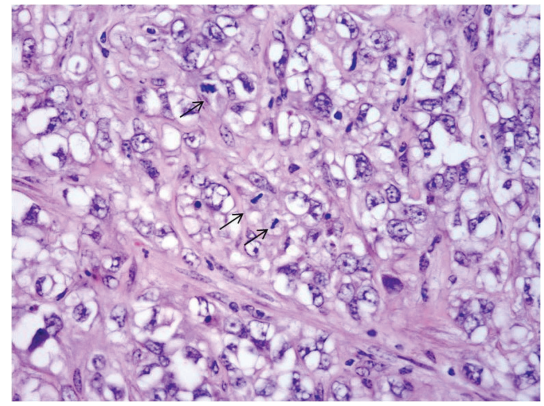

Figure 4: Bladder primary lymphoma composed of atypical cells showing vesicular nuclei, prominent nucleoli, and abnormal mitosis (arrows) (H&E, objective 40x).

Tumors of muscle origin represent approximately 6% (16/253) of the mesenchymal tumors of the present series (Table 1). We found five leiomyoma and eight malignant tumors, the microscopic patterns of which are consistent with the diagnosis of leiomyosarcoma. Histologically, these tumors are similar to those seen in other sites. We also found three cases of rhabdomyosarcoma. The microscopic patterns were characterized by a suburothelial (cambium layer) proliferation of round cells showing scant cytoplasm and vesicular nuclei containing prominent nucleoli. Rhabdomyosarcomas composed of small and spindle cells, some of them showing a deeply acidophilic cytoplasm, were also seen (Figures 3(a) and 3(b)).

3.3. Miscellaneous Mesenchymal Neoplastic Lesions of the Urinary Bladder. We found other neoplastic lesions arising in the bovine bladder. Three cases of malignant lymphoma were composed of numerous pleomorphic, hyperchromatic and lymphocytic cells, embedded in a delicate edematous stroma (Figure 4). Two fibromas and three stromal fibrous

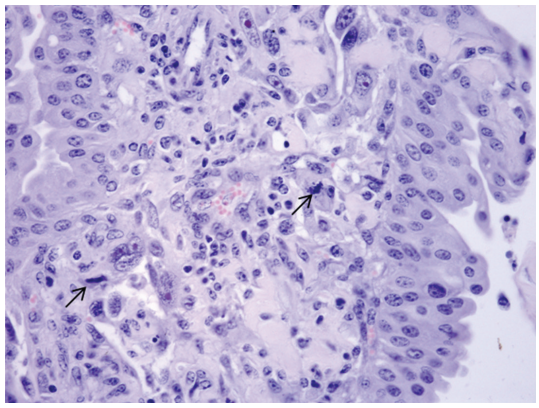

Figure 5: Carcinosarcoma shows an association of malignant epithelial and mesenchymal components. The latter is composed of large, abnormal cells with numerous mitoses (arrows) (H&E, objective 40x).

reactions, two fibrosarcomas, six true myxomas, and seven stromal mixomatous reactions were also seen.

Finally, three cases of carcinosarcomas, in which the mesenchymal component was composed of round cells with nuclear pleomorphism and hyperchromasia, were also documented (Figure 5).

3.4. Colocalization of E5 and PDGF b Receptors in Bladder Mesenchymal Tumours. In forty vascular tumors, the colocalization of E5 oncoprotein with the overexpressed and phosphorylated PDGFβR was clearly revealed by the yellow fluorescence of the merged image by laser-scanning confocal microscopy (LSCM) in endothelial cells (Figures 6(a), 6(b), and 6(c)). LSCM failed to detect this complex in normal endothelial cells (Figures 7(a), 7(b), and 7(c)). These findings show that BPV-2 virus, the DNA of which was already documented in tumor samples from soft tissue tumors collected by the laser microdissection method as previously reported [37], produces an active infection in mesenchymal cells of the urinary bladder and also plays an important role in the development of cancers of the soft tissue of the bovine urinary bladder.

4. Discussion

In human medicine mesenchymal tumors of the urinary bladder are uncommon neoplasms [35]. Soft tissue tumors and tumor-like lesions of the bladder are generally described in isolated case reports and short series [30, 35] and are by far less common than epithelial lesions.

Mesenchymal tumors are quite common in cattle harboring papillomavirus infection and grazing on lands rich in bracken fern, which shows that E5 protein, the major oncoprotein of BPV-2 and ptaquiloside and the major oncogenic factor of bracken fern, may play a synergistic role also in mesenchymal cancerogenesis of the urinary bladder.

It has been suggested that hemangiomas are congenital lesions arising from embryonic angioblastic stem cell [32, 39]. Some authors prefer to include arteriovenous malformation (AVM) of the urinary bladder in the spectrum of hemangiomas [35]. Furthermore, it is believed that hemangiomas diagnosed in adults are malformations detected later in life [30].

We never observed hemangiomas of the urinary bladder alone. These lesions were seen in association with other mesenchymal tumors but, mostly, with urothelial tumors in adult cattle. In addition, we detected, for the first time, that E5 oncoprotein binds to the activated (phosphorylated) form of PDGFβR that appears to be overexpressed in the endothelial cells of some hemangiomas. These findings allow us to suggest that bladder hemangiomas in cattle are not congenital malformations. We believe that the partnership between E5 oncoprotein and PDGFβR plays a crucial role also in mesenchymal bladder cancerogenesis in cattle. These observations confirm that BPV-2 is able to infect mesenchymal cells and corroborate our previous reports in which we showed that E5 oncoprotein interaction with PDGFβR is responsible for urothelial cell transformation [20]. It is worthwhile remembering that PDGF-B/PDGFβR is constitutively expressed in endothelial as well as in vascular smooth muscle cells (vSMCs) and pericytes, thus appearing to play a central role in vascular development [40]. Abnormal expression of PDGF-B and PDGFβR is associated with a severe vascular pathology [40]. Furthermore, it has been shown that CD4(+) and CD8(+) lymphocytes represent the most important reservoir of active BPV-2 in the blood of cattle as E5 oncoprotein has been detected in defined subsets of the peripheral blood mononuclear cells (PBMCs) [41]. Very likely, the high incidence of vascular tumors found in cattle suffering from chronic enzootic hematuria must be attributable to the transformation potential of E5 oncoprotein via the activation of the PDGFβR, which makes cattle unique among large animals.

There are fewer than 30 cases of primary angiosarcomas of the urinary bladder in man [35]. They are considered to be aggressive, high-grade tumors. Prognosis is poorer than angiosarcomas in other sites. Regional lymph nodes are typically spared but local recurrence with distant metastasis is the rule [42]. These patients tend to have rapidly progressing disease and poor long-term survival.

In cattle angiosarcomas of the urinary bladder are the most frequent malignant mesenchymal tumors. Most of them are epithelioid angiosarcomas, the cells of which share many morphological features with human angiosarcoma cells. Despite an aggressive appearance histologically, bovine angiosarcoma has a very low potential of metastasis. Out of 23 angiosarcoma in this series, only one showed metastasis to distant organs.

In papillomavirus-associated bladder tumors, severe diffuse inflammation is invariably present in the stroma of both urothelial and mesenchymal tumors [4, 43]. It is well known that papillomavirus L1 protein plays a central role both in infection and immunogenicity [44]. It has just been shown that L1 protein is surprisingly expressed in high-grade bladder cancer of ruminants [45]. L1 protein expression may contribute to chronic inflammation of tumor stroma known to have an important role in the progression and metastasis

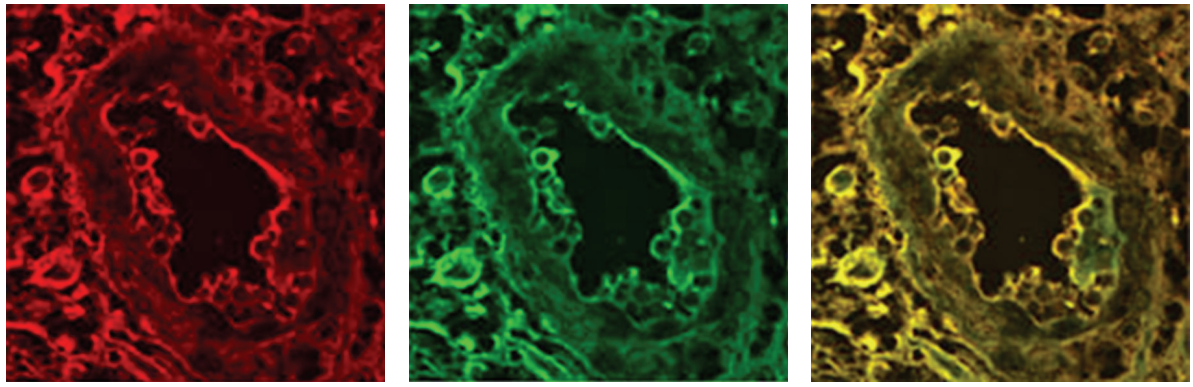

(a) (b) (c)

Figure 6: Hemangioma observed by confocal microscopy: (a) red immunofluorescence shows the overexpression and phosphorylation of the PDGFβ receptor, (b) green immunofluorescence detects the expression of the E5 oncoprotein, and (c) colocalization of the receptor and the oncoprotein documented by yellow immunofluorescence of the merged image.

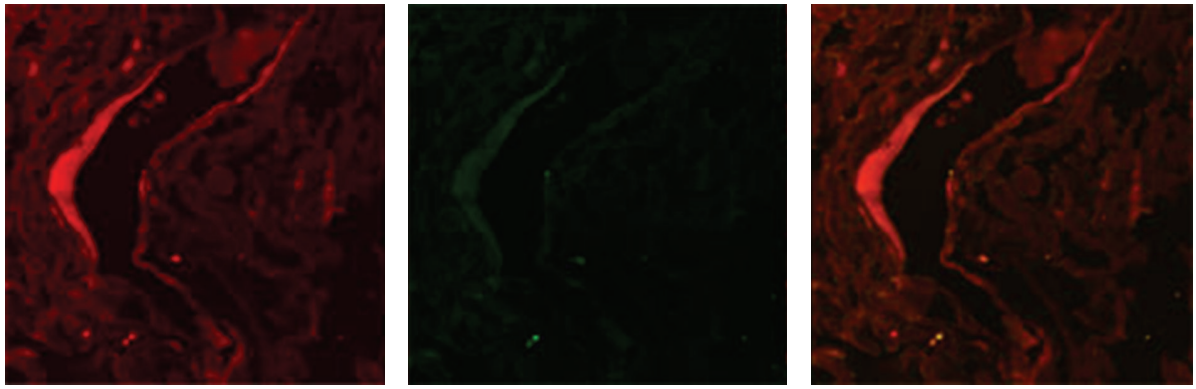

(a) (b) (c)

Figure 7: Normal vessel observed by confocal microscopy: (a) red immunofluorescence shows the expression and phosphorylation of the constitutive PDGFβ receptor, (b) green immunofluorescence shows no E5 oncoprotein, and (c) immunofluorescence of the merged image failed to show any colocalization of E5 oncoprotein with PDGFβ receptor.

of tumors. It has been suggested that immune cells play an emerging role in controlling tumor metastasis [46, 47].

Therefore, it is reasonable to believe that the L1-mediated severe inflammation of tumor stroma might play a role in controlling the metastatic potential of bladder tumors. Better understanding of the relationship, if any, between biological behavior of urothelial and mesenchymal tumors of ruminants and their stromal inflammation will be an important area of work in the future.

Finally, we report the first cases of IPEH of the urinary bladder in animals. Our work seems to strengthen the hypothesis that IPEH is not a true tumor but rather an exuberant organization and recanalization of a thrombus.

As spontaneous bladder pathology is quite common in cattle grazing on fern-infested pastures, we suggest that this species may serve as a spontaneous biological model that should prove rich ground for future research in papillomavirus biology and comparative bladder oncogenesis.

Conflict of Interests

The authors have no conflict of interests to declare.

Acknowledgments

This work was in part supported by grants from the Ministero dell'Università e della Ricerca Scientifica (MIUR) (PRIN 2009) and from the Ministero delle Politiche Agricole, Agroalimentari e Forestali.

References

[1] M. G. Maxie and S. J. Newman, "The urinary system," in *Jubb, Kennedy, and Palmer's Pathology of Domestic Animals*, M. G. Maxie, Ed., pp. 518–520, Saunders, San Diego, Calif, USA, 2007.

[2] A. M. Pamukcu, J. M. Price, and G. T. Bryan, "Naturally occurring and bracken fern induced bovine urinary bladder

tumors. Clinical and morphological characteristics," *Veterinary Pathology*, vol. 13, no. 2, pp. 110–122, 1976.

[3] A. Gava, D. Da Silva Neves, D. Gava, T. De Moura Saliba, A. L. Schild, and F. Riet-Correa, "Bracken fern (Pteridium aquilinum) poisoning in cattle in Southern Brazil," *Veterinary and Human Toxicology*, vol. 44, no. 6, pp. 362–365, 2002.

[4] S. Roperto, G. Borzacchiello, R. Brun et al., "A review of bovine urothelial tumours and tumour-like lesions of the urinary bladder," *Journal of Comparative Pathology*, vol. 142, no. 2-3, pp. 95–108, 2010.

[5] T. Carvalho, C. Pinto, and M. C. Peleteiro, "Urinary bladder lesions in bovine enzootic haematuria," *Journal of Comparative Pathology*, vol. 134, no. 4, pp. 336–346, 2006.

[6] I. A. Evans and J. Mason, "Carcinogenic activity of bracken," *Nature*, vol. 208, no. 5013, pp. 913–914, 1965.

[7] I. Hirono, "Carcinogenic principles isolated from bracken fern," *Critical Reviews in Toxicology*, vol. 17, no. 1, pp. 1–22, 1986.

[8] M. Shahin, B. L. Smith, and A. S. Prakash, "Bracken carcinogens in the human diet," *Mutation Research*, vol. 443, no. 1-2, pp. 69–79, 1999.

[9] R. M. Gil da Costa, P. A. Oliveira, M. M. S. M. Bastes et al., "Ptaquiloside-induced early-stage urothelial lesions show increased cell proliferation and intact β-Catenin and E-Cadherin expression," *Enviromental Toxicology*, vol. 27, no. 8, pp. 1–5, 2012.

[10] M. Shahin, M. R. Moore, S. Worrall, B. L. Smith, A. A. Seawright, and A. S. Prakash, "H-ras activation is an early event in the Ptaquiloside-induced carcinogenesis: comparison of acute and chronic toxicity in rats," *Biochemical and Biophysical Research Communications*, vol. 250, no. 2, pp. 491–497, 1998.

[11] R. M. Gil da Costa, P. A. Oliveira, M. Vilanova, M. M. S. M. Bastos, C. C. Lopes, and C. Lopes, "Ptaquiloside-induced, B-cell lymphoproliferative and early-stage urothelial lesions in mice," *Toxicon*, vol. 58, no. 6-7, pp. 543–549, 2011.

[12] M. S. Campo, B. W. O'Neil, R. J. Barron, and W. F. H. Jarrett, "Experimental reproduction of the papilloma-carcinoma complex of the alimentary canal in cattle," *Carcinogenesis*, vol. 15, no. 8, pp. 1597–1601, 1994.

[13] M. S. Campo, W. F. H. Jarrett, R. Barron, B. W. O'Neil, and K. T. Smith, "Association of bovine papillomavirus type 2 and bracken fern with bladder cancer in cattle," *Cancer Research*, vol. 52, no. 24, pp. 6898–6904, 1992.

[14] G. Borzacchiello, G. Lovane, M. L. Marcante et al., "Presence of bovine papillomavirus type 2 DNA and expression of the viral oncoprotein E5 in naturally occurring urinary bladder tumours in cows," *Journal of General Virology*, vol. 84, no. 11, pp. 2921–2926, 2003.

[15] R. C. Stocco Dos Santos, C. J. Lindsey, O. P. Ferraz et al., "Bovine papillomavirus transmission and chromosomal aberrations: an experimental model," *Journal of General Virology*, vol. 79, no. 9, pp. 2127–2135, 1998.

[16] M. B. Lioi, R. Barbieri, G. Borzacchiello et al., "Chromosome aberrations in cattle with chronic enzootic haematuria," *Journal of Comparative Pathology*, vol. 131, no. 2-3, pp. 233–236, 2004.

[17] V. Peretti, F. Ciotola, S. Albarella et al., "Chromosome fragility in cattle with chronic enzootic haematuria," *Mutagenesis*, vol. 22, no. 5, pp. 317–320, 2007.

[18] A. O. Latorre, B. D. Caniceiro, H. Fukumasu et al., "Ptaquiloside reduces NK cell activities by enhancing metallothionein expression, which is prevented by selenium," *Toxicology*, vol. 304, pp. 100–108, 2013.

[19] P. V. Peixoto, T. D. Do Nascimento França, C. S. L. Barros, and C. H. Tokarnia, "Histopathological aspects of Bovine Enzootic Hematuria in Brazil," *Pesquisa Veterinaria Brasileira*, vol. 23, no. 2, pp. 65–81, 2003.

[20] G. Borzacchiello, V. Russo, F. Gentile et al., "Bovine papillomavirus E5 oncoprotein binds to the activated form of the platelet-derived growth factor β receptor in naturally occurring bovine urinary bladder tumours," *Oncogene*, vol. 25, no. 8, pp. 1251–1260, 2006.

[21] S. Roperto, R. de Tullio, C. Raso et al., "Calpain3 is expressed in a proteolitically active form in papillomavirus-associated urothelial tumors of the urinary bladder in cattle," *PLoS ONE*, vol. 5, no. 4, Article ID e10299, 2010.

[22] G. Borzacchiello, V. Russo, C. Spoleto et al., "Bovine papillomavirus type-2 DNA and expression of E5 and E7 oncoproteins in vascular tumours of the urinary bladder in cattle," *Cancer Letters*, vol. 250, no. 1, pp. 82–91, 2007.

[23] J. N. Eble, G. Sauter, J. I. Epstein et al., *World Health Organization Classification of Tumours. Pathology and Genetics of Tumours of the Urinary System and Male Genital Organs*, IARC Press, Lyon, France, 2004.

[24] R. Montironi and A. Lopez-Beltran, "The 2004 WHO classification of bladder tumors: a summary and commentary," *International Journal of Surgical Pathology*, vol. 13, no. 2, pp. 143–153, 2005.

[25] S. Lott, A. Lopez-Beltran, R. Montironi, G. T. MacLennan, and L. Cheng, "Soft tissue tumors of the urinary bladder. Part II: malignant neoplasms," *Human Pathology*, vol. 38, no. 7, pp. 963–977, 2007.

[26] S. Lott, A. Lopez-Beltran, G. T. MacLennan, R. Montironi, and L. Cheng, "Soft tissue tumors of the urinary bladder, part I: myofibroblastic proliferations, benign neoplasms, and tumors of uncertain malignant potential," *Human Pathology*, vol. 38, no. 6, pp. 807–823, 2007.

[27] K. P. Clearkin and F. M. Enzinger, "Intravascular papillary endothelial hyperplasia," *Archives of Pathology and Laboratory Medicine*, vol. 18, pp. 441–444, 1976.

[28] G. Pelosi, A. Sonzogni, and G. Viale, "Intravascular papillary endothelial hyperplasia of the renal vein," *International Journal of Surgical Pathology*, vol. 19, no. 4, pp. 518–520, 2011.

[29] J. Rosai, "Soft tissues," in *Rosai and Ackerman's Surgical Pathology*, J. Rosai and L. V. Ackerman, Eds., vol. 2, pp. 2288–2290, Mosby, Edinburgh, UK, 2004.

[30] F. Tavora, E. Montgomery, and J. I. Epstein, "A series of vascular tumors and tumorlike lesions of the bladder," *American Journal of Surgical Pathology*, vol. 32, no. 8, pp. 1213–1219, 2008.

[31] H. D. Herrera, A. G. Duchene, J. O. Croxatto, N. Burgués, and H. Amusquibar, "Intravascular papillary endothelial hyperplasia of the conjunctiva in a horse," *Veterinary Ophthalmology*, vol. 6, no. 3, pp. 269–272, 2003.

[32] L. Cheng, A. G. Nascimento, R. M. Neumann et al., "Hemangioma of the urinary bladder," *Cancer*, vol. 86, no. 3, pp. 498–504, 2009.

[33] L. Cheng, "Heamangioma," in *World Health Organization Classification of Tumors. Pathology and Genetics of Tumours of the Urinary System and Male Genital Organs*, J. N. Eble, G. Sauter, J. I. Epstein, and I. A. Sesterhenn, Eds., p. 146, IARC Press, Lyon, France, 2004.

[34] I. Pires, F. Silva, F. L. Queiroga et al., "Epithelioid hemangiosarcomas of the bovine urinary bladder: a histologic, immunohistochemical, and ultrastructural examination of four tumors,"

Journal of Veterinary Diagnostic Investigation, vol. 22, no. 1, pp. 116–119, 2010.

[35] F. Tavora, O. N. Kryvenko, and J. I. Epstein, "Mesenchymal tumours of the bladder and prostate: an update," *Pathology*, vol. 45, pp. 104–115, 2013.

[36] I. Pires, F. L. Queiroga, F. Silva, C. Pinto, and C. Lopes, "Kaposi-like vascular tumor of the urinary bladder in a cow," *Journal of Veterinary Medical Science*, vol. 71, no. 6, pp. 831–833, 2009.

[37] S. Roperto, G. Borzacchiello, R. Brun et al., "Multiple glomus tumors of the urinary bladder in a cow associated with bovine papillomavirus type 2 (BPV-2) infection," *Veterinary Pathology*, vol. 45, no. 1, pp. 39–42, 2008.

[38] C. B. Jones Jr. and H. A. Oberman, "Rhabdomyosarcoma of the bladder: occurrence in childhood and in advanced age," *The Journal of urology*, vol. 91, pp. 533–537, 1964.

[39] D. F. Brobst and C. Olson, "Neoplastic and proliferative lesions of the bovine urinary bladder," *American Journal of Veterinary Research*, vol. 24, pp. 105–111, 1963.

[40] J. Andrae, R. Gallini, and C. Betsholtz, "Role of platelet-derived growth factors in physiology and medicine," *Genes and Development*, vol. 22, no. 10, pp. 1276–1312, 2008.

[41] S. Roperto, S. Comazzi, E. Ciusani et al., "PBMCS are additional sites of productive infection of bovine papillomavirus type 2," *Journal of General Virology*, vol. 92, no. 8, pp. 1787–1794, 2011.

[42] J. D. Engel, T. M. Kuzel, M. C. Moceanu, M. G. Oefelein, and A. J. Schaeffer, "Angiosarcoma of the bladder: a review," *Urology*, vol. 52, no. 5, pp. 778–784, 1998.

[43] S. Roperto, V. Russo, A. Ozkul et al., "Bovine papillomavirus type 2 infects the urinary bladder of water buffalo (Bubalus bubalis) and plays a crucial role in bubaline urothelial carcinogenesis," *Journal of General Virology*, vol. 94, no. 2, pp. 403–408, 2013.

[44] Y. Modis, B. L. Trus, and S. C. Harrison, "Atomic model of the papillomavirus capsid," *EMBO Journal*, vol. 21, no. 18, pp. 4754–4762, 2002.

[45] S. Roperto, V. Russo, A. Ozkul et al., "Productive infection of bovine papillomavirus type 2 in the urothelial cells of naturally occurring urinary bladder tumors in cattle and water buffaloes," *PLoS One*, vol. 8, no. 5, Article ID e62227, 2013.

[46] D. G. DeNardo, M. Johansson, and L. M. Coussens, "Immune cells as mediators of solid tumor metastasis," *Cancer and Metastasis Reviews*, vol. 27, no. 1, pp. 11–18, 2008.

[47] F. I. Staquicini, A. Tandle, S. K. Libutti et al., "A subset of host B lymphocytes controls melanoma metastasis through a melanoma cell adhesion molecule/MUC18-dependent interaction: evidence from mice and humans," *Cancer Research*, vol. 68, no. 20, pp. 8419–8428, 2008.

Hindawi Publishing Corporation
BioMed Research International
Volume 2013, Article ID 251098, 7 pages
http://dx.doi.org/10.1155/2013/251098

Research Article

Long Noncoding RNA HOTAIR Is Associated with Motility, Invasion, and Metastatic Potential of Metastatic Melanoma

Lihua Tang,[1] Wei Zhang,[2,3] Bing Su,[2,3] and Bo Yu[1,3,4,5]

[1] *The Affiliated Shenzhen Hospital, Anhui Medical University, Hefei, Anhui 230001, China*
[2] *Biomedical Research Institute, Shenzhen PKU-HKUST Medical Center, Shenzhen, Guangdong 518036, China*
[3] *Shenzhen Key Lab for Translational Medicine of Dermatology, Shenzhen PKU-HKUST Medical Center, Shenzhen, Guangdong 518036, China*
[4] *Shenzhen Key Discipline of Dermatology, Shenzhen Hospital, Peking University, Shenzhen, Guangdong 518036, China*
[5] *Department of Dermatology, Shenzhen Hospital, Peking University, Shenzhen, Guangdong 518036, China*

Correspondence should be addressed to Bing Su; bsu2@buffalo.edu and Bo Yu; yubomd@163.com

Received 22 February 2013; Accepted 21 May 2013

Academic Editor: Marcelo Palma Sircili

Metastatic melanoma, the primary cause of skin cancer-related death, warrants new therapeutic approaches that target the regulatory machinery at molecular level. While long noncoding RNAs (lncRNAs) are dysregulated in a number of cancer types, limited data are available on the expression and function of lncRNAs in melanoma metastasis. The primary objective of this study was to investigate the role of 6 metastasis-related lncRNAs in pairs of primary melanoma and matched lymph node metastatic tissues. Among the tested lncRNAs, HOTAIR was the most highly expressed in lymph node metastasis. The role of HOTAIR in melanoma cell motility and invasion was further evaluated by knocking down HOTAIR with siRNAs. Knockdown of HOTAIR resulted in the reduction of motility and invasion of human melanoma cell line A375, as assessed by wound healing assay and Matrigel-based invasion assay. siHOTAIR also suppressed the degradation of gelatin matrix, suggesting that HOTAIR promotes gelatinase activity. Together, our study shows that HOTAIR is overexpressed in metastatic tissue, which is associated with the ability of HOTAIR to promote melanoma cell motility and invasion. These data indicate that lncRNAs may be involved in the metastasis of melanoma and provide support for further evaluation of lncRNAs in melanoma.

1. Introduction

Although the incidence of malignant melanoma accounts for only approximately 1% of cutaneous tumors, it is among the few cancers with a remarkably high mortality rate. This is mainly due to its high potential to metastasize to the vital organs such as lungs, liver, and brain. Approximately 80% of skin cancer-related mortality is due to melanoma (http://www.chinaswzl.com/cancer/hsslby/2493.html).

The worldwide incidence of melanoma is increasing [1]. Statistical analysis of the melanoma cases collected in recent years in our department shows that the incidence of melanoma is much higher than the Chinese national average and is still increasing, especially in the younger population in southern industrial cities in China. This phenomenon may be caused by complex environmental factors and long sun exposure (Yu B, unpublished data).

Noncoding RNAs (ncRNAs) are emerging as new regulators in the cancer paradigm. They have demonstrated potential roles in both oncogenic and tumor suppressive pathways [2, 3]. ncRNAs are largely grouped into two major classes based on transcript sizes: small ncRNAs (<200 kb) and long ncRNAs (lncRNAs) (>200 kb) [4, 5]. Small ncRNAs include a broad range of well-known and newly discovered RNA species, with many being associated with 5′ or 3′ regions of genes. This class includes the well-documented miRNAs. It has been widely reported that cancer-specific miRNAs can be

detected in the blood, sputum, and urine of cancer patients and serve as diagnostic and prognostic markers [6–8].

LncRNAs, ranging from 200 nucleotides to over 10 kb, are abundantly transcribed by the mammalian genome [9, 10]. LncRNAs have been found to be dysregulated in a wide range of human diseases and disorders, including various cancers. For example, PCGEM [11] and DD3 [12] are overexpressed in prostate cancer as compared to adjacent normal prostate tissue, implicating a role for these lncRNAs in prostate tumorigenesis [13]. BC200 RNA overexpression is correlated with the progression of breast cancer and has been proposed to be a new molecular marker for breast cancer [14]. Increased expression of MALAT-1 RNA indicates a worse clinical outcome in lung cancer patients [15]. Gupta et al. recently revealed an important role for HOTAIR in breast cancer metastasis. HOTAIR is highly induced (up to 2,000-fold) in breast cancer metastatic tissues [16]. In addition, overexpression of HOTAIR in primary breast tumors is a powerful predictor of eventual metastasis and death [16]. These studies provide evidence and support that lncRNAs may be involved in tumorigenesis and tumor progression.

However, research on the expression and function of lncRNAs in melanoma is still limited. In this study, we analyzed the expression profiles of 6 well documented metastasis-related lncRNAs in 3 pairs of primary melanoma and matched lymph node metastatic tissues using real-time quantitative RT-PCR. Further, we investigated the role of HOTAIR in melanoma cell motility and invasion. Our study provides novel insights into the role of lncRNAs in the metastatic progression of melanoma and identifies a potential new target for the treatment of metastatic melanoma.

2. Materials and Methods

2.1. Tissue Samples. Three pairs of primary melanoma and matched lymph node metastatic tissues were obtained from the Department of Gastric Cancer and Soft Tissue Sarcoma Surgery at the Fudan University Shanghai Cancer Center. The protocol was approved by the Institutional Review Board of Fudan University. Patients enrolled in the study were provided with written informed consent. Fresh tissue samples were collected and cut into fragments <0.5 cm in any single dimension. The tissues were then immersed into 2 mL RNAlater (Ambion, Foster City, CA). All the tissue samples were frozen within 30 minutes after surgery and stored in liquid nitrogen until use. Tissue sections from each sample were reviewed and classified by a pathologist.

2.2. Cell Culture. Human metastatic melanoma cell line A375 was obtained from the Typical Cell Culture Collection Committee of the Chinese Academy of Sciences. A375 cells were maintained in Dulbecco's modified Eagle's media (DMEM) supplemented with 10% fetal bovine serum (FBS).

2.3. Quantitative Reverse Transcriptase PCR (qRT-PCR) of Six lncRNAs. Total RNA was isolated from melanoma and lymph node metastatic tissues using the RNeasy kit (Qiagen, Grand Island, NY) according to the manufacturer's instructions.

Table 1: Nucleotide sequence of primers for lncRNA qPCR.

lncRNA	Sequence
HOTAIR-F	5′-CAGTGGGGAACTCTGACTCG-3′
HOTAIR-R	5′-GTGCCTGGTGCTCTCTTACC-3′
HULC-F	5′-TCATGATGGAATTGGAGCCTT-3′
HULC-R	5′-CTCTTCCTGGCTTGCAGATTG-3′
MALAT1-F	5′-TAGGAAGACAGCAGCAGACAGG-3′
MALAT1-R	5′-TTGCTCGCTTGCTCCTCAGT-3′
MEG3-F	5′-GCCAAGCTTCTTGAAAGGCC-3′
MEG3-R	5′-TTCCACGGAGTAGAGCGAGTC-3′
NEAT1-F	5′-TGGCTAGCTCAGGGCTTCAG-3′
NEAT1-R	5′-TCTCCTTGCCAAGCTTCCTTC-3′
UCA1/CDUR-F	5′-CATGCTTGACACTTGGTGCC-3′
UCA1/CDUR-R	5′-GGTCGCAGGTGGATCTCTTC-3′

Reverse transcription (RT) reactions were performed with 1 μg total RNA using a PrimeScript RT reagent kit (TaKaRa BIO, Shiga, Japan). Random hexamer primers were used in the RT reactions. Real-time qPCR was performed on a Bio-Rad CFX-96 real-time PCR system (Bio-Rad, Hercules, CA) using SYBR Premix DimerEraser kit (TaKaRa, Shiga, Japan). GAPDH was used as an endogenous control for the qRT-PCR reactions (TaKaRa, Shiga, Japan). All assays were performed in triplicates. The $2^{-\Delta\Delta Ct}$ method was used to calculate the expression of each lncRNA. All the reactions were carried out with strict compliance with the MIQE (Minimum Information about Quantitative Real-Time PCR Experiments) guidelines. Sequences of the real-time PCR primers are listed in Table 1.

2.4. siRNA Transfection. A375 cells (3×10^4/well) were plated in 6-well plates overnight. Cells were then transfected with 50 nM nontargeting siRNA control (siControl), 50 nM siRNA against HOTAIR I (siHOTAIR I, SASI_Hs02_00380445), or siHOTAIR II (SASI_Hs02_00380446, Sigma Aldrich) for 24 h using Lipofectamine 2000 transfection reagent (Invitrogen, Grand Island, NY) according to the manufacturer's protocol. Following the transfections, A375 cells were then harvested for experiments as indicated.

2.5. Wound Healing Assay. A375 cells were transfected with siControl, siHOTAIR I, or siHOTAIR II and grew into confluent monolayers overnight. Scratches were generated with a sterile 200 μL pipette tip. Cell migration towards the wounds was monitored at 0 hours and 24 hours using a light microscope.

2.6. Invasion Assay. Modified Boyden chamber assay was performed to assess cell invasion by using BioCoat Matrigel invasion chambers with 8 μm pores (BD, Franklin Lakes, NJ). A375 cells (5×10^4/chamber, in 100 μL of serum-free DMEM) were added to the inserts of invasion chambers. FBS (10% in 600 μL DMEM) was added as a chemoattractant in the lower chambers. After 24 hours of incubation, cells that had not penetrated the membranes were removed from

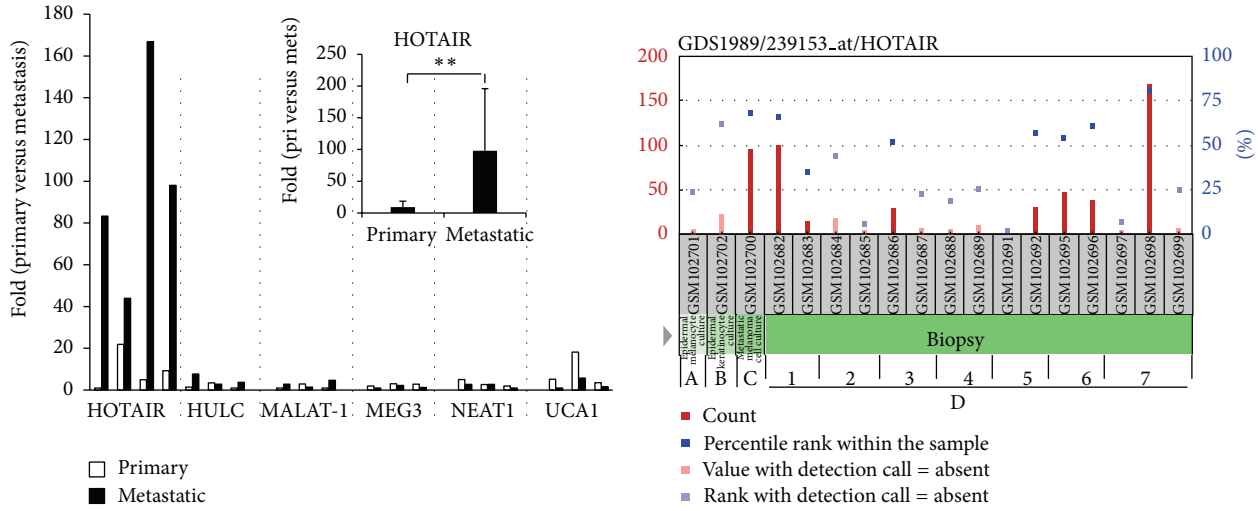

Figure 1: HOTAIR is upregulated in lymph node metastasis of melanoma. (a) Expression profiles of lncRNAs in melanoma and matched lymph node metastatic tissues. Quantitative RT-PCR was performed on 6 lncRNAs in melanoma and their matched metastatic tissue samples. HOTAIR expression was summarized in the insert. $^{**}P < 0.01$. (b) GEO analysis of HOTAIR in 4 types of specimens and several disease states related to melanoma. The image was adapted from the GEO website. (A) Epidermal melanocyte culture; (B) epidermal keratinocyte culture; (C) metastatic melanoma cell culture; (D) biopsy. (1) Normal; (2) benign nevus; (3) atypical nevus; (4) melanoma in situ; (5) vertical growth phase melanoma; (6) metastatic growth phase melanoma; (7) lymph node metastasis.

the upper chambers with cotton swabs. Chamber membranes were fixed and stained using Diff-Quik Stain Set (Dade Behring Inc., Newark, DE) and examined under a bright-field microscope. Invasion was assessed by counting 6 fields per membrane (×20 objective).

2.7. In Situ Zymography. Glass coverslips were coated with 0.2 mg/mL Oregon green 488-conjugated gelatin (Invitrogen), cross-linked in 0.5% glutaraldehyde for 15 minutes at 4°C, and incubated with 5 mg/mL $NaBH_4$ for 3 minutes. The coverslips were then sterilized with 70% ETOH for 15 minutes and incubated in serum-free media for 1 hour at 37°C. A375 cells transfected with siRNA-NS or siHOTAIR (I and II) were plated on gelatin-coated coverslips, incubated at 37°C for 24 hours, and processed by fluorescence microscopy procedures. Cell morphology was photographed under a light microscope.

2.8. Statistical Analysis. Statistical significances between groups were determined by two-tailed Student's t-test. For paired melanoma tissues, the difference of lncRNA expression was evaluated with Wilcoxon matched pairs signed ranks test. $P < 0.05$ was considered statistically significant.

3. Results

3.1. LncRNA Expression in Melanoma and Matched Lymph Node Metastatic Tissues. Expression profiles of 6 lncRNAs that have been found to be associated with cancer or metastasis [17] were examined by qRT-PCR in 3 pairs of primary melanoma and matched lymph node metastatic tissues. We observed that most of the lncRNAs (5 out of 6) were differentially regulated in melanomas versus matched metastatic tissues (Figure 1(a)). Among them, HOTAIR was significantly overexpressed in metastatic lymph nodes compared to matched primary melanoma ($P < 0.01$) (Figure 1(a)).

Further, data mining of publically available gene profiling database Gene Expression Omnibus (GEO) showed that HOTAIR expression is markedly higher in melanomas compared with nontumor tissues, and the highest expression was observed in tumors spread to regional lymph nodes (Figure 1(b)), suggesting that HOTAIR expression is linked to the progression and metastasis of melanoma.

3.2. Knockdown of HOTAIR Suppressed Metastatic Melanoma A375 Cell Motility. Cell migration is an essential step in metastasis. Therefore, we next examined the ability of HOTAIR to affect cell motility using the scratch "wound" healing assays in human metastatic melanoma cell line A375. HOTAIR expression in A375 cells was knocked down by siRNAs and confirmed by real-time qPCR (Figure 2(a)). The wound healing assay showed that siControl-transfected A375 cells covered almost the entire damaged area by 24 hours (Figure 2(b)). In contrast, the wounded area was only partially covered by siHOTAIR-transfected cells after 24 hours of incubation (Figure 2(b)), suggesting that HOTAIR promotes melanoma cell motility.

3.3. Knockdown of HOTAIR Decreased A375 Cell Invasion. To further examine the involvement of HOTAIR in melanoma cell invasion, Matrigel-based Boyden chamber assay was performed. Knockdown of HOTAIR by siRNAs resulted in a

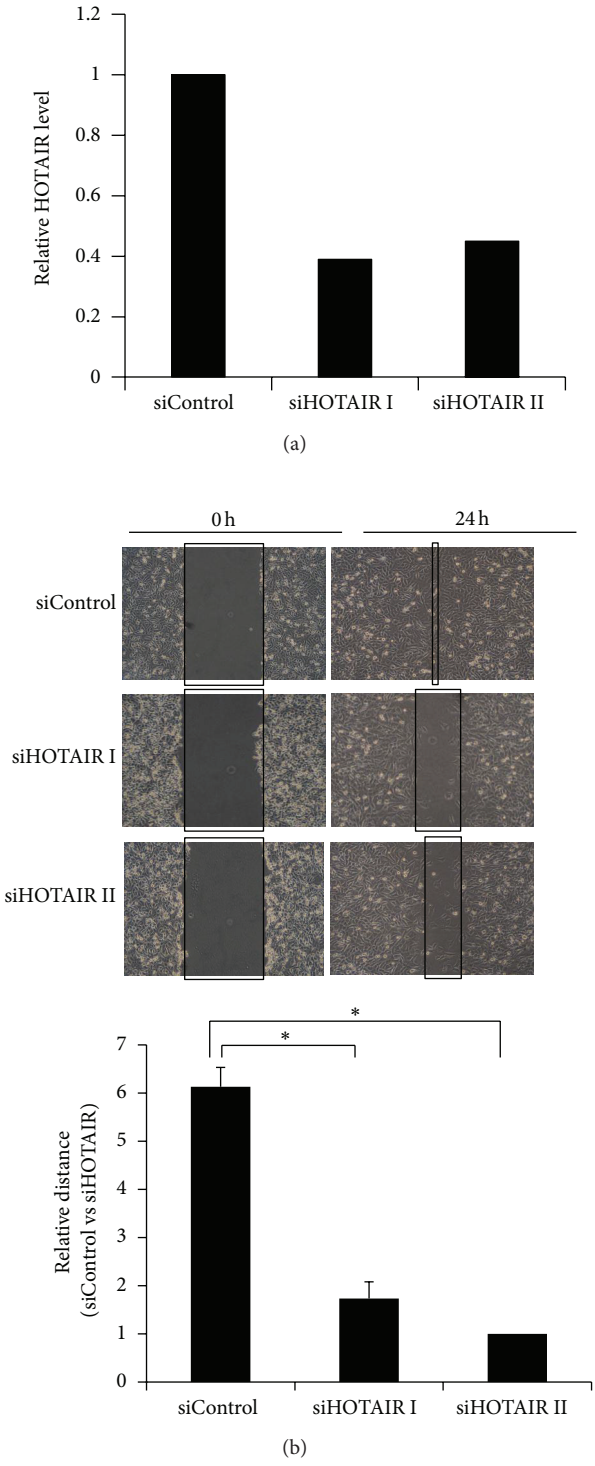

Figure 2: Knockdown of HOTAIR decreases melanoma A375 cell motility. (a) qRT-PCR analysis was performed to examine HOTAIR RNA levels in A375 cells transfected with siControl, siHOTAIR I, or siHOTAIR II. (b) Wounds were introduced by scratching confluent monolayers of A375 cells transfected with siControl, siHOTAIR I, or siHOTAIR II. Migration was monitored by light microscopy at 0 hours and 24 hours (upper panel). The widths of the gaps from 3 experiments were measured and the results are presented in a bar graph (lower panel). $^{*}P < 0.05$.

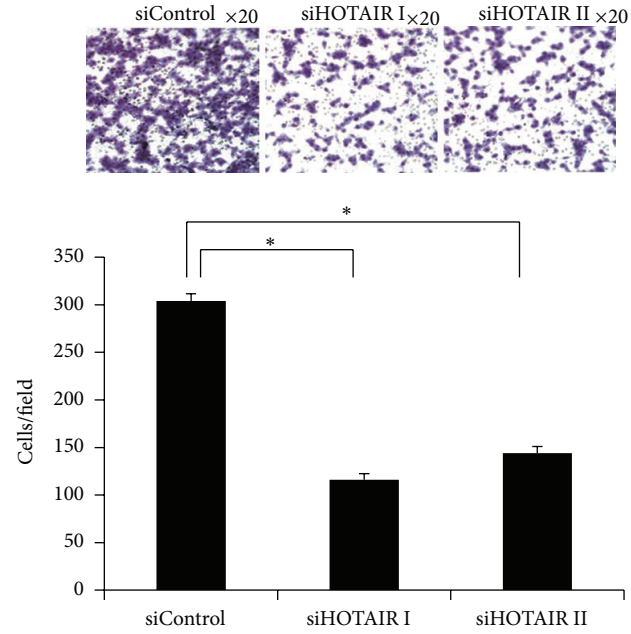

Figure 3: Knockdown of HOTAIR inhibits the invasion of melanoma A375 cells. Matrigel-based invasion assay was performed using modified Boyden chambers with 10% FBS as a chemoattractant. Representative images were presented. The cell numbers per field were counted and the results are summarized in a bar graph. $^{*}P < 0.05$.

~3-fold reduction of the invasiveness of A375 cells ($P < 0.01$; Figure 3). Taken together, these data indicate that knockdown of HOTAIR inhibits in vitro parameters associated with metastasis including motility and invasion.

3.4. Degradation of Matrix In Situ Was Suppressed by Knockdown of HOTAIR. Tumor cell invasion associated with metastasis requires both specialized cell migration and the ability to degrade basement membrane by secreted or membrane-bound proteases [18]. We sought to determine whether matrix metalloproteinase (MMPs), known to be upregulated in many metastatic tumors, might be responsible for HOTAIR-potentiated invasion. Gelatinase activity, indicating the activity of MMP-2 and MMP-9, was assessed by in situ zymography. The ability of A375 cells to degrade matrix in situ was markedly suppressed by siRNA-HOTAIR (I and II), as indicated by the reduced black holes representing matrix degradation (Figure 4(b)). This result suggests that HOTAIR promotes gelatinase activity in melanoma cells.

4. Discussion

Increasing studies provide evidence and support that ncRNAs are key factors in gene regulation and influence normal and cancer cell phenotypes [19–22].

LncRNAs belong to a novel class of ncRNA. They contain longer than 200 nucleotides and have no protein-coding

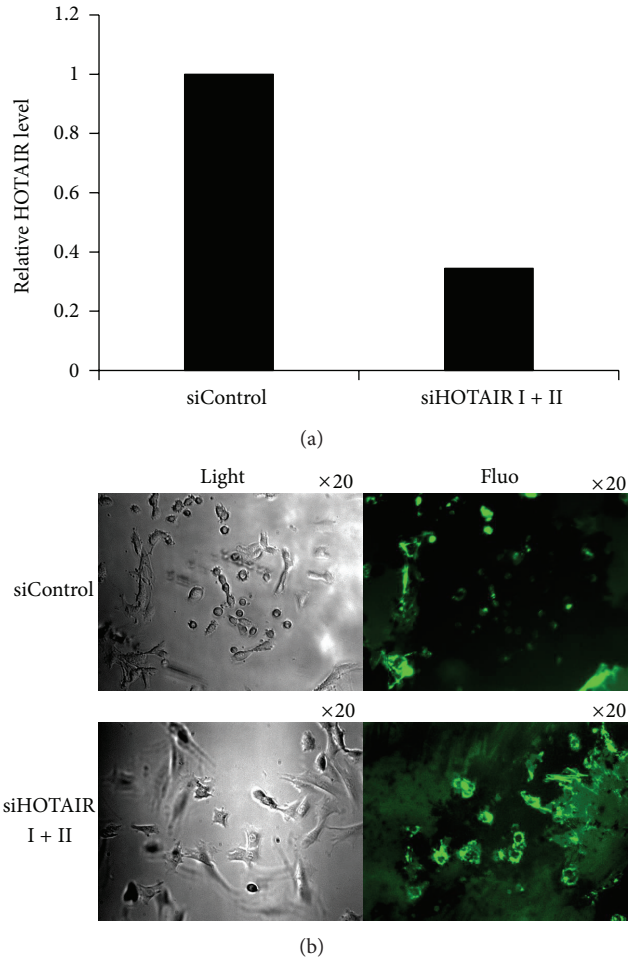

Figure 4: Degradation of matrix in situ is suppressed by knockdown of HOTAIR. (a) qRT-PCR analysis was performed to examine HOTAIR RNA levels in A375 cells transfected with siControl or siHOTAIR (I and II). (b) A375 cells were transfected with siControl or siHOTAIR (I and II) for 24 hours. In situ zymography was performed with Oregon green 488-conjugated gelatin. Cells were plated on gelatin matrix and incubated for 24 hours. The slides were observed by phase-contrast microscopy (left column), and gelatin degradation was visualized by fluorescence microscopy (right column).

capacity [23]. Several lncRNAs have been reported to control transcriptional alterations, implying that the difference in lncRNA profiling between normal and cancer cells is not just the secondary effect of cancer transformation [24]. On the contrary, lncRNAs are strongly associated with cancer progression [24]. However, little information regarding the expression profiles of lncRNAs in melanoma is available. Hence, in this study, we selected 6 well-documented lncRNAs associated with metastasis including MALAT1 [15, 16], HOTAIR [16], NEAT-1 [25], HULC [26], MEG-3 [27], and UCA1 [28] to evaluate their expression in primary melanoma and matched lymph node metastasis tissues. We observed that HOTAIR is the only consistently overexpressed lncRNA among the 6 lncRNAs in melanoma metastasis compared to matched primary tumors. Four other lncRNAs were differentially expressed in melanoma versus lymph node metastasis.

HOTAIR was initially identified as one of the 231 ncRNAs associated with human HOX loci [16]. HOTAIR promoted metastasis in breast cancer [16]. There is growing evidence that HOTAIR may have prometastasis activity in several cancer types, including breast [16], pancreatic [29], and hepatocellular carcinoma (HCC) [30]. Whether HOTAIR performs the same function in the progression of melanoma remains unknown. To understand the role of HOTAIR in melanoma progression, a series of in vitro assays were performed. Studies using wound healing assay demonstrate that knockdown of HOTAIR inhibits the migration of melanoma cells. The invasiveness of melanoma cells is also markedly suppressed by knocking down HOTAIR, as demonstrated by the Matrigel-based Boyden chamber assay. Recently, Geng et al. found that HOTAIR expression is elevated in HCC tumors compared with adjacent nontumor tissues [31]. HOTAIR expression is correlated with lymph node metastasis in HCC [31]. siRNA-mediated knockdown of HOTAIR in HCC cells was accompanied by a deduction in MMP-9, suggesting that MMP-9 may be involved in HOTAIR-mediated regulation of HCC progression [31]. As MMP-9 plays an important role in tumor metastasis, gelatinase activity (indicating the activity of MMP-2 and MMP-9) was assessed by in situ zymography, which is a unique technique for revealing proteolytic activity at specific sites in tissues or cell cultures. Results indicate that the degradation of matrix was suppressed by knockdown of HOTAIR, supporting the hypothesis that HOTAIR promotes the activity of MMP-9 and/or MMP-2. BRAF-activated noncoding RNA (BANCR) shows increased expression in melanoma [32]. Knockdown of BANCR reduced melanoma cell migration [32]. These data suggest that lncRNAs may play an important role in the progression of melanoma. Further research on lncRNA expression profiles is needed to define the impact of lncRNAs on the progress of melanoma.

Interestingly, in our study, the expression levels of lncRNA MALAT1 show no significant difference between primary melanoma and matched metastatic tissues. On the contrary, MALAT1 was documented by several studies to associate with metastasis in other cancer types [15]. Increased expression of MALAT1 was first observed in metastatic non-small cell lung cancer [15], followed by endometrial stromal sarcoma of the uterus [33], and more recently in six other types of cancer, including HCC, breast, pancreas, lung, colon, and prostate cancers [34]. Overall, these results suggest that the effect of lncRNAs on cancer progression may be cancer-type specific.

In conclusion, we demonstrate that HOTAIR lncRNA is predominantly upregulated in lymph node metastasis tissues compared with primary melanoma. Knockdown of HOTAIR inhibits the motility and invasiveness of melanoma cells, and the latter is associated with decreased degradation of extracellular matrix. Although further mechanistic investigation into the regulation of metastasis by HOTAIR is necessary, the observed prometastatic activity of HOTAIR in multiple preclinical model systems supports HOTAIR to be a potential target for melanoma metastasis therapy.

Conflict of Interests

The authors declare that they have no conflict interests.

Authors' Contribution

Lihua Tang and Wei Zhang equally contributed to the paper.

Acknowledgments

The study was supported by the Research Grants of Shenzhen Science and Technology project (ZYA201106080030A). The authors would like to thank Shenzhen Biomedical Research Support Platform for their excellent technical assistance.

References

[1] E. G. Little and M. J. Eide, "Update on the current state of melanoma incidence," *Dermatologic Clinics*, vol. 30, pp. 355–361, 2012.

[2] C. D. Malone and G. J. Hannon, "Small RNAs as guardians of the genome," *Cell*, vol. 136, no. 4, pp. 656–668, 2009.

[3] D. Moazed, "Small RNAs in transcriptional gene silencing and genome defence," *Nature*, vol. 457, no. 7228, pp. 413–420, 2009.

[4] C. A. Brosnan and O. Voinnet, "The long and the short of noncoding RNAs," *Current Opinion in Cell Biology*, vol. 21, no. 3, pp. 416–425, 2009.

[5] J. S. Mattick, "Non-coding RNAs: the architects of eukaryotic complexity," *EMBO Reports*, vol. 2, no. 11, pp. 986–991, 2001.

[6] N. Schöler, C. Langer, H. Döhner, C. Buske, and F. Kuchenbauer, "Serum microRNAs as a novel class of biomarkers: a comprehensive review of the literature," *Experimental Hematology*, vol. 38, no. 12, pp. 1126–1130, 2010.

[7] Y. Xie, N. W. Todd, Z. Liu et al., "Altered miRNA expression in sputum for diagnosis of non-small cell lung cancer," *Lung Cancer*, vol. 67, no. 2, pp. 170–176, 2010.

[8] L. Xing, N. W. Todd, L. Yu, H. Fang, and F. Jiang, "Early detection of squamous cell lung cancer in sputum by a panel of microRNA markers," *Modern Pathology*, vol. 23, no. 8, pp. 1157–1164, 2010.

[9] P. Bertone, V. Stolc, T. E. Royce et al., "Global identification of human transcribed sequences with genome tiling arrays," *Science*, vol. 306, no. 5705, pp. 2242–2246, 2004.

[10] P. Kapranov, J. Drenkow, J. Cheng et al., "Examples of the complex architecture of the human transcriptome revealed by RACE and high-density tiling arrays," *Genome Research*, vol. 15, no. 7, pp. 987–997, 2005.

[11] V. Srikantan, Z. Zou, G. Petrovics et al., "PCGEM1, a prostate-specific gene, is overexpressed in prostate cancer," *Proceedings of the National Academy of Sciences of the United States of America*, vol. 97, no. 22, pp. 12216–12221, 2000.

[12] M. J. G. Bussemakers, A. Van Bokhoven, G. W. Verhaegh et al., "DD3: a new prostate-specific gene, highly overexpressed in prostate cancer," *Cancer Research*, vol. 59, no. 23, pp. 5975–5979, 1999.

[13] G. Petrovics, W. Zhang, M. Makarem et al., "Elevated expression of PCGEM1, a prostate-specific gene with cell growth-promoting function, is associated with high-risk prostate cancer patients," *Oncogene*, vol. 23, no. 2, pp. 605–611, 2004.

[14] A. Iacoangeli, Y. Lin, E. J. Morley et al., "BC200 RNA in invasive and preinvasive breast cancer," *Carcinogenesis*, vol. 25, no. 11, pp. 2125–2133, 2004.

[15] P. Ji, S. Diederichs, W. Wang et al., "MALAT-1, a novel noncoding RNA, and thymosin β4 predict metastasis and survival in early-stage non-small cell lung cancer," *Oncogene*, vol. 22, no. 39, pp. 8031–8041, 2003.

[16] R. A. Gupta, N. Shah, K. C. Wang et al., "Long non-coding RNA HOTAIR reprograms chromatin state to promote cancer metastasis," *Nature*, vol. 464, no. 7291, pp. 1071–1076, 2010.

[17] T. Gutschner and S. Diederichs, "The Hallmarks of Cancer: a long non-coding RNA point of view," *RNA Biology*, vol. 9, no. 6, pp. 703–719, 2012.

[18] S. Boissier, M. Ferreras, O. Peyruchaud et al., "Bisphosphonates inhibit breast and prostate carcinoma cell invasion, an early event in the formation of bone metastases," *Cancer Research*, vol. 60, no. 11, pp. 2949–2954, 2000.

[19] K. V. Prasanth and D. L. Spector, "Eukaryotic regulatory RNAs: an answer to the "genome complexity" conundrum," *Genes and Development*, vol. 21, no. 1, pp. 11–42, 2007.

[20] D. S. Perez, T. R. Hoage, J. R. Pritchett et al., "Long, abundantly expressed non-coding transcripts are altered in cancer," *Human Molecular Genetics*, vol. 17, no. 5, pp. 642–655, 2008.

[21] M. Guttman, J. Donaghey, B. W. Carey et al., "LincRNAs act in the circuitry controlling pluripotency and differentiation," *Nature*, vol. 477, no. 7364, pp. 295–300, 2011.

[22] R. W. Carthew and E. J. Sontheimer, "Origins and mechanisms of miRNAs and siRNAs," *Cell*, vol. 136, no. 4, pp. 642–655, 2009.

[23] L. Lipovich, R. Johnson, and C.-Y. Lin, "MacroRNA underdogs in a microRNA world: evolutionary, regulatory, and biomedical significance of mammalian long non-protein-coding RNA," *Biochimica et Biophysica Acta*, vol. 1799, no. 9, pp. 597–615, 2010.

[24] M. Huarte and J. L. Rinn, "Large non-coding RNAs: missing links in cancer?" *Human Molecular Genetics*, vol. 19, no. 2, pp. R152–R161, 2010.

[25] Y.-S. Kim, J. Do Hwan, S. Bae, D.-H. Bae, and W. Ahn Shick, "Identification of differentially expressed genes using an annealing control primer system in stage III serous ovarian carcinoma," *BMC Cancer*, vol. 10, article 576, 2010.

[26] I. J. Matouk, I. Abbasi, A. Hochberg, E. Galun, H. Dweik, and M. Akkawi, "Highly upregulated in liver cancer noncoding RNA is overexpressed in hepatic colorectal metastasis," *European Journal of Gastroenterology and Hepatology*, vol. 21, no. 6, pp. 688–692, 2009.

[27] X. Zhang, R. Gejman, A. Mahta et al., "Maternally expressed gene 3, an imprinted noncoding RNA gene, is associated with meningioma pathogenesis and progression," *Cancer Research*, vol. 70, no. 6, pp. 2350–2358, 2010.

[28] X.-S. Wang, Z. Zhang, H.-C. Wang et al., "Rapid identification of UCA1 as a very sensitive and specific unique marker for human bladder carcinoma," *Clinical Cancer Research*, vol. 12, no. 16, pp. 4851–4858, 2006.

[29] K. Kim, I. Jutooru, G. Chadalapaka et al., "HOTAIR is a negative prognostic factor and exhibits pro-oncogenic activity in pancreatic cancer," *Oncogene*, vol. 32, pp. 1616–1625, 2013.

[30] Z. Yang, L. Zhou, L.-M. Wu et al., "Overexpression of long non-coding RNA HOTAIR predicts tumor recurrence in hepatocellular carcinoma patients following liver transplantation," *Annals of Surgical Oncology*, vol. 18, no. 5, pp. 1243–1250, 2011.

[31] Y. J. Geng, S. L. Xie, Q. Li, J. Ma, and G. Y. Wang, "Large intervening non-coding RNA HOTAIR is associated with

hepatocellular carcinoma progression," *Journal of International Medical Research*, vol. 39, no. 6, pp. 2119–2128, 2011.

[32] R. J. Flockhart, D. E. Webster, K. Qu et al., "BRAFV600E remodels the melanocyte transcriptome and induces BANCR to regulate melanoma cell migration," *Genome Research*, vol. 22, pp. 1006–1014, 2012.

[33] K. Yamada, J. Kano, H. Tsunoda et al., "Phenotypic characterization of endometrial stromal sarcoma of the uterus," *Cancer Science*, vol. 97, no. 2, pp. 106–112, 2006.

[34] R. Lin, S. Maeda, C. Liu, M. Karin, and T. S. Edgington, "A large noncoding RNA is a marker for murine hepatocellular carcinomas and a spectrum of human carcinomas," *Oncogene*, vol. 26, no. 6, pp. 851–858, 2007.

Hindawi Publishing Corporation
BioMed Research International
Volume 2013, Article ID 937918, 6 pages
http://dx.doi.org/10.1155/2013/937918

Research Article

Bovine Papillomavirus Type 2 Infection and Microscopic Patterns of Urothelial Tumors of the Urinary Bladder in Water Buffaloes

Paola Maiolino,[1] Ayhan Özkul,[2] Aylin Sepici-Dincel,[3] Franco Roperto,[4] Gözde Yücel,[2] Valeria Russo,[1] Chiara Urraro,[1] Roberta Lucà,[1] Marita Georgia Riccardi,[1] Manuela Martano,[1] Giuseppe Borzacchiello,[1] Iolanda Esposito,[1] and Sante Roperto[1]

[1] *Department of Veterinary Medicine and Animal Productions, Naples University Federico II, Via Delpino 1, 80137 Naples, Italy*
[2] *Department of Pathology, Faculty of Veterinary Medicine, Ankara University, 06110 Ankara, Turkey*
[3] *Faculty of Medicine, Gazi University, 06100 Ankara, Turkey*
[4] *Department of Biology, Naples University Federico II, 80134 Naples, Italy*

Correspondence should be addressed to Valeria Russo; valeria.russo@unina.it

Received 22 February 2013; Accepted 22 April 2013

Academic Editor: Rita de Cassia Stocco

Microscopic patterns of thirty-four urothelial tumors of the urinary bladder of water buffaloes from the Marmara and Black Sea Regions of Turkey are here described. All the animals grazed on lands rich in bracken fern. Histological diagnosis was assessed using morphological parameters recently suggested for the urinary bladder tumors of cattle. Papillary carcinoma was the most common neoplastic lesion (22/34) observed in this study, and low-grade carcinoma was more common (seventeen cases) than high-grade carcinoma (five cases). Papilloma, papillary urothelial neoplasm of low malignant potential (PUNLMP), and invasive carcinomas were less frequently seen. Carcinoma in situ (CIS) was often detected associated with some papillary and invasive carcinomas. De novo (primary) CIS was rare representing 3% of tumors of this series. A peculiar feature of the most urothelial tumors was the presence in the tumor stroma of immune cells anatomically organized in tertiary lymphoid organs (TLOs). Bovine papillomavirus type-2 (PV-2) E5 oncoprotein was detected by molecular and immunohistochemistry procedures. Early protein, E2, and late protein, L1, were also detected by immunohistochemical studies. Morphological and molecular findings show that BPV-2 infection contributes to the development of urothelial bladder carcinogenesis also in water buffaloes.

1. Introduction

Spontaneous tumors of the urinary bladder are very rare in cattle accounting for 0.01% of all bovine malignancies [1]. Conversely, they are common in adult cattle grazing on lands rich in bracken fern [2–4]. This plant contains toxic substances impairing the immune system and carcinogen principles such as ptaquiloside, the prolonged ingestion of which appears to be involved in bladder carcinogenesis. It has been suggested that ptaquiloside causes an increased cell proliferation in bladder urothelium resulting in urothelial dysplasia [5, 6]; furthermore, it is believed that ptaquiloside can act synergistically with bovine papillomavirus type 2 (BPV-2) thus causing bladder tumors in cattle [7].

Papillomavirus infection plays a central role in bladder carcinogenesis of large ruminants [7–11]. In particular, BPV-2 appears to be involved in many urothelial tumors in cattle and water buffaloes [4, 7, 12]. It has been shown that BPV-2 causes in vivo bladder carcinogenesis through the activation of PDGF β receptor [12, 13] and/or of Calpain 3 which is responsible for urothelial cell proliferation via E2F3 protein [14].

Tumors of the urinary bladder of buffaloes have sporadically been described [3]. However, BPV-2 infection has just been reported in urothelial tumors as well as in some nonneoplastic lesions of the urinary bladder of buffaloes [12].

The aim of the present paper is to report the microscopic patterns of thirty-four urothelial tumors of the urinary bladder of water buffaloes, twenty-seven of which were associated

with papillomavirus infection. All the animals were from the Marmara and Black Sea Regions of Turkey and grazed on pastures contaminated with bracken fern.

2. Materials and Methods

Thirty-four tumor samples of the urinary bladder were collected at public slaughterhouses of Marmara and Black Sea Region (Turkey) (Bafra, Coskun, Bartin) from 3- to 5-year-old castrated male water buffaloes daily grazing on fern-infested lands. Each sample was divided into two halves. One part was fixed in 10% neutral buffered formalin and was processed for paraffin embedding for morphological assessment; the other half was immediately frozen in liquid nitrogen, stored at –80°C until further processed for molecular procedures.

2.1. Histopathology and Immunohistochemistry. Histologic diagnosis of urinary bladder tumors was assessed on 4-μm-thick hematoxylin-eosin- (HE-) stained sections using morphological criteria suggested in a recent report on the new histological classification of urothelial tumors of the urinary bladder of cattle [4]. Immunohistochemistry was performed to detect both early (E) and late (L) papillomavirus proteins. Briefly, the sections were deparaffinized, and then endogenous peroxidase activity was blocked by incubation in 0.3% H_2O_2 in methanol for 20 min. Antigen retrieval was performed by pretreating with microwave heating (twice for 5 min each at 750 W) in citrate buffer pH 6.0. The slides were washed with phosphate buffered saline (PBS), pH 7.4, 0.01 M, then incubated for 1 h at room temperature with donkey serum (Sigma-Aldrich, Milan, Italy) diluted at 1 in 10 in PBS. A polyclonal sheep anti-BPV-2 E5 primary antibody (a kind gift from Dr. M. S. Campo, professor Emeritus of Glasgow University, UK) diluted at 1 in 40000 in PBS was applied for 1 h at room temperature in a humid chamber. The sections were rinsed with PBS before application of the donkey anti-sheep biotinylated secondary antibody (Santa Cruz Biotechnology Inc., CA, USA), diluted at 1 in 100 in PBS for 45 min at room temperature. For E2 and L1 detection, the slides were washed three times with PBS, pH 7.4, 0.01 M, then incubated for 1 h at room temperature with protein block serum free (DakoCytomation, Denmark). A polyclonal rabbit anti-BPV-2 E2 primary antibody (a kind gift from Dr. E. Androphy) diluted at 1 in 50 in PBS and a monoclonal mouse anti-HPV-16 L1 (late protein) primary antibody diluted at 1 in 200/300 in PBS were applied overnight at 4°C in a humid chamber. The sections were rinsed three times for 5 min with PBS, incubated for 40 min at room temperature with appropriate biotinylated secondary antibody (labelled streptavidin-biotin (LSAB) Kit; DakoCytomation, Denmark). Finally, all the sections were washed with PBS and then incubated with streptavidin-conjugated to horseradish peroxidase (LSAB Kit; DakoCytomation, Denmark).

Color development was obtained by treatment with diaminobenzidine (DakoCytomation, Denmark) for 5–20 min. Sections were counterstained with Mayer's hematoxylin. Negative control sections were incubated with PBS instead of primary antibody.

2.2. PCR Reaction. The DNA was extracted from the urinary bladders of water buffaloes using the DNeasy Tissue Kit (Qiagen TM, Germany) according to the manufacturer's instructions.

For the detection of BPV-2 E5 DNA, specific primers for the E5 ORF (forward primer, 5′-CACTGCCATTTGTTTTTTTC-3′; reverse primer, 5′-GGAGCACTCAAAATGATCCC-3′) were used. Furthermore, specific primers for the L1 region of the BPV-1 (forward primer, 5′-GGCTGAGGACGCTGCTGGTA-3′; reverse primer, 5′-TCTCCGAGCCCCCTCTGGTC-3′) were also employed. Aliquots 50–100 ng of purified DNA were amplified in 25 μL of reaction mixture containing 2 mM $MgCl_2$, 200 mM each dNTP, 480 nM of each primer, and 2.5 U of AmpliTaq Gold DNA Polymerase (Applied Biosystems, Monza, Italy). The reaction was carried out in a thermocycler (Veriti, Applied Biosystems) with an initial denaturation step of 3 min. Then, 35 cycles of amplification were carried out with a denaturation step at 95°C for 45 sec, an annealing step at 50°C, 45 sec, for BPV-2 E5, or at 65°C, 40 sec, for BPV-1 L1 and an extension step at 72°C for 1 min. A final extension step at 72°C for 7 min was performed. Detection of the amplified products was carried out by electrophoresis on ethidium bromide-stained agarose gel. In each experiment, a blank sample consisting of reaction mixture without DNA and a positive control composed of BPV-2 clone DNA (a kind gift from Dr. A. Venuti) or of BPV-1 positive sample were included. One μL of the amplified products was subjected to a second run of PCR under the same experimental conditions. Amplified products from the last PCR were electrophoresed in a 2,5% agarose gel and visualized by ethidium bromide stain.

2.3. RNA Extraction. Total RNA was extracted from urinary bladders of water buffaloes using the RNeasy Mini Kit (Qiagen TM, Germany), according to the manufacturer's instructions. The RNA quality was determined by agarose gel electrophoresis and ultraviolet spectrophotometer analysis.

2.4. cDNA-E5 Analysis. The reverse transcription reaction contained 4 μL 5x script reaction mix, 1 μL iScript reverse transcriptase, and 500 ng total RNA as the template. The volume was adjusted to 10 μL with RNase free water (Bio-Rad Laboratories, Milan, Italy). The reaction was incubated at 25°C for 5 min, 42°C for 30 min, 85°C for 5 min, and then kept at 4°C for 5 min. The synthesized cDNA was analyzed by PCR with specific primers for the E5 ORF (forward primer, 5′-CACTGCCATTTGTTTTTTTC-3′; reverse primer, 5′-GGAGCACTCAAAATGATCCC-3′). The total reaction volume was 25 μL containing 2.5 μL 10x Gold Buffer, 2 mM $MgCl_2$, 200 mM each dNTP, 480 nM of each primer, 2.5 U of AmpliTaq Gold DNA Polymerase (Applied Biosystems, Monza, Italy), and 100 ng reverse transcription products of cDNA as the template. The reaction procedure was as follows: predenaturation at 95°C for 3 min, 35 cycles (denaturation at 95°C for 45 sec, annealing at 50°C for 45 sec, and extension at 72°C for 1 min), and the final extension at 72°C for 7 min. Detection of the amplified products was carried out by electrophoresis on ethidium bromide-stained agarose

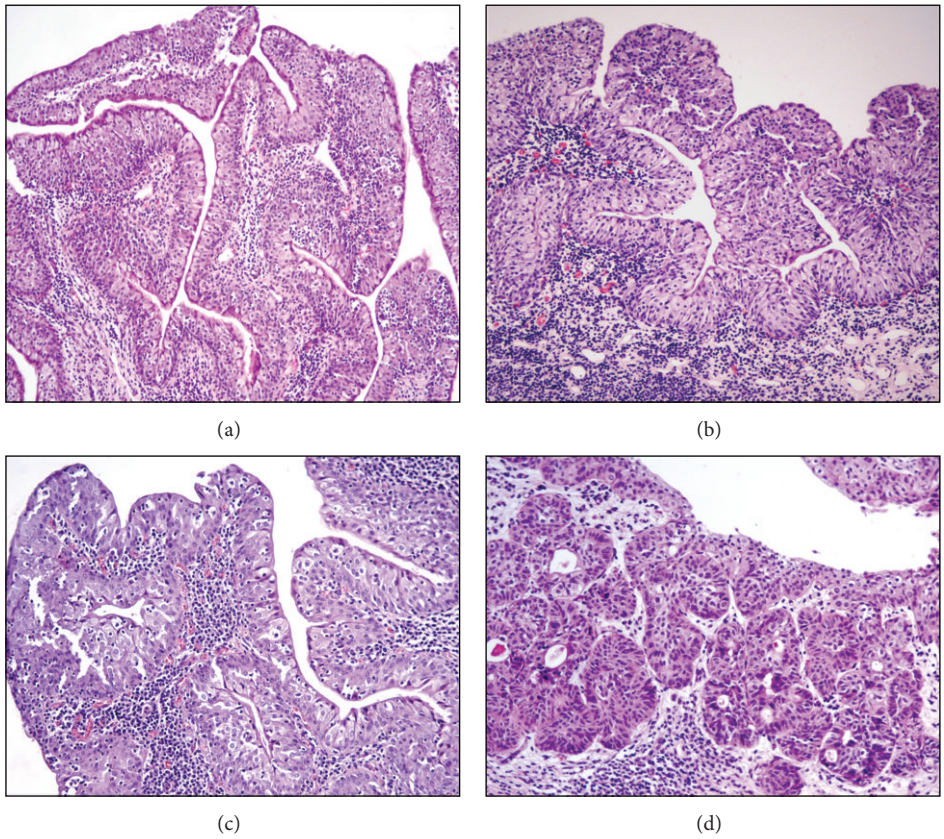

Figure 1: Morphological patterns of the bubaline urothelial tumors. Papilloma (a), H&E, Objective 10x; papillary urothelial neoplasm of low malignant potential (PUNLMP). Notice the diffuse reactive atypia, that is, the presence inflammatory cells into the urothelium (b) H&E, Objective 10x; papillary carcinoma (c) H&E, Objective 20x; invasive carcinoma (d) H&E, Objective 20x.

gel. In each experiment, a blank sample consisting of reaction mixture without DNA and a positive sample consisting of cloned BPV-2 (a kind gift from Dr. A. Venuti) were included.

3. Results

Histological examinations of the urinary bladder tumors detected microscopic patterns consistent with the diagnosis of urothelial papilloma in three cases, two of them showed an exophytic pattern and only one showed an inverted growth. Furthermore, three cases were diagnosed as papillary urothelial neoplasm of low malignant potential (PUNLMP); a diagnosis of papillary carcinoma was performed in twenty-two cases; five cases of invasive carcinomas were also found (Figure 1); de novo (primary) carcinoma in situ (CIS) was seen in only one case (Figure 2). Table 1 summarizes the results. Tumor-like lesions such as reactive atypia as well as flat and nodular hyperplasia were also seen.

Papillary carcinoma was the most common neoplastic lesion observed in this study, and low-grade carcinomas were more common (seventeen cases) than high grade carcinomas (five cases). CIS was seen to occur in three buffaloes with papillary carcinoma and in two with invasive bladder neoplasia. They were seen more frequently than the primary (de novo) CIS; the latter was seen in only one case thus representing about 3% of urothelial neoplasms. In all the examined cases, there was a strong inflammation of the tumor stroma; quite frequently, immune cells were anatomically organized in tertiary lymphoid organs (TLOs), in which clear germinal center and peripheral small dark and densely packed mantle lymphocytes without any fibrous encapsulation were seen (Figure 3).

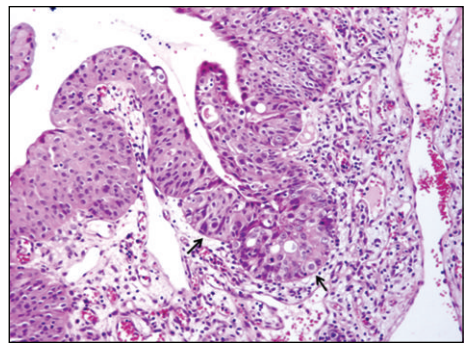

Figure 2: De novo (primary) carcinoma in situ (CIS) H&E, Objective 20x.

PCR analysis demonstrated the presence of E5 DNA in the samples from twenty-seven buffaloes suffering from uro-

Table 1: Histological types of thirty-four urothelial tumors of the urinary bladder in water buffaloes.

Microscopic patterns of tumors	Case no.
Papilloma	3
Papillary urothelial neoplasm of low malignant potential (PUNLMP)	3
Low-grade papillary urothelial carcinoma	17
High-grade papillary urothelial carcinoma	5
Low-grade invasive urothelial carcinoma	3
High-grade invasive urothelial carcinoma	2
De novo carcinoma *in situ* (CIS)	1

thelial bladder tumors in which a fragment of the expected size (154 bp) was amplified (Figure 4). Furthermore, in these samples, reverse transcriptase PCR analysis demonstrated the presence of E5 mRNA (Figure 5). No BPV-1 DNA was detected. Immunohistochemical studies confirmed the presence of E5 protein in the cytoplasm of many neoplastic cells; it was not detected in the cytoplasm of normal cells (Figure 6). Furthermore, a marked immunoreactivity for L1 protein expression was evident both in the cytoplasm and nuclei of the urothelial cells of neoplastic nests; it was not detectable in normal urothelial cells (Figure 7). Since it is known that E2 protein is essential for the viral life cycle and plays a part in productive infection, immunohistochemical studies on the expression of this protein were also carried out. E2 protein expression was detected both in the cytoplasm and nuclei of urothelial cells from neoplastic urinary bladder. Its expression was not manifested in normal urothelial cells (Figure 8).

4. Discussion

The present study reports the microscopic patterns of thirty-four spontaneous urothelial tumors of the urinary bladder in water buffaloes grazed on pasturelands rich in fern. A papillomavirus infection has been shown in twenty-seven tumors (~79%). Both benign and malignant lesions here described fell into the following categories: flat urothelial lesions, papillary urothelial lesions, and invasive urothelial tumors just reported in humans [15] and cattle [4]. No metastases were found in malignant tumors. Our findings corroborate that morphological criteria suggested for histological classification of urothelial tumors in cattle [4] may be used also in water buffaloes. Recently, we have shown that BPV-2 plays a central role also in bubaline bladder carcinogenesis. Like the case in bladder carcinogenesis of cattle, BPV-2 E5 oncoprotein binds to the activated form of platelet derived growth factor β receptor (PDGFβR) [12]. We document here a papillomavirus infection by western blot analysis, cDNA, and immunohistochemical investigations about the presence of BPV-2 E5 oncoprotein. The expression of BPV-2 L1 protein indicates that a complete life cycle of BPV-2 occurs also in bubaline neoplastic urothelial cells. These findings corroborate our previous results about the crucial role of BPV-2

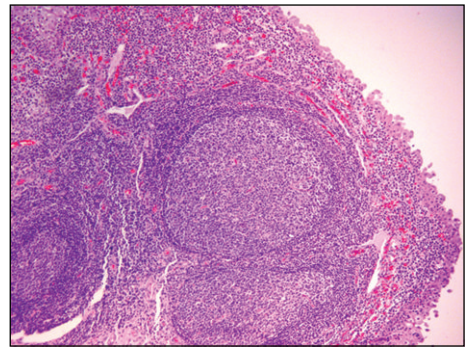

Figure 3: Lymphoid neogenesis. Tertiary lymphoid organs with an evident, clear germinal center and peripheral lymphocytes are evident in tumor stroma. H&E, Objective 10x.

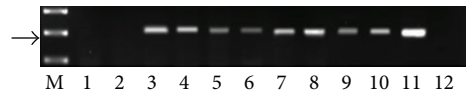

Figure 4: Detection of BPV-2 E5 DNA. M: 50 bp molecular marker (HyperLadder II Bioline); 1-2: urinary bladder samples from healthy buffaloes without BPV-2 E5 DNA; 3–10: some representative bladder tumors samples showing BPV-2 E5 DNA; 11: positive control (cloned BPV-2 DNA); 12: negative control (no DNA added). The arrow indicates the position of the 154 bp BPV-2 E5 PCR product.

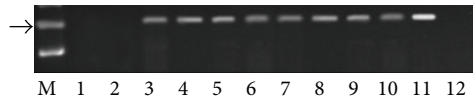

Figure 5: Assessment of BPV-2 E5 cDNA by reverse transcriptase polymerase chain reaction (RT-PCR). M: 50 bp molecular marker (HyperLadder II Bioline); 1-2: healthy urinary bladder samples; 3–10: bladder tumors samples; 11: positive control (cloned BPV-2 DNA); 12: negative control (no DNA added). The arrow indicates the position of the 154 bp BPV-2 E5 PCR product.

infection in urothelial cell transformation [12]. Toxic elements of the fern appear to play a synergistic role with BPV-2 infection also in bladder carcinogenesis of water buffaloes. As a matter of fact, when the buffalo breeding based on closed breeding techniques does not allow buffaloes to graze on pastures contaminated with bracken fern, the bladder disease is basically unknown although clinical cases of BPV infection can be seen, that is, papillomatosis of the skin. The microscopical findings of this study show that urothelial tumors of buffaloes share morphological characteristics with the human counterparts just like urothelial tumors of cattle [4, 15, 16]. A peculiar feature of most bubaline urothelial tumors was the presence of diffuse lymphocytes, plasma cells, and macrophages which can evolve into aggregates in the tumor stroma. These findings were also detected in the urothelial cancers of cattle [4], but in buffaloes the immune cells were often organized anatomically in de novo follicles leading to the formation of the so-called tertiary lymphoid organs (TLOs). Chronic follicular cystitis is frequently found in water buffaloes [17]. The pathophysiological significance of

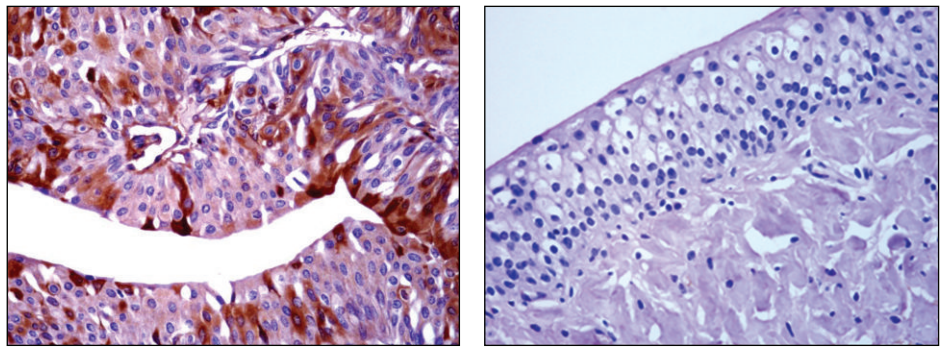

(a) (b)

Figure 6: E5 immunohistochemistry. Neoplastic cells show a strong cytoplasmatic E5 immunoreactivity (a), Objective 40x. No E5 immunoreactivity is evident in normal urothelial cells (b), Objective 20x.

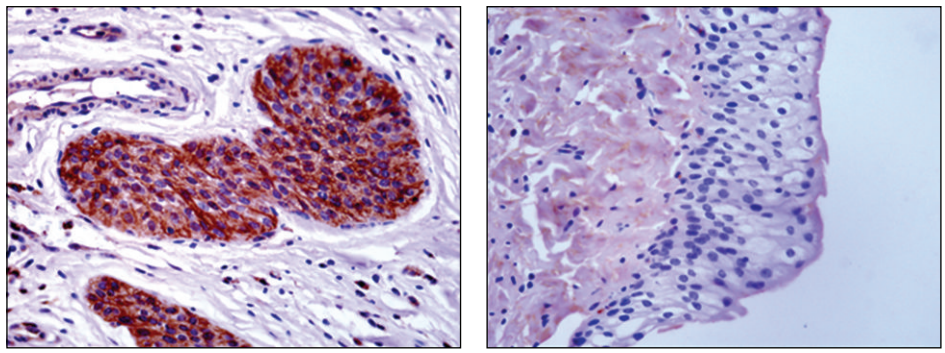

(a) (b)

Figure 7: L1 immunohistochemistry. Presence of L1 protein in urothelial neoplastic cells (a) Objective 40x. No L1 protein immunoreactivity was detected in normal urothelial cells (b), Objective 40x.

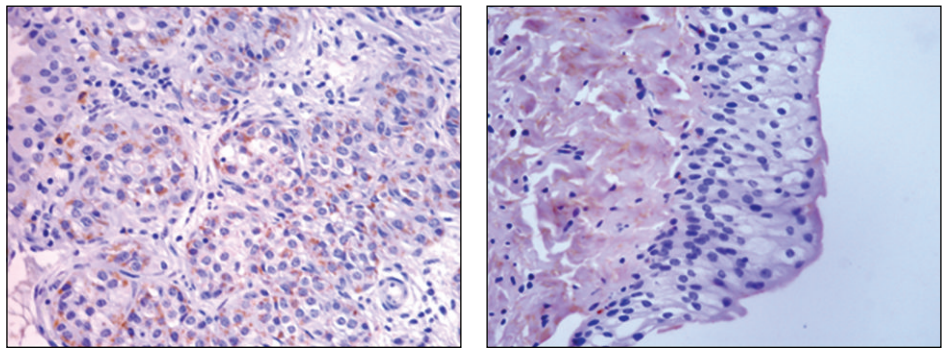

(a) (b)

Figure 8: E2 immunohistochemistry. Diffuse immunoreactivity of E2 protein in urothelial neoplastic cells (a), Objective 40x. No E2 protein immunoreactivity was detected in normal urothelial cells (b), Objective 40x.

the lymphoid neogenesis is still unclear. TLO formation is now recognized as a common feature of many chronic inflammatory diseases and might have a role in maintaining immune responses against persistent antigens. It has been suggested that the stimulus that triggers lymphoid neogenesis in infected tissues is the causative agent itself [18]. It is reasonable to suggest that, in our cases, L1 protein, expressed only in productive BPV-2 infection and known to play a central role both in infection and immunogenicity [19], stimulates adaptive immune responses thus leading to chronic inflammation of tumor stroma in which TLOs can develop. Furthermore, BPV E5 is known to impair the major histocompatibility class I complex (MHC I) thus allowing the persistence of the virus infection. This impairment and immunosuppressant of bracken fern may help maintain antigen stimuli responsible for a heavy cell infiltration which can

contribute to TLO formation [7, 20]. It has been suggested that chronic follicular cystitis in buffaloes is characterized by a very strong presence of lymphoid cells [17]. It is worth remembering that the most organized structures are generally found in highly infiltrated tissues [18]. Inflammatory cells of microenvironment and their secreted factors appear to be coresponsible for the fate of a tumor [21] being able to exert a strong anticancer immunosurveillance. Further studies are needed to gather insights into the relationship between tumor cells and their inflammatory microenvironment being a manner of debate [22]. In addition, we have to better understand the role of lymphoid neogenesis in infectious diseases as it has been suggested that, although so far it has been documented in only a few chronic diseases, lymphoid neogenesis might have a protective function by inducing an immune response against the infectious agent.

Conflict of Interests

The authors declare that they have no conflict of interests.

Acknowledgments

The authors thank Dr. M. S. Campo, Professor Emeritus of Glasgow University, for providing them with the E5 primary antibody; Dr. E. Androphy, University of Massachusetts Medical School, for providing them with the E2 primary antibody; Dr. A. Venuti, Laboratory of Virology, National Cancer Institute "Regina Elena," for giving them the BPV-2 DNA plasmid; Dr. G. Salvatore, Regione Basilicata for his technical help. This work was sponsored by grants from Ministero Italiano dell'Università e della Ricerca Scientifica (MIUR), Ministero Italiano delle Politiche Agricole, Alimentari e Forestali (MIPAAF), and Assessorato alla Sanità della Regione Basilicata.

References

[1] D. J. Meuten, "Tumors of the urinary bladder and urethra," in *Tumors in Domestic Animals*, D. J. Meuten, Ed., pp. 524–546, Iowa State Press, Ames, Iowa, USA, 2002.

[2] A. M. Pamukcu, J. M. Price, and G. T. Bryan, "Naturally occurring and bracken fern induced bovine urinary bladder tumors. Clinical and morphological characteristics," *Veterinary Pathology*, vol. 13, no. 2, pp. 110–122, 1976.

[3] I. A. Özkul and Y. Aydin, "Tumours of the urinary bladder in cattle and water buffalo in the black sea region of Turkey," *British Veterinary Journal*, vol. 152, no. 4, pp. 473–475, 1996.

[4] S. Roperto, G. Borzacchiello, R. Brun et al., "A review of bovine urothelial tumours and tumour-like lesions of the urinary bladder," *Journal of Comparative Pathology*, vol. 142, no. 2-3, pp. 95–108, 2010.

[5] R. M. Gil da Costa, M. M. Bastos, P. A. Oliveira, and C. Lopes, "Bracken-associated human and animal health hazards: chemical, biological and pathological evidence," *Journal of Hazardous Materials*, vol. 203-204, pp. 1–12, 2012.

[6] R. M. Gil da Costa, P. A. Oliveira, M. M. Bastos, C. C. Lopes, and C. Lopes, "Ptaquiloside-induced early-stage urothelial lesions show increased cell proliferation and intact β-catenin and e-cadherin expression," *Environmental Toxicology*, 2012.

[7] M. S. Campo, W. F. H. Jarrett, R. Barron, B. W. O'Neil, and K. T. Smith, "Association of bovine papillomavirus type 2 and bracken fern with bladder cancer in cattle," *Cancer Research*, vol. 52, no. 24, pp. 6898–6904, 1992.

[8] G. Borzacchiello, G. Lovane, M. L. Marcante et al., "Presence of bovine papillomavirus type 2 DNA and expression of the viral oncoprotein E5 in naturally occurring urinary bladder tumours in cows," *Journal of General Virology*, vol. 84, no. 11, pp. 2921–2926, 2003.

[9] S. R. Wosiacki, M. P. Claus, A. F. Alfieri, and A. A. Alfieri, "Bovine papillomavirus type 2 detection in the urinary bladder of cattle with chronic enzootic haematuria," *Memorias do Instituto Oswaldo Cruz*, vol. 101, no. 6, pp. 635–638, 2006.

[10] S. Roperto, R. Brun, F. Paolini et al., "Detection of bovine papillomavirus type 2 in the peripheral blood of cattle with urinary bladder tumours: possible biological role," *Journal of General Virology*, vol. 89, no. 12, pp. 3027–3033, 2008.

[11] S. Roperto, S. Comazzi, E. Ciusani et al., "PBMCS are additional sites of productive infection of bovine papillomavirus type 2," *Journal of General Virology*, vol. 92, no. 8, pp. 1787–1794, 2011.

[12] S. Roperto, V. Russo, A. Özkul et al., "Bovine papillomavirus type 2 infects the urinary bladder of water buffalo (*Bubalus bubalis*) and plays a crucial role in bubaline urothelial carcinogenesis," *Journal of General Virology*, vol. 94, pp. 403–408, 2013.

[13] G. Borzacchiello, V. Russo, F. Gentile et al., "Bovine papillomavirus E5 oncoprotein binds to the activated form of the platelet-derived growth factor β receptor in naturally occurring bovine urinary bladder tumours," *Oncogene*, vol. 25, no. 8, pp. 1251–1260, 2006.

[14] S. Roperto, R. de Tullio, C. Raso et al., "Calpain3 is expressed in a proteolitically active form in papillomavirus-associated urothelial tumors of the urinary bladder in cattle," *Plos One*, vol. 5, no. 4, Article ID e10299, 2010.

[15] J. N. Eble, G. Sauter, J. I. Epstein, and I. A. Sesterhenn, *World Health Organization Classification of Tumours: Pathology and Genetics of Tumours of the Urinary System and Male Genital Organs*, IARC Press, Lyon, France, 2004.

[16] A. M. Pamukcu, "Tumours of the urinary bladder," *Bulletin of the World Health Organization*, vol. 50, no. 1-2, pp. 43–52, 1974.

[17] R. Somvanshi, S. Pathania, N. Nagarajan, K. Pangty, and P. Kumar, "Pathological study of non-neolastic urinary bladder lesions in cattle and buffaloes: a preliminary report," *Tropical Animal Healthy Production*, vol. 44, no. 4, pp. 855–861, 2012.

[18] F. Aloisi and R. Pujol-Borrell, "Lymphoid neogenesis in chronic inflammatory diseases," *Nature Reviews Immunology*, vol. 6, no. 3, pp. 205–217, 2006.

[19] Y. Modis, B. L. Trus, and S. C. Harrison, "Atomic model of the papillomavirus capsid," *EMBO Journal*, vol. 21, no. 18, pp. 4754–4762, 2002.

[20] B. Marchetti, G. H. Ashrafi, E. Tsirimonaki, P. M. O'Brien, and M. S. Campo, "The bovine papillomavirus oncoprotein E5 retains MHC class I molecules in the Golgi apparatus and prevents their transport to the cell surface," *Oncogene*, vol. 21, no. 51, pp. 7808–7816, 2002.

[21] A. Viola, A. Sarukhan, V. Bronte, and B. Molon, "The pros and cons of chemokines in tumor Immunology," *Trends in Immunology*, vol. 33, pp. 496–504, 2012.

[22] R. M. Peek, S. Mohla, and R. N. DuBois, "Inflammation in the genesis and perpetuation of cancer: summary and recommendations from a National Cancer Institute-sponsored meeting," *Cancer Research*, vol. 65, no. 19, pp. 8583–8586, 2005.

Hindawi Publishing Corporation
BioMed Research International
Volume 2013, Article ID 425646, 6 pages
http://dx.doi.org/10.1155/2013/425646

Research Article

Detection of Bovine Leukemia Virus in Brains of Cattle with a Neurological Syndrome: Pathological and Molecular Studies

Rubens Henrique Ramos D'Angelino,[1] Edviges Maristela Pituco,[2] Eliana Monteforte Cassaro Villalobos,[3] Ricardo Harakava,[4] Fábio Gregori,[5] and Claudia Del Fava[6]

[1] *Pós-Graduação em Sanidade, Segurança Alimentar e Ambiental no Agronegócio, Instituto Biológico de São Paulo (IB), Avenida Conselheiro Rodrigues Alves 1252, Bairro Vila Mariana, 04014-002 São Paulo, SP, Brazil*
[2] *Laboratório de Viroses de Bovídeos, Centro de P & D de Sanidade Animal (CPDSA), IB, Avenida Conselheiro Rodrigues Alves 1252, Bairro Vila Mariana, 04014-002 São Paulo, SP, Brazil*
[3] *Laboratório de Raiva e Encefalites, CPDSA, IB, Avenida Conselheiro Rodrigues Alves 1252, Bairro Vila Mariana, 04014-002 São Paulo, SP, Brazil*
[4] *Laboratório de Bioquímica Fitopatológica, Centro de Sanidade Vegetal, IB, Avenida Conselheiro Rodrigues Alves 1252, Bairro Vila Mariana, 04014-002 São Paulo, SP, Brazil*
[5] *Laboratório de Biologia Molecular e Sorologia Aplicadas, Departamento de Medicina Veterinária Preventiva e Saúde Animal, VPS, Faculdade de Medicina Veterinária e Zootecnia da Universidade de São Paulo, Avenida Professor Dr. Orlando Marques de Paiva 87, Cidade Universitária, 05508-270 São Paulo, SP, Brazil*
[6] *Laboratório de Anatomia Patológica, CPDSA, IB, Avenida Conselheiro Rodrigues Alves 1252, Bairro Vila Mariana, 04014-002 São Paulo, SP, Brazil*

Correspondence should be addressed to Rubens Henrique Ramos D'Angelino; rhrdangelino@yahoo.com.br and Claudia Del Fava; delfava@biologico.sp.gov.br

Received 26 December 2012; Revised 8 March 2013; Accepted 12 March 2013

Academic Editor: Lubna Nasir

Bovine leukemia virus (BLV) was investigated in the central nervous system (CNS) of cattle with neurological syndrome. A total of 269 CNS samples were submitted to nested-PCR (BLV env gene gp51), and the viral genotypes were identified. The nested-PCR was positive in 4.8% (13/269) CNS samples, with 2.7% (2/74) presenting at histological examination lesions of nonpurulent meningoencephalitis (NPME), whereas 5.6% (11/195) not presenting NPME ($P > 0.05$). No samples presented lymphosarcoma. The PCR products (437 bp) were sequenced and submitted to phylogenetic analysis by neighbor-joining and maximum composite likelihood methods, and genotypes 1, 5, and 6 were detected, corroborating other South American studies. The genotype 6 barely described in Brazil and Argentina was more frequently detected in this study. The identity matrices showed maximum similarity (100%) among some samples of this study and one from Argentina (FJ808582), recovered from GenBank. There was no association among the genotypes and NPME lesions.

1. Introduction

Bovine encephalitis is an important group of usually fatal diseases that have a strong impact on public health, result in major economic losses worldwide, and present a sanitary barrier to international trade [1]. Agents associated with these diseases include viral, bacterial, parasitic, neoplastic, toxic, and metabolic agents, and all must be considered during differential diagnosis [2].

The importance of differential diagnosis of neurologic syndromes in cattle has increased since 1985, when bovine spongiform encephalopathy (BSE) was first identified in the United Kingdom [3]. Its association with the emergence of a new variant of the human disease Creutzfeldt-Jakob

Disease (CJD) increased its political, social, and public health significance. International health authorities require evidence from countries exporting meat, which includes Brazil, that their herds are free from BSE and that the causes of encephalitis and encephalopathy are diagnosed and clarified [4]. Decree no. 516 dated December 9, 1997, introduced a BSE surveillance component into the system of surveillance of Herbivore rabies as part of the National Rabies Control of herbivores (PNCRH) of the *Ministério da Agricultura, Pecuária e Abastecimento* (Ministry of Agriculture, Livestock and Supply, MAPA) [5]. Thus, animals with symptoms of central nerve system disorders must be submitted to a differential diagnosis for rabies and other encephalitides and encephalopathies. These rules are intended to improve specific epidemiological surveillance measures to ensure a country free of BSE [6]. The differential diagnosis and prevention of BSE and the livestock assets in Brazil is of fundamental importance, as is evaluating the risks related to public health and the economic outlook.

Analysis conducted by the Biological Institute from April to July 2002, of samples from 131 cattle with a CNS neurological syndrome [1], confirmed the etiologic agent in only 38.9% of the samples. Also 21.1% were positive for rabies (direct immunofluorescence and biological tests), 1.5% positive for Bovine Viral Diarrhea Virus (BVDV) (isolation, identification by immunoperoxidase and RT-PCR), 0.7% positive for BoHV-5 (PCR), and 0.7% were positive for *Neospora caninum* (conventional PCR). In 16.0% of the cases, isolation and identification of bacteria (*Listeria monocytogenes*, *Streptococcus* spp., *Clostridium perfringens*, *Arcanobacterium pyogenes*, *Enterobacter cloacae*, *Pseudomonas aeruginosa*, *Acinetobacter* spp., and *Staphylococcus* spp.) were obtained. In 61.1% of the samples, the agent could not be identified using available diagnostic methods (isolation and molecular) making it necessary to investigate other agents and employ other methods.

The Anatomopathology Laboratory of the Biological Institute of São Paulo has been accredited by MAPA resolution number 5 of January 8, 2004 (Federal Official Gazette of Brazil of 09.01.2004, Section 1, page 3), to perform histopathologic differential diagnosis of encephalitis and BSE, thus meeting MAPA's PNCRH criteria. From January 2004 to June 2007, 690 brains of cattle with clinical signs of nervous disorders associated with rabies (direct immunofluorescence) were submitted for histologic examination, with 40% (276) showing pathological changes and nonpurulent and nonspecific meningoencephalitis being the most frequent lesions observed, at 90.0% (249/276) [7]. This type of inflammatory mononuclear infiltrate indicates microorganisms (viral agents, bacteria, and parasites) causing encephalitis, necessitating sensitive, and specific tests to determine the causative agents.

Bovine leukemia virus (BLV), which causes bovine leukosis (BL), is widespread in all regions of Brazil with high incidence of seroreactivity in dairy herds and other livestock under intensive management [8], although lymphosarcoma in the CNS has been reported as a rare condition in cattle [9, 10].

Del Fava et al. [10] reported the occurrence of 0.03% (1/2867) intracerebral lymphosarcoma in bovine with neurological syndrome, in a surveillance period of seven years, in Brazil. The tumoral mass was positive to nested-PCR (BLV env gene gp51). The RFLPA analyses using enzyme *Bam* HI revealed a site in amplified segments of BLV env gene, providing information about its population polymorphism, and allowed to classify into the Japanese-North American subgroup. The amplified proviral DNA was analyzed using ABI Prism 377 DNA sequencer (Applied Biosystems), and the obtained sequence was aligned and compared with others present in GenBank, by program BLAST, confirming the subgroup.

Given that BLV induces seroconversion, causes persistent lymphocytosis, and may rarely lead to lymphosarcoma, and that there are many cases with non-purulent meningoencephalitis (NPME) in which a causative diagnosis cannot be made, the aim of this study was to investigate BLV as a possible cause of neurological syndrome in cattle testing negative for rabies.

2. Materials and Methods

Bovine leukemia virus infection was verified from CNS samples of 269 cattle with neurological symptoms referred to the *Centro de Pesquisa e Desenvolvimento de Sanidade Animal of Instituto Biológico* (Center of Research and Development of Animal Health of the Biological Institute) from January 2007 to December 2009, for differential diagnosis of neurological syndrome. The samples were collected by government and private veterinarians, and all samples were negative for rabies virus based on the antirabies conjugate labeled with fluorescein isothiocyanate (Sanofi) and *in vivo* testing [11].

Tissues were fixed in 10% buffered formalin, cut into smaller pieces, and then dehydrated, cleared, and embedded in paraffin; sections were cut at 5 μm and stained with hematoxylin and eosin [12].

DNA extraction was made from chilled tissue samples using the Wizard *Genomic* DNA *Purification* kit (Promega Corporation, Madison, WI, USA—Cat. no. A1120). Amplification of the segment that encodes the gp51 env gene of the BVL was conducted by nested PCR, using specific primers for amplifying a segment of 440 base pairs (bp) [13]. Briefly, the PCR reaction conditions were as follows: volume of DNA in the first and second amplification was 5 μL and 1.5 μL, respectively; concentration of external and internal primers, 0.2 and 0.1 μM; initial denaturation at 94°C for 2 min; 40 repeat cycles of denaturation at 95°C for 30 sec; annealing at 62°C for 30 sec in the first and 70°C for 30 sec in the second amplification; extension at 72°C for 1 min; final extension at 72°C for 4 min. Analysis of amplified products was by electrophoresis (100 V/60 min) agarose gel at 1.5% in Tris plug, sodium acetate, EDTA pH 8.0, and stained with ethidium bromide. The image of the gel under UV light was recorded using camera coupled to a computer.

The positive PCR products were purified with the Wizard Genomic DNA Purification kit (Promega Corporation, Madison, WI, USA—Cat. no. A7170) and subjected to

sequencing reaction by chain termination with dideoxynucleotides marked with fluorophores. The reaction was performed with 5.68 μL of the PCR product, 2 μL reagent Big Dye 3.1 (Applied Biosystems), 2 μL of dilution buffer (0.2 M Tris-HCl pH 9.0, 5 μL $MgCl_2$), and 0.32 μL of a primer used in PCR (final concentration 0.32 μL) to a total volume of 10 μL. Each sample was sequenced in both directions using forward and reverse primers. The samples were incubated in a thermocycler (PTC-100, MJ Research) for 25 cycles at 95°C for 10 sec and 60°C for 4 min. The sequencing reaction products were precipitated by adding 40 μL of 75% isopropanol and centrifugation R-5810 centrifuge (Eppendorf) at 3220 ×g for 30 min at room temperature. After discarding the supernatant, another 100 μL of 75% isopropanol was added for washing the precipitate, and the supernatant was again discarded, without centrifugation. The precipitate was dried by incubation at 37°C for 30–60 min. The precipitate was re-suspended in 2 μL of formamide, denatured at 95°C for 2 min, and subjected to electrophoresis in denaturing polyacrylamide gel in ABI377 automated sequencer (Applied Biosystems).

The generated sequences were analyzed by the program Bioedit v.7.0.9 [14] to generate a unique sequence from the bidirectional sequence data. They were then aligned to each other and to homologues retrieved from Genbank, using the Clustal W version 1.8.3 software [14].

After definition of a consensus block, a table of nucleotide and amino acid identity was constructed using the *software* Bioedit v.7.0.9 [14]. Phylogenetic inference was performed using the program Mega, version 5 [15]. The tree generated from the nucleotide sequence was constructed with the neighbor-joining method using the substitution pattern *maximum composite likelihood* for the partial region (437 nt) of the env glycoprotein 51 gene from the BLV (nt 5110–5546 having as reference a sample of BLV, Argentina Accession no. AF257515), representing approximately 50% of the total gene, with the bootstrap values defined from 1000 replicates, with values equal to or greater than 50 submitted to the next node.

The association between the histopathologic findings of non-purulent, nonspecific meningoencephalitis and results of nested PCR, positive or not, was evaluated using Fisher's two-tailed exact test with an alpha error 5% [16].

3. Results and Discussion

The 269 CNS tissue samples from cattle with a CNS neurological syndrome showed a high number with characteristic lesions of NPME, corroborating with Del Fava et al. [7], but the nested-PCR showed low positivity for BLV (Table 1). These data indicated that other infectious agents, including rabies, are important in the differential diagnosis of diseases of the CNS in cattle, as was demonstrated in southern Brazil [4].

Statistical analysis by Fisher's exact test [16] showed no significant (α = 5%, P = 0.52, CI = 0.1073 to 2.083) positive correlation between nested-PCR results and the presence of lesions characteristic of NPME.

Table 1: Correlation between histopathology of CNS of cattle with neurological syndrome and results of nested-PCR.

Histology (%)	Nested-PCR (%)		Total (%)
	Positive	Negative	
NPME	2 (0.7)[a]	72 (26.8)[a]	74 (27.5)
Without alterations	11 (5.6)[a]	184 (68.4)[a]	195 (72.5)
Total (%)	13 (4.8)	256 (95.2)	269 (100)

Same superscript letters between columns are not significantly different at 0.05.

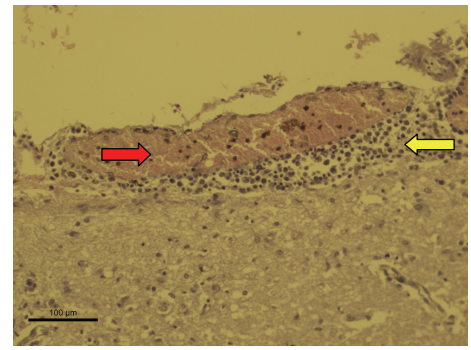

Figure 1: Nonpurulent meningitis (H & E 200x magnification). Bovine brain, positive for BLV, with accumulation of mononuclear inflammatory cells along the meninges (yellow arrows) and apparent congestion (red arrow).

Taking into account the high seroprevalence of BLV in recent decades in Brazil [17–19], especially in dairy herds, it is suspected that the low detection of genetic material (proviral DNA) of BLV by nested-PCR (13/269, 4.8%) may be due to low or absent neurotropism and/or in the difficulty of the virus in crossing the blood-brain barrier, even in animals with inflammatory changes of the CNS. The number of cases found positive with nested-PCR in samples with NPME (15.4%—2/13) was low in the present study. Another possible reason for this discrepancy is the connection of BLV with lymphoid tissue, particularly B lymphocytes [20, 21], and not the CNS itself. For this reason, a higher incidence of neoplastic changes is found in lymph nodes than in spleen, heart, uterus, abomasum, liver, and kidneys [22].

Positivity to BLV in animals with NPME may be due to the presence of the integrated virus in the lymphocyte genome, which is infiltrated in the tissues. On the other hand, in the positive nested-PCR animals that did not reveal NPME (84.6%—11/13), it can be assumed that the presence of proviral DNA in some samples may have been due to amplification of the genetic material from the intraluminal lymphocytes of cerebral blood vessels, taking into account that around 30%–70% of infected animals have shown persistent lymphocytosis [23].

In samples showing characteristics consistent with NPME, regardless of BLV status, meningeal inflammatory infiltration (Figure 1) and accumulation of inflammatory cells along the Virchow-Robin space were evident (perivascular cuffing) (Figure 2).

Table 2: Sequences with maximum and minimum similarity of nucleotides and of amino acids in the consensus region, when compared with one another and with GenBank sequences.

Similarity	Nucleotide Identity	Amino acid identity
Among the sequences of this study	Maximum (100%) (i) JN254633, JN254635, JN254637 and JN254638 (ii) JN254636 and JN254640	Maximum (100%) (i) JN254633, JN254635, JN254637 and JN254638 (ii) JN254636 and JN254640
	Minimum (95.8%) (i) JN254634 × JN254633, JN254635, JN254637 and JN254638	Minimum (96.5%) (i) JN254634 × JN254633, JN254635, JN254637 and JN254638
Among the sequences of the study before the other retrieved from GenBank	Maximum (100%) (i) JN254633, JN254635, JN254637, JN254638 and FJ808582 (ii) JN254636, JN254640 and EF065640	Maximum (100%) (i) JN254633, JN254635, JN254637, JN254638 and FJ808582 (ii) JN254636, JN254640 and EF065640 (iii) JN254639 and AY185360
	Minimum (94%) (i) JN254634 × EU266062	Minimum (92.4%) (i) EU266062 × JN254634, JN254634, JN254635, JN254638 and JN254638

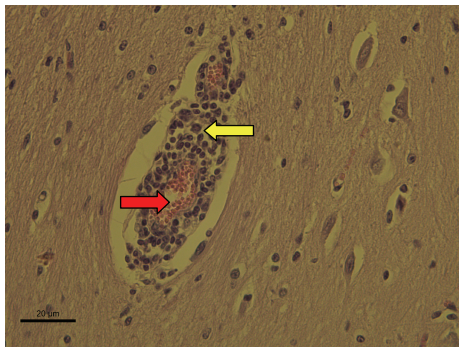

Figure 2: Non-purulent encephalitis (H & E 400x magnification). Bovine brain, positive for BLV, with mononuclear cell infiltrates in the Virchow-Robin space (yellow arrows) characterizing the perivascular cuffing. The red arrows indicate the vascular lumen, with red blood cells within.

Comparison of the nucleotide and amino acid identity matrix (Table 2) of the sequenced samples from this work showed 100% identity among the BLV samples JN254633, JN254637, and JN254638, all from São Paulo, and with BLV sample JN254635 from Mato Grosso State. When compared to GenBank sequences, these samples showed 100% identity with sequence FJ808582, originally from Argentina [24]. Maximum identity was also found between samples BLV 04 (JN254636) from São Paulo State and 13 (JN254640) from Mato Grosso, which were identical to the retrieved sequences from GenBank EF065640, originally described in Costa Rica [25].

A high mutation rate of retroviruses has been reported, linking this to reverse transcriptase due to the high number of replication cycles [26]. The rates of nucleotide mutation of BLV are 0.009% and 0.034% in regions corresponding to the env gene and long terminal repeat (LTR), respectively [27]. However, it was evident in the present work, based on minimal similarities of identity matrices, that both nucleotide (94%) and amino acid (92.4%) present a clear conservation of nucleotide sequences, confirming findings of Portetelle et al. [28] and Felmer et al. [29] that the BLV can conserve its genetic characteristics in different geographical areas for long periods.

Phylogenetic analysis of eight partial sequences of the env gene (gp51) of BLV showed the presence of three genotypes, they were represented in the phylogenetic tree (Figure 3), and they corresponded to the identity matrix and to the genotypes previously described [24, 30, 31]. Its topology confirmed the separate genotypes reported by these cited authors. Discussions and controversies have been generated concerning the number of genotypes of BLV but have evolved to consensus on the existence of at least seven genotypes, based both on studies using PCR-RFLP and those employing sequencing analyzes [24, 30, 32]. However, evidence for an eighth genotype was reported by Hemmatzadeh [33] and suggested by Matsumura et al. [31], which is why it was considered by this study.

Based on the phylogenetic analysis of the partial region of the env gene, none of the identified genotypes was associated with NPME in cattle with neurological syndrome. There is no currently available information on the pathogenicity of BLV genotypes to different organs, including the bovine CNS. Although the development of a tumoral form of bovine leukosis has been described as dependent on host susceptibility [34, 35], there is currently no evidence for whether some genotypes can influence or induce these neoplasias.

4. Conclusions

The results indicate that BLV has no tropism in the CNS, and it cannot be regarded as the primary causative agent of non-purulent meningoencephalitis in cattle. The observed genotypes corroborate previous studies conducted in Brazil. Bovine leukemia virus cannot be excluded from the differential diagnosis of neurological syndrome because, despite

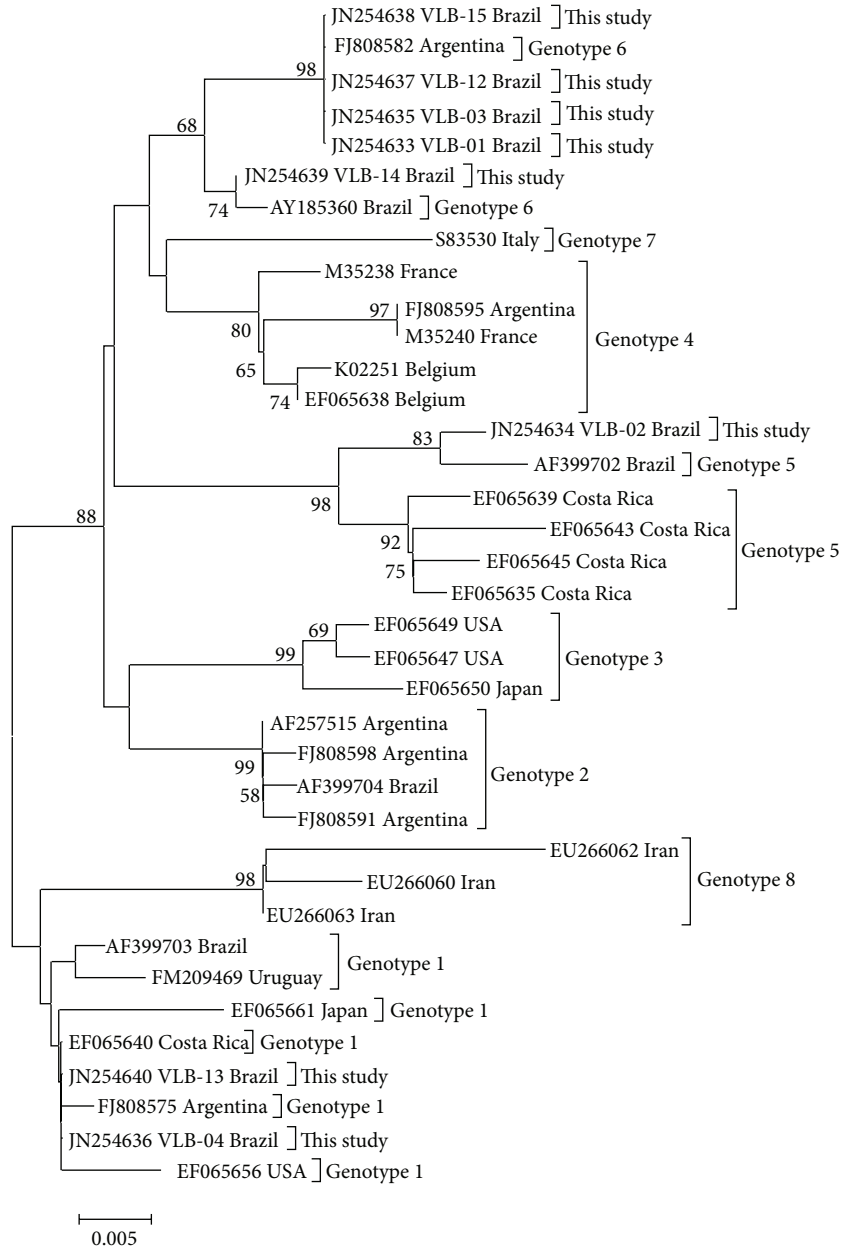

Figure 3: Phylogenetic tree developed by the neighbor-joining method with the substitution pattern *maximum composite likelihood* (Software Mega v. 5). The samples show identification *Accession Number*/country of study/genotype referring to the env gene. The numbers near each node represent the values of 1000 bootstrap replicates, showing only those greater than 50%. The scale represents the number of replacements/sites.

being rare, the presence of lymphosarcomas in the CNS has been reported in Brazil.

Acknowledgment

The authors would like to thank FAPESP (Research Support Foundation of São Paulo, SP, Brazil) for Masters Scholarship Process no. 2010/04692-6 and for Research Grant Process no. 2011/06513-4. They also want to thank the Scientific Researcher Alice Akimi Ikuno for her assistance.

References

[1] E. M. Pituco, E. M. S. Cunha, M. C. C. S. H. Lara et al., "Encefalites e encefalopatias dos bovinos: sistematização do diagnóstico diferencial," in *Proceedings of the 11th Latinoamerican Buiatrics Congress and the 5th Brazilian Buiatrics Congress*, p. 46, Brazilian Buiatrics Association, Salvador, Brazil, 2003.

[2] C. S. L. Barros, D. Driemeier, I. S. Dutra, and R. A. A. Lemos, *Doenças do Sistema Nervoso de Bovinos no Brasil*, Vallée, Montes Claros, Brazil, 2006.

[3] G. A. Wells, A. C. Scott, C. T. Johnson et al., "A novel progressive spongiform encephalopathy in cattle," *Veterinary Record*, vol. 121, no. 18, pp. 419–420, 1987.

[4] A. W. D. Sanches, I. M. Langohr, A. L. Stigger, and C. S. L. Barros, "Doenças do sistema nervoso central em bovinos no Sul do Brasil," *Pesquisa Veterinária Brasileira*, vol. 20, pp. 113–118, 2000.

[5] Ministério da Agricultura, Pecuária e Abastecimento—MAPA, Programa Nacional de Controle da Raiva e outras Encefalopatias—PNCRH, Brasília, Brazil, 2011, http://www.agricultura.gov.br/.

[6] C. S. L. Barros and G. H. F. Marques, *Procedimentos para o Diagnóstico de Doenças do Sistema Nervoso Central de Bovinos*, MAPA/SDA/DDA, Brasília, Brazil, 2003.

[7] C. Del Fava, R. Macruz, M. C. C. S. H. Lara et al., "Diagnóstico de encefalites e encefalopatias espongiformes transmissíveis em ruminantes no período de 2004 a 2007 no Estado de São Paulo, Brasil," *Archives of Veterinary Science*, vol. 12, pp. 83–84, 2007.

[8] C. Del Fava and E. M. Pituco, "Aspectos da infecção pelo vírus da leucose enzoótica bovina em bovinos no Brasil," *Biológico*, vol. 66, pp. 1–8, 2004.

[9] R. A. Fighera and C. S. L. Barros, "Intracerebral lymphosarcoma in a cow," *Ciência Rural*, vol. 34, pp. 943–945, 2004.

[10] C. Del Fava, A. A. Ikuno, R. Harakava, M. C. C. S. H. Lara, and E. M. Pituco, "Molecular study of bovine leukemia virus causing lymphosarcoma in bovine central nervous system," *Virus Reviews and Research*, vol. 16, no. 1, p. 232, 2011.

[11] D. J. Dean, M. K. Abelseth, and P. Atanasiu, "Routine laboratory procedures: the fluorescent antibody test," in *Laboratory Techniques in Rabies*, F. X. Meslin, M. M. Kaplan, and H. Koprowski, Eds., pp. 88–95, World Health Organization, Genebra, Switzerland, 4th edition, 1996.

[12] E. B. Prophet, B. Mills, J. B. Arrington, and L. H. Sobin, Eds., *Métodos Histotecnológicos*, Registro de Patologia de los Estados Unidos de América y Instituto de Patología de las Fuerzas Armadas de los Estados Unidos de América, Washington, DC, USA, 1992.

[13] D. Beier, P. Blankenstein, O. Marquardt, and J. Kuzmak, "Identification of different BLV provirus isolates by PCR, RFLPA and DNA sequencing," *Berliner und Munchener Tierarztliche Wochenschrift*, vol. 114, no. 7-8, pp. 252–256, 2001.

[14] T. A. Hall, "Bioedit: a user-friendly biological sequence alignment editor and analysis program for Windows 95/98/NT," *Nucleic Acids Symposium Series*, vol. 41, pp. 95–98, 1999.

[15] K. Tamura, J. Dudley, M. Nei, and S. Kumar, "MEGA4: Molecular Evolutionary Genetics Analysis (MEGA) software version 4.0," *Molecular Biology and Evolution*, vol. 24, no. 8, pp. 1596–1599, 2007.

[16] E. S. Berquó, J. M. P. Souza, and S. L. D. Gotlieb, *Bioestatística*, Editora Pedagógica e Universitária Ltda., São Paulo, Brazil, 1981.

[17] R. C. Leite, C. M. Modena, E. C. Moreira, and J. J. Abreu, "Evolução clínica da leucose enzoótica bovina," *Arquivo Brasileiro de Medicina Veterinária e Zootecnia*, vol. 36, pp. 47–57, 1984.

[18] E. H. Birgel Júnior, J. L. D'Angelino, F. J. Benesi, and E. H. Birgel, "Prevalência da infecção pelo vírus da Leucose dos bovinos, em animais da raça Jersey, criados no estado de São Paulo," *Pesquisa Veterinária Brasileira*, vol. 15, pp. 93–99, 1995.

[19] J. Megid, C. N. Nozaki, R. B. S. Kuroda, T. F. Cruz, and K. C. Lima, "Ocorrência de leucose enzoótica bovina na microrregião da Serra de Botucatu," *Arquivo Brasileiro de Medicina Veterinária e Zootecnia*, vol. 55, pp. 645–646, 2003.

[20] Y. Aida, M. Miyasaka, K. Okada et al., "Further phenotypic characterization of target cells for bovine leukemia virus experimental infection in sheep," *American Journal of Veterinary Research*, vol. 50, no. 11, pp. 1946–1951, 1989.

[21] I. Schwartz, A. Bensaid, B. Polack, B. Perrin, M. Berthelemy, and D. Levy, "*In vivo* leukocyte tropism of bovine leukemia virus in sheep and cattle," *Journal of Virology*, vol. 68, no. 7, pp. 4589–4596, 1994.

[22] A. L. Parodi, "Pathology of enzootic bovine leukosis: comparision with the sporadic form," in *Enzootic Bovine Leukosis and Bovine Leukemia Virus*, A. Burny and M. Mammerickx, Eds., pp. 15–49, Martinus Nijhoff, Boston, Mass, USA, 1987.

[23] J. F. Ferrer, "Bovine leukosis: natural transmission and principles of control," *Journal of the American Veterinary Medical Association*, vol. 175, no. 12, pp. 1281–1286, 1979.

[24] S. M. Rodriguez, M. D. Golemba, R. H. Campos, K. Trono, and L. R. Jones, "Bovine leukemia virus can be classified into seven genotypes: evidence for the existence of two novel clades," *Journal of General Virology*, vol. 90, no. 11, pp. 2788–2797, 2009.

[25] X. Zhao and G. C. Buehring, "Natural genetic variations in bovine leukemia virus envelope gene: possible effects of selection and escape," *Virology*, vol. 366, no. 1, pp. 150–165, 2007.

[26] L. M. Mansky and H. M. Temin, "Lower mutation rate of bovine leukemia virus relative to that of spleen necrosis virus," *Journal of Virology*, vol. 68, no. 1, pp. 494–499, 1994.

[27] L. Willems, R. Kettmann, F. Dequiedt et al., "*In vivo* infection of sheep by bovine leukemia virus mutants," *Journal of Virology*, vol. 67, no. 7, pp. 4078–4085, 1993.

[28] D. Portetelle, D. Couez, C. Bruck et al., "Antigenic variants of bovine leukemia virus (BLV) are defined by amino acid substitutions in the NH2 part of the envelope glycoprotein gp51," *Virology*, vol. 169, no. 1, pp. 27–33, 1989.

[29] R. Felmer, G. Muñoz, J. Zúñiga, and M. Recabal, "Molecular analysis of a 444 bp fragment of the bovine leukaemia virus gp51 env gene reveals a high frequency of non-silent point mutations and suggests the presence of two subgroups of BLV in Chile," *Veterinary Microbiology*, vol. 108, no. 1-2, pp. 39–47, 2005.

[30] G. Moratorio, G. Obal, A. Dubra et al., "Phylogenetic analysis of bovine leukemia viruses isolated in South America reveals diversification in seven distinct genotypes," *Archives of Virology*, vol. 155, no. 4, pp. 481–489, 2010.

[31] K. Matsumura, E. Inoue, Y. Osawa, and K. Okazaki, "Molecular epidemiology of bovine leukemia virus associated with enzootic bovine leukosis in Japan," *Virus Research*, vol. 155, no. 1, pp. 343–348, 2011.

[32] E. Inoue, K. Matsumura, K. Maekawa et al., "Genetic heterogeneity among bovine leukemia viruses in Japan and their relationship to leukemogenicity," *Archives of Virology*, vol. 156, no. 7, pp. 1137–1141, 2011.

[33] F. Hemmatzadeh, "Sequencing and phylogenetic analysis of gp51 gene of bovine leukaemia virus in iranian isolates," *Veterinary Research Communications*, vol. 31, no. 6, pp. 783–789, 2007.

[34] H. A. Lewin and D. Bernoco, "Evidence for BoLA-linked resistance and susceptibility to subclinical progression of bovine leukaemia virus infection," *Animal Genetics*, vol. 17, no. 3, pp. 197–207, 1986.

[35] O. M. Radostitis, C. C. Gay, D. C. Blood, and K. W. Hinchcliff, Eds., *Clínica Veterinária—Um Tratado de Doenças dos Bovinos, Ovinos, Suínos, Caprinos e Equinos*, Guanabara Koogan, Rio de Janeiro, Brazil, 9th edition, 2002.